eCAM Evidence-Based Complementary and Alternative Medicine

Traditional Chinese Medicine and Vascular Disease

Guest Editors: Yanwei Xing, Charles Antzelevitch, Dan Hu, and Zhang Tan

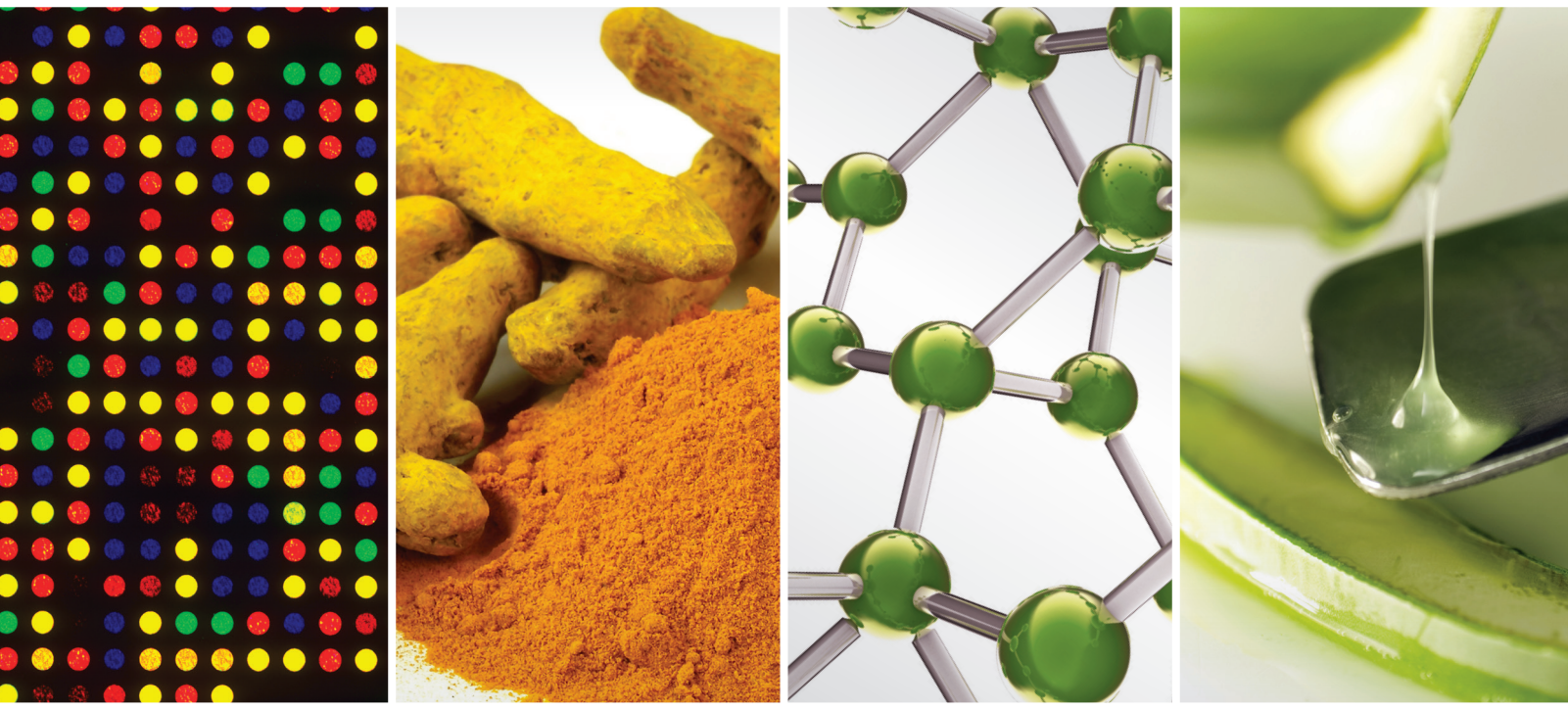

Traditional Chinese Medicine and Vascular Disease

Evidence-Based Complementary and Alternative Medicine

Traditional Chinese Medicine and Vascular Disease

Guest Editors: Yanwei Xing, Charles Antzelevitch, Dan Hu, and Zhang Tan

Editorial Board

Contents

Hindawi Publishing Corporation
Evidence-Based Complementary and Alternative Medicine
Volume 2015, Article ID 430818, 2 pages
http://dx.doi.org/10.1155/2015/430818

Editorial

Traditional Chinese Medicine and Vascular Disease

Yanwei Xing,[1] Dan Hu,[2] Tan Zhang,[3] and Charles Antzelevitch[2]

[1]*Department of Cardiology, Guang' anmen Hospital, China Academy of Chinese Medical Sciences, Beijing 100053, China*
[2]*Experimental Cardiology and Molecular Genetics, Masonic Medical Research Laboratory, Utica, USA*
[3]*Department of Internal Medicine, Gerontology and Geriatric Medicine, Wake Forest School of Medicine, Medical Center Boulevard, Winston-Salem, NC, USA*

Correspondence should be addressed to Yanwei Xing; xingyanwei12345@163.com and Dan Hu; dianah@mmrl.edu

Received 10 September 2015; Accepted 10 September 2015

According to the epidemiological survey, vascular disease is the leading cause of death in the world. Vascular disease includes any condition that affects your circulatory system, such as peripheral artery disease. This ranges from diseases of your arteries, veins, and lymph vessels to blood disorders that affect circulation. With the world population aging, hypertension, stroke, coronary heart disease, and diabetes incidences are increasing year by year. These diseases seem to be independent; in fact, vascular disease is able to cause all these diseases. However, the recent studies suggest that traditional Chinese medicine ("TCM") is a potential candidate for the preventative treatment of vascular disease. For example, Tongxinluo capsule for the treatment of atherosclerosis has been recognized around the world.

TCM is an integral part of Chinese culture, which includes pharmacology of traditional Chinese medical formulae, Chinese patent medicines, and Chinese herbal monomer. Today both of TCM and western medicine are being used in providing medical and health services in the whole world. TCM, with its unique diagnostic methods, systematic approach, abundant historical literature, and materials, has attracted many attentions from the international community. TCM has been very effective in the treatment of vascular disease, but it still has the following problems. (1) Many mechanisms of TCM for diseases are not clear. (2) Large-scale clinical trials based on evidence are lacking. Therefore, we encourage investigators to contribute original research articles as well as comprehensive review articles on the treatment of vascular diseases with TCM. We are particularly interested in articles reporting the clinical trials or revealing the action mechanisms of TCM by using cellular or animal models.

Cerebral Vascular Related Articles. X. Han et al. in their paper "The Clinical Relevance of Serum NDKA, NMDA, PARK7, and UFDP Levels with Phlegm-Heat Syndrome and Treatment Efficacy Evaluation of Traditional Chinese Medicine in Acute Ischemic Stroke" found that the serum PAPK7 and UFDP concentration exhibited diagnostic value for the phlegm-heat syndrome of TCM in patients. The serum NDKA, NDMA, PAPK7, and UFDP levels did not show a significant tendency of increase in day 7 compared to 3 days within onset, but UFDP, but not NDKA levels, exhibited a tendency of increase in day 14 compared to day 7.

X. Du et al. in their paper "Scutellarin Reduces Endothelium Dysfunction through the PKG-I Pathway" investigated the protective mechanism of scutellarin (SCU) in vitro and in vivo for human brain microvascular endothelial cells (HBMECs). SCU protects against cerebral vascular EtD through endothelial PKG pathway activation.

Mechanism of Chinese Herbal Medicine on the Protection of Renal Vascular. B. Liu et al. in their paper introduced to us the protective effects of curcumin on obesity-related glomerulopathy. Curcumin is able to alleviate the harmful reaction of leptin on podocytes and reduce the severity of ORG. The above protective effects are associated with the inhibition of Wnt/catenin signaling activation in podocytes.

L. Han et al. in their paper "The Renal Protective Effect of Jiangya Tongluo Formula, through Regulation of

Adrenomedullin and Angiotensin II, in Rats with Hypertensive Nephrosclerosis" make a conclusion that Jiangya Tongluo Formula can prevent nephrosclerosis through regulation of adrenomedullin and angiotensin II. JYTL may upregulate endogenous ADM level in the kidneys and antagonize Ang II during vascular injury by dilating renal blood vessels and improving ischemia, thus resulting in the protection of renal function.

Mechanism of Chinese Herbal Medicine on the Protection of Diabetic Vascular Disease. M. Li et al. in their paper "Tang-Tong-Fang Confers Protection against Experimental Diabetic Peripheral Neuropathy by Reducing Inflammation" have studied Chinese herbal medicine in the protection of diabetic vascular disease. TTF treatment also attenuated the effect of DPN on other parameters including histology and ultrastructural changes, expression of ICAM-1, MPO, and TNF-α in rat sciatic nerves, and plasma sICAM-1 and MPO levels. Together, our data suggest that TTF treatment may alleviate DPN via ICAM-1 inhibition.

Mechanism of Chinese Herbal Medicine Treatment on Atherosclerosis. Q. Kang et al. in their paper "Effect of Compound Chuanxiong Capsule on Inflammatory Reaction and PI3K/Akt/NF-κB Signaling Pathway in Atherosclerosis" suggested that Compound Chuanxiong Capsule can prevent atherosclerosis through regulation of the inflammatory reaction and PI3K/Akt/NF-κB signal pathway. They concluded that CCC can inhibit inflammatory reaction in the ApoE−/−mice fed with a high fat diet. Its mechanism may be related to regulation of PI3K/Akt/NF-κB signaling pathway.

S.-H. Lu et al. in their paper "Experimental Study of Antiatherosclerosis Effects with Hederagenin in Rats" studied that hederagenin had the effect of antiatherosclerosis. The results indicated that hederagenin can inhibit or improve the pathological changes that occur during atherosclerosis induced by a high-fat diet plus VD3 in rats. The underlying mechanism might be related to the regulation of lipid metabolism disorders, improvement of blood rheology, regulation of vascular endothelium imbalance, and inhibition of the IKKβ/NF-κB signaling pathway to reduce the amplification cascade of the inflammatory response.

M. Wu et al. in their paper "Polydatin Inhibits Formation of Macrophage-Derived Foam Cells" have studied that polydatin protected against atherosclerosis through inhibiting formation of macrophage-derived foam cells. Polydatin significantly inhibits the formation of foam cells derived from peritoneal macrophages. Further studies indicated that polydatin regulates the metabolism of intracellular lipid and possesses anti-inflammatory effects, which might be regulated through the PPAR-γ signaling pathways.

The accepted articles mainly introduced TCM which included pharmacology of traditional Chinese medical formulae, Chinese patent medicines, and Chinese herbal monomer, which protected against atherosclerosis through improving the vascular endothelial function, inhibiting the oxidative stress, and suppressing inflammatory reaction. In this special issue, the articles included are not only basic research, but also clinical research. The diseases to be intervened included diabetic vascular disease, cardiovascular disease, cerebrovascular disease, peripheral vascular diseases, microvascular diseases, and renal vascular diseases. TCM treatment of the vascular disease may be an effective method.

Yanwei Xing
Dan Hu
Tan Zhang
Charles Antzelevitch

Hindawi Publishing Corporation
Evidence-Based Complementary and Alternative Medicine
Volume 2015, Article ID 456354, 10 pages
http://dx.doi.org/10.1155/2015/456354

Research Article

Experimental Study of Antiatherosclerosis Effects with Hederagenin in Rats

Su-Hong Lu,[1] Jian-Hua Guan,[1] Yan-Li Huang,[1] Yu-Wei Pan,[1] Wei Yang,[1] Hai Lan,[1] Si Huang,[1] Jing Hu,[2] and Guo-Ping Zhao[1]

[1]*Medical School, Jinan University, 601 Huangpu Road West, Guangzhou, Guangdong 510632, China*
[2]*The First Affiliated Hospital of Jinan University, 613 Huangpu Road West, Guangzhou, Guangdong 510632, China*

Correspondence should be addressed to Guo-Ping Zhao; tguo428@163.com

Received 7 January 2015; Accepted 6 April 2015

Academic Editor: Zhang Tan

The research tries to establish Wistar rat's model of atherosclerosis for evaluating the antiatherosclerotic effect of hederagenin and exploring its antiatherosclerosis-related mechanisms. The statistical data have shown that hederagenin exhibits multiple pharmacological activities in the treatment of hyperlipidemia, antiplatelet aggregation, liver protection, and anti-inflammation, indicating that hederagenin may exert a protective effect on vascular walls by improving lipid metabolism disorders and lipid deposition. The results show that hederagenin can correct the imbalance of endothelial function by inhibiting the release of large amounts of iNOS and increasing eNOS contents and inhibits the IKKβ/NF-κB signaling pathway to reduce the release of IL-6, IFN-γ, TNF-α, and other inflammatory factors. The experimental results indicated that hederagenin can inhibit or ameliorate the pathological changes associated with AS, displaying an excellent preventive function against AS.

1. Introduction

Atherosclerosis (AS) is an inflammatory disease caused by the lesion-like deposition of lipids (primarily cholesterol and cholesterol ester), carbohydrates, and blood components on the vasculature intima or under the intima of the artery and its branches, in addition to the deposition of connective tissues and calcium. AS is accompanied by the migration of medial smooth muscle cells into the intima and the proliferation of these cells, causing intimal thickening and the formation of AS lesions or fibrous fatty plaque lesions. An inflammatory response is always present in AS. Deaths from cardiac and cerebrovascular accidents caused by AS account for the highest disease mortality in humans. Therefore, AS is referred to as the "number one killer" in western countries, and it is one of the most severe cardiovascular diseases that threaten human health. Hence, strategies for achieving early diagnosis and effective interventions for this disease are urgently required. Many studies have been conducted on the prevention and treatment of AS, both domestically and abroad. Most of these studies have investigated the pathogenesis of AS and attempted to delay the progression of the pathological changes associated with AS through drug interventions. Currently, hyperlipidemia is considered the primary factor involved in the occurrence and development of AS. Good control of blood lipids can significantly slow the progression of AS lesions and reduce morbidity and mortality associated with AS-related cardiovascular diseases. There have been drug studies on the prevention and treatment of atherosclerosis conducted to date. Statins can contribute to the prevention of atherosclerosis, but the liver damage they cause after long-term administration is drawing increasing attention [1–3]. Natural herbs present the characteristics of having many available varieties and low toxic side effects. Identifying single active components of natural herbs that can prevent and treat atherosclerosis is a trend in modern pharmaceutical research and development. Hederagenin, with a molecular formula of $C_{30}H_{48}O_4$, is a pentacyclic triterpenoid saponin that is relatively enriched in *Hedera nepalensisvar sinensis* of the Araliaceae *Hedera* L. genus, *Akebia trifoliata* of the Lardizabalaceae, and *Clematis armandii* Franch and *Holboellia fargesii* Reaub of the Ranunculaceae. Studies have

shown that hederagenin exhibits multiple pharmacological activities in the treatment of hyperlipidemia, antilipid peroxidation, antiplatelet aggregation, liver protection, antidepression, anti-inflammation, and diuresis [4–12], indicating that hederagenin may exert a protective effect on vascular walls by improving lipid metabolism disorders and lipid deposition. However, there are currently few reports regarding whether hederagenin can protect arteries from AS lesions through its lipid-lowering and anti-inflammatory functions. Therefore, the present study established a Wistar rat atherosclerosis model in which hederagenin was administered as a preventive intervention to evaluate its preventive function against atherosclerosis and to explore the underlying mechanism, providing an experimental basis for clinical drug administration.

2. Materials and Methods

2.1. Preparation of Drugs. Consider the following: hederagenin (purity 95%), Nanjing Spring and Autumn Biological Engineering Co., Ltd, batch number: 20131020; vitamin D_3, specifications: 1 mL: 7.5 mg, Shanghai General Pharmaceutical Co., Ltd., batch number: 121123; atorvastatin calcium (Lipitor), specifications: 20 mg $*$ 7 tablets, Pfizer, batch number: H54107; sodium carboxymethyl cellulose (CMC-Na), Shanghai Bohu Biological Technology Co., batch number: 20130513.

2.2. Animals and High-Fat Diet. Male, Specific Pathogen-Free- (SPF-) level Wistar rats with weights of 160–200 g, aged 5~6 weeks (provided by the Experimental Animal Center of Southern Medical University, license number: SCKK2011-0015, animal certificate number: 44002100002027), were used in this study. The animals were fed in animal experimental center of Jinan University SPF animal housing management and given free access to water and food; the feeding room temperature was set at 23°C–25°C, and the relative humidity was approximately 7%. After one week of feeding adaptation, the experiments were initiated. The high-fat diet was composed of 3% cholesterol, 0.5% sodium cholate, 0.2% propylthiouracil, 5% sugar, 10% lard, and 81.3% basic fodder, which were mixed well and irradiated with cobalt-60 (radiation dose 25.0 kGy) before feeding.

2.3. Experimental Design

2.3.1. Modeling [13–18]. After one week of adaptive feeding with basic rat fodder, 40 quarantined Wistar rats were selected and weighed. The rats were randomly divided into four groups according to a random number table. These groups included a normal group, model group, atorvastatin calcium (Lipitor) group and hederagenin group, with 10 rats in each group. With the exception of the normal group, the rats in all other groups were administered vitamin D_3 at 600,000 IU/kg/d via intraperitoneal injection, and they were also fed continuously with the high-fat diet. Furthermore, an additional 100,000 IU/kg of vitamin D_3 was administered to these rats via intraperitoneal injection in the 3rd, 6th, and 9th weeks of the experiments. The rats in the normal group were administered saline through intraperitoneal injection and were fed with normal fodder.

2.3.2. Grouping and Drug Administration

Doses and Methods. The rats in each group were administered the corresponding drugs for each intervention. The rats in the hederagenin group were administered hederagenin at 20 mg/kg/d via gavage. The rats in the atorvastatin calcium group were administered atorvastatin calcium tablets at 5 mg/kg/d via gavage. All drugs were prepared as suspension solutions with 0.5% sodium carboxymethyl cellulose (CMC-Na). The rats in the normal control group and the model group were administered an equal amount of 0.5% CMC-Na via gavage continuously for 12 weeks.

2.4. Determination of Indicators. At the end of 12 weeks, arteries were collected from the rats to perform HE staining and observe pathological changes under a light microscope and electron microscope. A Zeiss-Axioskop 20 microscope was used to observe the histological changes in HE-stained sections, and an Axiocan HRc camera was employed to obtain micrographs. Leica Qwin Image Processing and Analysis Software was used to analyze AS lesions and the cross-sectional area of the artery lumen and to calculate the relative area of atherosclerosis lesions (the ratio of the lesion area versus the lumen cross-sectional area), which is represented as a percentage (%). Blood lipids, liver lipids, blood rheology, inflammatory factors, and the gene expression and protein expression of eNOS, iNOS, IKKβ, p-IKKβ, and NF-κBp65 in artery tissue were examined.

2.5. Statistical Analysis of the Data. The experimental data were analyzed using Social Sciences (SPSS, USA) 16.0 statistical software. Measured data were represented as the mean ± standard deviation (SD), and comparisons of the means between two groups were carried out with one-way ANOVA. When the variance was homogeneous, the SNK test and Tukey test were applied, whereas when the variance was not homogeneous, the T2 test was used and probability value (P) less than 0.05 indicated that the difference was statistically significant.

3. Results

3.1. Observation of Pathological Changes in the Rat Aorta through Light and Electron Microscopy

3.1.1. Light Microscopy Observations of Rat Aorta HE Staining (200x)

Normal Control Group. Aorta morphology was normal; endothelial cells were intact; the intima was smooth; there was no local damage or thickening; the internal elastic lamina was continuous without breaks; the tunica media edge was clear; smooth muscle cells were arranged in an orderly fashion; no inflammatory cell infiltration was observed; and there was no excrescence in the lumen. Model group: significant

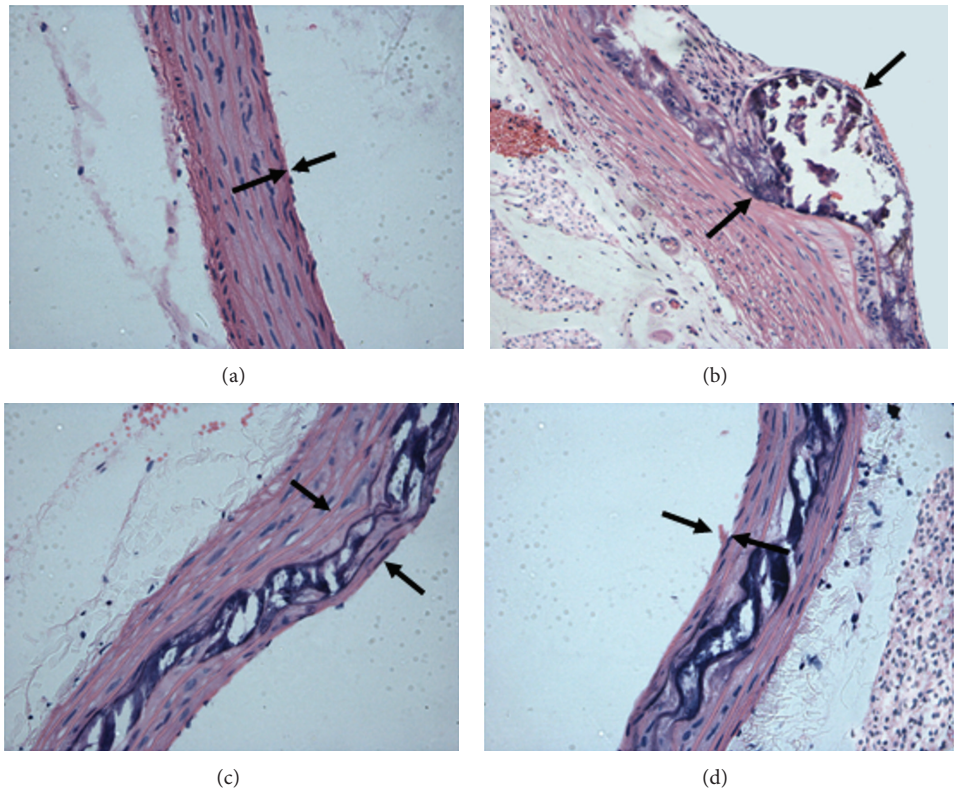

Figure 1: Histological changes of aorta morphology in different groups (HE stain ×200). (a) Normal control group. (b) Model group. (c) Lipitor group. (d) Hederagenin group.

intimal hyperplasia could be observed in the aorta, which appeared as continuous intimal damage, and a large number of foam cells, cholesterol crystals, intermittent calcification, and unstructured necrotic substances could be observed in the lumen, forming the fibrous cap of AS plaques. The tunica media was thickened, and a large number of smooth muscle cells aggregated and passed through the internal elastic lamina to gather at the tunica intima. Lipitor group: slight intimal thickening of rat aorta, protruding into the lumen, and a thickened tunica media were observed; smooth muscle cells were arranged in a relatively orderly fashion; calcification appeared between the intima and the tunica media; no unstructured necrotic substances were present; and there was a small amount of cholesterol crystal deposition. Hederagenin group: the aorta intima was relatively integral without thickening; only a small amount of damaged intima had detached; the tunica media exhibited intermittent calcification without unstructured necrotic substances; and there was a small amount of cholesterol crystal deposition (Figure 1).

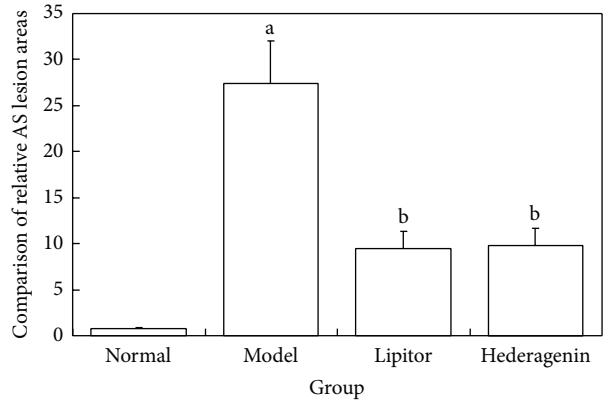

Figure 2: Comparison of relative AS lesion areas in the rat aorta in each group. [a]$P < 0.01$ versus normal group; [b]$P < 0.01$ versus model group.

3.1.2. Relative Area of Rat Aorta AS Lesions

The Experimental Results Demonstrated the Following (Figure 2). ① The relative area of model group rat aortic lesions was increased significantly compared with the normal control group, and the difference was statistically significant ($P < 0.01$). ② Compared with the model group, the relative lesion area in the Lipitor group and in the hederagenin group was decreased significantly, and these differences were statistically significant ($P < 0.01$).

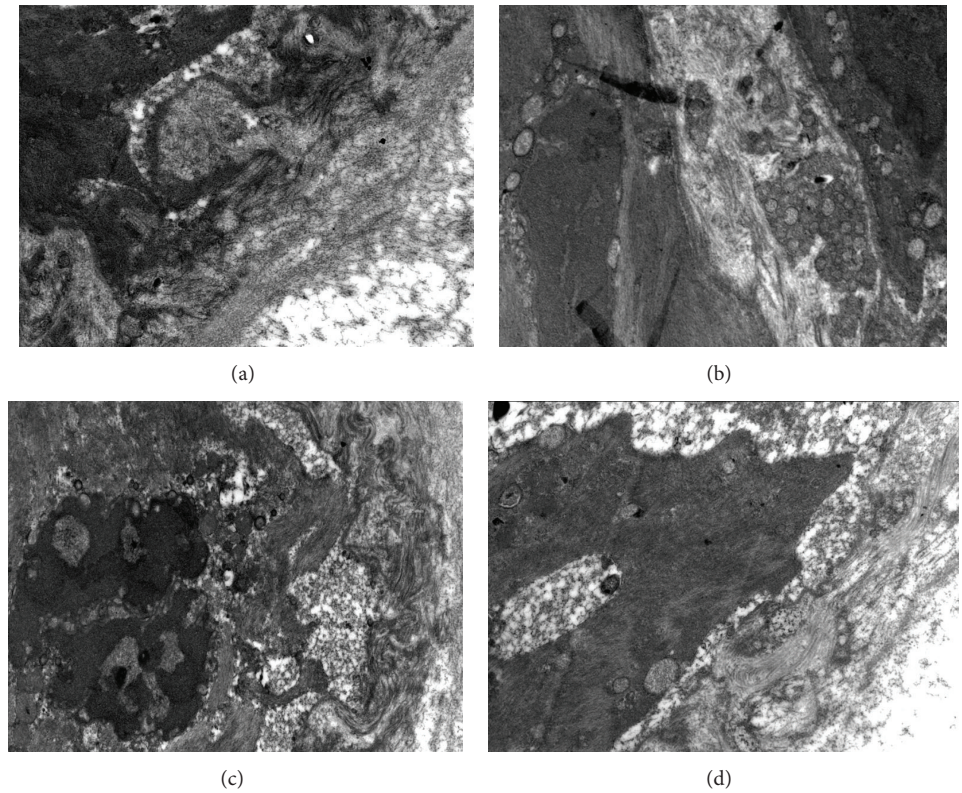

Figure 3: Electron microscopy observations of the rat aorta (12500x). (a) Normal control group. (b) Model group. (c) Lipitor group. (d) Hederagenin group.

3.1.3. Electron Microscopy Observations of the Rat Aorta (12500x)

Normal Control Group. Rat aorta endothelial cells presented a normal morphology; adjacent endothelial cells were closely connected; nuclei were integral; the internal elastic lamina was continuous, with a uniform thickness; no obvious lipid vacuoles or collagen fiber proliferation was observed. Model group: the rat aorta endothelial cells had detached completely; the cytoplasm was not dense; there was a large amount of disorganized lipid deposition. Many collagen fibers could be observed in the intercellular space. Endothelial cell necrosis was observed, where the endothelial cells disappeared and were replaced with cell debris and a large amount of a fiber-like substance. The continuity of the internal elastic lamina was severely damaged, with focal dissolution. There were large amounts of foam cell infiltration, and the number of collagen fibers was increased significantly. Lipitor group: endothelial cells were relatively integral with oval-shaped nuclei; the internal elastic lamina was not uniform, showing thinning with occasional breaks, and thickness was not uniform, with some areas showing a complete loss; the gap between the endothelial cells and the internal elastic lamina increased; collagen fiber deposition and a small number of lipid vacuoles could be observed under the endothelium. Hederagenin group: endothelial cell morphology was relatively normal; local endothelial cell damage could be detected, accompanied by a small amount of smooth muscle cell proliferation; a small number of collagen fibers could be observed in the intercellular space; no endothelial cell necrosis was observed; the structure of the internal elastic lamina was mostly integral; a small amount of collagen fiber deposition could be observed under the endothelium (Figure 3).

3.2. Comparison of Rat Serum Lipid Levels, Blood Rheology, and Liver Function in Each Group

3.2.1. Comparison of Rat Serum Lipid Levels in Each Group

Figures 4(a) and 4(b) Showed the Following. ① Compared with the normal control group, the model group animals exhibited increased TC, TG, and LDL-C levels and decreased HDL-C levels, and these differences were statistically significant ($P < 0.05$ or 0.01). ② Compared with the model group, the Lipitor group and the hederagenin group showed significantly reduced TC, TG, and LDL-C levels and significantly increased HDL-C levels, and these differences were statistically significant ($P < 0.01$).

3.2.2. Comparison of Rat Liver Function in Each Group

The Experimental Results Demonstrated the Following (Figure 5). ① Compared with the normal control group, the

Table 1: Comparison of rat hemorheological parameters in each group. [a]$P < 0.01$ versus normal group; [b]$P < 0.01$ versus model group; [c]$P < 0.05$ versus atorvastatin calcium group.

Group	Whole-blood viscosity/mpa·s				Hematocrit	Erythrocyte aggregation index	Platelet aggregation rate/%
	Low shear	Mid shear	High shear	Viscosity			
Normal	10.76 ± 0.83	7.15 ± 0.72	5.18 ± 0.42	1.28 ± 0.12	0.41 ± 0.04	5.12 ± 0.33	39.22 ± 3.69
Model	19.23 ± 2.51[a]	9.66 ± 0.89[a]	7.33 ± 0.76[a]	1.81 ± 0.23[a]	0.69 ± 0.12[a]	6.51 ± 0.87[a]	59.03 ± 5.17[a]
Lipitor	12.64 ± 0.97[b]	7.32 ± 0.83[b]	6.26 ± 0.58[b]	1.32 ± 0.15[b]	0.52 ± 0.05[b]	5.28 ± 0.39[b]	46.61 ± 4.09[b]
Hederagenin	12.58 ± 0.89[b]	7.27 ± 0.71[b]	5.66 ± 0.53[bc]	1.37 ± 0.14[b]	0.53 ± 0.03[b]	5.37 ± 0.45[b]	46.38 ± 4.19[b]

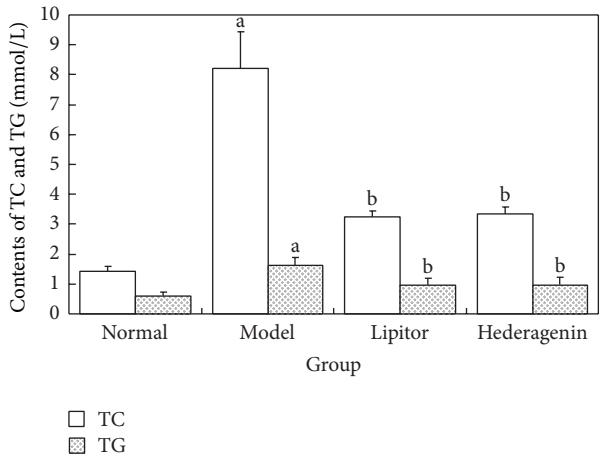

(a)

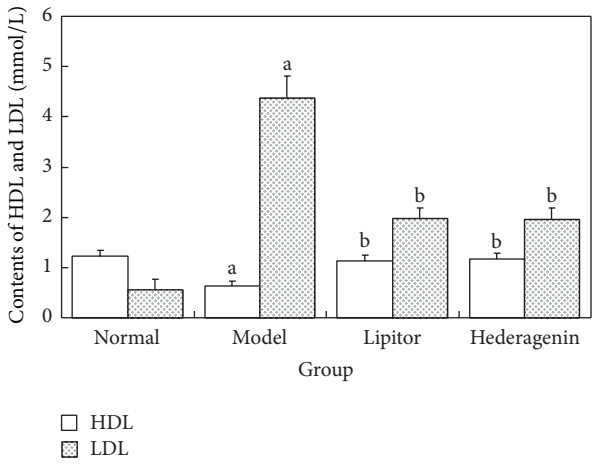

(b)

Figure 4: Comparison of rat serum TC, TG, HDL-C, and LDL-C contents in each group. [a]$P < 0.01$ versus normal group; [b]$P < 0.01$ versus model group.

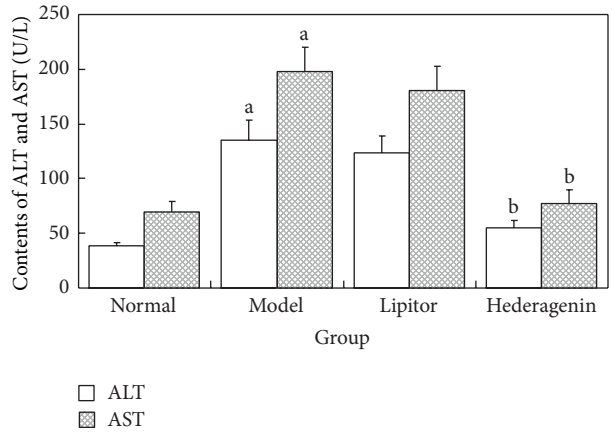

Figure 5: Comparison of rat serum ALT and AST contents. [a]$P < 0.01$ versus normal group; [b]$P < 0.01$ versus model group.

rats in the model group exhibited significantly increased ALT and AST contents, and these differences were statistically significant ($P < 0.01$). ② Compared with the model group, the hederagenin group showed significantly decreased ALT and AST contents, and these differences were statistically significant ($P < 0.01$). ③ Compared with the model group, the Lipitor group exhibited significantly increased ALT and AST contents, though these differences were not statistically significant ($P > 0.05$).

3.2.3. Comparison of Rat Hemorheological Parameters in Each Group

The Experimental Results Demonstrated the Following (Table 1). ① Compared with the normal control group, rat hemorheological parameters were significantly increased in the model group, and these differences were statistically significant ($P < 0.01$). ② Compared with the model group, rat hemorheological parameters in the Lipitor and hederagenin groups were decreased, and these differences were statistically significant ($P < 0.01$). ③ Compared with the Lipitor group, the hederagenin group exhibited an improved high shear whole-blood viscosity index, and this difference was statistically significant ($P < 0.05$).

3.3. Comparison of Rat Aortic Endothelial Function in Each Group

3.3.1. Comparison of Rat Serum NO and ET-1 Contents in Each Group

Figures 6(a) and 6(b) Showed the Following. ① Compared with the normal control group, the contents of NO significantly increased while ET-1 significantly decreased in

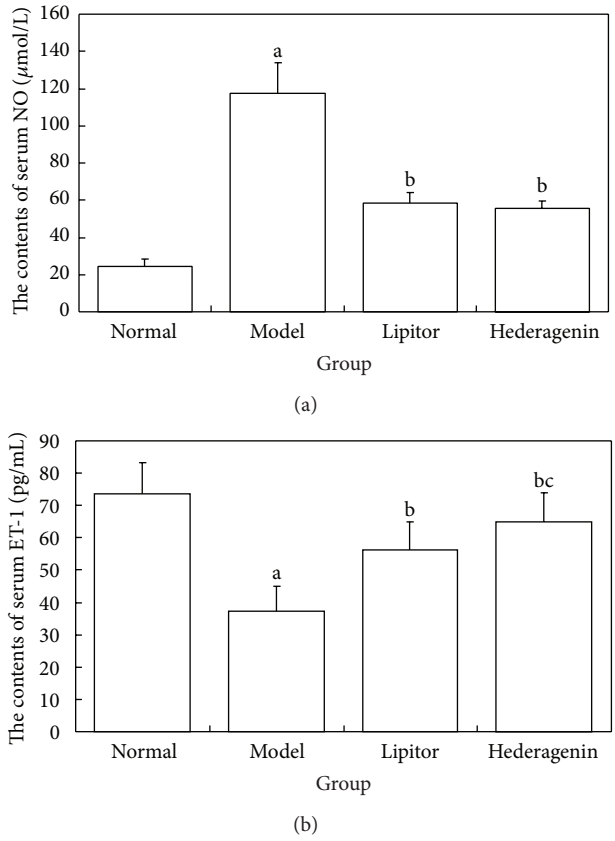

Figure 6: Comparison of rat serum NO and ET-1 contents. [a]$P < 0.01$ versus normal group; [b]$P < 0.01$ versus model group; [c]$P < 0.05$ versus atorvastatin calcium group.

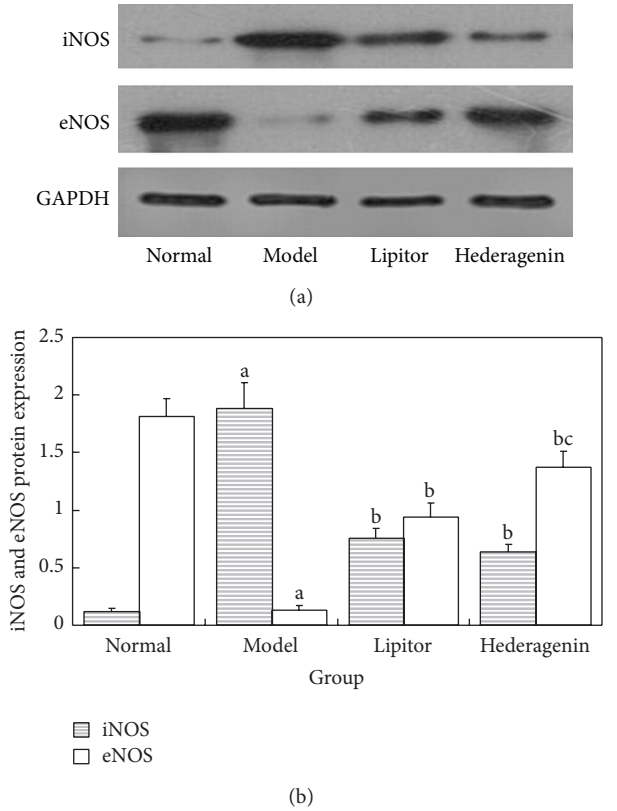

Figure 7: Comparison of rat aortic iNOS and eNOS protein expression levels. [a]$P < 0.01$ versus normal group; [b]$P < 0.01$ versus model group; [c]$P < 0.05$ versus atorvastatin calcium group.

the model group and these differences were statistically significant ($P < 0.01$). ② Compared with the model group, the contents of NO significantly decreased while ET-1 significantly increased in the Lipitor and hederagenin groups and these differences were statistically significant ($P < 0.01$). ③ Compared with the Lipitor group, the hederagenin group exhibited significantly increased ET-1 contents, and these differences were statistically significant ($P > 0.05$).

3.3.2. Comparison of Rat Aortic iNOS and eNOS Protein Expression Levels

Figures 7(a) and 7(b) Showed the Following. ① Compared with the normal control group, the contents of iNOS significantly increased while eNOS significantly decreased in the model group, and these differences were statistically significant ($P < 0.01$). ② Compared with the model group, the contents of iNOS significantly decreased while eNOS significantly increased in the Lipitor and hederagenin groups, and these differences were statistically significant ($P < 0.01$). ③ Compared with the Lipitor group, the hederagenin group exhibited significantly increased eNOS contents, and these differences were statistically significant ($P > 0.05$).

3.4. Comparison of the IKKβ/NF-κB Signaling Pathway and Relevant Inflammatory Factors in the Rat Aorta in Each Group

3.4.1. Contents of the Inflammatory Cytokines IL-6, IFN-γ, and TNF-α in the Rat Aorta

The Experimental Results Demonstrated the Following (Figure 8). ① Compared with the normal control group, the contents of IL-6, IFN-γ, and TNF-α significantly increased in the model group, and these differences were statistically significant ($P < 0.01$). ② Compared with the model group, the contents of IL-6, IFN-γ, and TNF-α significantly decreased in the Lipitor and hederagenin groups, and these differences were statistically significant ($P < 0.01$).

3.4.2. Relative Expression Levels of IKKβ and NF-κB mRNA in Rat Aortic Tissue in Each Group

The Experimental Results Demonstrated the Following (Figure 9). ① Compared with the normal control group, the model group animals exhibited increased gene expression levels of IKKβ and NF-κB, and these differences were statistically significant ($P < 0.01$). ② Compared with the model group, the Lipitor group and the hederagenin group showed significantly reduced gene expression levels of IKKβ

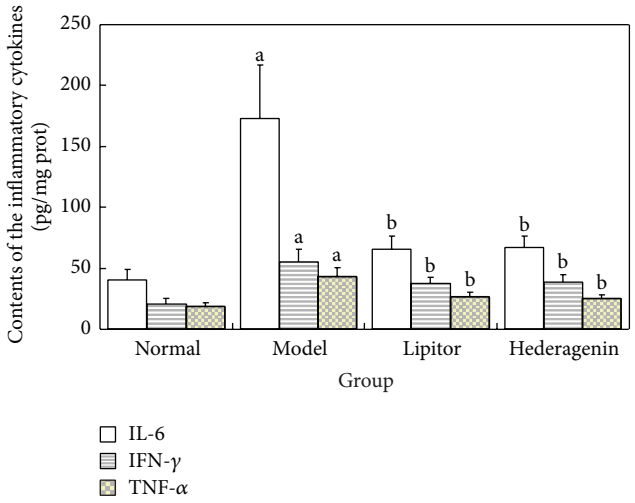

FIGURE 8: Contents of the inflammatory cytokines IL-6, IFN-γ, and TNF-α in the aorta. [a]$P < 0.01$ versus normal group; [b]$P < 0.01$ versus model group.

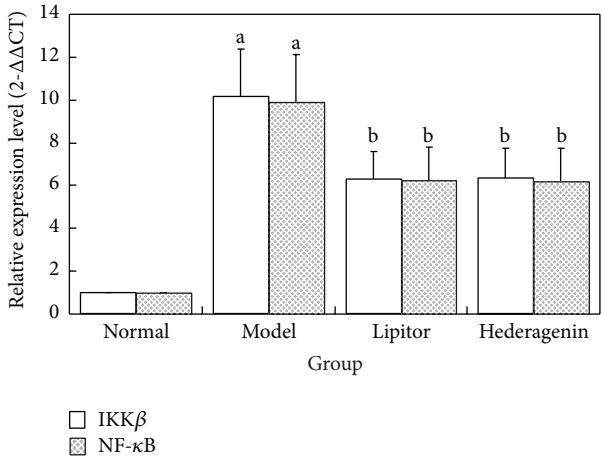

FIGURE 9: Relative expression level of IKKβ and NF-κB mRNA in the rat aorta. [a]$P < 0.01$ versus normal group; [b]$P < 0.01$ versus model group.

and NF-κB, and these differences were statistically significant ($P < 0.01$).

3.4.3. The Expression of Cytoplasmic IKKβ, p-IKKβ, and Nuclear NF-κBp65 Proteins in the Rat Aorta

Figures 10(a) and 10(b) Showed the Following. ① Compared with the normal control group, the model group animals exhibited increased protein content of IKKβ, p-IKKβ, and NF-κB, and these differences were statistically significant ($P < 0.01$). ② Compared with the model group, the Lipitor group and the hederagenin group showed significantly reduced protein content of IKKβ, p-IKKβ, and NF-κB, and these differences were statistically significant ($P < 0.01$).

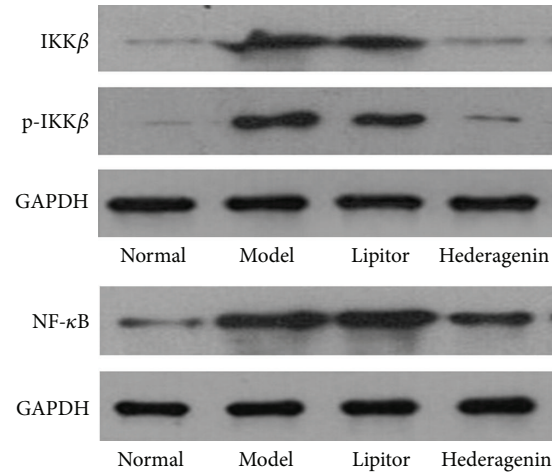

(a)

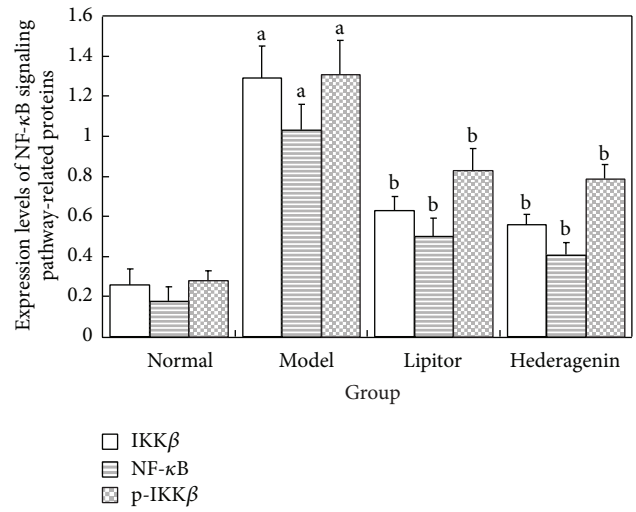

(b)

FIGURE 10: The expression levels of NF-κB signaling pathway-related proteins. [a]$P < 0.01$ versus normal group; [b]$P < 0.01$ versus model group.

4. Discussion

Atherosclerosis (AS) is a complicated pathological process resulting from interactions between various pathways and factors. The theory of AS pathogenesis primarily involves thrombosis theory, lipid filtration theory, endothelial dysfunction theory, oxidation stress theory, and inflammatory response theory. These theories correspondingly explain different aspects of the pathogenesis and progression of atherosclerosis. An increasing number of studies have shown that atherosclerosis is an inflammatory disease, and the inflammatory response is present throughout the process of the pathogenesis and progression of AS. During the early stage of atherosclerosis, when unstable plaques break, there are continuous activation and amplification of inflammation. Therefore, the early identification of unstable AS plaques, detecting sensitive and specific serological markers of these plaques and associated inflammation targets, in addition to

reducing and blocking atherosclerosis and other vascular events through early anti-inflammation treatment, represent current research hot spots that will continue to direct future research.

Hyperlipidemia and hemorheological abnormalities usually occur at the same time and promote each other's occurrence. Epidemiological studies have shown that, as an initiation factor of atherosclerosis, hyperlipidemia, accompanied by hemorheological abnormalities, is generally a risk factor for atherosclerosis. Studies have demonstrated that an increase of serum cholesterol levels is positively correlated with the occurrence of AS and can lead to abnormal plasma lipoproteins, thereby inducing artery wall lesions. Lipoproteins are the major form of lipids that exists in human plasma. Low density lipoprotein (LDL) plays an important role in the pathogenesis of atherosclerosis and is considered the major risk factor for atherosclerosis. Drug intervention experiments confirmed that lowering LDL levels can significantly reduce the risk of the occurrence of cardiovascular diseases for hypercholesterolemia patients and can also benefit patients with a normal level of LDL [19]. Studies have shown that one risk factor that causes AS is an overly low level of high density lipoprotein (HDL). HDL can carry out reverse transport of cholesterol to the liver for processing to lower body cholesterol levels, and HDL therefore exhibits an anti-AS function [20, 21]. Studies have shown that every stage of atherosclerosis is accompanied by endothelial dysfunction, and the occurrence of many coronary events is closely related to coronary artery endothelial dysfunction. Endothelial dysfunction is an early event in the occurrence of atherosclerosis, and all of the risk factors that cause atherosclerosis can also cause coronary artery endothelial dysfunction. Damage to the endothelium not only is the initiating step in the occurrence of AS but also serves as a clinical sign of AS disease, which plays an independent role in predicting the prognosis of AS [22–29].

AS is an inflammatory disease, and the inflammatory response is observed throughout the process of the occurrence and progression of AS [30, 31]. Studies have shown that the IKK/IκB/NF-κB signaling pathway plays a key role in the occurrence of AS. Throughout the course of AS, NF-κB is involved in multiple signaling pathways in the inflammatory process. The body's inflammatory response is not separable from the participation of various molecules [32], including IL-6, IL-8, IFN-γ, TNF-α, intercellular adhesion molecule-1 (ICAM-1), and vascular cell adhesion molecule-1 (VCAM-1), and a prerequisite for the activation of these molecules is activation of NF-κB. In other words, a prerequisite for the inflammatory response is the activation of NF-κB, and the inflammatory response is a prerequisite for AS occurrence [33–36]. As an important cytokine in the progression of AS, IL-6 was recently found to be positively correlated with atherosclerosis. The development of AS lesions is a slow and complicated process related to the inflammatory response. IL-6 represents the origin of the inflammatory response cascade, playing an extremely significant mediating function [37, 38]. IFN-γ is a cytokine that was recently found to be positively correlated with atherosclerosis. IFN-γ acts on multiple types of cells in AS plaques, regulating the expression of cytokines and cytokine receptors in these cells as well as the proliferation and apoptosis of the cells to promote the formation of AS plaques. Studies have shown that IFN-γ is a pro-AS cytokine. Macrophages and smooth muscle cells, which are found in AS plaques, show lipid accumulation and express the IFN-γ receptor [39–42]. Therefore, NF-κB activation leads to overexpression of inflammation-related factors, resulting in the inflammatory response [43]. Meanwhile, the increased production and release of inflammatory mediators and cytokines further activate NF-κB, resulting in continuous amplification of the initial inflammation signal and even loss of control of the inflammation response, eventually leading to AS.

Thus, in the present study, we explored and evaluated the antiatherosclerosis function of hederagenin by establishing a Wistar rat AS model, and we analyzed the antiatherosclerosis mechanism of hederagenin from the perspective of lipid metabolism disorders, liver function, blood rheology, endothelial function, and inflammation signaling pathways. Studies have shown that, in AS rat models induced by a high-lipid diet plus VD_3, hederagenin can effectively reduce serum lipid, ALT, and AST levels, in addition to improving liver function, relieving high blood coagulation, and slowing blood flow and stasis by improving blood rheology. Hederagenin can correct the imbalance of endothelial function by inhibiting the release of large amounts of iNOS and increasing eNOS contents. Hederagenin also inhibits the IKKβ/NF-κB signaling pathway to reduce the release of IL-6, IFN-γ, TNF-α, and other inflammatory factors.

5. Conclusion

In conclusion, the experimental results showed that hederagenin can inhibit or ameliorate the pathological changes associated with AS, displaying an excellent preventive function against AS. The mechanism of hederagenin action may be related to the regulation of lipid metabolism disorders, protection of liver function, improvement of blood rheology, regulation of endothelial dysfunction, and inhibition of the IKKβ/NF-κB signaling pathway, thereby reducing the amplification cascade of the inflammatory response, to reduce the release of IL-6, IFN-γ, TNF-α, and other inflammatory factors. Further study is needed to find out whether there are some other signal transduction pathways involved in the course.

Conflict of Interests

All of the authors of this paper declare that they have no direct financial relation with the commercial identities mentioned in this paper. And all of the authors declare that they have no competing interests.

Acknowledgment

The present work was supported by a grant (no. 81173189) from Natural Science Foundation of China.

References

[1] X. Li, C. J. Li, and H. Y. Tan, "Atorvastatin calcium induced liver damage," *Chinese Journal of Misdiagnosis*, vol. 11, no. 34, p. 8461, 2011.

[2] F. F. Sun, X. Q. Tan, and L. J. Guo, "Atorvastatin calcium induced abnormal liver function," *Journal of Pharmacoepidemiology*, vol. 20, no. 5, article 267, 2011.

[3] G. Li, "Atorvastatin calcium induced abnormal liver function," *Adverse Drug Reactions Journal*, vol. 9, no. 3, p. 181, 2007.

[4] B. F. Liang, H. B. Guo, and X. Yuan, "Evaluation of hederagenin antidepressant efficacy," *Chinese Journal of Pharmacology and Toxicology*, vol. 26, no. 3, pp. 447–448, 2012.

[5] J. Wang, X. Z. Zhao, Q. Qi et al., "Macranthoside B, a hederagenin saponin extracted from Lonicera macranthoides and its anti-tumor activities in vitro and in vivo," *Food and Chemical Toxicology*, vol. 47, no. 7, pp. 1716–1721, 2009.

[6] J. Yamahara, Y. Takagi, T. Sawada et al., "Effects of crude drugs on congestive edema," *Chemical and Pharmaceutical Bulletin*, vol. 27, no. 6, pp. 1464–1468, 1979.

[7] H.-M. Ma and B.-L. Zhang, "Comparison among families of Mutong," *China Journal of Chinese Materia Medica*, vol. 27, no. 6, pp. 412–418, 2002.

[8] I. Gülçin, V. Mshvildadze, A. Gepdiremen, and R. Elias, "The antioxidant activity of a triterpenoid glycoside isolated from the berries of *Hedera colchica*: 3-*O*-(β-D-glucopyranosyl)-hederagenin," *Phytotherapy Research*, vol. 20, no. 2, pp. 130–134, 2006.

[9] D. Jiang, Q. P. Gao, S. P. Shi, and P. F. Tu, "Triterpenoid saponins from the fruits of Akebiae quinata," *Chemical and Pharmaceutical Bulletin*, vol. 54, no. 5, pp. 595–597, 2006.

[10] M. W. Lee, S. U. Kim, and D.-R. Hahn, "Antifungal activity of modified hederagenin glycosides from the leaves of Kalopanax pictum var. chinense," *Biological and Pharmaceutical Bulletin*, vol. 24, no. 6, pp. 718–719, 2001.

[11] J. Choi, Y. N. Han, K.-T. Lee et al., "Anti-lipid peroxidative principles from the stem bark of Kalopanax pictus Nakai," *Archives of Pharmacal Research*, vol. 24, no. 6, pp. 536–540, 2001.

[12] L. J. Jing, Y. L. Yong, E. H. Jung, S. Lee, M. K. Jeong, and S. Y.-C. Hye, "Anti-platelet pentacyclic triterpenoids from leaves of *Campsis grandiflora*," *Archives of Pharmacal Research*, vol. 27, no. 4, pp. 376–380, 2004.

[13] Y. Quan and M.-Z. Qian, "Effect and mechanism of gypenosides on the inflammatory molecular expression in high-fat induced atherosclerosis rats," *Chinese Journal of Integrative Medicine*, vol. 30, no. 4, pp. 403–406, 2010.

[14] J. Pang, Q. Xu, X. Xu et al., "Hexarelin suppresses high lipid diet and vitamin D3-induced atherosclerosis in the rat," *Peptides*, vol. 31, no. 4, pp. 630–638, 2010.

[15] X. L. Yang, X. X. Zhao, F. Wang et al., "A new modeling of atherosclerostic in rats," *Journal of Ningxia Medical College*, vol. 29, no. 4, pp. 879–882, 2007.

[16] P. Y. Yang, Y. C. Rui, and Y. B. Jiao, "Establishment of experimental atherosclerosis model in rats," *Academic Journal of Second Military Medical University*, vol. 24, no. 7, pp. 802–804, 2003.

[17] S. Y. Xu, R. L. Bian, and X. Chen, *Methodology of Pharmacological Experiment*, People's Medical Publishing House, Beijing, China, 3rd edition, 2002.

[18] H. Zhou, X. X. Wu, Y. B. Yuan et al., "Comparison of methods for establishing a rat model of atherosclerosis using three-doses of vitamin D3 and atherogenic diet," *Chinese Journal of Arteriosclerosis*, vol. 20, no. 11, pp. 995–998, 2012.

[19] H. Motoshima, B. J. Goldstein, M. Igata, and E. Araki, "AMPK and cell proliferation-AMPK as a therapeutic target for atherosclerosis and cancer," *Journal of Physiology*, vol. 574, no. 1, pp. 63–71, 2006.

[20] P. P. Toth, "High-density lipoprotein as a therapeutic target: clinical evidence and treatment strategies," *The American Journal of Cardiology*, vol. 96, no. 9, supplement 1, pp. 50–58, 2005.

[21] G. C. Fonarow, "Treating to goal: new strategies for initiating and optimizing lipid-lowering therapy in patients with atherosclerosis," *Vascular Medicine*, vol. 7, no. 3, pp. 187–194, 2002.

[22] J. Sun, "NO pathway and atherosclerosis," *Journal of Chengdu Medical College*, vol. 2, no. 1, p. 71, 2007.

[23] J. W. Li, "Research progress of vascular endothelial contraction and relaxation factor," *Chinese Journal of Extracorporeal Circulation*, vol. 2, no. 1, p. 61, 2004.

[24] J. Li and F. Y. Liu, "The change of vasomotor function in atherosclerosis," *Chinese Journal of Cardiovascular Rehabilitation Medicine*, vol. 18, no. 5, p. 501, 2009.

[25] K. Mujynya-Ludunge, H. Viswambharan, R. Driscoll et al., "Endothelial nitric oxide synthase gene transfer restores endothelium-dependent relaxations and attenuates lesion formation in carotid arteries in apolipoprotein E-deficient mice," *Basic Research in Cardiology*, vol. 100, no. 2, pp. 102–111, 2005.

[26] E. Gkaliagkousi and A. Ferro, "Nitric oxide signalling in the regulation of cardiovascular and platelet function," *Frontiers in Bioscience*, vol. 16, no. 5, pp. 1873–1897, 2011.

[27] V. Zancan, S. Santagati, C. Bolego, E. Vegeto, A. Maggi, and L. Puglisi, "17β-estradiol decreases nitric oxide synthase II synthesis in vascular smooth muscle cells," *Endocrinology*, vol. 140, no. 5, pp. 2004–2009, 1999.

[28] W. Y. Z. Di and Y. Y. Yan, "Effects of Rou Tong Decoction on plasma ET-1 and serum NO content in experimental atherosclerosis rabbits," *Modern Traditional Chinese Medicine*, vol. 25, no. 6, article 12, 2005.

[29] S. L. Bourque, S. T. Davidge, and M. A. Adams, "The interaction between endothelin-1 and nitric oxide in the vasculature: new perspectives," *The American Journal of Physiology—Regulatory, Integrative and Comparative Physiology*, vol. 300, no. 6, pp. R1288–R1295, 2011.

[30] R. Ross, "Atherosclerosis—an inflammatory disease," *The New England Journal of Medicine*, vol. 340, no. 2, pp. 115–126, 1999.

[31] P. Libby, "Inflammation in atherosclerosis," *Nature*, vol. 420, no. 6917, pp. 868–874, 2002.

[32] H. X. Xu, J. J. Li, and G. S. Li, "Nuclear factor kappa B and atherosclerosis," *Chinese Journal of Arteriosclerosis*, vol. 9, no. 2, pp. 179–181, 2001.

[33] J. Mestas and K. Ley, "Monocyte-endothelial cell interactions in the development of atherosclerosis," *Trends in Cardiovascular Medicine*, vol. 18, no. 6, pp. 228–232, 2008.

[34] B. C. H. Lutters, M. A. Leeuwenburgh, C. C. M. Appeldoorn, T. J. M. Molenaar, T. J. C. van Berkel, and E. A. L. Biessen, "Blocking endothelial adhesion molecules: a potential therapeutic strategy to combat atherogenesis," *Current Opinion in Lipidology*, vol. 15, no. 5, pp. 545–552, 2004.

[35] V. Benson, A. C. McMahon, and H. C. Lowe, "ICAM-1 in acute myocardial infarction: a potential therapeutic target," *Current Molecular Medicine*, vol. 7, no. 2, pp. 219–227, 2007.

[36] S.-R. Kim, Y.-H. Bae, S.-K. Bae et al., "Visfatin enhances ICAM-1 and VCAM-1 expression through ROS-dependent NF-κB activation in endothelial cells," *Biochimica et Biophysica Acta: Molecular Cell Research*, vol. 1783, no. 5, pp. 886–895, 2008.

[37] A. R. Brasier, "The nuclear factor-B-interleukin-6 signalling pathway mediating vascular inflammation," *Cardiovascular Research*, vol. 86, no. 2, pp. 211–218, 2010.

[38] N. Li and M. Karin, "Ionizing radiation and short wavelength UV activate NF-κB through two distinct mechanisms," *Proceedings of the National Academy of Sciences of the United States of America*, vol. 95, no. 22, pp. 13012–13017, 1998.

[39] A. H. Wagner, M. Gebauer, B. Pollok-Kopp, and M. Hecker, "Cytokine-inducible CD40 expression in human endothelial cells is mediated by interferon regulatory factor-1," *Blood*, vol. 99, no. 2, pp. 520–525, 2002.

[40] E. Gallmeier, C. Schäfer, P. Moubarak et al., "JAK and STAT proteins are expressed and activated by IFN-γ in rat pancreatic acinar cells," *Journal of Cellular Physiology*, vol. 203, no. 1, pp. 209–216, 2005.

[41] S. Agrawal, M. Febbraio, E. Podrez, M. K. Cathcart, G. R. Stark, and G. M. Chisolm, "Signal transducer and activator of transcription 1 is required for optimal foam cell formation and atherosclerotic lesion development," *Circulation*, vol. 115, no. 23, pp. 2939–2947, 2007.

[42] M. Horiuchi, W. Hayashida, M. Akishita et al., "Interferon-γ induces AT_2 receptor expression in fibroblasts by Jak/STAT pathway and interferon regulatory factor-1," *Circulation Research*, vol. 86, no. 2, pp. 233–240, 2000.

[43] N. Li and M. Karin, "Ionizing radiation and short wavelength UV activate NF-κB through two distinct mechanisms," *Proceedings of the National Academy of Sciences of the United States of America*, vol. 95, no. 22, pp. 13012–13017, 1998.

Hindawi Publishing Corporation
Evidence-Based Complementary and Alternative Medicine
Volume 2015, Article ID 904273, 10 pages
http://dx.doi.org/10.1155/2015/904273

Research Article

Yiqihuoxuejiedu Formula Restrains Vascular Remodeling by Reducing the Inflammation Reaction and Cx43 Expression in the Adventitia after Balloon Injury

Hong Chang,[1] Huan Lei,[1] Yizhou Zhao,[1] Ruixue Yang,[1] Aiming Wu,[1] Yingqiu Mao,[2] Youliang Huang,[2] Xiying Lv,[1] Jiuli Zhao,[1] Lixia Lou,[1] Dongmei Zhang,[1] Yingkun He,[1] Ying Xu,[1] Tao Yang,[1] and Mingjing Zhao[1]

[1]*Key Laboratory of Chinese Internal Medicine of Ministry of Education and Dongzhimen Hospital, Beijing University of Chinese Medicine, Beijing 100700, China*
[2]*Beijing University of Chinese Medicine, Bei San Huan Dong Lu 11, Chao Yang District, Beijing 100029, China*

Correspondence should be addressed to Mingjing Zhao; mjgx2004@163.com

Received 6 May 2015; Revised 30 July 2015; Accepted 9 August 2015

Academic Editor: Dan Hu

Vascular remodeling is closely related to hypertension, atherosclerosis, and restenosis after PCI. Considerable evidence indicates that the activation and proliferation of adventitial fibroblasts play key roles in vessel injury. The inflammatory response and high expression of connexins contribute to adventitial remodeling. Therefore, reducing inflammation reaction and connexins expression in adventitia may become a new target to prevent vascular remodeling. Yiqihuoxuejiedu formula, composed of TCM therapeutic principle of supplementing qi, activating blood and detoxification, can inhibit restenosis after intimal injury. To further investigate the effect of Yiqihuoxuejiedu formula on inflammation and connexins, we established a carotid artery injury model. In model rats, hyperplasia in the intima was mild but obvious in the adventitia; CRP heightened; expressions of MCP-1, CD68, and Cx43 increased. Yiqihuoxuejiedu formula relieved intimal hyperplasia and adventitial area, obviously diminished the expressions of CD68 and Cx43 in the adventitia, and reduced CRP but did not lower MCP-1. These results indicated that Yiqihuoxuejiedu formula inhibited vascular remodeling especially adventitial hyperplasia by reducing the inflammation reaction including lowering macrophages infiltration and systemic nonspecific inflammatory response and also restraining gap junction connexins leading to less communication among cells. This study provides new ideas and methods for the prevention and treatment of vascular remodeling.

1. Introduction

Vascular remodeling is a structural and functional variation of vessels to adapt to the intracorporal environment. For a long time, vascular smooth muscle cells (VSMCs) in the media have been regarded as a central link and the adventitia has been known to play only supportive functions [1]. However, the adventitia is an essential regulator of vascular wall structure and function. Adventitial fibroblasts (AFs, the major component of the adventitia) are activated and transfer into myofibroblasts, proliferate, and migrate to media and intima to participate in the progression of vascular remodeling [2, 3].

In the initial stages of intimal balloon injury, one of the key triggers of vascular remodeling is early inflammation in the adventitia [4] including the infiltration of macrophages [5] and neutrophils [6] and the release of inflammatory factors, such as interleukin- (IL-) 1β, IL-6, IL-8, and MCP-1 [7, 8]. Research in patients also found that in-stent restenosis is related to macrophage infiltration [9]. Meanwhile myofibroblasts release various proinflammatory cytokines, for instance, MCP-1, recruiting macrophages and neutrophils to infiltrate into the adventitia [10, 11]. These inflammatory responses promote activation and proliferation of adventitial fibroblasts, resulting in adventitial remodeling.

Cellular interaction in blood vessels is maintained by multiple communication pathways, including gap junctions. Gap junctions (GJs) arise from the docking of two hemichannels or connexons, formed by the assembly of six connexins (Cxs), and achieve direct cellular communication by allowing the transport of small metabolites, second messengers, and ions between two adjacent cells [12]. Although Cx37, Cx40, and Cx43, respectively, are expressed in different layers of vessel wall, Cx43 is common in all the three layers [13–16]. Accumulating evidence supports the results that Cx43 has been deeply investigated in cardiovascular diseases. In atherosclerosis, Cx43 promoted leukocyte to adhere to endothelium and infiltrate into the media, which deteriorated atherosclerosis [17]. Further investigation showed that reduced Cx43 expression could inhibit atherosclerotic lesion formation in low-density lipoprotein receptor-deficient mice [18]. Meanwhile, upregulation of Cx43 promoted SMC phenotypic transformation and accelerated intimal hyperplasia, leading to vascular restenosis [19, 20]. In view of the function of Cx43, its expression and relationship with inflammation in the adventitia need to be illustrated.

In 2011 PCI guideline, treatment and prevention after PCI mainly include antihypertensive therapy including β-receptor blockers, angiotensin-converting enzyme inhibitors (ACEI), lipid-lowering therapy with statins, and antiplatelet/anticoagulant therapy with aspirin and clopidogrel [21]. Of these drugs, statins not only lower lipid concentration but also diminish inflammation and expression of GJ [22, 23]. Though western medicine has gained success, a number of potential risks remain, and we need to find new drugs to prevent vascular remodeling.

Myofibroblasts play pivotal role in the tissue repair and remodeling and are also a key player in pathological hypertrophic scars and organ fibrosis. The vascular remodeling after PCI is similar to local wound repair. Based on this idea, as well as the traditional Chinese medicine treatment of supplementing qi, activating blood plus detoxification, Yiqihuoxuejiedu formula was prescribed to prevent and treat vascular remodeling. The prescription is composed of astragalus, salvia, honeysuckle, and other components. Previous researches have shown that the prescription can reduce vessel stenosis, lower blood lipids [24], inhibit the activation and proliferation of the adventitial fibroblasts, and decrease collagen content and type I/III collagen ratio in the adventitia [25].

In this study, we used a vascular remodeling model of intimal injury with balloon injury and made Atorvastatin a positive control to explore the underlying mechanism of Yiqihuoxuejiedu's inhibition on adventitial inflammation and regulation of GJs at the early stages of injury (7 days). This study may provide a new approach to prevent vascular remodeling.

2. Materials and Methods

2.1. Animals. Male Sprague-Dawley (SD) rats weighing 380 to 420 g were purchased from Beijing Weitong Lihua Experimental Animal Technology Co., Ltd., Beijing, China (certificate number SCXK (Beijing) 2012-0001). Rats were raised in SPF room in Beijing University of Chinese Medicine. All the procedures were conformed to the National Institute of Health's Guide for the Use and Care of Laboratory Animals.

2.2. Establishment of Balloon Injury Model. One hour before anesthesia, a deep subcutaneous injection of heparin was given to each rat by 500 U/kg. Next, rats were anesthetized with 40 mg/kg sodium pentobarbital. As showed in the past study [25], a Fogarty 2 F balloon catheter (diameter of balloon 2 mm, length 20 mm, Medtronic Company, USA) was introduced through the left external carotid artery and advanced 4–4.5 cm into the thoracic aorta while the internal carotid artery was blocked. The balloon was inflated with normal saline at 0.5 atm to 0.7 atm to distend the artery. Then it was pulled back to the entry point. The entire procedure was repeated three times to denude the endothelium and cause vascular injury. After removing the catheter, the external carotid artery was ligated and the blood circulation of the internal carotid artery restored. In the sham group, only the external carotid artery was ligated. The above surgical operation was done in sterile condition.

2.3. Medications and Grouping. The Yiqihuoxuejiedu formula (Cat. Number 120603), composed of astragalus, salvia, honeysuckle, and other components, was produced by the Chinese Herbal Company of Beijing University of Chinese Medicine (Beijing, China) and the final concentration of crude drug was 1.2 g/mL.

Rats with balloon injury were randomly divided into three groups: the model group, the Atorvastatin group, and the Yiqihuoxuejiedu group. The sham group served as a control. Rats in the Atorvastatin group were orally administered with 13.33 mg/kg/d of Atorvastatin calcium (Pfizer), while they were administered with 12 g/kg in the Yiqihuoxuejiedu group and 10 mL/kg/d distilled water in the sham and model groups. Both doses for the two groups were based on the typical daily clinical dosages for adults, corresponding with 10 times of clinical dosages. Rats were administered once a day and seven days later, perfused with 4% paraformaldehyde through the left ventricle to fix specimen and make paraffin sections.

2.4. Histomorphometric Analysis. Carotid artery sections (5 μm) were stained with hematoxylin-eosin. Next, the sections were examined with a microscope (magnification ×100) and photographed for morphological analysis. Image analysis software (Image-Pro Plus 6.0) was used to analyze the following morphological indicators: lumen radius (lumen perimeter/2π), neointimal thickness (internal elastic membrane perimeter/2π − lumen perimeter/2π), and adventitial area (total area of vessel − area circled by external elastic membrane).

2.5. Radioimmunoassay Measurement and Analysis of CRP. For radioimmunoassay of CRP, a nonequilibrium method was used. The corresponding antibody was used to the standard and sample solutions, mixed well, and placed at 4°C

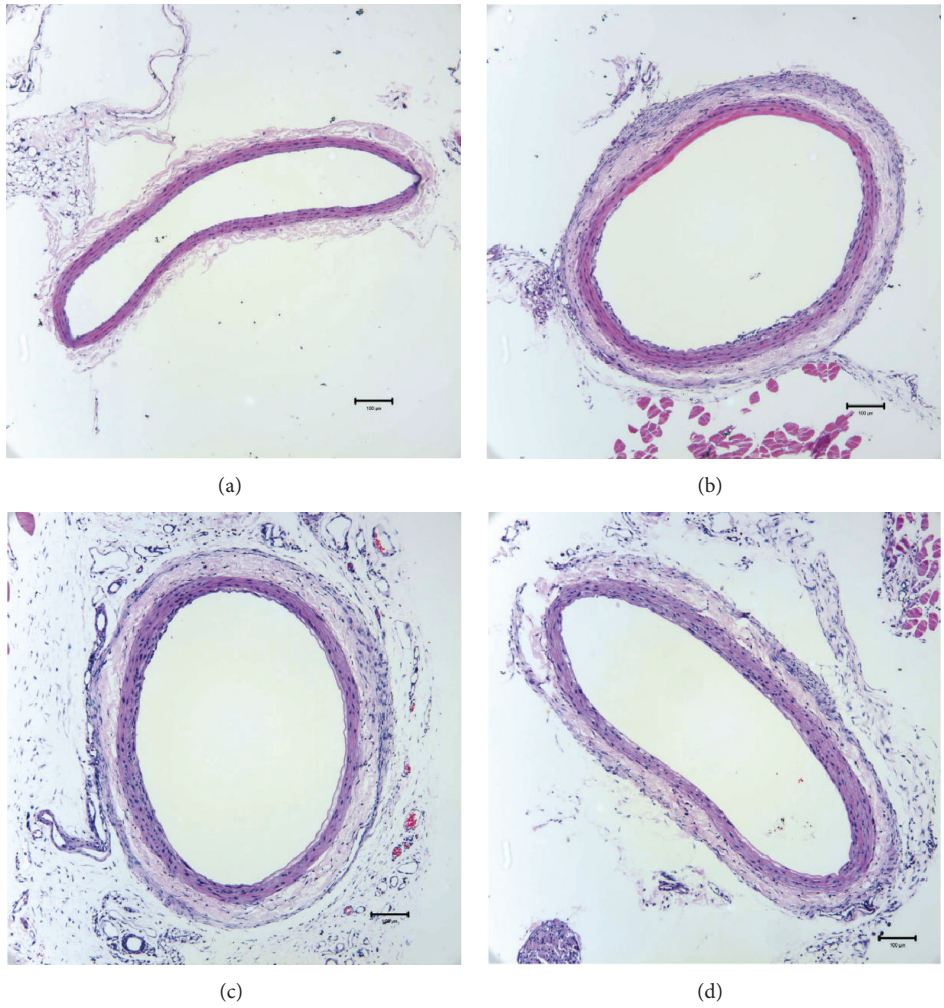

FIGURE 1: Left common carotid artery slices with HE 7 days after injury. (a) Sham group, (b) model group, (c) Atorvastatin group, and (d) Yiqihuoxuejiedu group.

for 24 h. Next, 125I-VIP (125I-SP, 125I-SS, Beijing Huaying Biotechnology Institute) was added, mixed well, and placed at 4°C for another 24 h. After that, appropriate secondary antibody was added, mixed thoroughly, and placed at room temperature for 20 min. Then samples were centrifuged 3500 r for 20 min, and the supernatants were discarded. The radionuclide blink count of precipitation was tested and converted to mg/L according to the standard curve.

2.6. Immunohistochemistry Measurement and Analysis of MCP-1, CD68, and Cx43. Different antibodies were used to detect the expressions of MCP-1, CD68, and Cx43 in the vascular wall. All samples were repaired in a microwave and incubated in 0.3% hydrogen peroxide before using primary antibodies (MCP-1, Abcam, UK; CD68 and Cx43, Santa Cruz Biotechnology, USA) and secondary antibody-HRP multimer (Zhongshan Golden Bridge Biotechnology Company, China). Samples were then visualized with diaminobenzidine substrate. The positive expressions of CD68, Cx43, and MCP-1 appeared as brownish-yellow or a brown granulation in the cytoplasm. The typical images were captured with SPOT V3.0II software, and the average optical density or the positive area was measured and analyzed by image-Pro Plus 6.0.

2.7. Statistical Analysis. Mean differences among groups were statistically analyzed using one-way analysis of variance (ANOVA) and between two groups by a TSD test. The level of statistical significance was considered to be $P < 0.05$.

3. Results

3.1. Lumen Radius and Changes of Neointimal Thickness. Seven days after balloon injury, there was small reduction of lumen radius in the model group but had no significant difference compared with the sham group, neither in Atorvastatin nor in Yiqihuoxuejiedu groups. Intimal hyperplasia appeared obviously in the model group compared to the sham group ($P < 0.01$). Compared with the model group, the Yiqihuoxuejiedu formula could reduce neointimal thickness ($P < 0.01$, Figures 1 and 2).

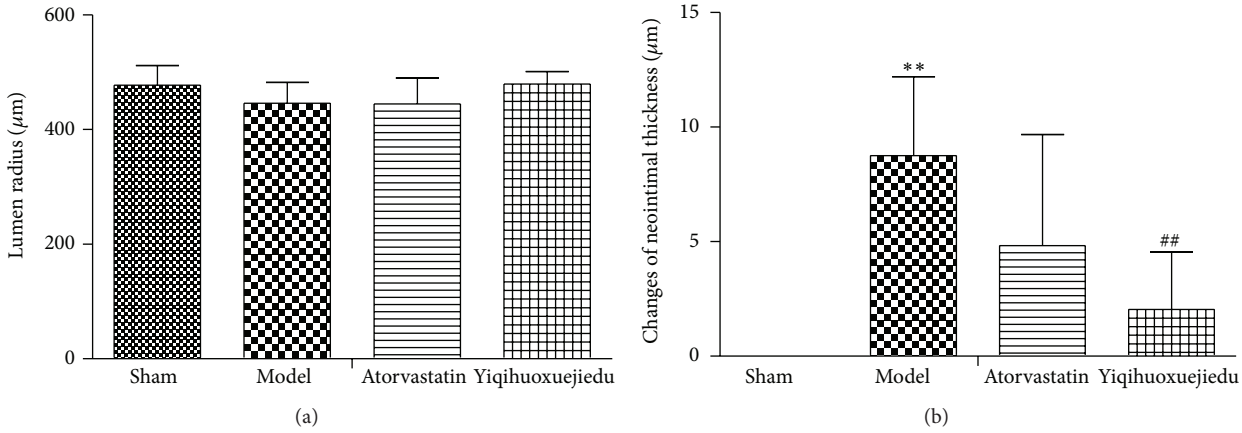

Figure 2: Lumen radius and changes of neointimal thickness 7 days after balloon injury. (a) Lumen radius. (b) Changes of neointimal thickness. **Compared with sham group, $P < 0.01$. ##Compared with model group, $P < 0.01$.

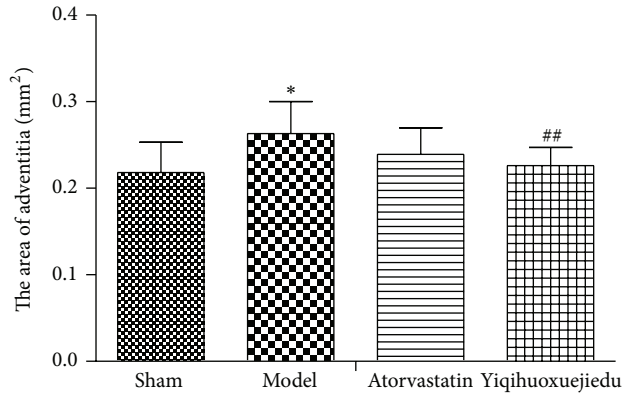

Figure 3: The area of adventitia 7 days after balloon injury. *Compared with sham group, $P < 0.05$. ##Compared with model group, $P < 0.01$.

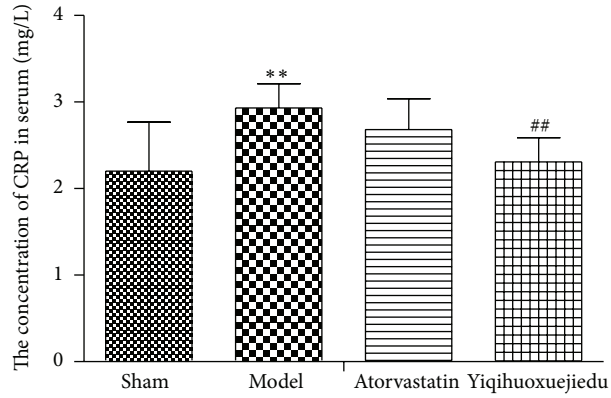

Figure 4: The concentration of CRP in serum. **Compared with sham group, $P < 0.01$. ##Compared with model group, $P < 0.01$.

3.2. The Area of the Adventitia. There was a significant increase in the area of the adventitia in model group ($P < 0.05$). Compared with the model group, the area of the adventitia in the Yiqihuoxuejiedu group was decreased ($P < 0.01$, Figures 1 and 3).

3.3. The Concentration of CRP in Serum. At the early period of injury, CRP increased markedly in the serum, especially in the model group ($P < 0.01$). The Yiqihuoxuejiedu formula decreased CRP ($P < 0.01$), while Atorvastatin only had a trend in reducing CRP (Figure 4).

3.4. The Expression of MCP-1 in Vascular Wall. Immunohistochemistry showed that the expression of MCP-1 in the three layers of vascular wall increased after balloon injury, especially in the adventitia of the model group. The average optical density (OD) in the treatment groups was all decreased; the adventitial positive expression in the Atorvastatin group had an apparent reduction compared with the model group ($P < 0.01$, Figure 5).

3.5. The Expression of CD68 in Vascular Wall. Compared with the sham group, CD68 expression of media and adventitia in the model group had a significant increase ($P < 0.05$ for media, $P < 0.01$ for adventitia). The Yiqihuoxuejiedu formula inhibited positive expression of CD68 in the adventitia ($P < 0.01$), and it had a stronger effect than Atorvastatin ($P < 0.05$, Figure 6).

3.6. The Expression of Cx43 in Vascular Wall. There were no significant changes in the average OD in the vascular wall when determining Cx43 expression. However, the positive areas of Cx43 in surgery groups were increased, and there was significant difference between the model group and the sham group ($P < 0.05$). Compared with model group, the positive area of Cx43 in adventitia significantly decreased in the Yiqihuoxuejiedu group ($P < 0.05$). We observed the same trend in the media but without any significant differences (Figure 7).

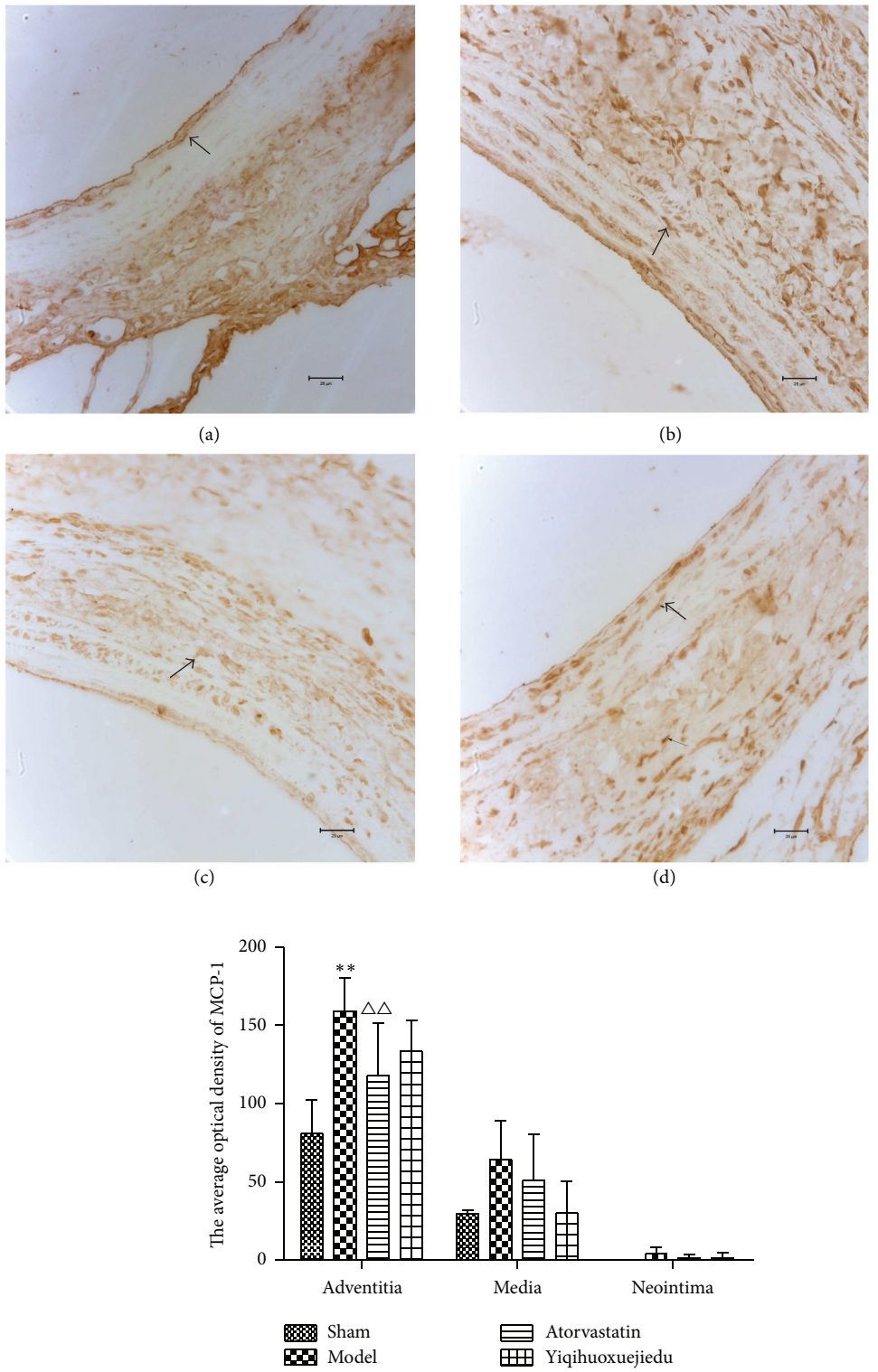

Figure 5: The expression of MCP-1 in vascular wall. (a) Sham group, (b) model group, (c) Atorvastatin group, and (d) Yiqihuoxuejiedu group. **Compared with sham group, $P < 0.01$. $^{\#\#}$Compared with model group, $P < 0.01$.

4. Discussion

PCI can lead to two types of vascular remodeling, positive remodeling and negative remodeling [26]. Positive remodeling means that the vessels provide compensatory dilation, and the lumen diameter does not change significantly, while negative remodeling means that vessels shrink, and the lumen diameter narrows. In the early remodeling, adventitial fibroblasts play principal roles, although VSMCs also contribute to the pathological change. In this

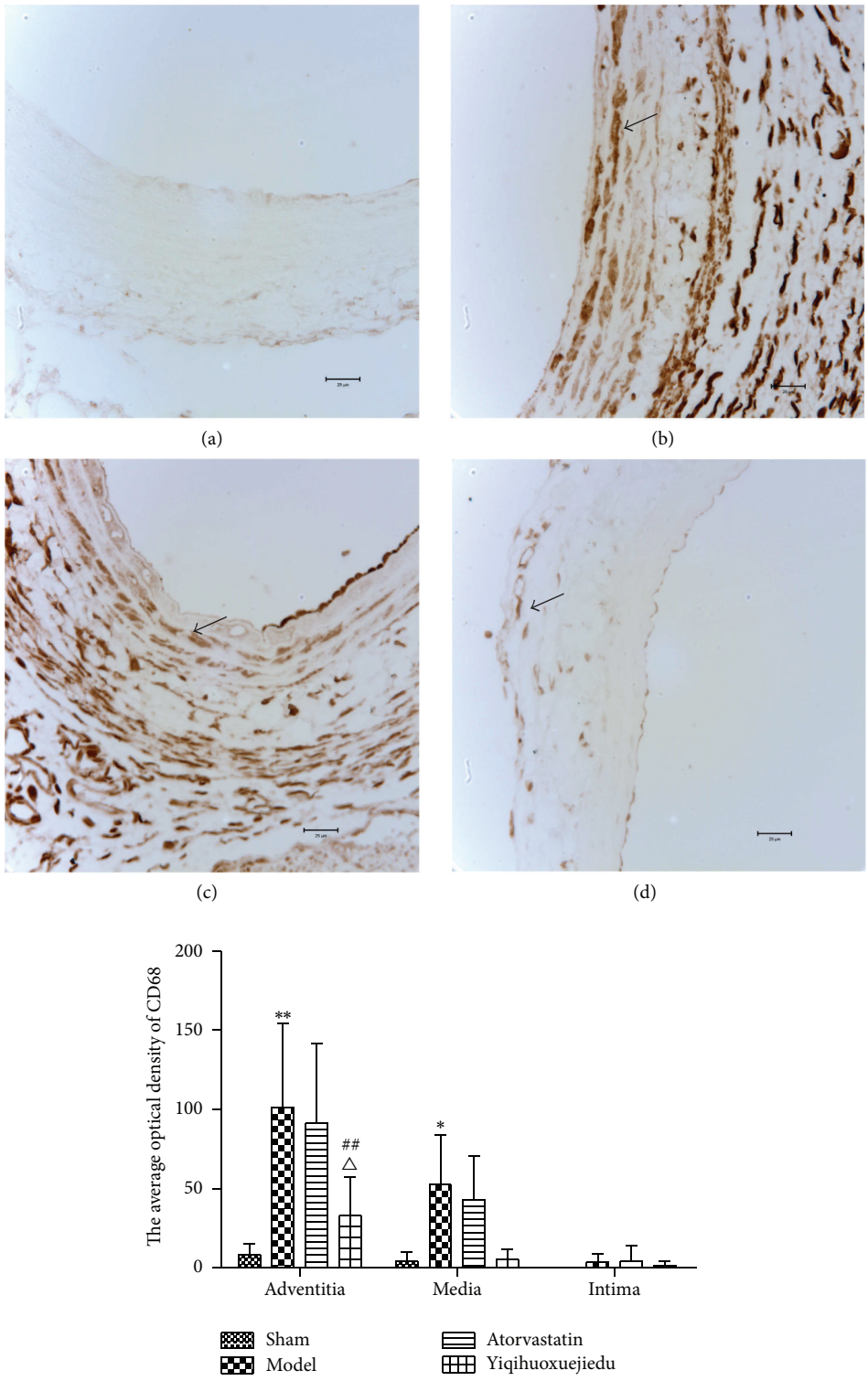

Figure 6: The expression of CD68 in vascular wall. (a) Sham group, (b) model group, (c) Atorvastatin group, and (d) Yiqihuoxuejiedu group. **Compared with sham group, $P < 0.01$. $^{\#\#}$Compared with model group, $P < 0.01$. $^{\triangle}$Compared with Atorvastatin group, $P < 0.05$.

study, neointimal thickness slowly increased and lumen showed no stenosis, but the adventitial area rapidly grew in model animals. Thus, positive remodeling dominated vascular remodeling at the early phase of intimal injury. The Yiqihuoxuejiedu formula could inhibit neointimal thickness and reduce the adventitial area. Our previous study demonstrated that α-SMA expression of the adventitia increased in model group at 7 days after balloon injury, which indicated

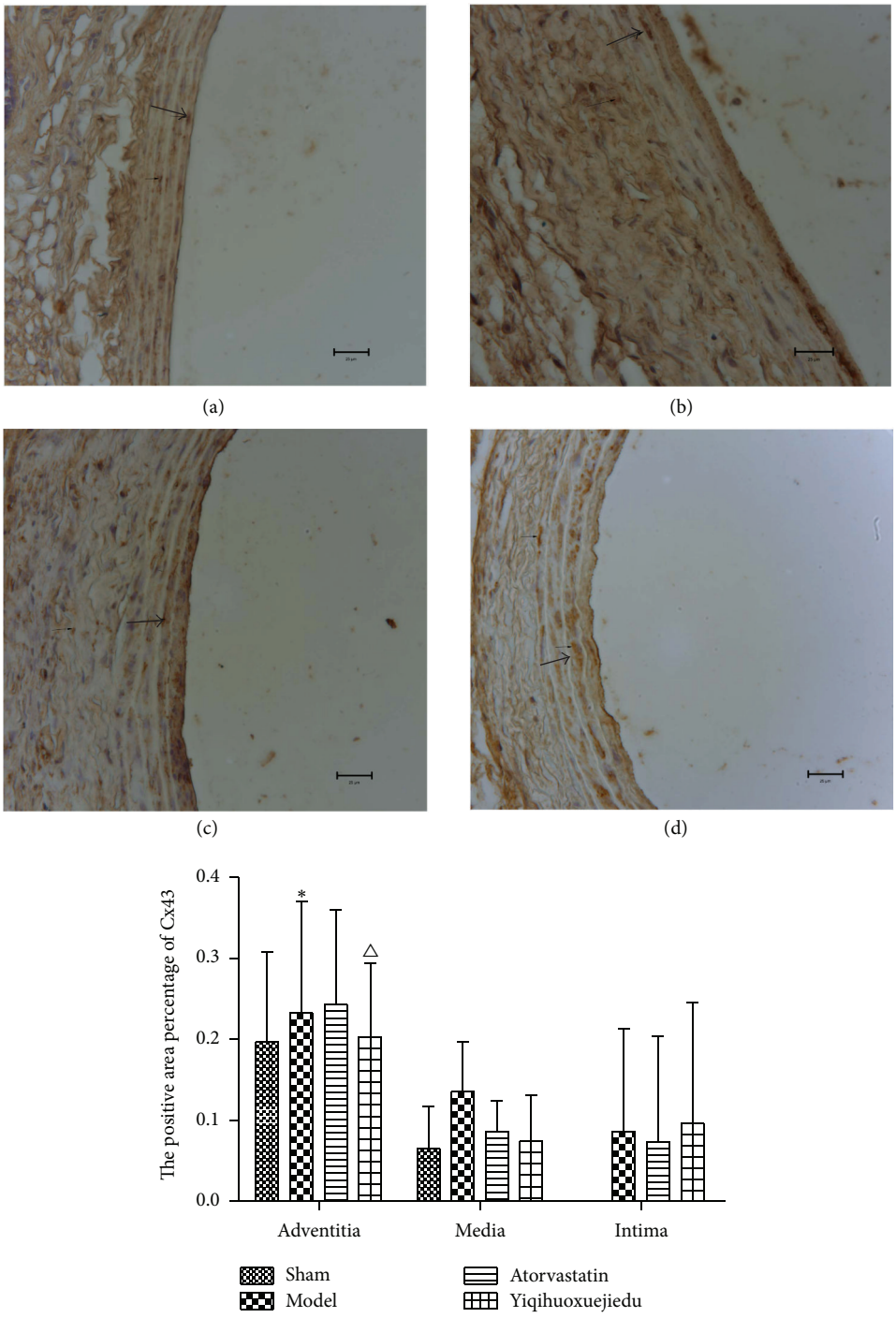

Figure 7: The expression of Cx43 in vascular wall. (a) Sham group, (b) model group, (c) Atorvastatin group, and (d) Yiqihuoxuejiedu group. *Compared with sham group, $P < 0.05$. #Compared with model group, $P < 0.05$.

activation and proliferation of the adventitial fibroblasts [25].

C-reactive protein (CRP) not only serves as one of the most widely known biomarkers of cardiovascular disease and underlying inflammation but also promotes activation of endothelial cells and monocytes, leading to vascular remodeling [27, 28]. The concentration of CRP increases when inflammation occurs in the adventitia [8]. In our study, CRP increased highly in serum, particularly in the model group ($P < 0.01$), while the Yiqihuoxuejiedu formula could diminish CRP ($P < 0.01$).

Lesion of the intima can lead to an early inflammatory response, including infiltration of macrophages and neutrophils and the release of inflammatory factors, especially

in the adventitia [29]. MCP-1 is secreted by monocytes-macrophages and adventitial fibroblasts [30, 31], and it can stimulate VSMCs to proliferate and migrate [32, 33] and promote monocytes to gather in the adventitia, leading to AFs proliferation and adventitial thickness [7]. In our study, MCP-1 expression increased in all the three layers of the vessel wall and markedly increased in the adventitia ($P < 0.01$). The concentration of MCP-1 was higher in the adventitia than in the media and neointima, indicating severe adventitial inflammation after vascular injury. The positive medicine, Atorvastatin, significantly reduced MCP-1 expression to restore the body's balance between proinflammatory and anti-inflammatory responses [34], but the Yiqihuoxuejiedu formula had no effect on MCP-1.

Thirty minutes after intimal injury, the inflammatory cells can be detected in the adventitia, with earlier time and higher concentration than in the media [6]. Macrophages can release cytokines and promote neointimal hyperplasia [35–37]. CD68 is a special marker of macrophages. Our study showed that macrophages infiltrated into the media and adventitia, particularly in the latter. The Yiqihuoxuejiedu formula limited the infiltration of macrophages dramatically, and its effect was better than that of Atorvastatin ($P < 0.05$), while Atorvastatin failed to do this.

GJs are important channels for exchanging matter, energy, and information between cells. They are closely associated with vascular function. Connexins (Cxs) are the main components of GJs, and Cx43 is expressed mostly in the vascular wall [16, 38]. Previous studies have indicated that Cx43 in vessel wall increased after PCI and played a promoting role in vascular remodeling by encouraging VSMCs to proliferate and be activated together, leading to inflammation in injured vessels [39–41]. One of the drug targets is to reduce the level of Cxs and communication among cells to prevent and treat remodeling. The present study showed that Cx43 expression increased in the vessel wall, especially in the adventitia, and cell communication strengthened, leading to cell proliferation and inflammation. Yiqihuoxuejiedu formula significantly reduced Cx43 ($P < 0.05$). Atorvastatin downregulated Cx43, but the change was not significant. Other studies found different results with Atorvastatin, mostly showing that the drug caused limited Cx43 expression in VSMCs to achieve an antiproliferative role [23]. Different drug doses may account for the different results. We used 10 times the clinical dose in our study, but other studies used higher doses [42, 43]. Thus, it is unclear whether stains have an effective role in GJs under clinical doses.

Yiqihuoxuejiedu formula is composed of astragalus, salvia, honeysuckle, and other components based on Chinese medicine principle of strengthening qi, activating the blood plus detoxication. Our previous studies have demonstrated that this formula reduced levels of lipids and TGF-β [24], limited neointimal hyperplasia, and diminished the collagen deposition in neointimal formation [44]. Astragalus, salvia, and tetramethylpyrazine, the main ingredients, play effective roles in anti-inflammation, downregulating MCP-1 and inhibiting SMC proliferation and migration [45–50]. All of these targets are the vital pharmacological bases for the Yiqihuoxuejiedu formula to inhibit neointimal formation and reduce macrophages infiltration and Cx43 expression in present study.

5. Conclusion

In summary, the injured vessel presents positive remodeling with slight neointimal hyperplasia and remarkable adventitial remodeling, and it also elicits inflammatory reactions with high expressions of MCP-1, CD68, and Cx43, particularly in the adventitia at the early phase of intimal injury. Yiqihuoxuejiedu formula restrained expression of CD68 and Cx43 remarkably in the adventitia and reduced the concentration of CRP and diminished intimal hyperplasia and area of the adventitia. These results indicated that this formula could inhibit vascular remodeling by limiting macrophages infiltration in the adventitia, depressing systemic nonspecific inflammatory response and AFs proliferation, and reducing GJs between cells. This study provides new ideas and methods for the prevention and treatment of vascular remodeling.

Conflict of Interests

The authors declare that they have no conflict of interests.

Authors' Contribution

Hong Chang, Huan Lei, Yizhou Zhao, and Ruixue Yang contributed equally to this study.

Acknowledgment

This paper was supported by the National Natural Science Foundation Project of China (no. 81173234).

References

[1] J. B. Koenig and I. Z. Jaffe, "Direct role for smooth muscle cell mineralocorticoid receptors in vascular remodeling: novel mechanisms and clinical implications," *Current Hypertension Reports*, vol. 16, no. 5, article 427, 2014.

[2] B. Yang, R. Janardhanan, P. Vohra et al., "Adventitial transduction of lentivirus-shRNA-VEGF-A in arteriovenous fistula reduces venous stenosis formation," *Kidney International*, vol. 85, no. 2, pp. 289–306, 2014.

[3] K. R. Stenmark, M. E. Yeager, K. C. El Kasmi et al., "The adventitia: essential regulator of vascular wall structure and function," *Annual Review of Physiology*, vol. 75, pp. 23–47, 2013.

[4] A. Fedorov, A. Kostareva, J. Raud, J. Roy, U. Hedin, and A. Razuvaev, "Early changes of gene expression profiles in the rat model of arterial injury," *Journal of Vascular and Interventional Radiology*, vol. 25, no. 5, pp. 789.e7–796.e7, 2014.

[5] W. Lan, F. Yang, Z. Li et al., "Human urine kininogenase attenuates balloon-induced intimal hyperplasia in rabbit carotid artery through transforming growth factor β1/Smad2/3 signaling pathway," *Journal of Vascular Surgery*, 2015.

[6] E.-I. Okamoto, T. Couse, H. De Leon et al., "Perivascular inflammation after balloon angioplasty of porcine coronary arteries," *Circulation*, vol. 104, no. 18, pp. 2228–2235, 2001.

[7] B. C. Tieu, X. Ju, C. Lee et al., "Aortic adventitial fibroblasts participate in angiotensin-induced vascular wall inflammation and remodeling," *Journal of Vascular Research*, vol. 48, no. 3, pp. 261–272, 2011.

[8] P. Liu, C. Zhang, Y. X. Zhao et al., "Gax gene transfer inhibits vascular remodeling induced by adventitial inflammation in rabbits," *Atherosclerosis*, vol. 212, no. 2, pp. 398–405, 2010.

[9] M. Zhang, N. Cresswell, F. Tavora, E. Mont, Z. Zhao, and A. Burke, "In-stent restenosis is associated with neointimal angiogenesis and macrophage infiltrates," *Pathology Research and Practice*, vol. 210, no. 12, pp. 1026–1030, 2014.

[10] G. Li, S.-J. Chen, S. Oparil, Y.-F. Chen, and J. A. Thompson, "Direct in vivo evidence demonstrating neointimal migration of adventitial fibroblasts after balloon injury of rat carotid arteries," *Circulation*, vol. 101, no. 12, pp. 1362–1365, 2000.

[11] S. Sartore, A. Chiavegato, E. Faggin et al., "Contribution of adventitial fibroblasts to neointima formation and vascular remodeling: from innocent bystander to active participant," *Circulation Research*, vol. 89, no. 12, pp. 1111–1121, 2001.

[12] A. C. Brisset, B. E. Isakson, and B. R. Kwak, "Connexins in vascular physiology and pathology," *Antioxidants & Redox Signaling*, vol. 11, no. 2, pp. 267–282, 2009.

[13] N. J. Severs, S. Rothery, E. Dupont et al., "Immunocytochemical analysis of connexin expression in the healthy and diseased cardiovascular system," *Microscopy Research and Technique*, vol. 52, no. 3, pp. 301–322, 2001.

[14] M. J. A. van Kempen and H. J. Jongsma, "Distribution of connexin37, connexin40 and connexin43 in the aorta and coronary artery of several mammals," *Histochemistry and Cell Biology*, vol. 112, no. 6, pp. 479–486, 1999.

[15] T. L. Little, E. C. Beyer, and B. R. Duling, "Connexin 43 and connexin 40 gap junctional proteins are present in arteriolar smooth muscle and endothelium in vivo," *American Journal of Physiology—Heart and Circulatory Physiology*, vol. 268, no. 2, part 2, pp. H729–H739, 1995.

[16] J.-A. Haefliger, P. Nicod, and P. Meda, "Contribution of connexins to the function of the vascular wall," *Cardiovascular Research*, vol. 62, no. 2, pp. 345–356, 2004.

[17] L. P. Véliz, F. G. González, B. R. Duling, J. C. Sáez, and M. P. Boric, "Functional role of gap junctions in cytokine-induced leukocyte adhesion to endothelium in vivo," *The American Journal of Physiology—Heart and Circulatory Physiology*, vol. 295, no. 3, pp. H1056–H1066, 2008.

[18] B. R. Kwak, N. Veillard, G. Pelli et al., "Reduced connexin43 expression inhibits atherosclerotic lesion formation in low-density lipoprotein receptor-deficient mice," *Circulation*, vol. 107, no. 7, pp. 1033–1039, 2003.

[19] T. Matsushita, A. Rama, N. Charolidi, E. Dupont, and N. J. Severs, "Relationship of connexin43 expression to phenotypic modulation in cultured human aortic smooth muscle cells," *European Journal of Cell Biology*, vol. 86, no. 10, pp. 617–628, 2007.

[20] X. Han, M. Chen, T. Hong et al., "Lentivirus-mediated RNAi knockdown of the gap junction protein, Cx43, attenuates the development of vascular restenosis following balloon injury," *International Journal of Molecular Medicine*, vol. 35, no. 4, pp. 885–892, 2015.

[21] G. N. Levine, E. R. Bates, J. C. Blankenship et al., "2011 ACCF/AHA/SCAI Guideline for Percutaneous Coronary Intervention. A report of the American College of Cardiology Foundation/American Heart Association Task Force on Practice Guidelines and the Society for Cardiovascular Angiography and Interventions," *Journal of the American College of Cardiology*, vol. 58, no. 24, pp. e44–e122, 2011.

[22] N. Tahara, A. Tahara, J. Narula, and T. Imaizumi, "Statin therapy resolves coronary artery inflammation," *JACC: Cardiovascular Imaging*, vol. 6, no. 10, pp. 1119–1120, 2013.

[23] J. Shen, L.-H. Wang, L.-R. Zheng, J.-H. Zhu, and S.-J. Hu, "Lovastatin inhibits gap junctional communication in cultured aortic smooth muscle cells," *Journal of Cardiovascular Pharmacology and Therapeutics*, vol. 15, no. 3, pp. 296–302, 2010.

[24] M. J. Zhao, S. R. Wang, Q. M. Li et al., "Experimental study of Yiqihuoxuejiedu decoction on inhibiting restenosis after percutaneous transluminal angiography in rabbits," *Chinese Journal of Experimental Traditional Medical Formulae*, vol. 13, no. 3, pp. 32–36, 2007.

[25] M.-J. Zhao, A.-M. Wu, J. Wang et al., "Yiqihuoxuejiedu formula inhibits vascular remodeling by reducing proliferation and secretion of adventitial fibroblast after balloon injury," *Evidence-Based Complementary and Alternative Medicine*, vol. 2014, Article ID 849167, 8 pages, 2014.

[26] G. H. Gibbons and V. J. Dzau, "The emerging concept of vascular remodeling," *The New England Journal of Medicine*, vol. 330, no. 20, pp. 1431–1438, 1994.

[27] F. G. Hage, "C-reactive protein and Hypertension," *Journal of Human Hypertension*, vol. 28, no. 7, pp. 410–415, 2014.

[28] N. Mahajan and V. Dhawan, "In vitro modulation of peroxisome proliferator-activated receptor-γ and its genes by C-reactive protein. Role of atorvastatin," *Archives of Medical Research*, vol. 41, no. 3, pp. 154–161, 2010.

[29] M.-L. Kortelainen and K. Porvari, "Adventitial macrophage and lymphocyte accumulation accompanying early stages of human coronary atherogenesis," *Cardiovascular Pathology*, vol. 23, no. 4, pp. 193–197, 2014.

[30] K. G. Battiston, B. Ouyang, R. S. Labow, C. A. Simmons, and J. P. Santerre, "Monocyte/macrophage cytokine activity regulates vascular smooth muscle cell function within a degradable polyurethane scaffold," *Acta Biomaterialia*, vol. 10, no. 3, pp. 1146–1155, 2014.

[31] B. C. Tieu, C. Lee, H. Sun et al., "An adventitial IL-6/MCP1 amplification loop accelerates macrophage-mediated vascular inflammation leading to aortic dissection in mice," *The Journal of Clinical Investigation*, vol. 119, no. 12, pp. 3637–3651, 2009.

[32] Y. J. Yang, L. S. Wu, B. Shu, and M. Z. Qian, "MCPIP1 mediates MCP-1-induced vascular smooth muscle cell proliferation," *Acta Physiologica Sinica*, vol. 65, no. 6, pp. 616–622, 2013.

[33] V. Kundumani-Sridharan, N. K. Singh, S. Kumar, R. Gadepalli, and G. N. Rao, "Nuclear factor of activated T cells c1 mediates p21-activated kinase 1 activation in the modulation of chemokine-induced human aortic smooth muscle cell F-actin stress fiber formation, migration, and proliferation and injury-induced vascular wall remodeling," *The Journal of Biological Chemistry*, vol. 288, no. 30, pp. 22150–22162, 2013.

[34] B. Mirjanic-Azaric, M. Rizzo, L. Sormaz et al., "Atorvastatin in stable angina patients lowers CCL2 and ICAM1 expression: pleiotropic evidence from plasma mRNA analyses," *Clinical Biochemistry*, vol. 46, no. 15, pp. 1526–1531, 2013.

[35] J. R. Hoch, V. K. Stark, N. van Rooijen, J. L. Kim, M. P. Nutt, and T. F. Warner, "Macrophage depletion alters vein graft intimal hyperplasia," *Surgery*, vol. 126, no. 2, pp. 428–437, 1999.

[36] J. Yu, C. Fernández-Hernando, Y. Suarez et al., "Reticulon 4B (Nogo-B) is necessary for macrophage infiltration and tissue

repair," *Proceedings of the National Academy of Sciences of the United States of America*, vol. 106, no. 41, pp. 17511–17516, 2009.

[37] Y. Kondo, C. C. Jadlowiec, A. Muto et al., "The Nogo-B-PirB axis controls macrophage-mediated vascular remodeling," *PLoS ONE*, vol. 8, no. 11, Article ID e81019, 2013.

[38] S. Morel and B. R. Kwak, "Vascular connexins in restenosis after balloon injury," *Methods in Molecular Biology*, vol. 1037, pp. 381–398, 2013.

[39] H. Zhong, Q.-H. Hu, E.-B. Wang et al., "Roles of gap junctions in proliferation mediated by Hcy in the spontaneous hypertensive rat vascular smooth muscle cells," *Zhongguo ying yong sheng li xue za zhi*, vol. 28, no. 4, pp. 289–293, 2012.

[40] C. N. Joshi, D. N. Martin, P. Shaver, C. Madamanchi, B. J. Muller-Borer, and D. A. Tulis, "Control of vascular smooth muscle cell growth by connexin 43," *Frontiers in Physiology*, vol. 3, article 220, 2012.

[41] L. Wang, J. Chen, Y. Sun et al., "Regulation of connexin expression after balloon injury: possible mechanisms for antiproliferative effect of statins," *American Journal of Hypertension*, vol. 18, no. 9, pp. 1146–1153, 2005.

[42] D. D. Li, W. Z. Zhang, Y. Q. Chen, and L. Ma, "Effects of atorvastatin on angiotensin II-inducing ventricular connexin 43 remodeling in rats," *South China Journal of Cardiovascular Diseases*, vol. 17, no. 1, pp. 55–59, 2011.

[43] L. Li, X. Y. Zhao, G. Q. Liu, P. L. Yang, Y. L. Chen, and W. J. Dong, "The effects of atorvastatin on left ventricular remodeling in spontaneously hypertensive rats," *Chinese Journal of Hypertension*, vol. 17, no. 7, pp. 636–640, 2009.

[44] M. J. Zhao, S. R. Wang, and Q. M. Li, "Comparative study of Yiqihuoxuejiedu decoction and Xuefuzhuyu capsule on inhibiting extracellular matrix in restenosis," *Chinese Journal of Integrative Medicine on Cardio-/Cerebrovascular Disease*, vol. 3, no. 12, pp. 1061–1063, 2005.

[45] S. Ohkawara, Y. Okuma, T. Uehara, T. Yamagishi, and Y. Nomura, "Astrapterocarpan isolated from *Astragalus membranaceus* inhibits proliferation of vascular smooth muscle cells," *European Journal of Pharmacology*, vol. 525, no. 1–3, pp. 41–47, 2005.

[46] G.-F. Wang, C.-G. Shi, M.-Z. Sun et al., "Tetramethylpyrazine attenuates atherosclerosis development and protects endothelial cells from ox-LDL," *Cardiovascular Drugs and Therapy*, vol. 27, no. 3, pp. 199–210, 2013.

[47] J. Lu, X. Chen, Y. Zhang et al., "Astragalus polysaccharide induces anti-inflammatory effects dependent on AMPK activity in palmitate-treated RAW264.7 cells," *International Journal of Molecular Medicine*, vol. 31, no. 6, pp. 1463–1470, 2013.

[48] L. Sun, R. Zhao, L. Zhang et al., "Salvianolic acid A inhibits PDGF-BB induced vascular smooth muscle cell migration and proliferation while does not constrain endothelial cell proliferation and nitric oxide biosynthesis," *Molecules*, vol. 17, no. 3, pp. 3333–3347, 2012.

[49] S. Xu, P. J. Little, T. Lan et al., "Tanshinone II-A attenuates and stabilizes atherosclerotic plaques in apolipoprotein-E knockout mice fed a high cholesterol diet," *Archives of Biochemistry and Biophysics*, vol. 515, no. 1-2, pp. 72–79, 2011.

[50] G. Ma, S. Ding, Y. Feng, C. Shen, L. Chen, and Z. Chen, "Tetramethylpyrazine-eluting stents prevented in-stent restenosis in a porcine model," *Journal of Cardiovascular Pharmacology*, vol. 50, no. 2, pp. 201–205, 2007.

Hindawi Publishing Corporation
Evidence-Based Complementary and Alternative Medicine
Volume 2015, Article ID 634172, 9 pages
http://dx.doi.org/10.1155/2015/634172

Research Article

Effect of α-Allocryptopine on Delayed Afterdepolarizations and Triggered Activities in Mice Cardiomyocytes Treated with Isoproterenol

Bin Xu,[1] Yicheng Fu,[1] Li Liu,[1] Kun Lin,[1] Xiaojing Zhao,[1] Yu Zhang,[1] Xi Chen,[1] Zhongqi Cao,[1] Yun Huang,[2] and Yang Li[1]

[1]*Department of Cardiology, General Hospital of Chinese People's Liberation Army, Beijing 100853, China*
[2]*Department of Gerontology, Union Hospital, Tongji Medical College, Huazhong University of Science and Technology, Wuhan 430030, China*

Correspondence should be addressed to Yun Huang; huangyun1207@163.com and Yang Li; liyangbsh@163.com

Received 7 May 2015; Revised 7 August 2015; Accepted 13 August 2015

Academic Editor: Dan Hu

Objective. To investigate the effect of α-allocryptopine (ALL) on delayed afterdepolarization (DAD) incidence and triggered activity (TA) in mice administered isoproterenol (ISO). *Methods*. Mouse ventricular myocytes were isolated. And the cellular electrophysiological properties of ventricular myocytes were investigated. *Results*. We found that the incidences of DADs and TA in mouse myocytes were increased by ISO treatment. In sharp contrast, triggered arrhythmia events were rarely observed in myocytes with 10 μM ALL treatment. Transient inward current (I_{ti}) was reduced significantly with ALL treatment, which contributed to DAD-related triggered arrhythmia. Compared to Iso-treated group, the L-type calcium current ($I_{Ca,L}$) densities were decreased after exposure to ALL, along with slower activation, quicker inactivation, and longer time constant of recovery from inactivation kinetics. *Conclusion*. There is less triggered arrhythmia events in ventricular myocytes treated with ALL. This effect may be associated with the inhibition of I_{ti} and $I_{Ca,L}$.

1. Introduction

It is widely believed that the incidences of delayed afterdepolarizations (DADs) and triggered activities (TAs) have dramatically increased in heart failure patients [1, 2]. DAD-mediated TA is believed to play an important role in abnormal autorhythmicity, which causes the majority of sudden cardiac death during nonischemic heart failure by contributing to intracellular Ca^{2+} overload. DAD-mediated TA leads to activation of sodium-calcium exchanger (NCX) that extrudes Ca^{2+} in exchange for Na^{+} and generates a net inward current (I_{ti}) [3, 4]. The larger $I_{Ca,L}$ plays a vital role in producing I_{ti}. I_{ti} induces DADs that may reach threshold and trigger premature beats [5]. Currently, there is no effective strategy for the treatment of triggered arrhythmias. Available clinical antiarrhythmic drugs have a narrow therapeutic index, which identifies the need for researchers to explore the safety profile and effectiveness of alternative drugs.

α-Allocryptopine (ALL), a derivative of tetrahydropalmatine, is extracted from *Corydalis decumbens* (Thunb.) Pers. Papaveraceae [6]. Previous studies have indicated that ALL has antiarrhythmic effects in various animal models, which could be accounted for by the electrophysiological effects of ALL in prolonging the action potential duration [7]. However, it is not clear whether ALL reduces DADs and TAs in ventricular myocardium to resist the development of triggered arrhythmias. The present study aimed to characterize the action and mechanism of ALL on DADs and TAs in mouse ventricular myocytes by using the whole cell patch-clamp technique.

2. Materials and Methods

All experimental procedures and protocols were carried out according to the Chinese law on animal experimentation and approved by the Animal Experimental Committee of Chinese

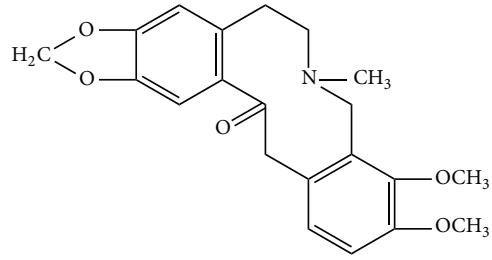

Figure 1: Chemical formula of ALL, an alkaloid extracted from *Corydalis decumbens* (Thunb.) Pers. Papaveraceae.

PLA General Hospital. This study conforms to the Guide for the Care and Use of Laboratory Animals published by the US National Institutes of Health (NIH Publication number 85-23, revised 1996).

2.1. Alpha-Allocryptopine Preparation and Treatment. Alpha-allocryptopine (ALL, formula is shown in Figure 1) was supplied by the Pharmaceutical Department of Lanzhou University (molecular weight: 365), melting point 168°C, as a white crystal powder, and 99.0% purity. ALL was dissolved in dimethyl sulfoxide (DMSO) to obtain a stock solution of 1.0 M. The effect of ALL was investigated at a maximum concentration of 0.5 mM. Based on the highest employed drug concentrations, DMSO was added to the media to produce a final concentration of 0.1%. The drug stock solution was added to the culture media or bath solution to produce the final concentration as reported in Section 3.

2.2. Patch-Clamp Experiments. Mouse cardiac myocytes were isolated using an established enzymatic digestion protocol. Cell pellets were resuspended and plated on laminin-coated 35 mm dishes. Only quiescent, Ca^{2+}-tolerant, and rod-shaped cells were used. Transmembrane action potentials and currents were recorded in whole cell configuration as previously described using a MultiClamp 700B amplifier (Axon Instruments) [7]. Correction for liquid junction potentials (which averaged −10 mV) was applied only for resting potential and reversal potential values.

Action potentials and current were recorded using the whole cell patch-clamp technique with a MultiClamp 700B amplifier (Axon Instruments). Data were sampled at 10 kHz and subsequently filtered at 5 kHz for analysis (Digidata 1440A, Axon Instruments). Patch pipettes were pulled from borosilicate glass on a P-97 horizontal puller (Sutter Instruments). The resistance electrodes of 2 MΩ ~5.5 MΩ were used to record action potentials and currents. A routine series resistance compensation was performed for values >80% to minimize voltage clamp errors. Thus, the uncompensated R_{series} was < 2 MΩ. The membrane capacitance was measured on each of the cells and was compensated by approximately 80% ~90% of their initial value.

2.3. Stimulation Parameters of Cardiac Myocytes. Myocytes were electrically stimulated for 3 ms with a 1.5 nA depolarizing pulse. Action potentials were induced in cardiac myocytes by 30 trains of suprathreshold current pulses at frequencies of 1.0, 2.0, 3.0, 4.0, and 5.0 Hz while the cells were under current clamp. DAD is defined as a depolarization >5 mV for >10 ms occurring during diastole (phase 4) immediately after an action potential. TA is defined as a spontaneous action potential arising from DADs.

To record transient inward current (I_{ti}), serial voltage steps were preceded by 20 conditioning pulses with each pulse lasting 150 ms from −80 mV to +50 mV at intervals of 100 ms. Following conditioning, serial voltage steps were applied for 2 s from −100 mV to +30 mV at 10 mV increments. Successive trains were 6 seconds apart. I_{ti} amplitude was measured as the difference between the peak and the base of the transient current with the first peak taken for analysis.

Using an extracellular solution with 0.05 mM TTX to inhibit Na^+ current and 5.0 mM CsCl to inhibit K^+ current, L-type calcium current ($I_{Ca,L}$) was recorded with 200 ms depolarizing pulses from a holding potential of −40 mV, with 10 mV steps from −40 mV to +60 mV. Current-voltage (I-V) curves were obtained with 10 mV voltage steps (−40 mV to +60 mV) from a holding potential of −40 mV.

2.4. Statistical Analysis. Statistical analyses were performed using SPSS version 17.0. One-way ANOVA with a Bonferroni post hoc test or Student's t-test was used. Chi-square tests (Fisher exact tests) were used to compare differences in the occurrence of DADs and TAs. Data were expressed as mean ± SEM. $p < 0.05$ was considered statistically significant.

3. Results

3.1. DADs and TA Incidences in Mouse Ventricular Myocytes of Mice with ALL Treatment. Under fast frequency pacing pulse (5.0 Hz), DADs were elicited in 20% (5/25) of cardiac myocytes following 30 nM ISO treatment (Figures 2(a) and 2(b)). The occurrence of DADs was significantly decreased in cardiac myocytes treated with 30 nM ISO treatment when administered 10 nM ALL (9%, 3/25, $p < 0.01$, Figures 2(a) and 2(b)). Only 4% of untreated myocytes had DADs (1/25, Figures 2(a) and 2(b)). Twelve percent of TA events were observed in cells treated with ISO. In myocytes administered ISO and then treated with 10 μM ALL, only 4% had TA events ($p < 0.01$, Figures 2(a) and 2(c)).

3.2. Frequency Characteristics of ALL on DADs and TA Incidences. Action potentials were recorded from ventricular myocytes that were stimulated at 1 to 5 Hz. Figure 3(a) displays 30 continuous driven action potentials at each pacing frequency with the development of DADs and TAs when pacing was discontinued. DADs and TAs were observed after relatively faster pacing frequencies. Compared to control myocytes, the occurrence of DADs and TAs progressively increased following treatment with 30 nM ISO at higher frequencies. The numbers of DADs or TAs were reduced after exposure to 10 μM ALL, and this effect was more significant during high frequency stimulation (Figures 3(b) and 3(c)).

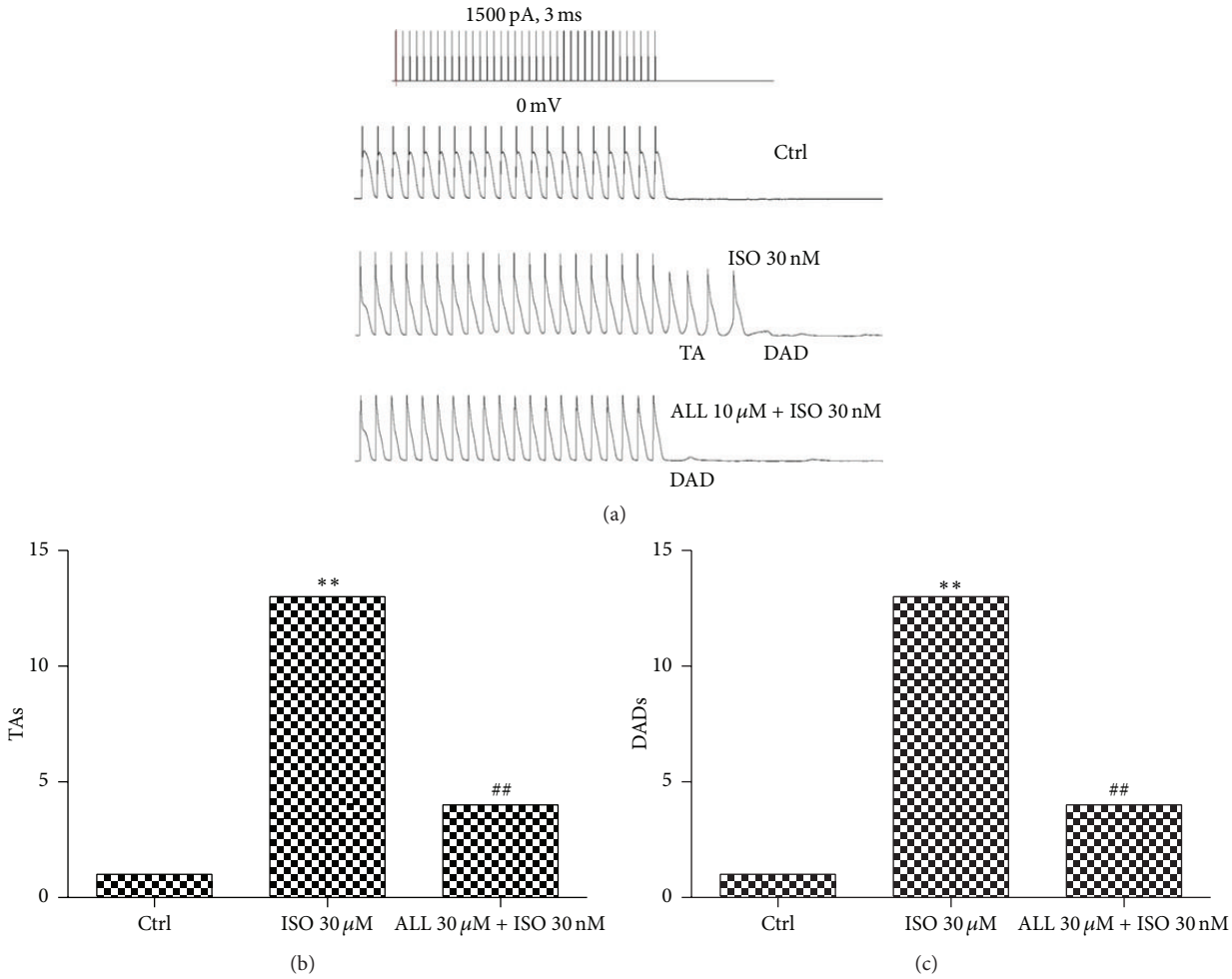

Figure 2: Effects of ALL on DADs and TA in mouse ventricular myocytes with 5.0 Hz stimulation. (a) The events of DADs or TAs induced with ISO were decreased after exposure to 10 μM ALL. The percent of DADs and TA events is shown in (b and c). $^{**}p < 0.01$, compared to control myocytes; $^{\#\#}p < 0.01$, compared to myocytes with ISO treatment.

3.3. I_{ti} of Mouse Ventricular Myocytes with ALL Treatment. It is known that the occurrence of DADs is due to instigation by I_{ti}. To evaluate the role of I_{ti} in development of DADs and TA, we recorded I_{ti} among three groups. Compared to control cells, there was a notable increase of I_{ti} found under exposure to 30 nM ISO. On average, the peak current densities of I_{ti} increased from -1.03 ± 0.12 pA/pF to -2.38 ± 0.08 pA/pF, which was markedly reduced by 10 μM ALL to -1.21 ± 0.14 pA/pF ($p < 0.05$, $n = 10$, Figures 4(a) and 4(b)). Current-voltage relationship curves indicated that maximal inward current density of I_{ti} was at the potential of -60 mV. Also, the current density of I_{ti} was greater in myocytes with ISO treatment, ranging from -80 mV to -20 mV, compared to untreated myocytes. The ISO-induced increase of current in myocytes was reduced by ALL treatment (Figure 4(c)).

3.4. $I_{Ca,L}$ of Mouse Ventricular Myocytes with ALL Treatment. Since DAD events were augmented by both ISO and ALL treatment, we mainly measured currents of L-type calcium currents. The $I_{Ca,L}$ currents of three groups were showed in Figure 5(a). The current densities of $I_{Ca,L}$ in myocytes with 30 nM ISO treatment were significantly larger, with -8.5 ± 0.6 pA/pF in the control group and -15.5 ± 0.3 pA/pF in the ISO-treated group at 0 mV of test potential. $I_{Ca,L}$ was reduced to -10.3 ± 0.4 pA/pF in ISO-treated myocytes that were cotreated with 10 μM of ALL ($p < 0.01$, $n = 12$, Figure 5(b)). The concentration-dependent inhibition of ALL on $I_{Ca,L}$ is shown in Figure 5(c), with IC_{50}: 16.08 ± 1.23 μM and Hill coefficient: 0.84. The current-voltage relationship demonstrated that current densities of $I_{Ca,L}$ from myocytes treated with ISO were significantly larger than in control myocytes from -20 mV to $+20$ mV. This effect was alleviated by 10 μM ALL treatment (Figure 5(d)).

Steady-state activated curves and steady-state inactivated curves of $I_{Ca,L}$ were fitted by the Boltzmann equation function. The steady-state activated curve of $I_{Ca,L}$ was shifted to more negative potential in the presence of 30 nM ISO. Meanwhile, the steady-state inactivated curve was shifted to

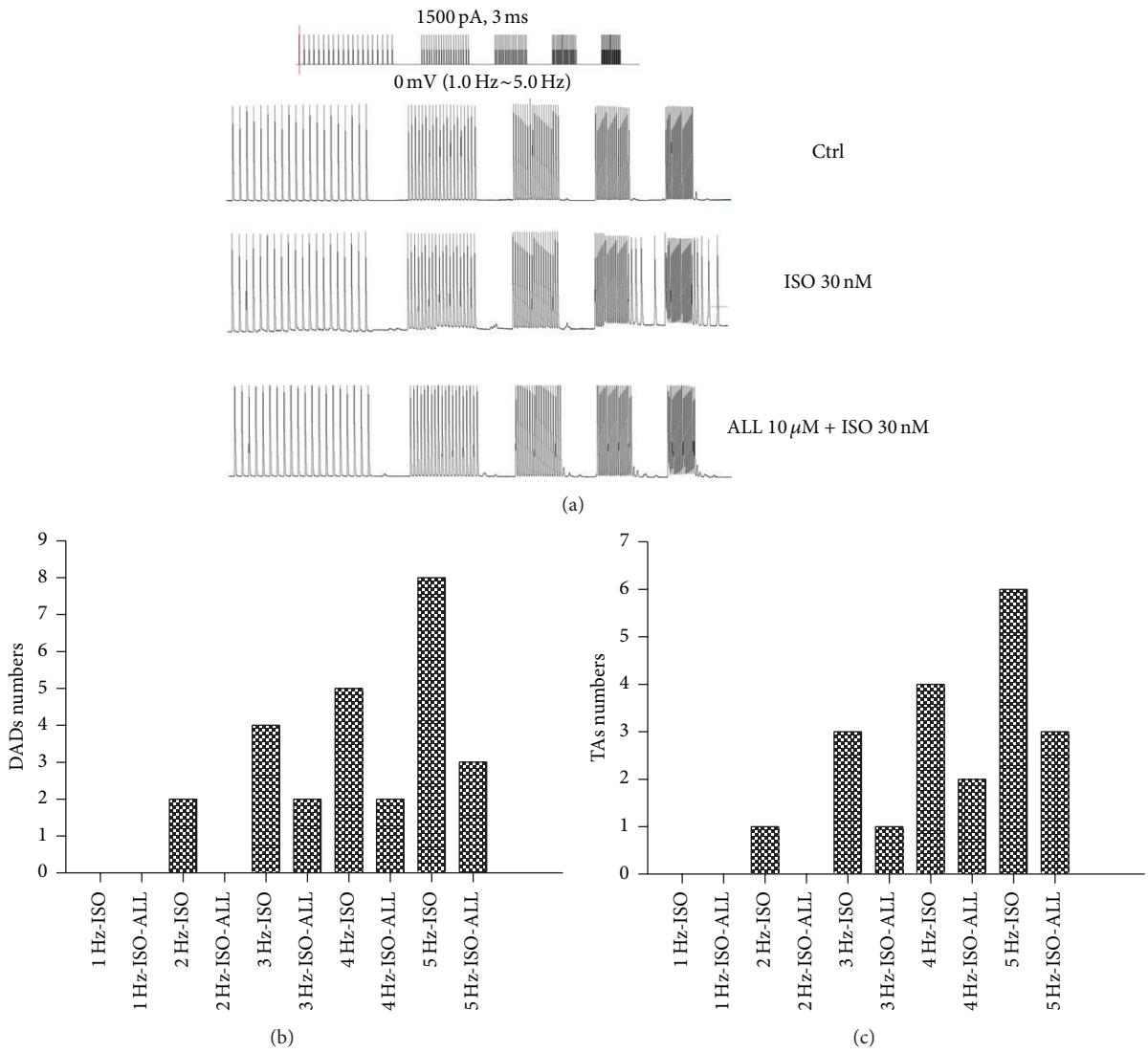

Figure 3: Frequency characteristics of ALL on DADs and TAs. (a) Hold potential at 0 mV, applying 30 wave pulses at 1500 pA for 3 ms at frequencies of 1.0, 2.0, 3.0, 4.0, and 5.0 Hz. Compared with untreated myocytes, the events of DADs and TAs progressively increased and had accelerated frequency following treatment with 30 nM ISO. Numbers of DADs or TAs were reduced in myocytes treated with ISO after exposure to 10 μM ALL in (b and c).

more positive potential by ISO treatment (Figures 6(a) and 6(c)). This suggests a slower activated procedure and faster inactivated procedure of $I_{Ca,L}$. Changes to the steady-state (in)activated curves were reversed by treatment with 10 μM ALL. $V_{1/2,act}$ and $V_{1/2,inact}$ were significantly different between the three groups, whereas k_{act} and k_{inact} values in the three groups had no significant difference (Figures 6(b) and 6(d)).

A faster recovery from inactivation of $I_{Ca,L}$ in myocytes with ISO treatment was reversed by 10 μM ALL treatment. The representative currents of recovery from inactivation before and after Iso and ALL treatment were recorded and shown in Figure 7(a). The average recovery time constants from inactivation were 895 ± 20 ms in the control group, 312 ± 16 ms in the ISO-treated myocytes, and 545 ± 22 ms in myocytes cotreated with ISO and ALL, respectively ($p < 0.01$, $n = 10$, Figure 7(b)).

4. Discussion

The major finding of the present study is that mouse ventricular myocytes exhibited a lower incidence of ISO-induced DADs and TAs in response to 10 μM ALL, which suggests that ALL has potential antitriggered arrhythmic effects. TAs have been easily induced by DADs in ventricular myocytes following the addition of isoproterenol and high calcium [8]. Furthermore, in isolated mouse ventricular myocytes, the effect of ALL on depressing DADs and DAD-induced TAs is largely rate-dependent showing stronger inhibitory effects at higher pulse frequencies.

DADs are generally thought to be initiated by spontaneous Ca^{2+} release from the sarcoplasmic reticulum (SR) and a Ca^{2+}-activated transient, depolarizing inward current (I_{ti}) [9, 10]. Several Ca^{2+}-activated currents have been proposed

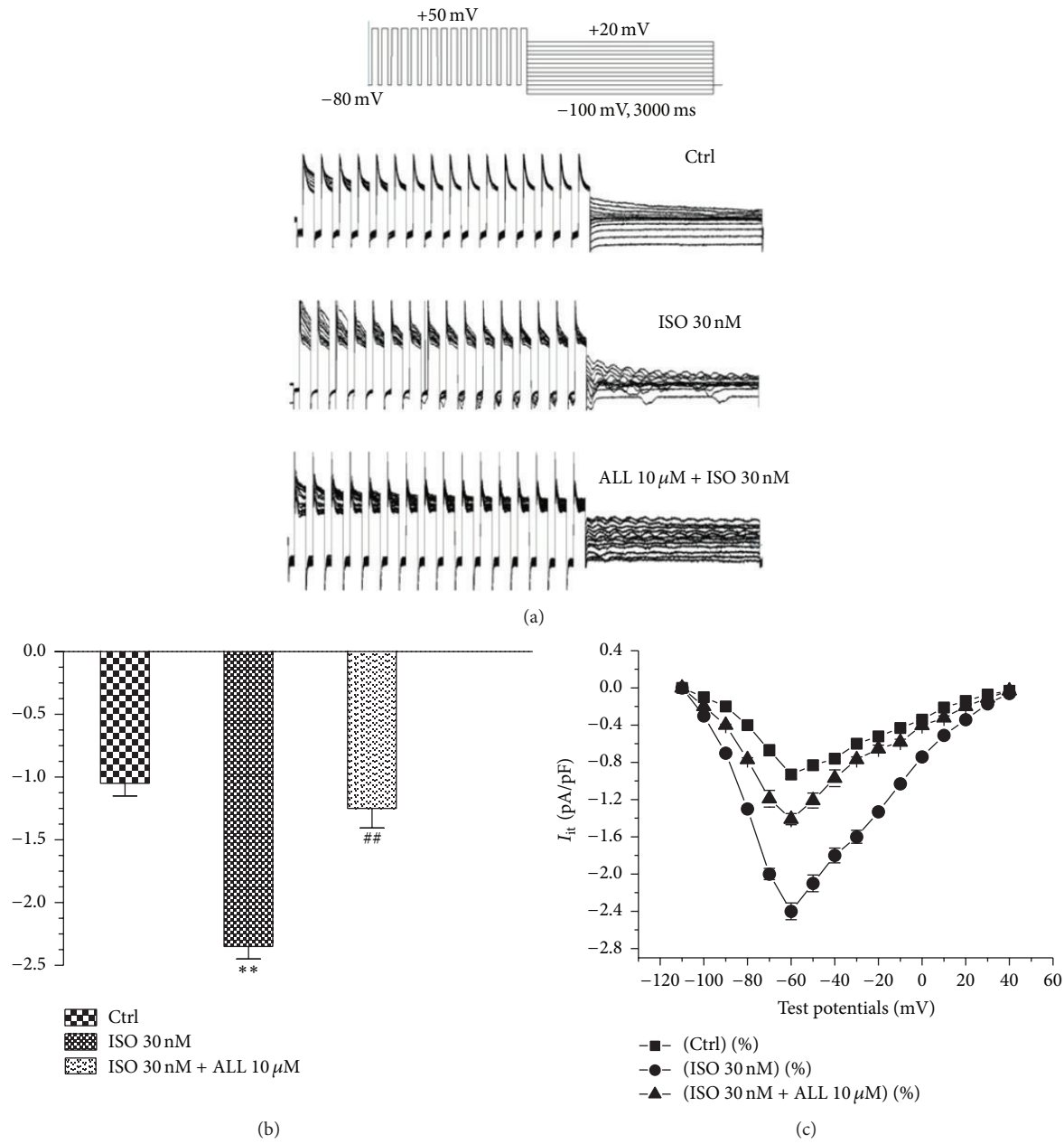

FIGURE 4: Effect of ALL on I_{ti} in mouse ventricular myocytes. (a) The left inset shows current traces obtained by applying train pulses from −100 mV to +30 mV for 2 s after conditioned stimulus ranging from −80 to +50 mV at intervals of 150 ms. (b) The larger current densities induced by ISO were significantly reduced with 10 μM ALL treatment. (c) Current-voltage relationship showed that densities of inward I_{ti} ranging from −80 mV to 0 mV were decreased by treatment with ALL with the largest reduction of peak current at −60 mV. $^{**}P < 0.01$, versus control myocytes; $^{\#\#}P < 0.01$, versus myocytes with ISO treatment.

to participate in I_{ti}, namely, the NCX exchange ($I_{Na/Ca}$) and calcium activated chloride channels ($I_{Cl,Ca}$) [11, 12]. Recently, Asakura et al. [4] reported that activation of the ryanodine receptor results in an explicit Ca^{2+} release initiated by the subthreshold Ca^{2+} accumulation and the progressive accumulation of $[Ca^{2+}]_i$, which rapidly increases the rate of DAD events. During heart failure, it has been shown that there is an increase in magnitude of I_{Na} and $I_{Ca,L}$ and NCX exchange protein can double. Together, this will increase $I_{Na/Ca}$ and will double I_{ti} amplitude, which depolarizes the cell towards TA threshold. I_{ti} induces DADs during the diastolic interval that may trigger premature beats by reaching threshold potential. Triggered arrhythmias cause the majority of sudden cardiac death during nonischemic heart failure [2]. Our data demonstrates the ability of ALL to suppress DADs and DAD-induced TA and that this effect could be explained by its action to reduce I_{ti} currents. Current-voltage relationships of myocytes undergoing stimulation showed that densities

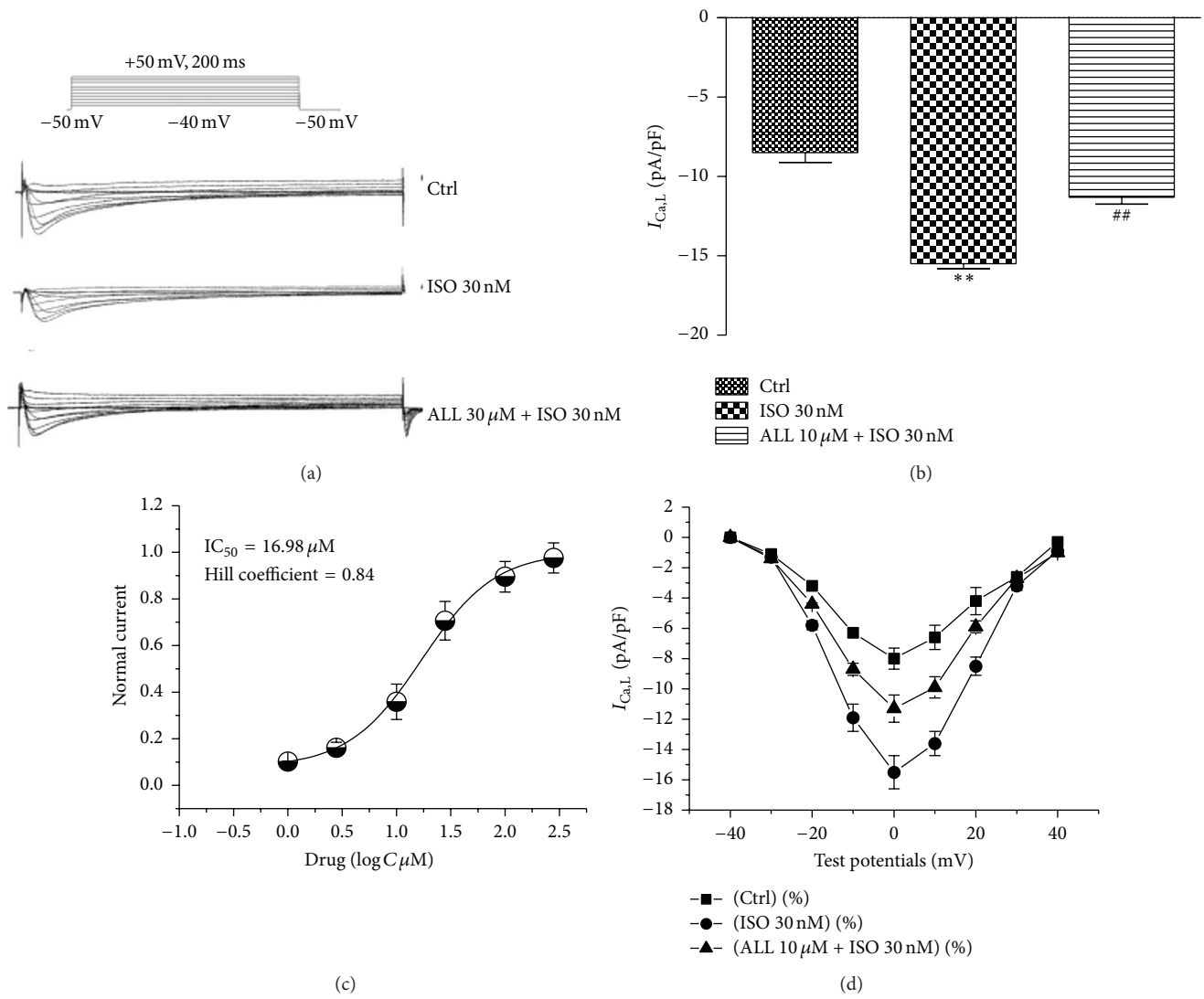

Figure 5: Effect of ALL on $I_{Ca,L}$ in mouse ventricular myocytes. (a) Representative $I_{Ca,L}$ traces in mouse ventricular myocytes of the indicated three groups. Current amplitudes of $I_{Ca,L}$ with ISO treatment were significantly higher and were reduced by treatment with ALL (b). The concentration-dependent inhibition of ALL on $I_{Ca,L}$ is shown in (c), with IC_{50}: 16.08 μM and Hill coefficient: 0.84. The current-voltage relationship demonstrated that current densities of $I_{Ca,L}$ from myocytes with ISO treatment were significantly larger than in control myocytes. The effect of ISO on $I_{Ca,L}$ was alleviated by 10 μM ALL treatment (d). $^{**}p < 0.01$, versus control myocytes; $^{\#\#}p < 0.01$, versus myocytes with ISO treatment.

of inward I_{ti} range from −80 mV to 0 mV were decreased by ALL, with the largest reduction peak current at −60 mV. The lower amplitude of I_{ti} leads to fewer events of DADs and subsequent DAD-induced TAs.

During heart failure, $I_{Ca,L}$ is essential for the electrical and biochemical function of the heart because they are the primary pathway for Ca^{2+} influx into cardiac myocytes. We found a notable $I_{Ca,L}$ increase in myocytes with ISO treatment. The steady-state activated curve of $I_{Ca,L}$ was shifted to negative potential, while the steady-state inactivated curve was shifted to positive potential by ISO treatment. The main mechanism of channel gating is a shorter time constant of recovery from inactivation in ISO-treated cells. The time constant of recovery from inactivation was prolonged and changes of the steady-state (in)activated curves were reversed by ALL treatment. Also, the increased effect of ISO on $I_{Ca,L}$ was alleviated by ALL with less DAD events as a response. For these reasons and more, the effects of ALL on $I_{Ca,L}$ and I_{ti} may attenuate ISO-induced arrhythmogenesis by decreasing the genesis of DADs.

The data in this study should be interpreted with caution because of its potential limitations. First, normal mouse ventricular myocytes are employed to determine the effect of ALL on DADs and TAs. As we know, triggered arrhythmias are prone to develop in heart failure. It is difficult to establish a heart failure model in mice, but normal cells do not mirror disease states. Therefore, ventricular myocytes isolated from mice with heart failure should be adopted in future research.

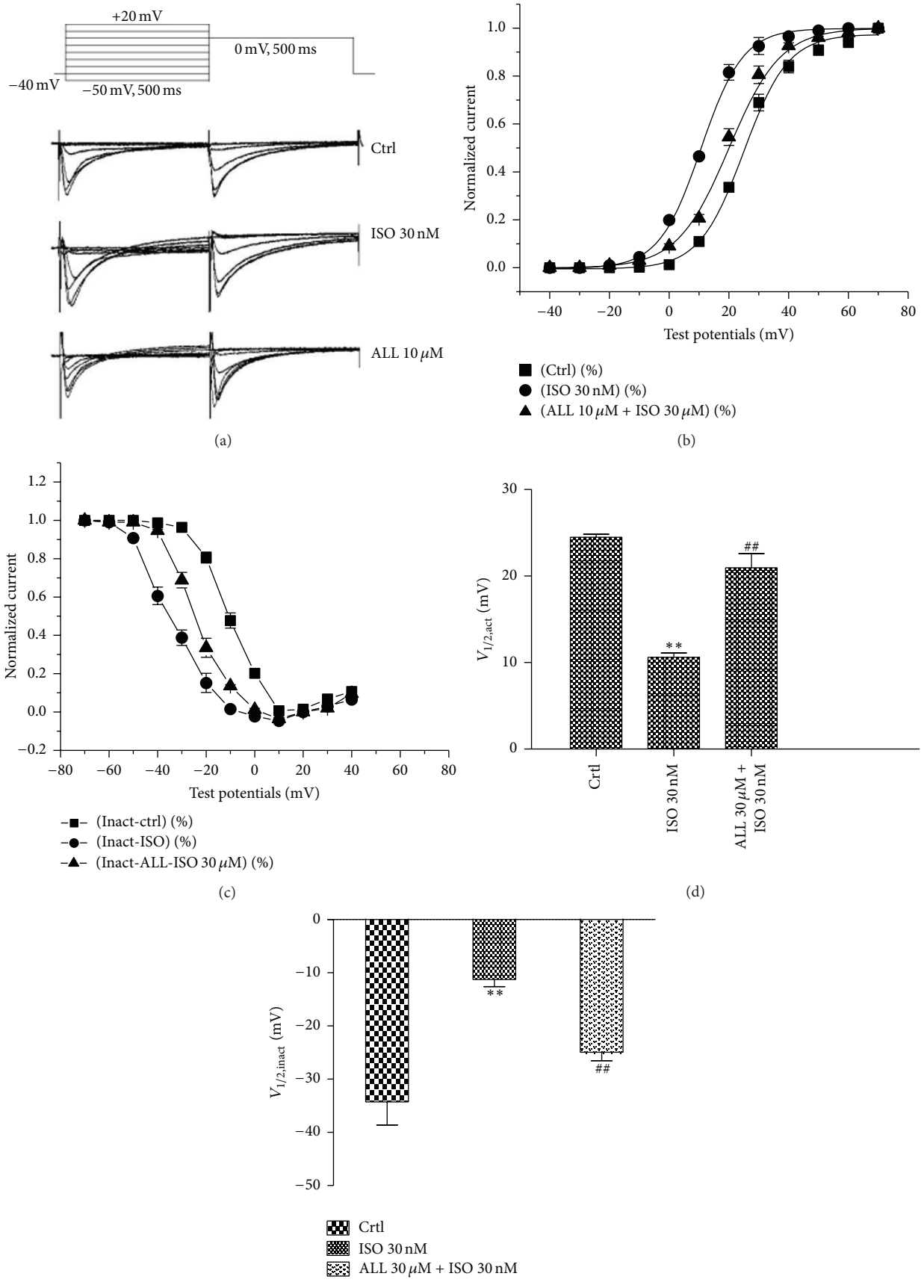

Figure 6: Continued.

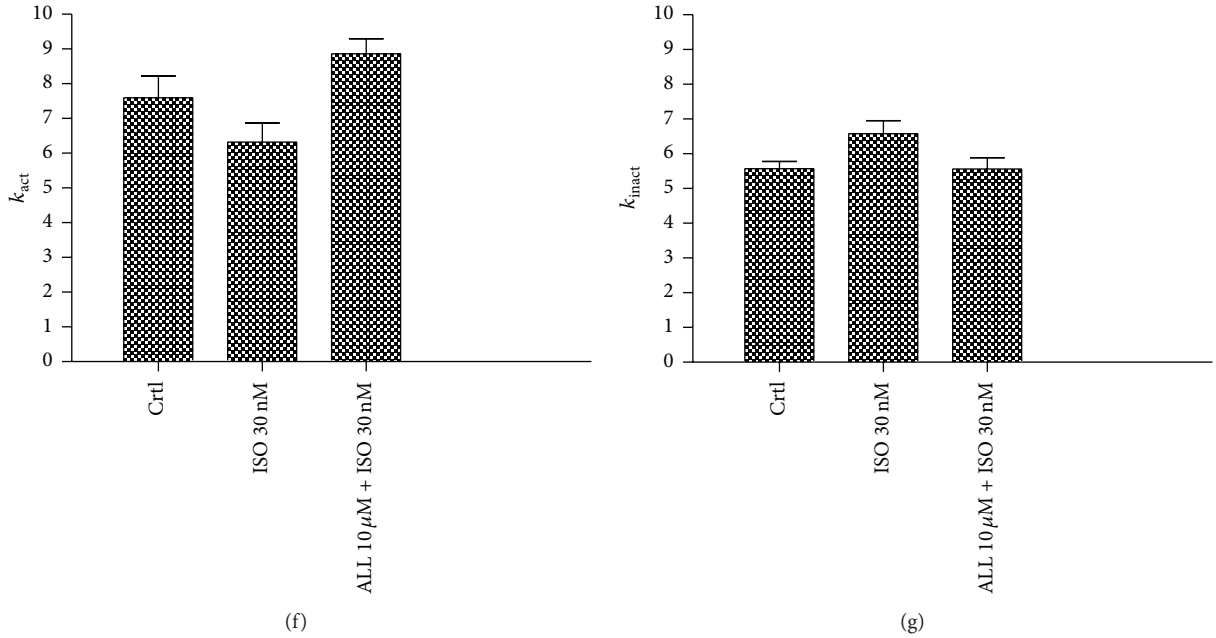

FIGURE 6: Effect of ALL on steady-state activated and inactivated curve of $I_{Ca,L}$. (a) The representative currents of $I_{Ca,L}$ activation and inactivation before and after being treated with Iso 30 nM and ALL 10 μM. (b and c) The steady-state activated curve of $I_{Ca,L}$ was shifted to negative potential, while the steady-state inactivated curve was shifted to positive potential following ISO treatment. Changes of steady-state (in)activated curves were reversed with 10 μM ALL treatment. $V_{1/2,act}$ and $V_{1/2,inact}$ were shown in (d and e); k_{act} and k_{inact} were shown in (f and g). $^{**}P < 0.01$, versus control myocytes; $^{\#\#}P < 0.01$, versus myocytes with ISO treatment.

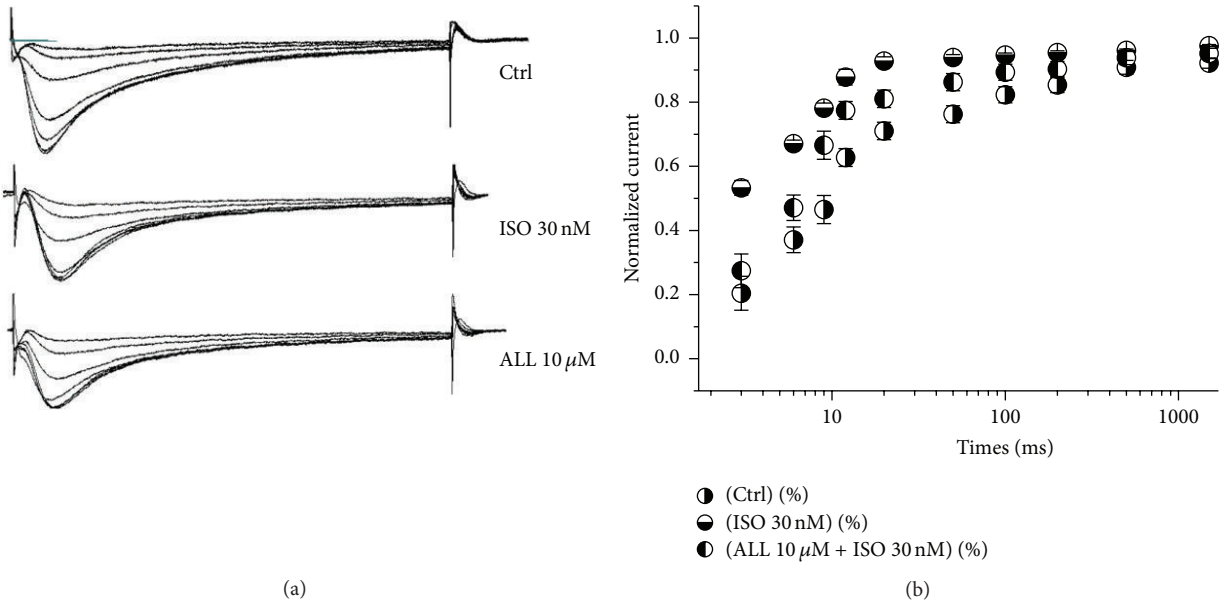

FIGURE 7: Effect of ALL on recovery from inactivation of $I_{Ca,L}$. (a) The representative currents of $I_{Ca,L}$ recovery from inactivation after being treated with Iso 30 nM and ALL 10 μM. (b) A faster recovery from inactivation of $I_{Ca,L}$ in myocytes treated with Iso was observed. The time constant of recovery from inactivation was prolonged in myocytes treated with ALL.

Second, DADs and TA events are regulated by many currents such as $I_{Ca,L}$, I_{ti}, I_{K1}, I_{NCX}, and $I_{Cl,Ca}$ [13, 14]. We only investigated $I_{Ca,L}$ and I_{ti} in this study. The effects of ALL on other currents should be investigated in future research.

In conclusion, DADs and TA events were decreased in mice ventricular cells treated with ALL. The underlying mechanism through which these cells exhibited a lower incidence of triggered arrhythmias was unclear. A possible explanation is that the decrease of $I_{Ca,L}$ leads to NCX exchanger inhibition and generates I_{ti}. On the other hand, I_{ti} current can be directly blocked by ALL. Together, these effects on I_{ti} will explain the reduced incidence of DADs and TAs in mouse by ALL.

Disclosure

Bin Xu is the first author.

Disclaimer

The funders had no role in study design, data collection and analysis, decision to publish, or preparation of the paper.

Conflict of Interests

There are no competing interests to declare.

Authors' Contribution

Bin Xu, Yicheng Fu, and Li Liu contributed equally to this work.

Acknowledgment

This work was supported by the National Natural Science Foundation of China (nos. 81170177, 81030002, and 8147054).

References

[1] S. Despa and D. M. Bers, "Na^+ transport in the normal and failing heart—remember the balance," *Journal of Molecular and Cellular Cardiology*, vol. 61, pp. 2–10, 2013.

[2] S.-H. Wu, Y.-C. Chen, S. Higa, and C.-I. Lin, "Oscillatory transient inward currents in ventricular myocytes of healthy versus myopathic Syrian hamster," *Clinical and Experimental Pharmacology and Physiology*, vol. 31, no. 10, pp. 668–676, 2004.

[3] Y.-T. Zhao, C. R. Valdivia, G. B. Gurrola, J. J. Hernández, and H. H. Valdivia, "Arrhythmogenic mechanisms in ryanodine receptor channelopathies," *Science China Life Sciences*, vol. 58, no. 1, pp. 54–58, 2015.

[4] K. Asakura, C. Y. Cha, H. Yamaoka et al., "EAD and DAD mechanisms analyzed by developing a new human ventricular cell model," *Progress in Biophysics and Molecular Biology*, vol. 116, no. 1, pp. 11–24, 2014.

[5] M. Fukuda, T. Yamamoto, S. Nishimura et al., "Enhanced binding of calmodulin to RyR2 corrects arrhythmogenic channel disorder in CPVT-associated myocytes," *Biochemical and Biophysical Research Communications*, vol. 448, no. 1, pp. 1–7, 2014.

[6] Y.-Z. Chen, G.-Z. Liu, Y. Shen, B. Chen, and J.-G. Zeng, "Analysis of alkaloids in Macleaya cordata (Willd.) R. Br. using high-performance liquid chromatography with diode array detection and electrospray ionization mass spectrometry," *Journal of Chromatography A*, vol. 1216, no. 11, pp. 2104–2110, 2009.

[7] Y. Li, L. Wang, R. Cheng, P. Liu, and Q. Xue, "Effects of allocryptopine on arrhythmia of animals and action potential of the papillary muscles of guinea pigs," *Chinese Journal of Multiple Organ Diseases in the Elderly*, vol. 4, pp. 123–126, 2005.

[8] Y.-K. Lin, Y.-C. Chen, J.-H. Huang et al., "Leptin modulates electrophysiological characteristics and isoproterenol-induced arrhythmogenesis in atrial myocytes," *Journal of Biomedical Science*, vol. 20, article 94, 2013.

[9] D. Terentyev, J. A. Rochira, R. Terentyeva, K. Roder, G. Koren, and W. Li, "Sarcoplasmic reticulum Ca^{2+} release is both necessary and sufficient for SK channel activation in ventricular myocytes," *American Journal of Physiology—Heart and Circulatory Physiology*, vol. 306, no. 5, pp. H738–H746, 2014.

[10] A. Llach, C. E. Molina, J. Fernandes, J. Padró, J. Cinca, and L. Hove-Madsen, "Sarcoplasmic reticulum and L-type Ca^{2+} channel activity regulate the beat-to-beat stability of calcium handling in human atrial myocytes," *The Journal of Physiology*, vol. 589, no. 13, pp. 3247–3262, 2011.

[11] A. O. Verkerk, MW. Veldkamp, and A. C. G. van Ginneken, "Cl^- current blockade reduces triggered activity based on delayed afterdepolarisations," *Netherlands Heart Journal*, vol. 9, no. 4-5, pp. 172–176, 2001.

[12] O. F. Köster, G. P. Szigeti, and D. J. Beuckelmann, "Characterization of a $[Ca^{2+}]_i$-dependent current in human atrial and ventricular cardiomyocytes in the absence of Na^+ and K^+," *Cardiovascular Research*, vol. 41, no. 1, pp. 175–187, 1999.

[13] G. Szigeti, Z. Rusznák, L. Kovács, and Z. Papp, "Calcium-activated transient membrane currents are carried mainly by chloride ions in isolated atrial, ventricular and Purkinje cells of rabbit heart," *Experimental Physiology*, vol. 83, no. 2, pp. 137–153, 1998.

[14] A. C. Zygmunt, R. J. Goodrow, and C. M. Weigel, "I Na(Ca) and ICl(Ca) contribute to isoproterenol-induced delayed afterdepolarizations in midmyocardial cells," *The American Journal of Physiology*, vol. 44, pp. H1979–H1992, 1998.

Hindawi Publishing Corporation
Evidence-Based Complementary and Alternative Medicine
Volume 2015, Article ID 430271, 12 pages
http://dx.doi.org/10.1155/2015/430271

Research Article

Scutellarin Reduces Endothelium Dysfunction through the PKG-I Pathway

Xiaohua Du,[1,2] Chen Chen,[1] Min Zhang,[3] Donghua Cai,[1] Jiaqi Sun,[1] Jian Yang,[1] Na Hu,[1] Congji Ma,[3] Liyan Zhang,[2] Jun Zhang,[4] and Weimin Yang[1]

[1] *School of Pharmaceutical Science and Yunnan Key Laboratory of Pharmacology for Natural Products, Kunming Medical University, Kunming 650500, China*
[2] *Department of Respiratory Medicine, First Affiliated Hospital of Kunming Medical University, Kunming 650032, China*
[3] *Pharmacy Department, First Affiliated Hospital of Kunming Medical University, Kunming 650032, China*
[4] *Department of Clinical Pharmacy, First Affiliated Hospital of Kunming Medical University, Kunming 650032, China*

Correspondence should be addressed to Jun Zhang; zhangjunyang@126.com and Weimin Yang; ywmbessie@yeah.net

Received 4 May 2015; Revised 25 July 2015; Accepted 4 August 2015

Academic Editor: Dan Hu

Purpose. In this report, we investigated the protective mechanism of scutellarin (SCU) *in vitro* and *in vivo* which could be involved in endothelial cGMP-dependent protein kinase (PKG), vasodilator stimulated phosphoprotein (VASP) pathway, and vascular endothelium dysfunction (EtD). *Method*. Human brain microvascular endothelial cells (HBMECs) with hypoxia reoxygenation (HR) treatment and rats with cerebral ischemia reperfusion (CIR) treatment were applied. Protein and mRNA expression of PKG, VASP, and p-VASP were evaluated by Western blot and RT-PCR methods. Vascular EtD was assessed by using wire myography to determine endothelium-dependent vasorelaxation in isolated rat basilar artery (BA). *Result*. In cultured HBMECs, SCU (0.1, 1, and 10 μM) increased cell viability, mRNA, protein level, and phosphorylative activity of PKG and VASP against HR injury. In HR model of BA, SCU increased protein level of P-VASP. In rat CIR model, wire myography demonstrated that SCU (45 and 90 mg/kg, i.v.) significantly reduced ischemic size by partially restoring the endothelium dependent vasodilation of BA; PKG inhibitor Rp-8-Br-cGMPS (50 μg/kg, i.v.) reversed this protection of SCU in CIR rats. *Conclusion*. SCU protects against cerebral vascular EtD through endothelial PKG pathway activation.

1. Introduction

Vascular endothelium has complex physiological functions such as maintaining vascular tone, inhibiting platelet aggregation, reducing endothelial permeability, reducing adhesion molecules expression, and inhibiting vascular smooth muscle cell (VSMC) proliferation [1]. Endothelial cells, in easily damaged anatomical functional interface, are firstly affected by a variety of injuries including ischemia reperfusion (IR), that stimulating effect leads to the damage of structural integrity and reduce of function and then endothelial dysfunction (EtD) occurs. EtD may be an important basis for a number of diseases [1, 2]. Vascular tension adjustment disorders and abnormal expression of adhesion molecules are the main manifests of EtD. Study has shown that IR produces vascular EtD as defined by abrogated endothelium-dependent dilation [2]. In addition, previous study indicated that hypoxia reoxygenation (HR) caused selective inhibition of response to acetylcholine (ACh) in the cerebral arteries [3].

Ischemia reperfusion (IR) leads to tissue injury in various pathophysiological conditions. IR directly affects the vascular wall and luminal surface of blood vessel, causing damages including hemorrhage, capillary plugging, adhesion and infiltration of granulocytes, impaired vascular permeability, and endothelial dysfunction (EtD) [4]. Endothelial cells, while being particularly susceptible to IR injury, play an active role in IR-induced organ damage [5]. EtD reduces perfusion to ischemia areas and thereby exacerbates tissue injury and subsequent damage [6].

cGMP-dependent protein kinase (PKG) is a serine/threonine protein kinase that is activated by cGMP. Accumulating evidences are demonstrating that PKG phosphorylates

a number of biologically important targets which are needed to accomplish multiple cellular functions and its dysregulation has been incriminated in many diseases, such as hypertension, atherosclerosis, chronic heart failure, left ventricular hypertrophy, ventricular remodelling, IR injury, diabetes, and cancer [7]. Among the three isoforms of PKG-Iα, PKG-Iβ, and PKG-II, PKG-Iα is the strongest vascular tone modulator regulating cell motility, migration, proliferation, and vascular tone [8].

Moreover, there was report that PKG is involved in testosterone-induced vasodilation of human umbilical artery [9]. Upon activation, PKG phosphorylates VASP, which in turn activates downstream ion channels, leading to vascular smooth muscle relaxation and vasodilation. Previous reports have suggested that vasorelaxant effects of baicalin are mainly attributed to voltage-dependent Ca^{2+} channel (VDCC) inhibition and BKCa channel activation through PKA and PKG pathways [10].

Vasodilator stimulated phosphoprotein (VASP) belongs to the Ena/VASP protein family and is an important PKG-I substrate and actin regulatory protein. Studies [11] suggested that phosphorylated VASP at serine 239 (p-VASP) has been shown to be a useful monitor for PKG-I activity in intact cells.

Scutellarin (SCU), 4′,5,6-trihydroxy flavonoid-7-glucuronide, was reported to be the primary active ingredient of breviscapine, which is a mixture of flavonoid glycosides isolated from a Chinese traditional medicine plant *Erigeron breviscapus* (Vant.) Hand. Mazz. [12]. The plant extracts and SCU have been used in China to treat a variety of disorders including cardiovascular, cerebrovascular, and inflammatory diseases for many years [13]. In animal studies, SCU has been reported to be neuroprotective in rat cerebral ischemia reperfusion (CIR) models [14] via augmentation of antioxidant defense capacity [13]. In addition, SCU prevented EtD in diabetic rats and inhibited translocation of protein kinase C in diabetic thoracic aorta of the rat [15]. Our earlier study [16, 17] showed that relaxation effect of SCU on artery was predominantly endothelium dependent and partially involved the catalase-sensitive nitric oxide synthase signaling pathway.

Based on these observations, we hypothesize that SCU reduces EtD through the PKG-I pathway. To verify this hypothesis, we test the protein level and mRNA expression of PKG-I, VASP, and p-VASP in human brain microvascular endothelial cells (HBMECs). The effects of SCU on EtD of brain basilar artery (BA) and infarct size were checked in rats with CIR injury.

2. Materials and Methods

2.1. Chemicals and Drugs. SCU was obtained from Kunming Longjin Pharmaceutical Co. (Kunming, China). Cell culture reagents DMEM, modified RPMI-1640 medium, and fetal bovine serum were obtained from the Hyclone (Thermo Scientific, USA). Other items include Wire Myograph System DMT (Danish Myo Technology Company, Denmark) and Power Lab data recording and analytical system (ADInstruments Ltd., Australia). HBMECs were purchased from Yangsen Biology Limited Company (Shanghai, China). U46619 was purchased from Cayman Chemical Company. PKG inhibitor Rp-8-Br-cGMPS was purchased from Santa Cruz Biotechnology (Dallas, TX, USA). 3-(4,5-Dimethylthiazol-2-yl)-2,5-diphenyltetrazolium bromide (MTT), triphenyl tetrazolium chloride (TTC), and ACh were purchased from Sigma-Aldrich (St. Louis, MO, USA).

2.2. Animals. Sprague-Dawley rats (180–220 g, male and female in each half) were provided by the animal center of Kunming Medical University. All animals were housed in microisolation under conditions of constant temperature and controlled illumination (light on 12-hour light/dark cycle). Food and water were available ad libitum. All the animals used in the experiment received humane care. All surgical and experimental procedures were in accordance with the institutional animal care guidelines. The animal study was approved by the Animal Care and Use Committee of Kunming Medical University and conformed to the standards set by the Yunnan Experimental Animal Management Board.

2.3. Methods

2.3.1. Endothelial Cell Culture and HR Treatment. HBMECs were obtained from the Shanghai Yangsen Biochemical Technology Company (Shanghai, China) and grown in 1640 medium supplemented with 10% fetal bovine serum and 1% penicillin/streptomycin antibiotics. Tightly confluent monolayers of HBMECs from 4th–15th passage were used in all experiments. In experiments checking the effects of SCU under normal condition, cells were treated with vehicle control (NS) or SCU (0.1, 1.0, and 10.0 μM) at different concentrations for 26 hours. In experiments with HR treatments, cells were divided into 5 groups including control, HR model, HR + SCU 0.1 μM, HR + SCU 1 μM, and HR + SCU 10 μM group. Control cells were cultured in parallel and kept in normal culture condition for the entire time period (26 h). Simulated HR injury was induced according to previously described procedures [18] with minor modifications. Briefly, HBMECs were placed in a humidified hypoxic chamber (HF100, Heal Force Biotech Co., Shanghai, China) for 12 h of hypoxia (5% CO_2 + 2% O_2 + 93% N_2) with medium free of glucose and serum at 37°C, followed by 12 h of reoxygenation (5% CO_2 + 95% air) in complete medium containing glucose and serum. For HR + SCU groups, cells were incubated with SCU at different concentrations for 2 h prior to hypoxia treatment and during hypoxia (12 h) and reoxygenation (12 h) injury. For control group, cells were treated with vehicle control (NS) for 26 h, and for SCU groups, cells were given different concentrations of SCU for 26 h separately. At the end of the experiment, cell viability was examined using MTT assay as described below. Furthermore, cells of each group were also collected for RT-PCR assay and Western blotting assay as described in the following sections. All experiments were performed in triplicate.

2.3.2. MTT Assay of Cell Viability. For MTT assay, cells were plated in 96-well flat-bottomed plates at a density of 3×10^4 cells/mL and 90 μL/well. Cells were cultured in

normal culture condition or treated with simulated HR injury as described above. After the treatments, 20 μL of MTT (5 mg/mL) was added to each well and the plates were incubated for 4 h at 37°C. Then, 100 μL of lysis buffer (20% sodium dodecyl sulfate [SDS] in 50% N,N-dimethylformamide, containing 0.4% [v : v] 1 N HCL and 0.5% [v : v] 80% acetic acid) was added to each well and incubated overnight. Cell viability was determined by measuring the ability of metabolically active cells to convert the yellow tetrazolium salt MTT (5 mg/mL, PH = 7.4) into purple formazan crystals with a microplate reader at 570 nm. Results of three independent experiments (each conducted in triplicate) were used for statistical analysis.

2.3.3. Western Blot Analysis. The PKG-I, VASP, and p-VASP protein levels in lyzed cell were examined by Western analysis. Protein concentrations were determined by using BCA Protein Assay Kit (Beyotime Biotechnology, Haimen, Jiangsu, China). Total protein (20 μg) was fractionated on 10% SDS-PAGE and transferred to nitrocellulose membranes. Membranes were blocked with 10% defatted milk powder solution at room temperature for 2 h and incubated overnight at 4°C with the rabbit antibodies against VASP (concentration 1 : 500, Cell Signaling Technology, Inc., USA), p-VASP (Ser239) (concentration 1 : 2000, Santa Cruz Biotechnology, USA), and PKG-I (concentration 1 : 1000, Santa Cruz Biotechnology, USA). After three washes, membranes were incubated with horseradish peroxidase conjugated goat anti-rabbit IgG antibody (Santa Cruz Biotechnology, USA) for 1.5 h at room temperature. Then four washes were repeated, and the protein was visualized with enhanced chemiluminescence kit (Sigma, USA). The density values of bands were quantified by densitometric analysis of scanned images (Scion Image 4.03). The relative protein ratio was calculated by determining the integrated intensity of the bands of each treated group as a ratio of the control condition.

2.3.4. RT-PCR. Total RNAs were isolated from the cells by using Trizol reagent (TaKaRa, Japan). The sequences of primers (human PKG-Iα and GAPDH) used in this study were PKG-Iα (forward, AGCGGATCGAAGCAGGAGGC and reverse, TGACGGTCGCTGTCCGGGTA, 728 bp) and GAPDH (forward, AATCCCATCACCATCTTCC and reverse, GAGTCCTTCCACGATACCAA, 309 bp), respectively.

Total RNA (1 μg) was reverse-transcribed into cDNA using a Quantscript RT Kit (Tiangen, China). PCR was performed using a PCR MasterMix Kit (BioTeke, China) in a GeneAmp PCR system 9600 (ABI Int.). cDNA was amplified under the thermocycling conditions as follows: 3 min initial denaturation at 94°C (1 cycle), 30 s denaturation at 94°C (35 cycles), 30 s annealing at 57°C for human PKG and VASP, and 45 s extension at 72°C. The last amplification was followed by a final 7 min incubation at 72°C. PCR products were separated by electrophoresis through 1% agarose gel, stained with ethidium bromide, and visualized by UV transillumination in a Tocan Gel Imaging System (Tocan Co., Shanghai, China). GAPDH was used as an internal control. The mRNA level was calculated by determining the integrated intensity of the bands of each treated group as a ratio of the control. Each sample was measured in triplicate and the mean threshold cycle (Ct) value was calculated.

2.3.5. Rat CIR Model and Evaluation of Cerebral Infarct Volume. At room temperature (22 ± 2°C) conditions, the rats with 10% chloral hydrate (0.035 mL/kg) intraperitoneal injection of anesthesia were supinely fixed on the operating table, giving the tail vein injection of drugs while starting surgery. The right external carotid artery was ligated, and then right middle cerebral artery was given reperfusion 24 h after occlusion for 1 h [19]. At the end of the reperfusion, rats were decapitated. The brains were rapidly removed and frozen immediately at −20°C for 15 min, and then the brains were cut into 2 mm thick coronal sections which were stained with 1% TTC at 37°C for 10 min followed by fixation with 4% paraformaldehyde for 1 hour. Unstained areas were defined as ischemic lesions, whereas normal tissue was stained red. The infarct areas were traced and quantified with IPP software. Infarct areas of all sections were added to derive the total infarct area, which was multiplied by the thickness of the brain sections to obtain the infarct volume. To compensate for the effect of brain edema, the corrected infarct volume was calculated as previously described [20]. Corrected infarct volume equals total infarct volume multiply contralateral hemisphere volume/ipsilateral hemisphere volume.

To evaluate the effects of SCU on CIR injury, SD rats were divided into four groups (n = 10–12 in each group): sham, CIR model, and two SCU groups (45 or 90 mg/kg, i.v.). In another experiment, the influence of PKG inhibitor on the effects of SCU was assessed. The rats were divided into four groups (n = 10–15 each): CIR model, SCU (90 mg/kg, i.v.), PKG inhibitor (50 μg/kg, i.v.), and SCU (90 mg/kg, i.v.) + PKG inhibitor (50 μg/kg, i.v.) treated group. Drug infusion was initiated intravenously during surgery via the tail vein (2 mL/h). The sham and CIR model groups were given normal saline (NS).

2.3.6. Evaluation of EtD in Isolated BA from CIR Rats. The above treated rats were sacrificed and the BA was gently excised and rinsed off blood in 4°C PSS buffer solution (140 mM NaCl, 4.7 mM KCl, 1.6 mM $CaCl_2$, 1.2 mM $MgSO_4$, 1.2 mM MOPS, 1.4 mM Na_2HPO_4, 0.02 mM EDTA, and 5.6 mM D-glucose. The PH of PSS was preadjusted to 7.4 at 37°C). The BA was cleaned of fat and surrounding tissue, and then was cut into approximately 1-2 mm rings..

An integrated wire myograph system (Model 620 M, DMT Asia Ltd., Shanghai, China) was applied with a Motic SMZ168-TL stereomicroscope to mount BA rings on 60 μm steel wires in separated tissue baths of the wire myograph system for tension recording. The tissue baths were filled with PSS solution (PH 7.4) at 37 ± 1°C and aerated with O_2. Washout was performed by draining and replacing the bathing solution using a syringe. Isometric tension signals were recorded and data were collected by a PowerLab data acquisition system (ADInstruments Asia, Shanghai, China). Each ring was stretched to an optimal tension of 1 mN and permitted to equilibrate for 90 minutes before the experiment started. The rings were contracted by U46619 (1 μmol/L)

and relaxed using cumulative addition of ACh (0.001–1000 μmol/L) to test the endothelial-dependent vasodilation by calculating EC_{50} and E_{max} values.

2.3.7. Preparation of HR Model of Isolated BA and Treatment with SCU. Rats were sacrificed by intraperitoneal injection of 10% (0.1 mL/100 g) urethane. BA was removed and dissected free from brain tissues. Isolated BA segments were placed in anaerobic sugar-free physical salt solution (PSS) with 3-(N-morpholino)propanesulfonic acid sodium polystyrene sulfonate (MOPS), which leads to nitrogen hypoxia for 2 hours; then the BA segments were changed into normal MOPS-PSS solution with restoring oxygen and glucose for 2 hours. During HR damage, SCU (50 μM, 100 μM) was incubated along in SCU groups, while HR model group was given vehicle (NS). Control group was the normal BA. At the end of HR injury, BA transferred into a precooled glass homogenizer containing 200 μL precooled RIPA buffer (50 mM Tris-HCl, 150 mM NaCl, 1 mM EDTA, 1 mM PMSF, 1 mM Na_3VO_4, 1 mM NaF, 1% NP-40, 0.25% Na-deoxycholate, 10% glycerol, and 1 mg/mL of each of the phosphatase inhibitors aprotinin, leupeptin, and pepstatin, PH 7.4). Vessel tissues were then homogenized for 10 min, transferred to a 1.5 mL Eppendorf tube, and centrifuged at 18,000 rpm for 10 min at 4°C. The supernatant was collected by decantation and stored at −80°C until Western blot analysis.

2.3.8. Calculations and Statistical Analysis. Data were expressed as means ± SEM. Statistical analysis was performed using statistical software Sigma Stat 3.5. The E_{max} value represents the maximal vasodilative response that drug caused; EC_{50} is the concentration in which drug makes 50% of the maximum vasodilative effect. Nonlinear regression analysis for individual concentration-response curves was performed using a Hill algorithm in Sigma Plot 10.0, allowing for an individual geometric "EC_{50}" value to be calculated. E_{max} = [(the maximal stress of precontraction − the minimal stress)/the maximal stress of precontraction] ∗ 100%. Comparisons were made using one-way ANOVA analysis. $P < 0.05$ was considered statistically significant.

3. Results

3.1. Effect of SCU on PKG-I and Cell Viability in Normal Cultured HBMECs. As seen from Figures 1(a), 1(b), and 1(d), SCU (0.1, 1 and 10 μM) treatment increased the protein levels PKG-I, p-VASP, and VASP in normal HBMECs compared with control group. In addition, the ratio of p-VASP to VASP that indicated the activity of PKG was also increased under SCU treatment (Figure 1(c)). Particularly, there was apparent increase in protein levels of PKG-I, P-VASP, VASP, and PKG activity in normal HBMECs with SCU (1 and 10 μM) treatment.

As shown in Figures 2(a) and 2(b), under normal condition, SCU (0.1, 1, and 10 μM) incubation increased mRNA level of PKG-Iα, especially in SCU 1 μM group.

In our preliminary experiments checking the influence of SCU on cell viability of normal HBMECs, SCU with dose < 0.1 μM did not cause significant changes in cell viability while SCU with dose >100 μM exhibited cytotoxicity (data not shown). Therefore, SCU at doses of 0.1, 1, and 10 μM was used in the present study. As shown in Figure 2(c), results of MTT assay indicated that SCU 10 μM incubation raised apparently cell viability under normal culture condition, while there are not significant changes in SCU 0.1 and 1 μM group.

3.2. Effect of SCU on PKG-I and Cell Viability in HBMECs with HR Treatment. The effects of SCU on protein expression of PKG-I, VASP, and phosphorylation of VASP (p-VASP) under HR injury were shown in Figure 3. Compared with control, HR injury decreased p-VASP, VASP, and PKG, especially p-VASP; compared with model, SCU preincubations could significantly raise the protein expression of p-VASP, VASP, and PKG-I (Figures 3(a), 3(b), and 3(d)). HR injury also reduced PKG activity in model group (ratio of p-VASP and VASP) while SCU pretreatment could significantly augment it, especially in SCU 10 μM (Figure 3(c)).

As seen from Figures 4(a) and 4(b), the expression of PKG-Iα mRNA was significantly reduced in HR model group, while SCU (0.1, 1, and 10 μM) pretreatment increased it sharply (Figure 4(b)). The results indicated SCU could upregulate mRNA expression of PKG-Iα and antagonized the HR-induced injury.

As shown in Figure 4(c), HR injury greatly reduced cell viability of HBMECs, and pretreatment of SCU (0.1, 1, and 10 μM) could protect cells from HR-induced injury, especially the obvious effect of SCU (10 μM) on viability (Figure 4(c)). The data indicated that SCU has the protective effects on HBMECs against HR injury.

3.3. The Effect of SCU and PKG Inhibitor in Rats with CIR Treatment. As seen from Figures 5(a) and 5(b), compared with model group, SCU (45, 90 mg/kg) attenuated infarct size in rats with CIR treatment, especially in SCU 45 mg/kg group. Moreover, the values of vascular tension were reduced in SCU (90 mg/kg) group (Figure 5(c)), while the values of vascular tension in SCU (45 mg/kg) have no significant change.

There was similar change in the values of BA cumulative-response curves of ACh, EC_{50}, and E_{max} in CIR rats. CIR injury caused BA EC_{50} and E_{max} to be higher, while in CIR rats handled with SCU (90 mg/kg) pretreatment, the values of BA cumulative-response curves of ACh, EC_{50}, and E_{max} were low apparently. These above results showed that SCU (90 mg/kg) pretreatment has a protective effect on vascular EtD induced by CIR, and endothelium-dependent vasodilation in response to ACh was significantly impaired in BA exposed to CIR treatment, which showed that CIR model was successfully made.

In order to check the mechanism of SCU, the PKG inhibitor was used before the CIR rats were given SCU treatment. The results showed that PKG inhibitor reversed the effects of SCU on improving infarct size and BA values of EC_{50} and E_{max} in CIR rats dealt with SCU. As presented in Figures 5(d) and 5(e), infarct sizes in rats treated with SCU and PKG inhibitor were bigger than those in rats handled with SCU alone. Meanwhile, similar changes occurred in the EC_{50}, E_{max}, and the values of BA cumulative-response curves of ACh in CIR rats handled with SCU and PKG inhibitor

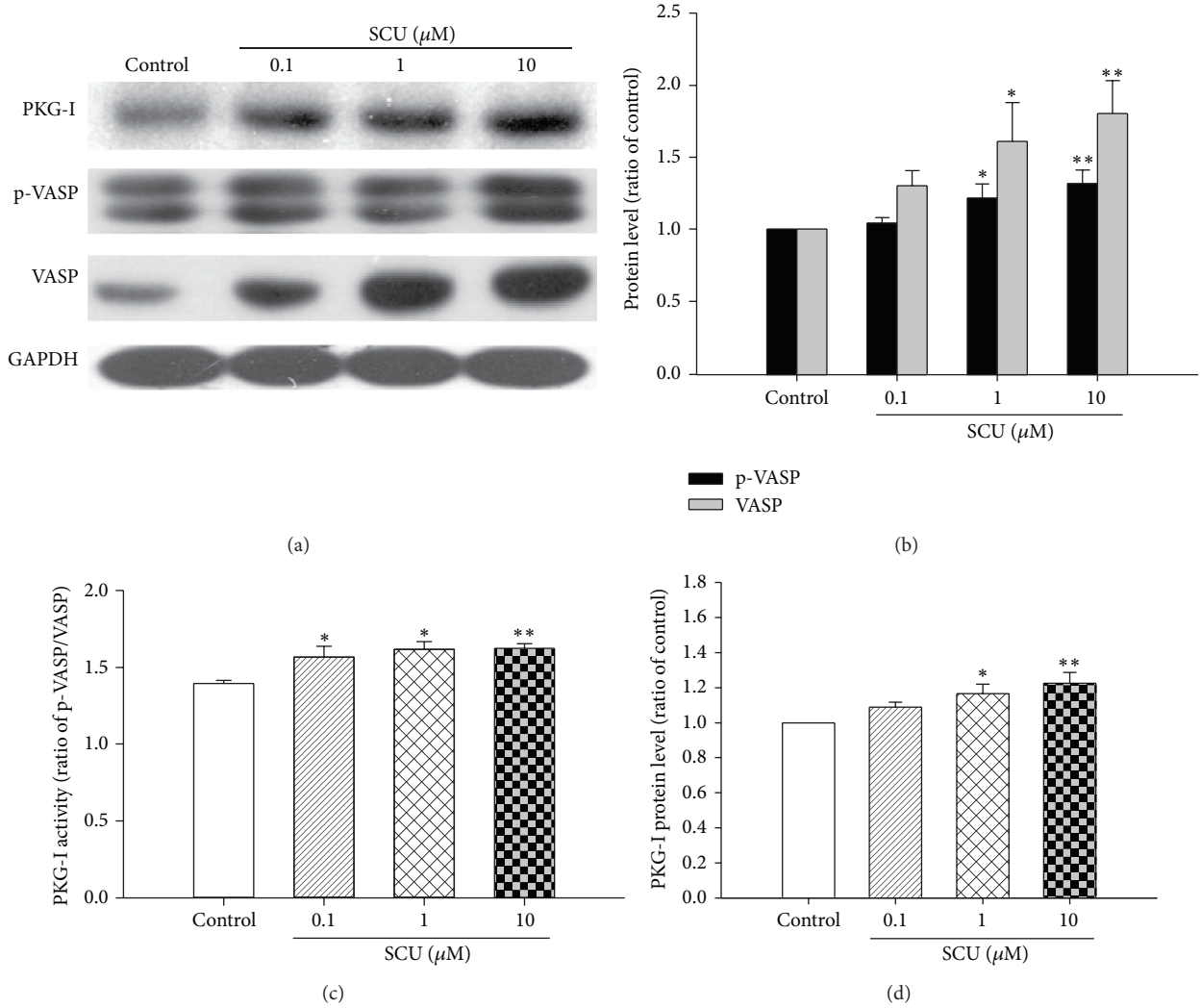

Figure 1: The effect of SCU on the protein level of PKG-I, VASP, and p-VASP protein in normal HBMECs. (a) Representative immunoblot and quantification of PKG-I, p-VASP, and VASP protein expression in normal HBMECs with SCU treatment. (b) The ratio of p-VASP and VASP compared with control in normal HBMECs with SCU treatment. Protein ratio of control was calculated by determining band integrated intensity as ratio of control. (c) The ratio of p-VASP compared with VASP in normal HBMECs with SCU treatment. (d) The ratio of PKG-I compared with control in normal HBMECs with SCU treatment. Protein ratio of control was calculated by determining band integrated intensity as ratio of control. Normal HBMECs, under normal culture condition: cells were incubated with SCU (0.1, 1, and 10 μM) for 24 h except control group. One-way ANOVA on Rank followed by SNK test, $^{*}P < 0.05$, $^{**}P < 0.01$, compared to control. Data are means ± SEM; $n = 3$ independent experiments with independent culture.

(Figure 5(c) and Table 1). The results indicated that PKG inhibitor reversed the effect of SCU on BA of rats with CIR treatment through inhibiting improvement of endothelium vasodilation and suggested that SCU might protect against CIR via PKG signal pathway.

3.4. The Effect of SCU on p-VASP in Isolated BA of Rats with HR Treatment. The effects of SCU on protein expression of phosphorylation of VASP (p-VASP) under HR injury were shown in Figures 6(a) and 6(b). HR injury significantly decreased p-VASP while SCU treatment could significantly increase the protein level of p-VASP. This shows that SCU can fight against HR injury in isolated BA blood vessel involved in PKG pathway.

4. Discussion

This study advances not only our understanding about the regulation of VASP and PKG-I, but also a mechanism underlying the beneficial effects of SCU in treating cerebrovascular diseases. In the present study, we found firstly, to our knowledge, that SCU increased the protein and mRNA expression of PKG and VASP in HBMECs with HR treatment. Moreover, compared with model group, SCU increased the cell viability and simultaneously raised the viability of PKG-I in HBMECs with HR treatment. This suggested the protective effects of SCU on the injury of HBMECs with HR involved in PKG-I/VASP signaling pathway. In our cell experiment, we found that the effect of SCU on normal HBMECs is sharply

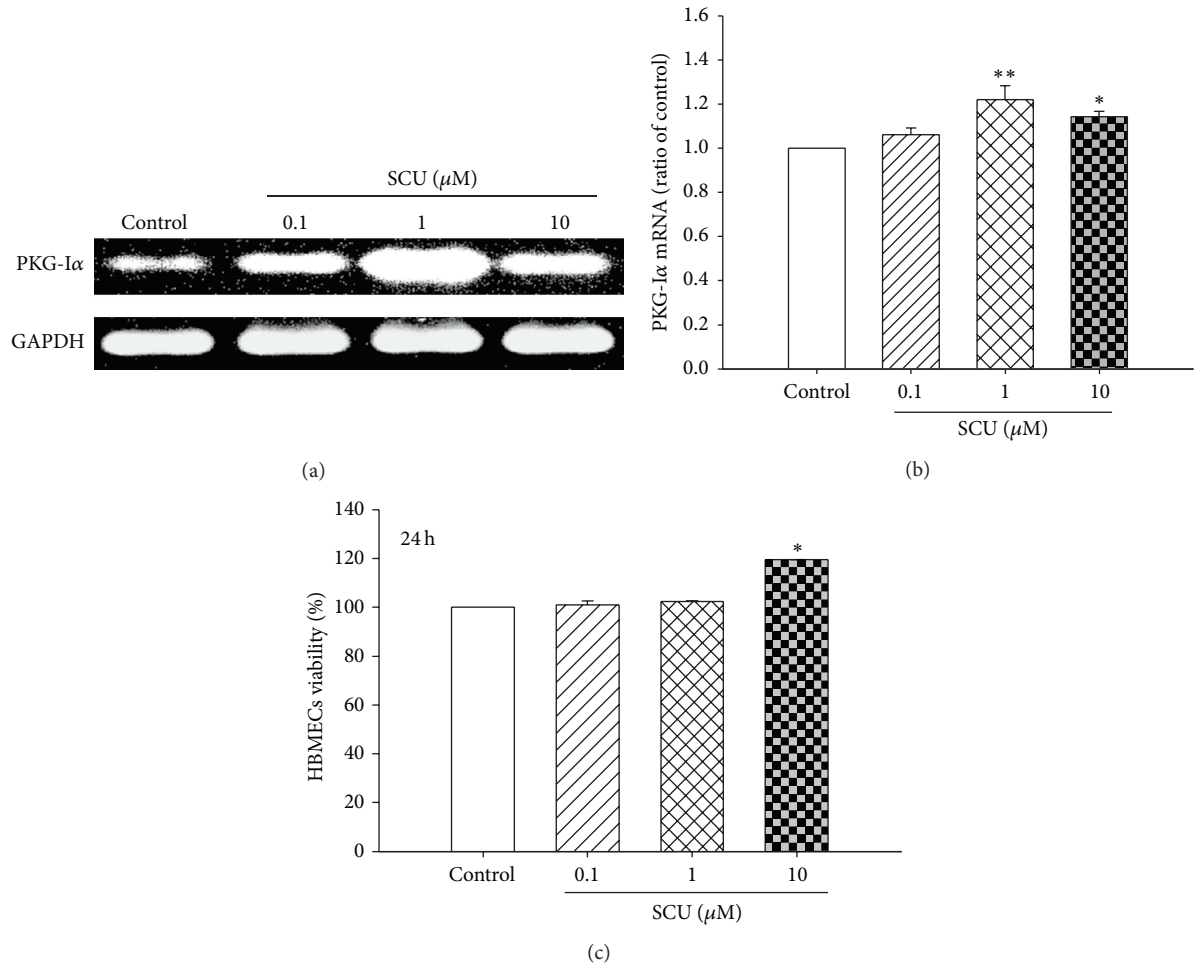

Figure 2: The effect of SCU on mRNA expression of PKG-I and cell viability in normal HBMECs. (a) Representative electrophotogram and quantification of PKG-Iα mRNA expression in normal HBMECs. (b) The mRNA ratio of PKG-Iα in normal HBMECs. Ratio of control was calculated by determining band integrated intensity as ratio of control. (c) The ratio of cell viability compared with control in normal HBMECs with SCU (0.1, 1, and 10 μM) treatment. Cell viability was examined using MTT assay. Normal HBMECs, under normal culture condition: cells were incubated with SCU (0.1, 1, and 10 μM) for 24 h except control group. One-way ANOVA on Rank followed by SNK test, $^{*}P < 0.05$, $^{**}P < 0.01$, compared to control. Data are means ± SEM; $n = 3$ independent experiments with independent culture.

weaker than that of HBMECs with HR treatment; this result showed that SCU could fight against HR injury.

In CIR rats, SCU preincubations could significantly decrease brain infarct size, vascular tension, and the values of BA cumulative-response curves of ACh, EC_{50}, and E_{max} and increase protein level of p-VASP in HR BA. These above results showed that SCU (90 mg/kg) pretreatment has a protective effect on vascular EtD induced by CIR, and endothelium-dependent vasodilation in response to ACh was significantly impaired in BA exposed to CIR treatment, which showed that CIR model was successfully made. Moreover, our results showed that SCU decreased the cerebral infarct size; this is consistent with the previous studies by Lin et al. [21, 22].

In order to check the mechanism of SCU, the PKG inhibitor was used before the CIR rats were given SCU treatment. The result shows that PKG inhibitor reversed the effects of SCU on improving infarct size, vascular tension, and the BA values of EC_{50} and E_{max} in CIR rats dealt with SCU. This result indicated that PKG inhibitor reversed the effect of SCU on BA of rats with CIR treatment through inhibiting improvement of endothelium vasodilation and suggested that SCU protects against CIR partially via PKG signal pathway.

Endothelial cells play an important role in controlling local vascular tension. In this study, we proposed one of the mechanisms of SCU-attenuated EtD induced by IR via PKG-I/VASP signaling pathway. Our results showed SCU attenuated the EC_{50} and E_{max} values of ACh in isolated BA induced by CIR, but the PKG inhibitor reversed the effects of SCU on improving EC_{50} and E_{max} values of BA in CIR rats. This confirmed our hypothesis that SCU attenuated EtD induced by IR via PKG-I/VASP signaling pathway and supported our group's previous studies that SCU vasorelaxation was predominantly endothelium dependent and involved nitric oxide synthase signaling pathway [17]. Meanwhile, we found that PKG inhibitor blocked the effect of SCU on reducing the cerebral infarction size. This mechanism contributes, at least in part, to elucidating the beneficial effects of SCU in CIR injury via PKG-I signal pathway.

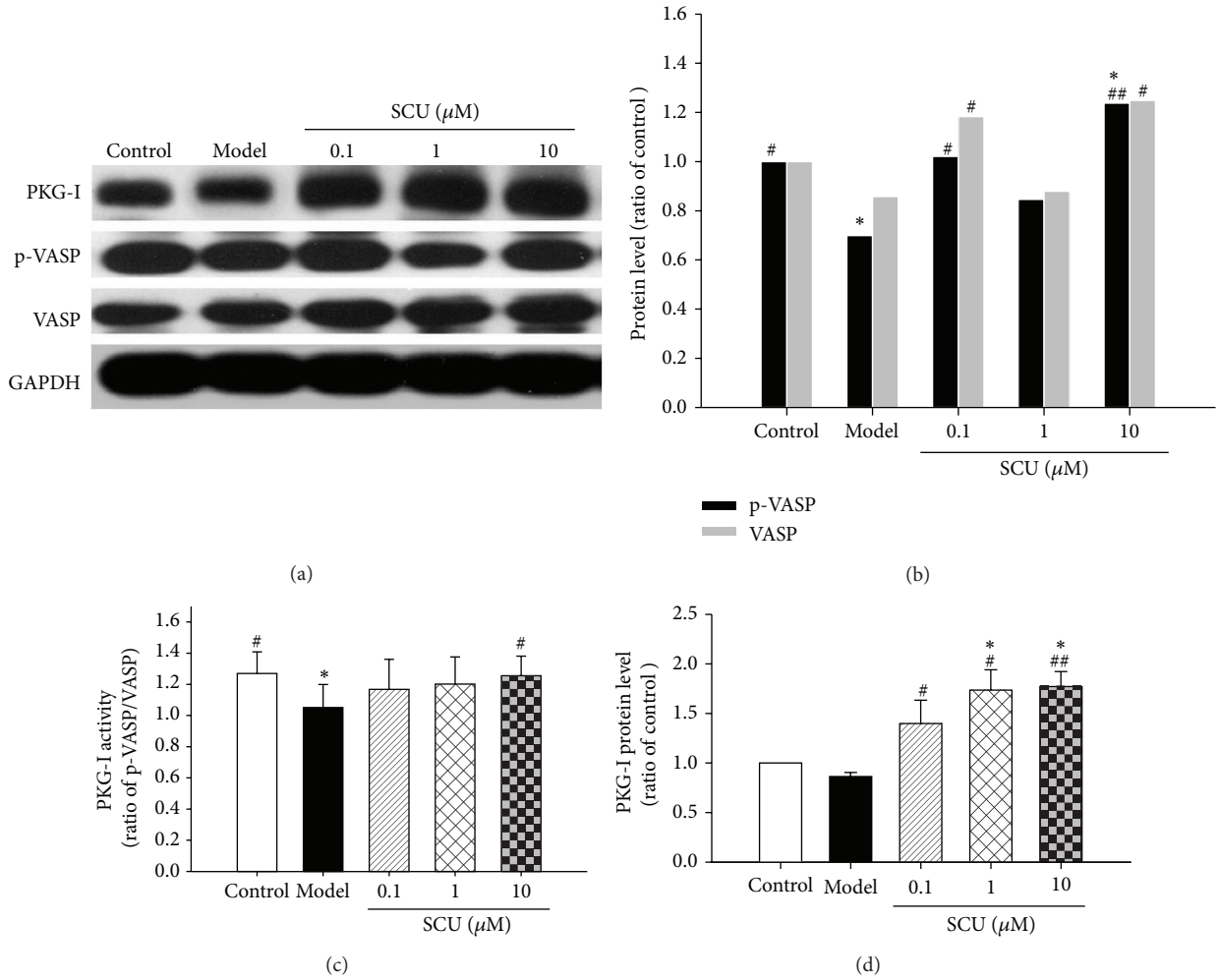

Figure 3: The effect of SCU on the protein level of PKG-I, VASP, and p-VASP in HR HBMECs. (a) Representative immunoblot and quantification of PKG-I, p-VASP, and VASP protein expression in HR HBMECs with SCU treatment. (b) The ratio of p-VASP and VASP compared with control in HR HBMECs with SCU treatment. Protein ratio of control was calculated by determining band integrated intensity as ratio of control. (c) The ratio of p-VASP compared with VASP in HR HBMECs with SCU treatment. (d) The ratio of PKG-I compared with control in HR HBMECs with SCU treatment. Protein ratio of control was calculated by determining band integrated intensity as ratio of control. Control group: cells were treated with vehicle control (NS) under normal culture condition for 26 h. Model group: cells were incubated under normal culture condition for 2 h and then given HR treatment (hypoxia 12/reoxygenation 12 hours). SCU groups: cells were incubated with SCU for 2 h prior to HR injury. One-way ANOVA followed by SNK test, $^{\#}P < 0.05$, $^{\#\#}P < 0.01$, compared to model of HR group, $^{*}P < 0.05$, $^{**}P < 0.01$, compared to control group. Data are means ± SEM; $n = 3$ independent experiments with independent culture.

SCU may exert its protection effects in IR by preventing generation of ROS, directly scavenging ROS or indirectly through enhancement of cellular antioxidant enzymes [23, 24]. Moreover, SCU could promote angiogenesis in endothelial cells [25], inhibit the apoptosis and the apoptosis inducing factor pathway [26–28], and attenuate mucus production *in vitro* and *in vivo* involving the inhibition of PKC-ERK signaling pathway [29]. SCU benzyl ester has a remarkable protective effect against myocardial ischemic injury and the protective mechanism may associate with its antiapoptotic effect by inhibiting cytochrome C release and caspase-3 activation and attenuate inflammation [30], antitumor [31, 32], antiviral [33], and neuroprotective effect [24]. Long-term administration of SCU improved the cardiac function of MI rats by inhibiting interstitial fibrosis, and the mechanisms may involve the suppression of profibrotic cytokine TGFβ1 expression and inhibition of p38 MAPK and ERK1/2 phosphorylation [22]. SCU exerts protective effects against IR injury through inhibiting PKC [15, 34]. However, the current study demonstrates that the PKG/VASP pathway plays an important role in pharmacological studies of SCU *in vivo* combining *in vitro* IR model. This observation may have further pharmacy implications because it may contribute to the clarification of the mechanisms behind the observed decreases in cardiocerebral vascular morbidity and mortality in patients receiving SCU or other flavonoids. Studies in another flavonoid baicalin suggest that vasodilator properties were attributed to endothelium-dependent relaxation through the PKG pathway [10]. There are evidences suggesting that ischemia followed by reperfusion causes local

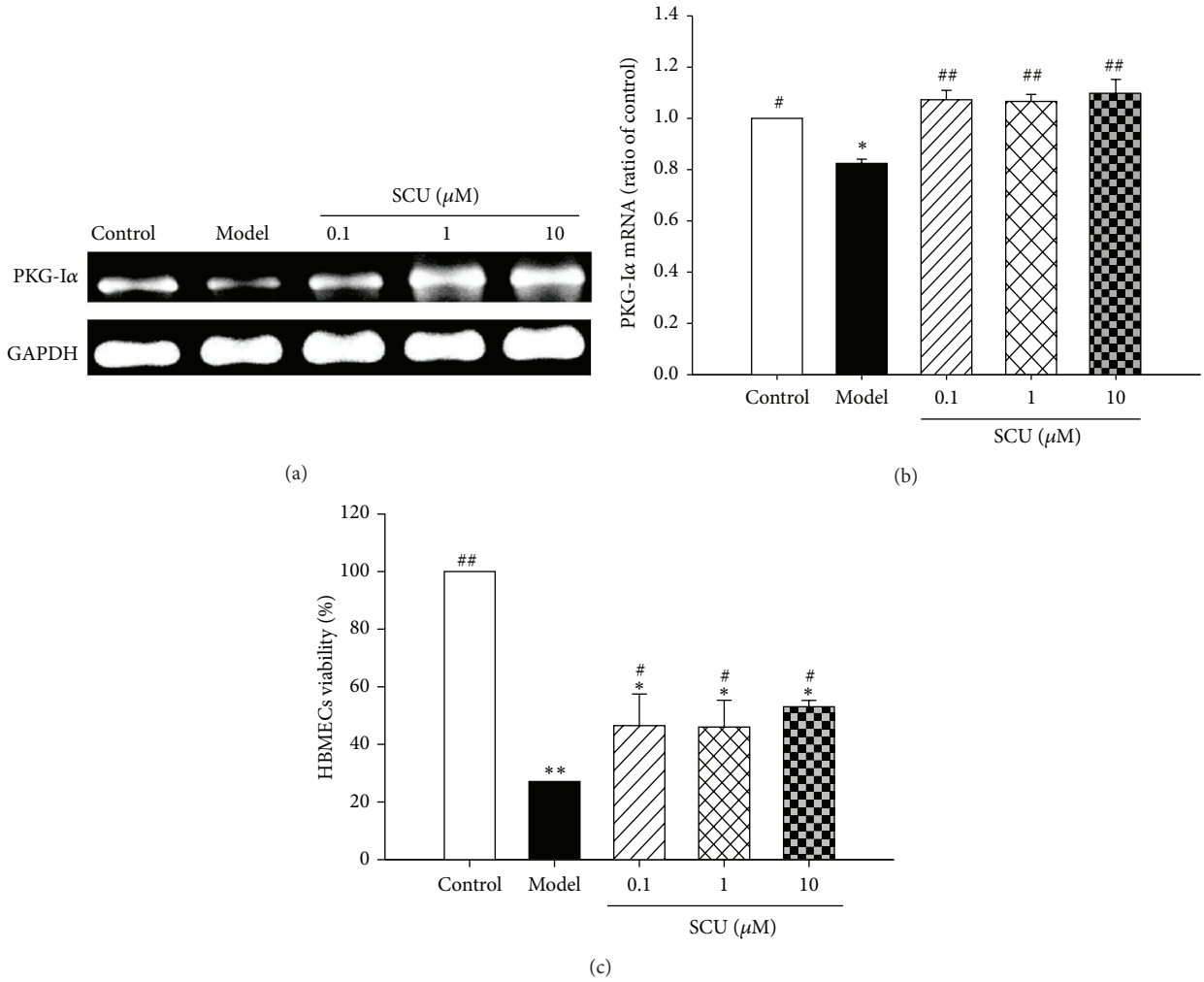

FIGURE 4: The effect of scutellarin (SCU) on mRNA expression of PKG and cell viability in HR HBMECs. (a) Representative electrophotogram and quantification of PKG-Iα mRNA expression in HR HBMECs. (b) The mRNA ratio of PKG-Iα in HR HBMECs. Ratio of control was calculated by determining band integrated intensity as ratio of control. (c) SCU increases cell viability in hypoxia reoxygenation- (HR-) treated human brain microvascular endothelial cells (HBMECs). Cell viability was examined using MTT assay and expressed as ratio of control. Control group: cells were treated with vehicle control (NS) under normal culture condition for 26 h. Model group: cells were incubated under normal culture condition for 2 h and then given HR treatment (hypoxia 12/reoxygenation 12 hours). One-way ANOVA followed by SNK test, $^{\#}P < 0.05$, $^{\#\#}P < 0.01$, compared to model of HR group, $^{*}P < 0.05$, $^{**}P < 0.01$, compared to control group. Data are means ± SEM; $n = 3$ independent experiments with independent culture.

dysfunction including EtD [35]. Hypoxia and reoxygenation are two essential elements of ischemia and reperfusion injury. HR may cause different forms of vascular injury, such as hemorrhage, change in vascular permeability, and EtD, including impaired endothelium-dependent vasodilation. Our study showed that IR caused EtD of BA with CIR, and SCU had protective effect on the EtD of BA *in vivo*. This observation was also in accordance with our previous result that SCU could relax isolated aortic rings of rat [17].

The roles of PKG-I isozymes have been documented in many processes including gastrointestinal motility, blood flow, neuronal plasticity, erectile function, lower urinary tract functions, endothelial permeability, and cardiac protection [7, 36–38]. Moreover, there was report that PKG is involved in testosterone-induced vasodilation of human umbilical artery [9]. Upon activation, PKG phosphorylates VASP, which in turn activates downstream ion channels, leading to vascular smooth muscle relaxation and vasodilation. Previous reports have suggested that cGMP/PKG/ROS/calmodulin/CaMKII signaling pathway may regulate cardiomyocyte excitability by opening K_{ATP} channels and contribute to cardiac protection against IR injury [39]. In vascular endothelial cells, PKG-I regulates cell motility, migration, and proliferation. These functions are reported to be essential for vascular permeability and angiogenesis. Experiments with PKG-I deficient vascular model systems have recently established that NO donor-induced VASP phosphorylation is primarily mediated by PKG-I [11]. Our result showed that the actions of PKG-I/VASP signaling may be a novel therapy target for IR injury of BA.

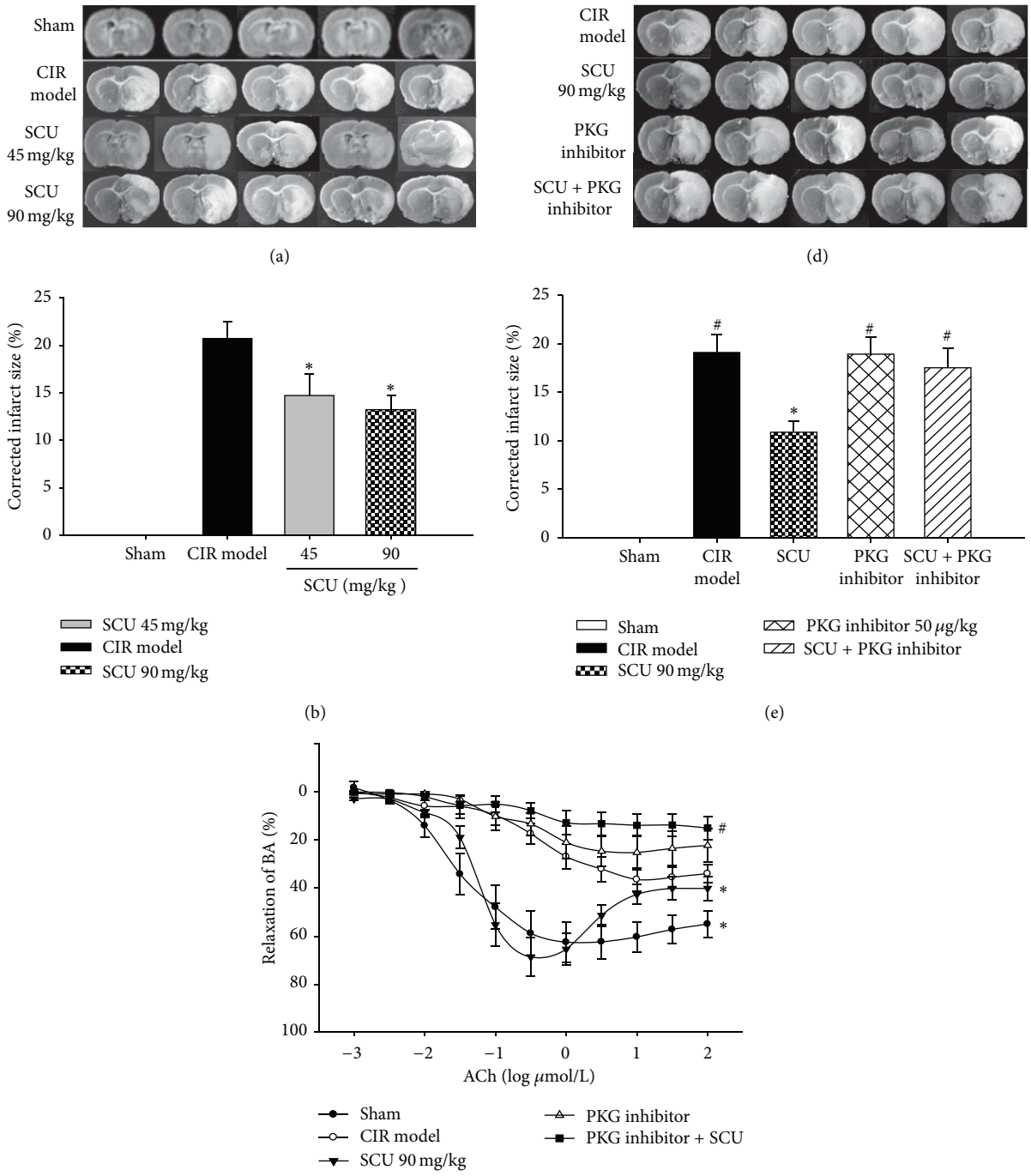

Figure 5: The effect of SCU and PKG inhibitor in rats with CIR treatment. (a) Representative images of triphenyl tetrazolium chloride (TTC) staining of ischemic brain slices from CIR (ischemia 60 minutes/reperfusion 24 hours) rats with SCU treatment. (b) Quantification of the corrected cerebral infarct volume in CIR rats with SCU treatment. $n = 10$ rats in each group. One-way ANOVA followed by SNK test versus model, $^{**}P < 0.01$, $^{***}P < 0.001$. (c) Cumulative concentration response curves of acetylcholine chloride (ACh) in isolated basilar artery (BA) segments from normal or CIR rats which were given SCU (90 mg/kg, i.v.) or PKG inhibitor treatment. Relaxation in response to ACh is expressed as a percent of precontraction with U46199 (1 μmol/L). $n = 8$ segments obtained from 3 rats with different treatments. Two-way ANOVA test versus model, $^{*}P < 0.05$, versus SCU, $^{\#}P < 0.05$. (d) Representative images of TTC staining of ischemic brain slices from CIR (ischemia 60 minutes/reperfusion 24 hours) rats, with SCU (90 mg/kg i.v.) and PKG inhibitor (Rp-8-Br-cGMPS, 50 μg/kg i.v.) alone and combined (SCU 90 mg/kg + Rp-8-Br-cGMPS 50 μg/kg) treatments. (e) Quantification of the corrected cerebral infarct size in CIR rats administered with SCU and PKG inhibitor. $n = 10$ rats in each group. One-way ANOVA followed by SNK test versus model, $^{*}P < 0.05$, versus SCU, $^{\#}P < 0.05$. Data are means ± SEM.

Table 1: Effect of SCU and PKG inhibitor administrations on ACh EC_{50} and E_{max} in BA rings.

Group	Dosage (i.v.)	n	EC_{50} (μM)	E_{max} (% of U46619)
Sham	NS	12	0.39 ± 0.14	$79.06 \pm 6.57^{**}$
Model	NS	11	1.11 ± 0.47	$36.46 \pm 4.90^{\#\#}$
SCU	45 mg/kg	8	NA	$22.47 \pm 7.59^{\#}$
SCU	90 mg/kg	11	0.30 ± 0.17	$64.33 \pm 4.40^{**}$
PKG inhibitor	50 μg/kg	8	NA	$25.24 \pm 7.19^{\#}$
SCU + PKG inhibitor	90 mg/kg + 50 μg/kg	15	NA	$15.1 \pm 4.90^{*\#}$

Data are means ± SEM; PKG inhibitor: Rp-8-Br-cGMPS; E_{max} is the maximum vasodilative effect that ACh caused; EC_{50} is the ACh concentration that makes 50% of the maximum vasodilative effect. n: BA segments' number; in each group blood vessel rings were obtained from 3-4 rats with different treatments. Blood vessel rings in each group were pretreated by tail intravenous injection with SCU or NS; NA: not available as relaxative response is too weak to be tested; NS: normal saline; one-way ANOVA on Rank Kruskal-Wallis test, E_{max} versus model, $^{*}P < 0.05$; $^{**}P < 0.01$, versus SCU (90 mg/kg), $^{\#}P < 0.05$, $^{\#\#}P < 0.01$.

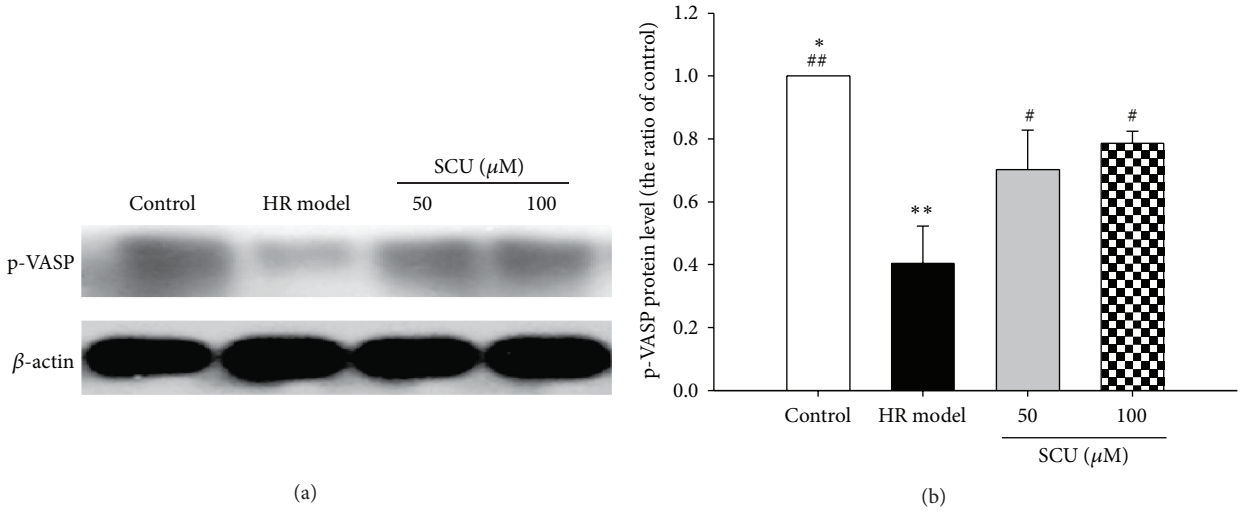

Figure 6: The effect of SCU on p-VASP in isolated BA of rats with HR treatment. (a) Representative immunoblot and quantification of p-VASP protein expression in rat BA with CIR and SCU treatment. (b) The ratio of p-VASP compared with control and CIR model in BA of rats with treatment of SCU and CIR injury. Protein ratios of control and model were calculated by the ratio of each bar compared to the control ratio and to the model ratio separately after the band integrated intensity as ratio of internal control (β-actin). $n = 8$ rats in each group. One-way ANOVA followed by SNK test versus control, $^{*}P < 0.05$, $^{**}P < 0.01$, versus model, $^{\#}P < 0.05$, $^{\#\#}P < 0.01$. Data are means ± SEM.

Among the downstream targets of PKG is vasodilator-stimulated phosphoprotein (VASP), a protein implicated in the control of cytoskeletal dynamics and cell migration [40]. Ser239 is the major site of action PKG. Phosphorylation of VASP at Ser239 by PKG inhibits growth of vascular smooth muscle [41], in part, by capping actin filaments, resulting in filament retraction [42, 43]. The determination of P-VASP levels could be a novel indicator of both PKG-I activity and endothelium integrity under physiological and pathophysiological conditions in human tissue [11]. Our study suggested that VASP and P-VASP protein levels were depressed in IR model group, but elevated after being given SCU treatment, which was accompanied with the PKG-I fluctuation and the change of EtD of BA. Our result showed that the actions of PKG-I/VASP signaling may be a novel therapy target for IR injury of BA.

In summary, SCU produces a marked pharmacologic action and regulates cellular function through multiple pathways. Our present study firstly provides important evidence that SCU induced expression and activation of PKG-I and increased VASP expression in normal cultured and HR treated HBMECs. In CIR rats, SCU treatment decreased cerebral infarct size and augmented the endothelium-dependent relaxation in isolated BA against EtD caused by CIR, while the protective effects of SCU could be reversed by PKG inhibitor. These suggest that SCU protects endothelial cells against HR injury and improves endothelium-dependent relaxation which involves PKG/VASP signaling pathway. Our studies provide a new mechanism to explain cerebral protective effects of SCU.

Abbreviations

SCU: Scutellarin
HR: Hypoxia reoxygenation
CIR: Cerebral ischemia reperfusion
IR: Ischemia reperfusion
PKG: cGMP-dependent protein kinase
EtD: Endothelial dysfunction
BA: Basilar artery
ACh: Acetylcholine
HBMECs: Human brain microvascular endothelial cells

p-VASP: Phosphorylated VASP
VASP: Vasodilator stimulated phosphoprotein.

Conflict of Interests

The authors declare that they have no conflict of interests.

Authors' Contribution

Weimin Yang designed experiments and revised the paper. Xiaohua Du wrote the paper. Other authors performed experiments. Xiaohua Du and Chen Chen contributed equally to this study.

Acknowledgments

This work was partly supported by the National Natural Science Foundation of China (nos. 30960450 and 81173110) and Yunnan Provincial Science and Technology Department (nos. 2011FA022, 2014FA010, 2012BC012, 2014FB037, 2008CD054, and 2014BC012). The authors thank Mr. Renwei Zhang and Xianer Fang for the gift of SCU compound. They also thank Dr. Yongxiao Cao and his group members for their technical assistance with wire myography and Yiping Wang and his group for their technical assistance with CIR animal model assessments.

References

[1] A. R. Pries and W. M. Kuebler, "Normal endothelium," in *The Vascular Endothelium I*, vol. 176 of *Handbook of Experimental Pharmacology*, part 1, pp. 1–40, Springer, Berlin, Germany, 2006.

[2] T. W. Hein, C. Zhang, W. Wang, C.-I. Chang, N. Thengchaisri, and L. Kuo, "Ischemia-reperfusion selectively impairs nitric oxide-mediated dilation in coronary arterioles: counteracting role of arginase," *The FASEB Journal*, vol. 17, no. 15, pp. 2328–2330, 2003.

[3] H. Xie, P. E. Ray, and B. L. Short, "NF-κB activation plays a role in superoxide-mediated cerebral endothelial dysfunction after hypoxia/reoxygenation," *Stroke*, vol. 36, no. 5, pp. 1047–1052, 2005.

[4] H. K. Eltzschig and C. D. Collard, "Vascular ischaemia and reperfusion injury," *British Medical Bulletin*, vol. 70, no. 1, pp. 71–86, 2004.

[5] K. Laude, P. Beauchamp, C. Thuillez, and V. Richard, "Endothelial protective effects of preconditioning," *Cardiovascular Research*, vol. 55, no. 3, pp. 466–473, 2002.

[6] R. K. Kharbanda, M. Peters, B. Walton et al., "Ischemic preconditioning prevents endothelial injury and systemic neutrophil activation during ischemia-reperfusion in humans in vivo," *Circulation*, vol. 103, no. 12, pp. 1624–1630, 2001.

[7] S. H. Francis, J. L. Busch, and J. D. Corbin, "cGMP-dependent protein kinases and cGMP phosphodiesterases in nitric oxide and cGMP action," *Pharmacological Reviews*, vol. 62, no. 3, pp. 525–563, 2010.

[8] H. Sellak, C.-S. Choi, N. B. Dey, and T. M. Lincoln, "Transcriptional and post-transcriptional regulation of cGMP-dependent protein kinase (PKG-I): pathophysiological significance," *Cardiovascular Research*, vol. 97, no. 2, pp. 200–207, 2013.

[9] E. Cairrão, A. J. Santos-Silva, and I. Verde, "PKG is involved in testosterone-induced vasorelaxation of human umbilical artery," *European Journal of Pharmacology*, vol. 640, no. 1–3, pp. 94–101, 2010.

[10] Y.-L. Lin, Z.-K. Dai, R.-J. Lin et al., "Baicalin, a flavonoid from *Scutellaria baicalensis* Georgi, activates large-conductance Ca^{2+}-activated K^+ channels via cyclic nucleotide-dependent protein kinases in mesenteric artery," *Phytomedicine*, vol. 17, no. 10, pp. 760–770, 2010.

[11] E. Schulz, N. Tsilimingas, R. Rinze et al., "Functional and biochemical analysis of endothelial (Dys)function and NO/cGMP signaling in human blood vessels with and without nitroglycerin pretreatment," *Circulation*, vol. 105, no. 10, pp. 1170–1175, 2002.

[12] M. Gao, W. Huang, and C.-Z. Liu, "Separation of scutellarin from crude extracts of *Erigeron breviscapus* (vant.) Hand. Mazz. by macroporous resins," *Journal of Chromatography B: Analytical Technologies in the Biomedical and Life Sciences*, vol. 858, no. 1-2, pp. 22–26, 2007.

[13] H. Guo, L.-M. Hu, S.-X. Wang et al., "Neuroprotective effects of scutellarin against hypoxic-ischemic-induced cerebral injury via augmentation of antioxidant defense capacity," *Chinese Journal of Physiology*, vol. 54, no. 6, pp. 399–405, 2011.

[14] X.-M. Hu, M.-M. Zhou, X.-M. Hu, and F.-D. Zeng, "Neuroprotective effects of scutellarin on rat neuronal damage induced by cerebral ischemia/reperfusion," *Acta Pharmacologica Sinica*, vol. 26, no. 12, pp. 1454–1459, 2005.

[15] Y. Su, W. Liu, L. Ma, X. Liu, Z. Liu, and B. Zhu, "Scutellarin inhibits translocation of protein kinase C in diabetic thoracic aorta of the rat," *Clinical and Experimental Pharmacology and Physiology*, vol. 39, no. 2, pp. 136–140, 2012.

[16] W. Yang, A. Bofferding, R. M. Lust, and C. J. Wingard, "Effect of scutellarin on contractile behavior of isolated thoracic aorta rings of the mouse," *The FASEB Journal*, vol. 21, no. 6, Article ID A1160, 2007.

[17] W. Yang, R. M. Lust, A. Bofferding, and C. J. Wingard, "Nitric oxide and catalase-sensitive relaxation by scutellarin in the mouse thoracic aorta," *Journal of Cardiovascular Pharmacology*, vol. 53, no. 1, pp. 66–76, 2009.

[18] D. S. Burley, P. Ferdinandy, and G. F. Baxter, "Cyclic GMP and protein kinase-G in myocardial ischaemia-reperfusion: opportunities and obstacles for survival signaling," *British Journal of Pharmacology*, vol. 152, no. 6, pp. 855–869, 2007.

[19] Z. Wang, T. Liu, L. Gan et al., "Shikonin protects mouse brain against cerebral ischemia/reperfusion injury through its antioxidant activity," *European Journal of Pharmacology*, vol. 643, no. 2-3, pp. 211–217, 2010.

[20] X. Zeng, S. Zhang, L. Zhang, K. Zhang, and X. Zheng, "A study of the neuroprotective effect of the phenolic glucoside gastrodin during cerebral ischemia in vivo and in vitro," *Planta Medica*, vol. 72, no. 15, pp. 1359–1365, 2006.

[21] L.-L. Lin, A.-J. Liu, J.-G. Liu, X.-H. Yu, L.-P. Qin, and D.-F. Su, "Protective effects of scutellarin and breviscapine on brain and heart ischemia in rats," *Journal of Cardiovascular Pharmacology*, vol. 50, no. 3, pp. 327–332, 2007.

[22] Z. Pan, W. Zhao, X. Zhang et al., "Scutellarin alleviates interstitial fibrosis and cardiac dysfunction of infarct rats by inhibiting TGFβ1 expression and activation of p38-MAPK and ERK1/2," *British Journal of Pharmacology*, vol. 162, no. 3, pp. 688–700, 2011.

[23] H. Hong and G.-Q. Liu, "Scutellarin protects PC12 cells from oxidative stress-induced apoptosis," *Journal of Asian Natural Products Research*, vol. 8, no. 6, pp. 471–479, 2006.

[24] S. Wang, H. Wang, H. Guo, L. Kang, X. Gao, and L. Hu, "Neuroprotection of Scutellarin is mediated by inhibition of microglial inflammatory activation," *Neuroscience*, vol. 185, pp. 150–160, 2011.

[25] Z.-X. Gao, D.-Y. Huang, H.-X. Li et al., "Scutellarin promotes in vitro angiogenesis in human umbilical vein endothelial cells," *Biochemical and Biophysical Research Communications*, vol. 400, no. 1, pp. 151–156, 2010.

[26] H. Dai, J. Gu, L.-Z. Li, L.-M. Yang, H. Liu, and J.-Y. Li, "Scutellarin benzyl ester partially secured the ischemic injury by its anti-apoptosis mechanism in cardiomyocytes of neonatal rats," *Journal of Chinese Integrative Medicine*, vol. 9, no. 9, pp. 1014–1021, 2011.

[27] L.-L. Guo, Z.-Z. Guan, Y. Huang, Y.-L. Wang, and J.-S. Shi, "The neurotoxicity of β-amyloid peptide toward rat brain is associated with enhanced oxidative stress, inflammation and apoptosis, all of which can be attenuated by scutellarin," *Experimental and Toxicologic Pathology*, vol. 65, no. 5, pp. 579–584, 2013.

[28] H.-F. Zhang, X.-M. Hu, L.-X. Wang, S.-Q. Xu, and F.-D. Zeng, "Protective effects of scutellarin against cerebral ischemia in rats: evidence for inhibition of the apoptosis-inducing factor pathway," *Planta Medica*, vol. 75, no. 2, pp. 121–126, 2009.

[29] D.-P. Jiang, Q. Li, J. Yang, J. M. Perelman, V. P. Kolosov, and X.-D. Zhou, "Scutellarin attenuates human-neutrophil-elastase-induced mucus production by inhibiting the PKC-ERK signaling pathway in vitro and in vivo," *The American Journal of Chinese Medicine*, vol. 39, no. 6, pp. 1193–1206, 2011.

[30] P. Luo, Z.-H. Tan, Z.-F. Zhang, H. Zhang, X.-F. Liu, and Z.-J. Mo, "Scutellarin isolated from *Erigeron multiradiatus* inhibits high glucose-mediated vascular inflammation," *Yakugaku Zasshi*, vol. 128, no. 9, pp. 1293–1299, 2008.

[31] H. Xu and S. Zhang, "Scutellarin-induced apoptosis in HepG2 hepatocellular carcinoma cells via a STAT3 pathway," *Phytotherapy Research*, vol. 27, no. 10, pp. 1524–1528, 2013.

[32] Y. Feng, S. Zhang, J. Tu et al., "Novel function of scutellarin in inhibiting cell proliferation and inducing cell apoptosis of human Burkitt lymphoma Namalwa cells," *Leukemia and Lymphoma*, vol. 53, no. 12, pp. 2456–2464, 2012.

[33] G.-H. Zhang, Q. Wang, J.-J. Chen, X.-M. Zhang, S.-C. Tam, and Y.-T. Zheng, "The anti-HIV-1 effect of scutellarin," *Biochemical and Biophysical Research Communications*, vol. 334, no. 3, pp. 812–816, 2005.

[34] W. Xu, R.-P. Zha, W.-Y. Wang, and Y.-P. Wang, "Effects of scutellarin on PKCγ in PC12 cell injury induced by oxygen and glucose deprivation," *Acta Pharmacologica Sinica*, vol. 28, no. 10, pp. 1573–1579, 2007.

[35] B. H. Neo, S. Kandhi, M. Ahmad, and M. S. Wolin, "Redox regulation of guanylate cyclase and protein kinase G in vascular responses to hypoxia," *Respiratory Physiology and Neurobiology*, vol. 174, no. 3, pp. 259–264, 2010.

[36] A. Aicher, C. Heeschen, S. Feil et al., "CGMP-dependent protein kinase I is crucial for angiogenesis and postnatal vasculogenesis," *PLoS ONE*, vol. 4, no. 3, Article ID e4879, 2009.

[37] B. Kemp-Harper and H. H. H. W. Schmidt, "cGMP in the vasculature," in *cGMP: Generators, Effectors and Therapeutic Implications*, vol. 191 of *Handbook of Experimental Pharmacology*, pp. 447–467, Springer, Berlin, Germany, 2009.

[38] D. Atochin, E. Buys, H. Swanson et al., "Abstract T P225: cGMP-dependent protein kinase I in smooth muscle cells protects against stroke injury in mice," *Stroke*, vol. 45, supplement 1, Article ID ATP225, 2014.

[39] Y. Chai, D.-M. Zhang, and Y.-F. Lin, "Activation of cGMP-dependent protein kinase stimulates cardiac ATP-sensitive potassium channels via a ROS/calmodulin/CaMKII signaling cascade," *PLoS ONE*, vol. 6, no. 3, Article ID e18191, 2011.

[40] J. E. Bear, J. J. Loureiro, I. Libova, R. Fässler, J. Wehland, and F. B. Gertler, "Negative regulation of fibroblast motility by Ena/VASP proteins," *Cell*, vol. 101, no. 7, pp. 717–728, 2000.

[41] L. Chen, G. Daum, K. Chitaley et al., "Vasodilator-stimulated phosphoprotein regulates proliferation and growth inhibition by nitric oxide in vascular smooth muscle cells," *Arteriosclerosis, Thrombosis, and Vascular Biology*, vol. 24, no. 8, pp. 1403–1408, 2004.

[42] T. M. Gomez and E. Robles, "The great escape: phosphorylation of Ena/VASP by PKA promotes filopodial formation," *Neuron*, vol. 42, no. 1, pp. 1–3, 2004.

[43] X. Wang, J. L. Pluznick, D. C. Settles, and S. C. Sansom, "Association of VASP with TRPC4 in PKG-mediated inhibition of the store-operated calcium response in mesangial cells," *American Journal of Physiology - Renal Physiology*, vol. 293, no. 6, pp. F1768–F1776, 2007.

Hindawi Publishing Corporation
Evidence-Based Complementary and Alternative Medicine
Volume 2015, Article ID 729017, 8 pages
http://dx.doi.org/10.1155/2015/729017

Research Article

Polydatin Inhibits Formation of Macrophage-Derived Foam Cells

Min Wu,[1] Meixia Liu,[2] Gang Guo,[3] Wengao Zhang,[4] and Longtao Liu[2]

[1]*Department of Cardiovascular Diseases, Guang'anmen Hospital, China Academy of Chinese Medical Sciences, Beijing 100053, China*
[2]*Xiyuan Hospital, China Academy of Chinese Medical Sciences, Beijing 100091, China*
[3]*Qilu Hospital of Shandong University, Jinan 250012, China*
[4]*Shandong University of Traditional Chinese Medicine, Shandong 250355, China*

Correspondence should be addressed to Longtao Liu; liulongtao1976@126.com

Received 1 March 2015; Accepted 4 May 2015

Academic Editor: Dan Hu

Rhizoma Polygoni Cuspidati, a Chinese herbal medicine, has been widely used in traditional Chinese medicine for a long time. Polydatin, one of the major active ingredients in *Rhizoma Polygoni Cuspidati*, has been recently shown to possess extensive cardiovascular pharmacological activities. In present study, we examined the effects of Polydatin on the formation of peritoneal macrophage-derived foam cells in Apolipoprotein E gene knockout mice ($ApoE^{-/-}$) and explored the potential underlying mechanisms. Peritoneal macrophages were collected from $ApoE^{-/-}$ mice and cultured *in vitro*. These cells sequentially were divided into four groups: Control group, Model group, Lovastatin group, and Polydatin group. Our results demonstrated that Polydatin significantly inhibits the formation of foam cells derived from peritoneal macrophages. Further studies indicated that Polydatin regulates the metabolism of intracellular lipid and possesses anti-inflammatory effects, which may be regulated through the PPAR-γ signaling pathways.

1. Introduction

Complications of atherosclerosis are the leading causes of death throughout the world. Atherosclerosis is a chronic, inflammatory disorder characterized by the deposition of excess lipids in the arterial intima [1–3]. Macrophage-derived foam cells play essential roles in all stages of atherosclerosis [4]. From early fatty-streak lesions to advanced plaques, macrophage-derived foam cells are integral to the development and progression of atherosclerosis. Lipid homeostasis, especially cholesterol homeostasis, plays a crucial role in the formation of foam cells [5]. Macrophage foam cell formation is a prominent feature of human atherosclerotic plaques, usually considered to be correlated to uptake of and inflammatory response to oxidized low density lipoproteins (ox-LDL) [6]. The limited efficacy of current treatment strategies for atherosclerosis and its complications highlights the urgent need for new therapeutic options [7].

Recruitment of macrophages and their subsequent uptake of ox-LDL by scavenger receptors are major cellular events contributing to fatty-streak formation [8]. Among the scavenger receptors, cluster of differentiation antigen 36 (CD36) is known to be the principal receptor in the process of foam cell formation [9, 10]. The most convincing data supporting a critical role of CD36 in foam cell formation and atherosclerosis are from studies of a CD36-null engineered mouse model. Macrophages isolated from CD36-deficient animals are profoundly defective in uptake of ox-LDL and foam cell formation. Accordingly, knockout of CD36 in proatherogenic ApoE-null mice protects the development of atherosclerosis lesions in these animals. Compared to CD36-intact ApoE-null mice fed with a western diet, these animals showed a more than 70% reduction in aortic lesion size [11].

Cholesterol efflux is considered as the most important key point with regard to maintenance of cholesterol homeostasis and atherosclerosis. One of the major potential cholesterol efflux pathways in macrophages is mediated by ATP-binding cassette transporter A1 (ABCA1). It promotes efflux of phospholipids and cholesterol to lipid-poor ApoA-I in a process that involves the direct binding of ApoA-I to the transporter.

So ABCA1 was considered as the key mediator of macrophage cholesterol efflux to mature HDL [12]. The intracellular cholesterol homeostasis in macrophages is dynamically regulated by cholesterol uptake and cholesterol efflux, processes that are tightly controlled by these scavenger receptors, such as CD36 and ABCA1 [13].

Peroxisome proliferators-activated receptor gamma (PPAR-γ) is a nuclear transcription factor that is highly expressed in macrophages and macrophage-derived foam cells in atherosclerotic lesions. PPAR-γ regulates cholesterol metabolism and attenuates inflammation [14]. It inhibits macrophage foam cell formation and atherosclerosis [15]. PPAR-γ promotes monocyte/macrophage differentiation and the uptake of ox-LDL by enhancing CD36 expression [16]. PPAR-γ is in the first step of the reverse-cholesterol-transport pathway through the activation of ABCA1-mediated cholesterol efflux in human macrophages [17]. Disruption of the PPAR-γ gene suppresses the expression of ABCA1 in macrophage and reduces cholesterol efflux. So PPAR-γ plays a critical role in the regulation of cholesterol homeostasis by controlling the expression of a group of genes that mediate cholesterol efflux from cells and its transport in plasma [18].

Rhizoma Polygoni Cuspidati, a traditional Chinese herbal medicine, was thought to have actions of "dispelling dampness, alleviating jaundice, clearing heat, subsiding toxin, activating blood, and removing stasis" [19]. Polydatin, one of its chief active ingredients, has been shown to possess extensive cardiovascular pharmacological activities in recent pharmacological studies. Polydatin was shown to markedly affect the regulation of blood lipid, protecting cardiomyocytes, dilating blood vessels, antagonizing platelet aggregation, thrombosis, and atherosclerosis [20]. However, the direct effects of Polydatin on the uptake of ox-LDL by macrophages and formation of foam cells have not yet been elucidated. The mechanism of the antiatherosclerotic effects of Polydatin also remains unclear.

To clarify the effect of Polydatin on peritoneal macrophage-derived foam cells of ApoE$^{-/-}$ mice, we investigated the action of Polydatin on the uptake of ox-LDL, the metabolism of intracellular lipid, the expression of inflammatory factors, and mRNA expression of PPAR-γ, ABCA1, and CD36 in peritoneal macrophage. Our results demonstrated that Polydatin significantly inhibits the formation of foam cells in peritoneal macrophages. Polydatin has significant anti-inflammatory effects and regulates the metabolism of lipid, possibly through the PPAR-γ signaling pathways.

2. Materials and Methods

2.1. Animals. Six-week-old ApoE$^{-/-}$ mice were purchased from the Jackson Laboratory (USA) and bred by the Laboratory Animal Center of Beijing University, weighing 19 to 21 g.

2.2. Reagents and Chemicals. Polydatin was extracted and purified from *Rhizoma Polygoni Cuspidati* by Xi'an Guanyu BioTech Co. Ltd. The purity of Polydatin is 99.42%. Lovastatin was purchased by Beijing Winsunny Co. Ltd. RPMI 1640, fetal bovine serum (FBS), and antibiotics (streptomycin/penicillin) were purchased from Gibco (BRL Life Technologies, Grand Island, NY). TNF-α and IL-6 ELISA kits were purchased from Shanghai Westang BioTech Inc., Ltd., Shanghai.

2.3. Isolation and Culture of Mouse Peritoneal Macrophages. The ApoE$^{-/-}$ mice were sacrificed by cervical dislocation, in accordance with the Principles of Laboratory Animal Care (NIH publication number 85-23, revised 1985) and the Guidelines of the Animal Investigation Committee of Peking University. Sterile ice-cold phosphate-buffered saline (PBS) was injected into the peritoneal cavity of each mouse and peritoneal lavage was performed. This fluid was carefully collected and centrifuged at 1,000 rpm for 6 min. After centrifugation, the supernatant was then discarded, and the cell pellet was resuspended in RPMI 1640 medium (containing 100 IU/mL of penicillin, 100 μg/mL of streptomycin, and 100 μg/mL of l-glutamine) and plated in 6-well tissue culture plates (Costar) at 1.5×10^6 cells per well. Cells were incubated in a humidified atmosphere of 5% CO_2 at 37°C for 2-3 h to allow adherence, and nonadherent cells were rinsed away with prewarmed RPMI 1640 medium and 2 mL of complete RPMI 1640 medium (supplemented with 10% fetal bovine serum) was added. Media with all additions were replaced daily and macrophages were used within 5 days from harvesting for further analysis [21, 22].

2.4. LDL Modification. LDL was exposed to 5 μmol/L $CuSO_4$ for 24 hours at 37°C. Cu^{2+} was then removed by extensive dialysis. The extent of modification was determined by measurement of thiobarbituric acid-reactive substances. ox-LDL containing 30–60 nmol thiobarbituric acid-reactive substances defined as malondialdehyde equivalents per milligram of LDL protein was used for experiments [23].

2.5. Groups. Peritoneal macrophages of ApoE$^{-/-}$ mice were collected and divided into 4 groups: Control group (treated with calf serum 250 μL), Model group (treated with calf serum 250 μL and ox-LDL 250 μg), Lovastatin group (treated with calf serum 250 μL, ox-LDL 250 μg, and 110 μg/mL Lovastatin), and Polydatin group (treated with calf serum 250 μL, ox-LDL 250 μg, and 8.9 μg/mL Polydatin). Culture fluid was added to make up for 2.5 mL in all groups.

2.6. Ultrastructural Structure Observation of Macrophage Cells. After being loaded with ox-LDL, Polydatin, and Lovastatin for 48 h, those macrophages were centrifuged at 400 g for 10 min, and the pellets produced were washed with PBS and then mixed with 2% (v/v) P-formaldehyde-glutaraldehyde in 0.05 M cacodylate buffer (pH 7.4) for 4 hours at 4°C. After that, the pellets were prepared for transmission electron microscope (JEM-1200EX).

2.7. Intracellular Lipid Analysis in Macrophages. Intracellular lipids in macrophages were extracted with hexane/isopropyl alcohol (3 : 2) after 0, 24, and 48 h of incubation with ox-LDL, Polydatin, and Lovastatin, evaporated, and then dissolved in isopropyl alcohol containing 10% Triton X-100 for preparation of a sample solution. Free cholesterol and total cholesterol were determined by commercial assay

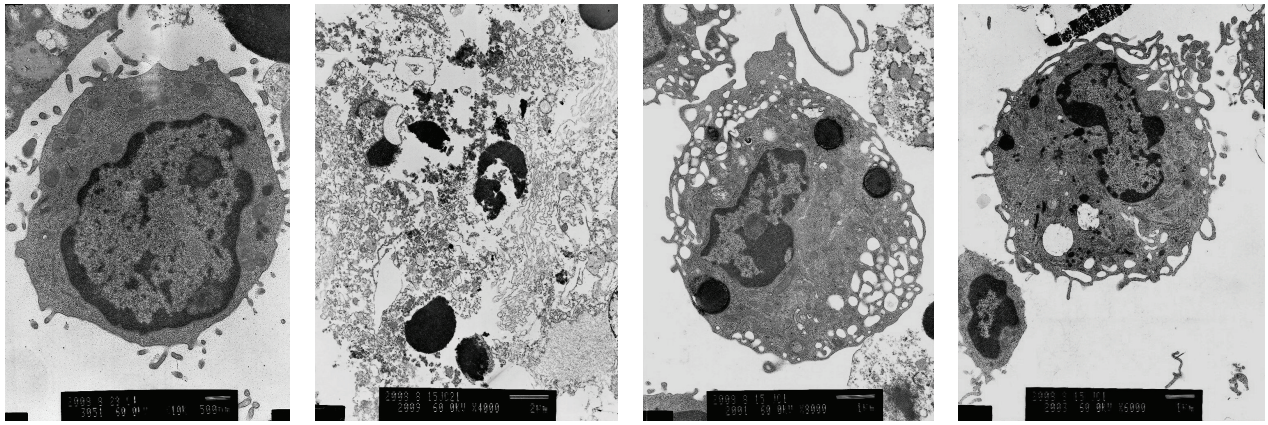

(a) (b) (c) (d)

Figure 1: Polydatin protects the ultrastructure of peritoneal macrophage. (a) Control group, (b) Model group, (c) Lovastatin group, (d) Polydatin group.

systems (Wako Chemicals). Cholesterol ester was estimated by subtracting free cholesterol from total cholesterol. The experiment was repeated at three times.

2.8. Protein Levels of TNF-α and IL-1β Detection with ELISA. After 24 h and 48 h of incubation with ox-LDL, the levels of TNF-α and IL-6 in the cultured media were measured by ELISA kits according to the manufacturer's instructions (Shanghai Westang BioTech Inc., Ltd., Shanghai). The ELISA data were obtained at least at three independent experiments.

2.9. RT-PCR Analysis of Expression of PPAR-γ, ABCA1, and CD36 mRNA. The total RNA was extracted from cultured peritoneal macrophages using RNA isolation kit (Sangong BioTech Co., Ltd., Shanghai), according to the manufacturer's instructions. cDNAs were prepared from 0.3 μg of RNA.

RT-PCR was performed according to the manufacturer's instructions, using oligonucleotide primers to detect PPAR-γ, ABCA1, and CD36 mRNA (Sangong BioTech Co., Ltd., Shanghai), PPAR-γ (403 bp): sense 5′-CCCTGGCAAAGC-ATTTGTAT-3′, antisense 5′-AATCCTTGGCCCTCTGAG-AT-3′; ABCA1 (364 bp): sense 5′-CAGATGCCCTACCCC-TGTTA-3′, antisense 5′-GGGAGAAGAGCGTGCTAATG-3′; CD36 (418 bp): sense 5′-CCTTAAAGGAATCCCCGT-GT-3′, antisense 5′-CCAATGGTCCCAGTCTCATT-3′; β-actin (302 bp): sense 5′-TCCTCCCTGGAGAAGAGCTA-3′, antisense, 5′-TCA GGA GGA GCA ATG ATC TTG-3′ [24]. This experiment was repeated at least three times.

2.10. Statistical Analysis. The results are expressed as mean ± SD values for the number of experiments. Statistical significance was compared in each treated group with the negative control and determined by one-way ANOVA test. Each experiment was repeated at least three times. SPSS version 13.0 (SPSS Inc., IL, USA) was used for analysis. Values with $P < 0.05$ were considered significant.

3. Results

3.1. Polydatin Protects the Ultrastructure of Peritoneal Macrophage Cells. To examine the potential effects of Polydatin on macrophage cells, the mouse macrophages were incubated with ox-LDL for 48 h in the absence or presence of Polydatin and the ultrastructure was evaluated under electron microscope. The normal structure of macrophage is shown in Figure 1(a). In comparison, the structure of macrophages in the Model group was completely damaged and the organelles in the periplasm disappeared. The nucleus split into multiple shivers with different sizes. The structure of the nuclear membrane, nucleoli, and euchromatin disappeared (Figure 1(b)). In Polydatin and Lovastatin group, the structure of nucleus was integrated. The nuclear membrane, nucleolus, and abundant euchromatin were observed. A part of the organelles was damaged and vacuolization was observed. These suggested that peritoneal macrophage of ApoE$^{-/-}$ mice had favorable response and phagocytosis ability to ox-LDL. Combined treatment with Polydatin/Lovastatin and ox-LDL significantly reduced the damage of ox-LDL on intracellular ultrastructure in macrophages compared to the group of ox-LDL treatment alone (Figures 1(c) and 1(d)).

3.2. Polydatin Regulates the Metabolism of Intracellular Lipid in Peritoneal Macrophage Cells. After being loaded with ox-LDL for 24 h and 48 h, the levels of total cholesterol, free cholesterol, and cholesterol ester in macrophages in Model group were elevated. The ratio of cholesterol ester to total cholesterol in macrophage was more than 50% in Model group, which is in accordance with the pathological change of foam cells. After treatment for 24 h and 48 h, Polydatin and Lovastatin significantly reduced cholesterol accumulation in ox-LDL loaded macrophages. There was no difference observed between Polydatin and Lovastatin group (Figures 2(a)–2(d)).

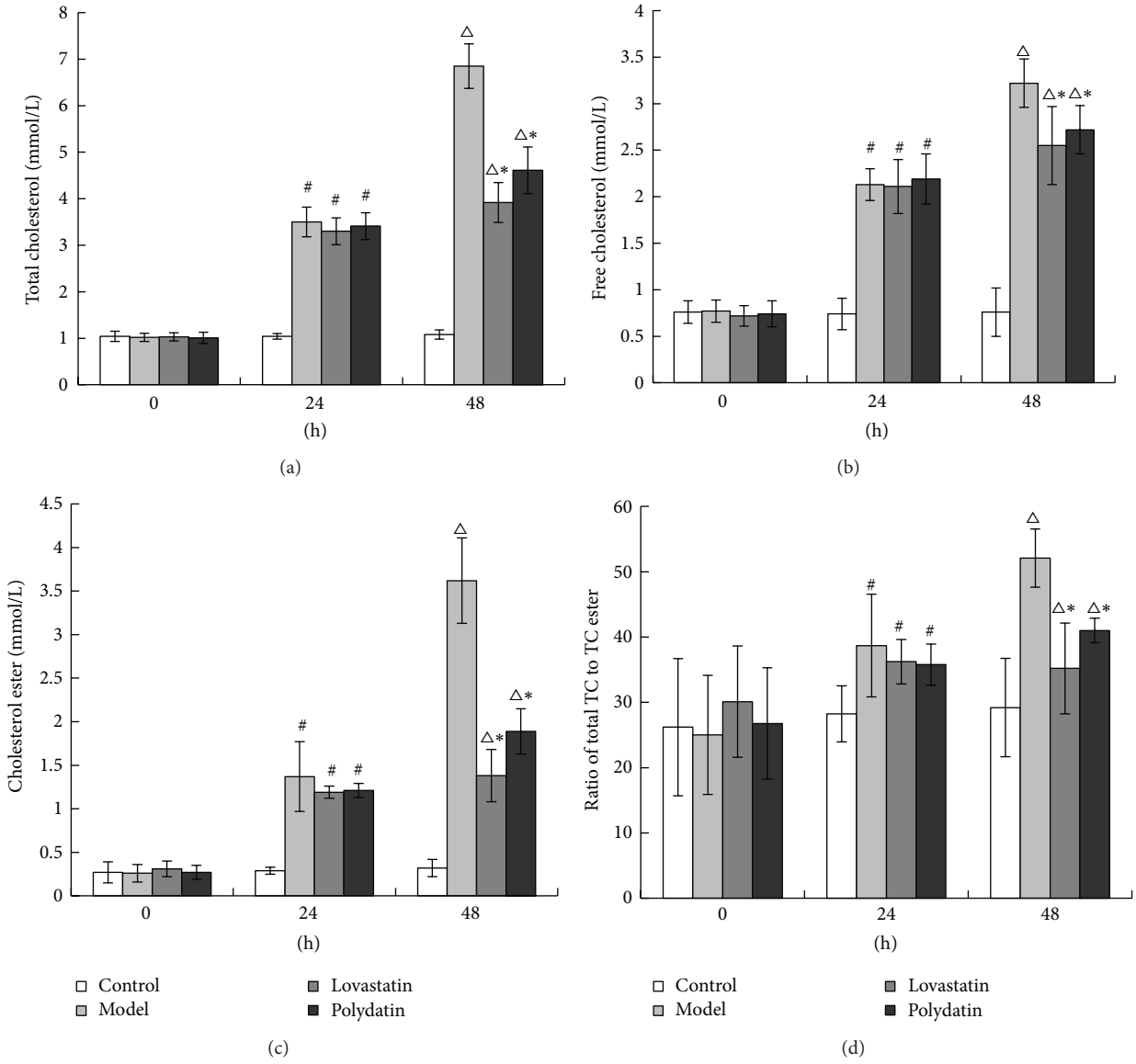

Figure 2: Polydatin regulates the metabolism of intracellular lipid in peritoneal macrophage cells. (a) Level of total cholesterol, (b) level of free cholesterol, (c) level of cholesterol ester, (d) ratio of cholesterol ester to total cholesterol. $^{\#}P < 0.01$, $^{\triangle}P < 0.01$, compared with the Control group. $^{*}P < 0.01$, compared with the Model group.

3.3. Polydatin Reduces Protein Levels of TNF-α and IL-1β in Peritoneal Macrophage Cells. To further investigate the potential effect of Polydatin on inflammatory factors, the expression of TNF-α and IL-1β in the peritoneal macrophage cells was evaluated by ELISA. After ox-LDL treatment for 24 h and 48 h, the protein level of TNF-α and IL-1β was significantly increased. Polydatin and Lovastatin reduced the expression of the TNF-α and IL-1β levels. And there was no difference between Polydatin and Lovastatin group (Figures 3(a) and 3(b)). This illustrated that chemotropism of peritoneal macrophages in ApoE$^{-/-}$ mice is enhanced by ox-LDL, accompanied by produce of abundant inflammatory factors, such as TNF-α and IL-1β.

3.4. Polydatin Regulates mRNA Expression of PPAR-γ, ABCA1, and CD36 in Peritoneal Macrophage Cells. The mRNA expression of PPAR-γ, ABCA1, and CD36 was examined by RT-PCR to determine whether Polydatin has a suppressive effect on the PPAR-γ pathway in the peritoneal macrophage cells. After ox-LDL treatment for 24 h and 48 h, the mRNA levels of PPAR-γ, ABCA1, and CD36 were remarkably increased in peritoneal macrophage cells. However, the mRNA expression of PPAR-γ and ABCA1 was found to increase in Polydatin and Lovastatin group after 24 and 48 h treatment, compared to the ox-LDL treatment group. But the mRNA expression of CD36 was reduced significantly in Polydatin and Lovastatin group after 24 h treatment. There

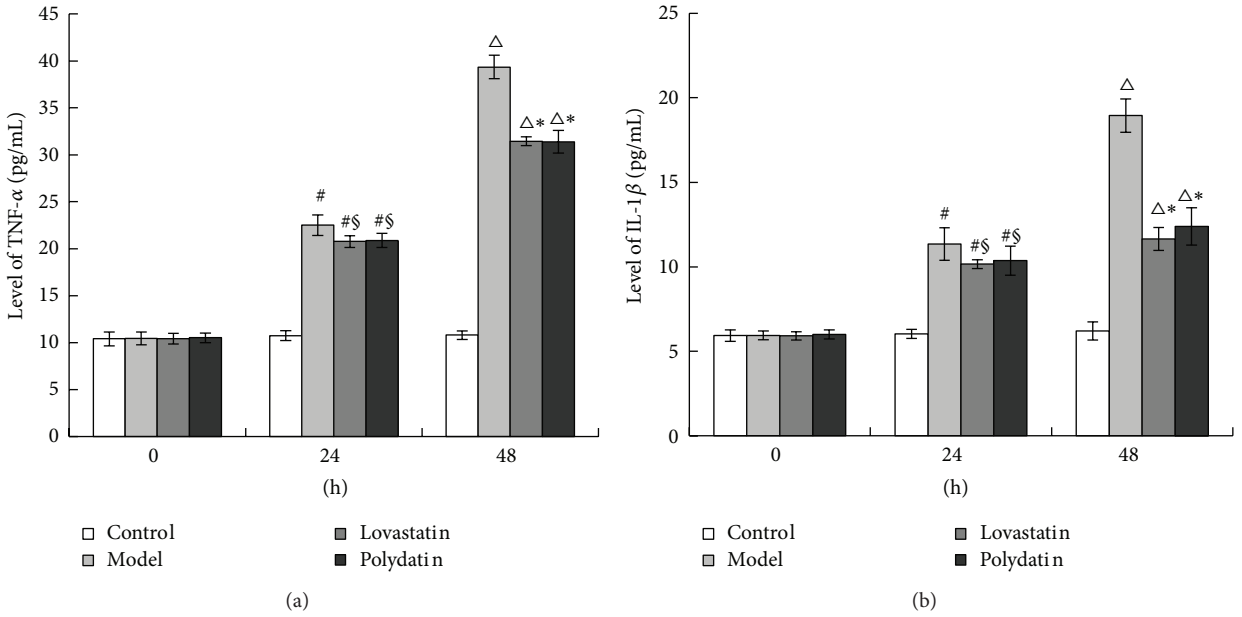

Figure 3: Polydatin reduces the protein level of TNF-α and IL-1β in peritoneal macrophage cells. (a) TNF-α level; (b) IL-1β level. $^{\#}P < 0.01$, $^{\triangle}P < 0.01$, compared with the Control group. $^{\S}P < 0.05$, $^{*}P < 0.01$, compared with the Model group.

was no difference in the mRNA expression of PPAR-γ and CD36 between the Polydatin and Lovastatin group. But the mRNA expression of ABCA1 in Polydatin group was higher than that in Lovastatin group ($P < 0.05$) (Figures 4(a)–4(f)).

4. Discussion

Atherosclerosis begins early in life and frequently leads to severe complications in later life with high morbidity and mortality. Macrophage cholesterol accumulation-induced foam cell formation is the hallmark of early atherosclerosis [25]. Elucidation of molecular and cellular processes involving macrophages has led to numerous therapeutic targets being suggested [7]. Cholesterol accumulation in macrophages can result from an unbalanced cellular cholesterol flux, increased uptake of atherogenic lipoproteins, and/or decreased cholesterol efflux from the cells [26–28]. In our study, we showed that Polydatin could increase cholesterol efflux from macrophage and decrease the uptake of ox-LDL, thus resulting in the inhibition of cholesterol accumulation in macrophage. Its mechanism is possibly induced in a PPAR-γ-dependent manner.

Large sample clinical trials have confirmed that the statins have antiatherosclerotic effects, including improving endothelial function, suppressing platelet aggregation, increasing anti-inflammatory effects, and stabilizing atherosclerotic plaque [29–32]. However, the statins result in some significant side effects. So we try to find the new medicine from Chinese herbs which have the antiatherosclerotic effects and regulate lipid, but with few side effects. The search for new drugs with antiatherosclerosis and lipid-regulation effects has gained momentum over the years, resulting in numerous reports on significant activities of natural agents. Many classes of dietary components and natural compounds have been tested to regulate serum lipid concentrations with the aim of lowering the incidence of atherosclerosis and coronary heart disease [20, 33]. Our research group found that Polydatin can decrease carotid intima-media thickness (IMT), plaque integral and reduce the level of plaque stability related serum indexes such as Hs-CRP, MMP-1, and TIMP in patients with carotid atherosclerosis [34, 35].

Rhizoma Polygoni Cuspidati is recorded first in the book named *Miscellaneous Records of Famous Physicians* (Ming Yi Bie Lu). Modern pharmacological studies have shown that it has obvious antibacterial, anti-inflammation, diuresis, purgation, and menstrual restoration effects [36]. As one of its main ingredients, Polydatin has multiple biological actions, such as liver protection, anti-inflammation, antitumor, and antipathogenic microbe, and is applied to prevent/treat cardiovascular diseases. Particularly, its cardiovascular pharmacological actions, such as cardiomyocyte (CM) protection, vascular smooth muscle dilation, platelet aggregation, thrombosis, and atherosclerosis prevention, have received great attention from scholars of related fields in latest years [37].

Cholesterol-loaded macrophages or foam cells are a major contributor to the atherosclerotic plaque. *In vitro* studies have shown that modified forms of low density lipoprotein cause accumulation of cholesterol esters in cultured macrophages [38]. In this study, we collected the peritoneal macrophages from ApoE$^{-/-}$ mice, which have become the most widely used rodent model for the study of atherosclerosis [39, 40]. Then we stimulated the macrophage cells by ox-LDL to get the "foam cell" model. The results showed that the ratio of cholesterol ester to total cholesterol in macrophage is more than 50% in Model group and this is consistent with the pathological change of foam cells. We used the MTT analysis method to decide the appropriate dosage of Polydatin and Lovastatin (data not showed). In our study,

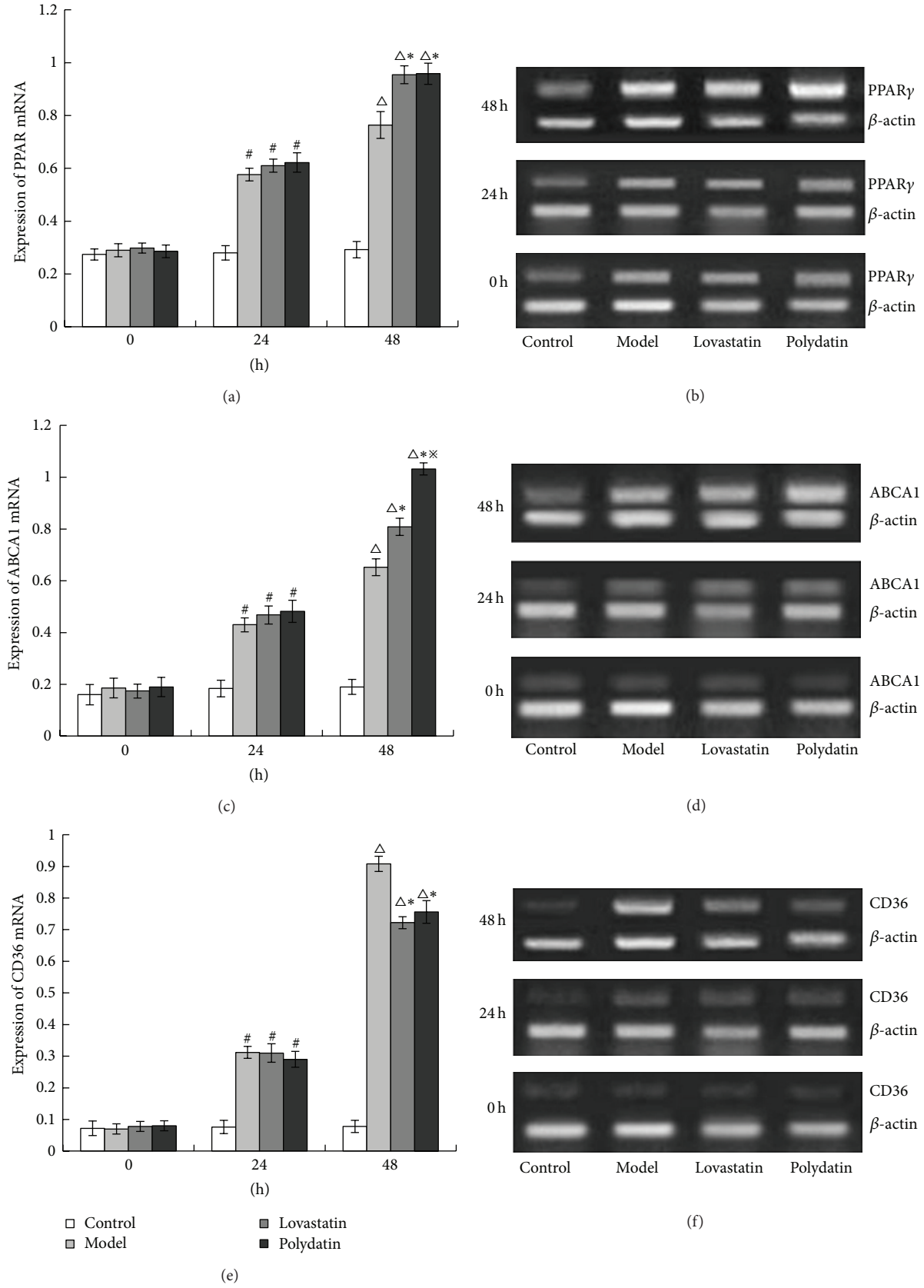

FIGURE 4: Polydatin regulates mRNA expression of PPAR-γ, ABCA1, and CD36 in peritoneal macrophage cells. Figures (b), (d), and (f) are the mRNA expression of PPAR-γ, ABCA1, and CD36. (a), (c), and (e) are quantitated from these results. $^{\#}P < 0.01$, $^{\triangle}P < 0.01$, compared with the Control group. $^{*}P < 0.01$, compared with the Model group, $^{※}P < 0.05$, compared with the Lovastatin group.

we found that combined treatment with Polydatin/Lovastatin and ox-LDL significantly relieve the damage of ox-LDL on intracellular ultrastructure in macrophages compared with the ox-LDL loaded cells. Polydatin and Lovastatin regulate the metabolism of intracellular lipid and so confer the protective role in the formation of macrophage foam cells.

In the study, we found that, after incubation with ox-LDL for 24 h and 48 h, peritoneal macrophage of ApoE$^{-/-}$ mice had favorable responsibility and phagocytosis ability to ox-LDL and abundant inflammatory factors were secreted. Working together, these effects could inhibit the elevation of TNF-α, IL-1β. We did not observe any difference between the Polydatin and Lovastatin group, suggesting the efficacy of Polydatin is comparable to Lovastatin.

CD36 and ABCA1 are the downstream target genes which are transcriptionally controlled by PPAR-γ. CD36 is correlated to intracellular cholesterol accumulation. ABCA1 can promote diffluence of free cholesterol and phosphatides from cells. The activated PPAR-γ by ox-LDL can induce CD36 expression in the macrophage, promote the uptake of ox-LDL, increase intracellular cholesterol accumulation, and then motivate foam cell formation [16]. This is the positive feedback pathway. At the same time, the activated PPAR-γ also upregulates ABCA1 expression, reduces cholesterol, and then inhibits foam cell formation. This is the negative feedback pathway. Therefore, the regulation of the ox-LDL-PPAR-γ-CD36 and ox-LDL-PPAR-γ-ABCA1 signaling pathways is important for inhibition of foam cell formation and antiatherosclerosis [41]. In our study, we examined whether the expression of PPAR-γ affects the expression of ABCA1 and CD36. After treating with ox-LDL, Polydatin, and Lovastatin for 24 h and 48 h, the expression of PPAR-γ, ABCA1, and CD36 at mRNA levels was increased. Polydatin and Lovastatin might upregulate the mRNA expression of PPAR-γ and ABCA1 and downregulate the mRNA expression of CD36. This suggests that Polydatin might regulate the expression of ABCA1 mRNA and CD36 mRNA through activating the PPAR-γ signaling, which sequentially inhibit the formation of macrophage foam cells.

In conclusion, our studies have indicated that Polydatin inhibits the formation of peritoneal macrophage-derived foam cells of ApoE$^{-/-}$ mice. Further investigation has shown that Polydatin has anti-inflammatory effects and regulates the metabolism of intracellular lipid, possibly through the PPAR-γ signaling pathway. Thus, our data have provided some experimental evidences to use Polydatin in prevention and cure of atherosclerosis.

Disclosure

The funders had no role in study design, data collection and analysis, decision to publish, or preparation of the paper.

Conflict of Interests

All the authors of this paper declare that they do not have a direct financial relation with the commercial identities mentioned in the paper.

Authors' Contribution

Min Wu and Meixia Liu equally contributed to the paper.

Acknowledgments

This work was supported by the National Natural Science Foundation of China (no. 81102721 and no. 81202805), A Planned Technologic Item of State Administration of Traditional Chinese Medicine (no. 04-05LP30), Chinese National Scientific Fund for Post-Doctor (no. 20070410622), Its Special Aid Item (no. 201003226), and the Key Technologies R & D Program of Shandong Province, China (no. 2010 GSF 10289).

References

[1] R. Ross, "Atherosclerosis—an inflammatory disease," *The New England Journal of Medicine*, vol. 340, no. 2, pp. 115–126, 1999.

[2] C. K. Glass and J. L. Witztum, "Atherosclerosis: the road ahead," *Cell*, vol. 104, no. 4, pp. 503–516, 2001.

[3] A. J. Lusis, "Atherosclerosis," *Nature*, vol. 407, no. 6801, pp. 233–241, 2000.

[4] T. Gui, A. Shimokado, Y. Sun, T. Akasaka, and Y. Muragaki, "Diverse roles of macrophages in atherosclerosis: from inflammatory biology to biomarker discovery," *Mediators of Inflammation*, vol. 2012, Article ID 693083, 14 pages, 2012.

[5] Y. Yuan, P. Li, and J. Ye, "Lipid homeostasis and the formation of macrophage-derived foam cells in atherosclerosis," *Protein & Cell*, vol. 3, no. 3, pp. 173–181, 2012.

[6] J. Persson, J. Nilsson, and M. W. Lindholm, "Cytokine response to lipoprotein lipid loading in human monocyte-derived macrophages," *Lipids in Health and Disease*, vol. 5, article 17, 2006.

[7] R. P. Choudhury, J. M. Lee, and D. R. Greaves, "Mechanisms of disease: macrophage-derived foam cells emerging as therapeutic targets in atherosclerosis," *Nature Clinical Practice Cardiovascular Medicine*, vol. 2, no. 6, pp. 309–315, 2005.

[8] M. Febbraio, D. P. Hajjar, and R. L. Silverstein, "CD36: a class B scavenger receptor involved in angiogenesis, atherosclerosis, inflammation, and lipid metabolism," *Journal of Clinical Investigation*, vol. 108, no. 6, pp. 785–791, 2001.

[9] V. V. Kunjathoor, M. Febbraio, E. A. Podrez et al., "Scavenger receptors class A-I/II and CD36 are the principal receptors responsible for the uptake of modified low density lipoprotein leading to lipid loading in macrophages," *Journal of Biological Chemistry*, vol. 277, no. 51, pp. 49982–49988, 2002.

[10] S. O. Rahaman, D. J. Lennon, M. Febbraio, E. A. Podrez, S. L. Hazen, and R. Silverstein, "A CD36-dependent signaling cascade is necessary for macrophage foam cell formation," *Cell Metabolism*, vol. 4, no. 3, pp. 211–221, 2006.

[11] M. Febbraio, E. A. Podrez, J. D. Smith et al., "Targeted disruption of the class B, scavenger receptor CD36 protects against atherosclerotic lesion development in mice," *Journal of Clinical Investigation*, vol. 105, no. 8, pp. 1049–1056, 2000.

[12] N. Wang, D. L. Silver, C. Thiele, and A. R. Tall, "ATP-binding cassette transporter A1 (ABCA1) functions as a cholesterol efflux regulatory protein," *The Journal of Biological Chemistry*, vol. 276, no. 26, pp. 23742–23747, 2001.

[13] D. Li, D. Wang, Y. Wang, W. Ling, X. Feng, and M. Xia, "Adenosine monophosphate-activated protein kinase induces

cholesterol efflux from macrophage-derived foam cells and alleviates atherosclerosis in apolipoprotein E-deficient mice," *The Journal of Biological Chemistry*, vol. 285, no. 43, pp. 33499–33509, 2010.

[14] A. C. Li, C. J. Binder, A. Gutierrez et al., "Differential inhibition of macrophage foam-cell formation and atherosclerosis in mice by PPARalpha, beta/delta, and gamma," *The Journal of Clinical Investigation*, vol. 114, no. 11, pp. 1564–1576, 2004.

[15] A. Castrillo and P. Tontonoz, "PPARs in atherosclerosis: the clot thickens," *The Journal of Clinical Investigation*, vol. 114, no. 11, pp. 1538–1540, 2004.

[16] P. Tontonoz, L. Nagy, J. G. A. Alvarez, V. A. Thomazy, and R. M. Evans, "PPARgamma promotes monocyte/macrophage differentiation and uptake of oxidized LDL," *Cell*, vol. 93, no. 2, pp. 241–252, 1998.

[17] G. Chinetti, S. Lestavel, V. Bocher et al., "PPAR-alpha and PPAR-gamma activators induce cholesterol removal from human macrophage foam cells through stimulation of the ABCA1 pathway," *Nature Medicine*, vol. 7, no. 1, pp. 53–58, 2001.

[18] T. E. Akiyama, S. Sakai, G. Lambert et al., "Conditional disruption of the peroxisome proliferator-activated receptor γ gene in mice results in lowered expression of ABCA1, ABCG1, and apoE in macrophages and reduced cholesterol efflux," *Molecular and Cellular Biology*, vol. 22, no. 8, pp. 2607–2619, 2002.

[19] X. H. Kong and L. Z. Zhou, "Study progress of glant knotweed rhizome," *Guiding Journal of Traditional Chinese Medicine and Pharmacy*, vol. 15, no. 5, pp. 107–110, 2009.

[20] L.-T. Liu, G. Guo, M. Wu, and W.-G. Zhang, "The progress of the research on cardio-vascular effects and acting mechanism of polydatin," *Chinese Journal of Integrative Medicine*, vol. 18, no. 9, pp. 714–719, 2012.

[21] M. Ogawa, S. Nakamura, Y. Saito, M. Kosugi, and Y. Magata, "What can be seen by ^{18}F-FDG PET in atherosclerosis imaging? The effect of foam cell formation on ^{18}F-FDG uptake to macrophages in vitro," *Journal of Nuclear Medicine*, vol. 53, no. 1, pp. 55–58, 2012.

[22] S. Xu, Y. Huang, Y. Xie et al., "Evaluation of foam cell formation in cultured macrophages: an improved method with Oil Red O staining and DiI-oxLDL uptake," *Cytotechnology*, vol. 62, no. 5, pp. 473–481, 2010.

[23] K.-Y. Lu, L.-C. Ching, K.-H. Su et al., "Erythropoietin suppresses the formation of macrophage foam cells: role of liver X receptor α," *Circulation*, vol. 121, no. 16, pp. 1828–1837, 2010.

[24] M. Ditiatkovski, B.-H. Toh, and A. Bobik, "GM-CSF deficiency reduces macrophage PPAR-γ expression and aggravates atherosclerosis in ApoE-deficient mice," *Arteriosclerosis, Thrombosis, and Vascular Biology*, vol. 26, no. 10, pp. 2337–2344, 2006.

[25] J. A. Berliner, M. Navab, A. M. Fogelman et al., "Atherosclerosis: basic mechanisms: oxidation, inflammation, and genetics," *Circulation*, vol. 91, no. 9, pp. 2488–2496, 1995.

[26] M. Aviram, "Interaction of oxidized low density lipoprotein with macrophages in atherosclerosis, and the antiatherogenicity of antioxidants," *European Journal of Clinical Chemistry and Clinical Biochemistry*, vol. 34, no. 8, pp. 599–608, 1996.

[27] D. Steinberg, "Low density lipoprotein oxidation and its pathobiological significance," *The Journal of Biological Chemistry*, vol. 272, no. 34, pp. 20963–20966, 1997.

[28] M. Kaplan, T. Hayek, A. Raz et al., "Pomegranate juice supplementation to atherosclerotic mice reduces macrophage lipid peroxidation, cellular cholesterol accumulation and development of atherosclerosis," *Journal of Nutrition*, vol. 131, no. 8, pp. 2082–2089, 2001.

[29] J. Tian, X. Gu, Y. Sun et al., "Effect of statin therapy on the progression of coronary atherosclerosis," *BMC Cardiovascular Disorders*, vol. 12, article 70, 2012.

[30] Y. Huang, W. Li, L. Dong, R. Li, and Y. Wu, "Effect of statin therapy on the progression of common carotid artery intima-media thickness: an updated systematic review and meta-analysis of randomized controlled trials," *Journal of Atherosclerosis and Thrombosis*, vol. 20, no. 1, pp. 108–121, 2013.

[31] O. Hegland, M. W. Kurz, P. S. Munk, and J. P. Larsen, "The effect of statin therapy on the progression of carotid artery stenosis in relation to stenosis severity," *Acta Neurologica Scandinavica*, vol. 121, no. 1, pp. 11–15, 2010.

[32] C. P. Cannon, E. Braunwald, C. H. McCabe et al., "Intensive versus moderate lipid lowering with statins after acute coronary syndromes," *The New England Journal of Medicine*, vol. 350, no. 15, pp. 1495–1504, 2004.

[33] J. Du, L.-N. Sun, W.-W. Xing et al., "Lipid-lowering effects of polydatin from *Polygonum cuspidatum* in hyperlipidemic hamsters," *Phytomedicine*, vol. 16, no. 6-7, pp. 652–658, 2009.

[34] L. T. Liu, M. Wu, W. G. Zhang et al., "Clinical study on treatment of carotid atherosclerosis with extraction of Polygoni Cuspidati Rhizoma et Radix and Crataegi Fructus: a randomized controlled trial," *China Journal of Chinese Materia Medica*, vol. 39, no. 6, pp. 1115–1119, 2014.

[35] L. T. Liu, G. J. Zheng, W. G. Zhang, G. Guo, and M. Wu, "Clinical study on treatment of carotid atherosclerosis with polydatin," *Beijing Journal of Traditional Chinese Medicine*, vol. 28, no. 3, pp. 172–175, 2009.

[36] S. H. Gao, S. L. Yang, and G. R. Fan, "Study progress of polydatin," *Journal Pharmaceutical Practice*, vol. 23, no. 6, pp. 145–147, 2005.

[37] S. Das and D. K. Das, "Resveratrol: a therapeutic promise for cardiovascular diseases," *Recent Patents on Cardiovascular Drug Discovery*, vol. 2, no. 2, pp. 133–138, 2007.

[38] M. Pataki, G. Lusztig, and H. Robenek, "Endocytosis of oxidized LDL and reversibility of migration inhibition in macrophage-derived foam cells in vitro. A mechanism for atherosclerosis regression?" *Arteriosclerosis and Thrombosis*, vol. 12, no. 8, pp. 936–944, 1992.

[39] J. L. Breslow, "Mouse models of atherosclerosis," *Science*, vol. 272, no. 5262, pp. 685–688, 1996.

[40] R. L. Reddick, S. H. Zhang, and N. Maeda, "Atherosclerosis in mice lacking Apo E. Evaluation of lesional development and progression," *Arteriosclerosis, Thrombosis, and Vascular Biology*, vol. 14, no. 1, pp. 141–147, 1994.

[41] Y. Zhu, W. G. Zhang, G. J. Zheng, and H. Jiang, "PPARγ with atherosclerosis and intervention study of traditional Chinese medicine," *Chinese Journal of Integrative Medicine on Cardio/Cerebrovascular Disease*, vol. 5, no. 3, pp. 225–227, 2007.

Hindawi Publishing Corporation
Evidence-Based Complementary and Alternative Medicine
Volume 2015, Article ID 709568, 6 pages
http://dx.doi.org/10.1155/2015/709568

Research Article

Nao-Xue-Shu Oral Liquid Improves Aphasia of Mixed Stroke

Yuping Yan,[1] Mingzhe Wang,[2] Liang Zhang,[3] Zhenwei Qiu,[4] Wenfei Jiang,[2] Men Xu,[2] Weidong Pan,[2] and Xiangjun Chen[5]

[1] *Shanghai Business School, Room 612, Administrative Building, No. 123, Fengpu Avenue, Fengxian District, Shanghai 201400, China*
[2] *Department of Neurology, Shuguang Hospital Affiliated to Shanghai University of TCM, No. 528, Zhang-Heng Road, Pu-Dong New Area, Shanghai 201203, China*
[3] *Department of Neurology, Shanghai Seventh Hospital, Shanghai University of Traditional Chinese Medicine, Shanghai 200137, China*
[4] *Department of Emergency, Shuguang Hospital Affiliated to Shanghai University of TCM, No. 528, Zhang-Heng Road, Pu-Dong New Area, Shanghai 201203, China*
[5] *Department of Neurology, Hua Shan Hospital Affiliated to Fu Dan University, No. 12, Wu Lu Mu Qi Zhong Road, Shanghai 200040, China*

Correspondence should be addressed to Weidong Pan; panwd@medmail.com.cn and Xiangjun Chen; xiangjunchen@hotmail.com

Received 11 March 2015; Accepted 27 April 2015

Academic Editor: Zhang Tan

Objective. The objective is to observe whether the traditional Chinese medicine (TCM) *Nao-Xue-Shu* oral liquid improves aphasia of mixed stroke. *Methods*. A total of 102 patients with aphasia of mixed stroke were divided into two groups by a single blind random method. The patients treated by standard Western medicine plus *Nao-Xue-Shu* oral liquid ($n = 58$) were assigned to the treatment group while the remaining patients treated only by standard Western medicine ($n = 58$) constituted the control group. Changes in the Western Aphasia Battery (WAB), Modified Rankin Scale (mRS), National Institutes of Health Stroke Scale (NIHSS), and hemorheology parameters were assessed to evaluate the effects of the treatments. *Results*. Excluding the patients who dropped out, 54 patients in the treatment group and 51 patients in the control group were used to evaluate the effects. Significant and persistent improvements in the WAB score, specifically comprehension, repetition, naming, and calculating, were found in the treatment group when the effects were evaluated at the end of week 2 and week 4, respectively, compared with baseline. The naming and writing scores were also improved at the end of week 4 in this group. The comprehension and reading scores were improved at the end of week 4 in the control group compared with the baseline, but the improvements were smaller than those in the treatment group. The percentages of patients at the 0-1 range of mRS were increased at the end of week 2 and week 4 in both groups, but the improvements in the treatment group were much larger than those in the control group. Greater improvements in the NIHSS scores and the hemorheology parameters in the treatment group were also observed compared with the control group at the end of week 2 and week 4. *Conclusion*. *Nao-Xue-Shu* oral liquid formulation improved aphasia in mixed stroke patients and thus might be a potentially effective drug for treating stroke aphasia.

1. Introduction

Mixed stroke, also known as hemorrhagic infarction or infarction with hemorrhage, presents as a cerebral infarction combined with intracerebral hemorrhage on computed tomography (CT) brain scans [1, 2]. Current clinical cases of mixed stroke are caused by middle cerebral artery territory and lead to massive temporal infarction with hemorrhage. Mixed stroke patients with brain infarction and hemorrhage have mutual promoting and mutual transforming characteristics that often appear as epilepsy, dementia, aphasia, and other kinds of advanced neural function damage. Also, there is a higher proportion of patients with mixed apoplexy aphasia, including aphasia and dysarthria, or both kinds of symptoms coexisting in patients that result in communication difficulties, and loss of the ability to communicate socially has

a serious impact on the patient's quality of life [3]. Western medicine treatment that consists of decreasing intracranial pressure and adjusting blood pressure and blood density and hemostatic measures can produce contradictory effects and, in other words, may lead to the development of ischemia and at the same time increase bleeding, and vice versa, causing contradiction to treat it [4]. In the theory of traditional Chinese medicine (TCM), one of the integrative medicines [5] has shown that *Nao-Xue-Shu* oral liquid may raise *Qi* and remove blood stasis, clear pathogenic "heat" and "cool" blood (make the abnormal activity of the blood quiet stop bleeding), and eliminate phlegm [6]. In Western medicine, the oral liquid can increase cerebral blood flow, improve microcirculation, prolong thrombus formation, bleeding, and clotting times, and inhibit platelet aggregation, so it can promote phagocytic function and accelerate the absorption of blood swollen in cerebral [6] and might be an effective prescription in the treatment of mixed stroke [7]. For these reasons, the aim of the present investigation was to evaluate whether *Nao-Xue-Shu* oral liquid can improve the aphasia of mixed stroke. We enrolled mixed stroke aphasia patients from the Department of Neurology of Shuguang Hospital affiliated to Shanghai University of Traditional Chinese Medicine and the Department of Neurology of Hua Shan Hospital affiliated to Fu Dan University based on whether or not they were taking *Nao-Xue-Shu* oral liquid in order to identify a reliable treatment for improving the prognosis of the patients.

2. Subjects and Methods

2.1. Subjects. A total of 116 mixed stroke patients with aphasia from our two hospitals were divided into a treatment group (treatment plus *Nao-Xue-Shu* oral liquid, $n = 58$) and a control group (treatment without *Nao-Xue-Shu* oral liquid, $n = 58$) in a single blind fashion. Inclusion criteria for the patients with aphasia of mixed stroke were (1) acute onset, neural function defect syndrome caused by a local brain blood circulation disorder, and duration of symptoms of at least 24 hours [8]; (2) diagnosis by CT and/or magnetic resonance imaging (MRI) of the brain clearly showing cerebral infarction accompanied by cerebral hemorrhage; (3) the patient in a conscious state and with the ability to speak and no comprehension difficulties, with or without dysarthria; and (4) the patient or their guardians providing signed informed consent. Exclusion criteria for those meeting the above inclusion criteria were (1) a patient with an existing consciousness disorder; (2) cerebral hemorrhage caused by another reason such as a tumor or brain trauma caused by cerebral infarction; (3) the existence of serious gastrointestinal bleeding, hemoptysis, or bloody urine; (4) the presence of other diseases caused by vascular dementia, frontotemporal dementia, Parkinson's disease (PD), Alzheimer's disease (AD), or a central nervous system disease such as a brain tumor, multiple sclerosis, encephalitis, epilepsy, normal pressure hydrocephalus (NPH), or other types of dementia; (5) alcohol and/or drug abuse or other known kinds of aphasia or dementia which prohibit the patient from cooperating with the examiner.

The mixed stroke patients with aphasia selected included 83 males and 33 females (age range, 39–87 y; mean ± SD, 64.28 ± 4.74 y), and time from onset to admission was 0.5~2.5 d (0.75 ± 1.08 d). There were 34 cases of left temporal infarction with hemorrhage, 23 cases of right temporal leaf infarction with hemorrhage, 14 cases of left putamen hemorrhage with right basal ganglia infarction, 12 cases of left putamen hemorrhage with right brain stem infarction, 11 cases of right basal ganglia infarction with hemorrhage in the left caudate nucleus, 9 cases of left cerebellar hemorrhage with right basal ganglia infarction, 8 cases of left thalamus hemorrhage with infarction in the right side of the basal ganglia area, and 5 cases of left basal ganglia infarction with right basal ganglia hemorrhage. No significant differences in gender, age, number of cases, duration, or types of diseases between the two groups were found, and the 2 groups were comparable (Table 1).

2.2. Treatment Methods. The control group underwent routine clinical treatments and measures according to the guidelines of Western medicine [9], including monitoring fluctuations in the electrocardiograph (ECG) and blood pressure. To control blood pressure and intracranial pressure, *mannitol* and/or *furosemidum* and *citicoline* were administered by intravenous infusion according to the patient's situation. The patients in the treatment group were treated using the same routine treatments as the control group and were also administered 10 mL of *Nao-Xue-Shu* oral liquid [6, 7] three times per day (Shandong *Wohua* Pharmaceutical Polytron Technologies Inc.), which consists of *Astragalus root*, *Hirudo, Acorus gramineus, Radix Achyranthis bidentatae, tree Peony bark, Rheum officinale,* and *Ligusticum wallichii* (batch numbers 5040504 and 5040708). The ratio formula of each herb or insect and the craftsmanship are protected by Chinese patent, but the effective elements could pass through the blood brain barrier to modify cerebral hemorrhage by study of cerebral hemorrhage model [10]. Patients who could not ingest the liquid orally were given it by nasal feeding. The patients in the treatment group took *Nao-Xue-Shu* oral liquid for 4 consecutive weeks. The clinical and laboratory parameters were measured before treatment (baseline), at the end of week 2, and at the end of week 4 to evaluate the effects of treatment in the two groups.

2.3. Assessments. (1) Western Aphasia Battery (WAB) [11] is the main outcome measure of aphasia. The examination not only detects fluctuations in aphasia but also assesses the use of visual spatial function, nonlinguistic intelligence abilities, spatial structure ability, ability to perform calculations, and other nonlinguistic function examinations. The WAB test has been used as a common tool in evaluating aphasia and is minimally influenced by race and cultural background in Western countries [12]. The six quotients developed by weighting WAB scores are as follows: comprehension, repetition, naming, reading, calculating, and writing, with the highest score being 100%.

(2) The Modified Rankin Scale (mRS) [13] is a simplification of the overall assessment of the patient's neurological function scale. The higher the score for neural function

Table 1: Background characteristics of the patients of mixed stroke with aphasia.

Group	n	Gender		Age (y)	Educational level (n)			Handedness (n)		Aphasia type (n)		
		M	F		Primary	Middle	College or more	L	R	Motor	Receptive	Mixed
Treatment group	54	38	16	63.32 ± 5.1	13	24	17	5	49	23	19	12
Control group	51	37	14	64.6 ± 4.9	11	23	17	4	47	21	17	13

Table 2: Quantitative changes of Western aphasia battery (WAB) between before and after the additional treatments in the treatment and control groups.

	Comprehension	Repetition	Naming	Reading	Calculating	Writing
Treatment group						
Before	0.68 ± 0.22	0.53 ± 0.17	0.46 ± 0.31	0.57 ± 0.26	0.43 ± 0.37	0.62 ± 0.25
Week 2	0.76 ± 0.17*	0.70 ± 0.32*	0.52 ± 0.28	0.67 ± 0.25*	0.56 ± 0.28*	0.67 ± 0.21
Week 4	0.87 ± 0.12$^{**\#}$	0.75 ± 0.21$^{**\#}$	0.62 ± 0.24$^{*\#}$	0.77 ± 0.18$^{**\#}$	0.67 ± 0.22$^{**\#}$	0.77 ± 0.12$^{*\#}$
Control group						
Before	0.69 ± 0.23	0.54 ± 0.12	0.46 ± 0.25	0.56 ± 0.21	0.45 ± 0.29	0.63 ± 0.28
Week 2	0.70 ± 0.21	0.60 ± 0.19	0.49 ± 0.21	0.58 ± 0.24	0.48 ± 0.27	0.65 ± 0.25
Week 4	0.77 ± 0.19*	0.63 ± 0.25	0.52 ± 0.17	0.65 ± 0.22*	0.53 ± 0.33	0.68 ± 0.19

Note: $^{*}p < 0.05$ and $^{**}p < 0.01$ compared with before for the same group; $^{\#}p < 0.05$ compared with control group at the same time.

defect, the more serious the condition; 0 means no movement dysfunction and 6 means death. After 2 and 4 weeks of treatment, an increased percentage in the range of 0-1 of mRS will be used as the main determinant of improvement for movement dysfunction.

(3) The National Institutes of Health Stroke Scale (NIHSS) [14] as the reference index of curative effect include consciousness, gaze, facial paralysis, limb activities, and so on for a total of 11 scoring categories, with 0 points being normal. The higher the score of NIHSS, the more serious the neurologic deficit, NIHSS as a predictor of acute onset for stroke.

(4) Blood hemorheology as a reference index of the curative effect include whole blood viscosity low shear (WBVLS), whole blood viscosity high shear (WBVHS), plasma viscosity (PV), erythrocyte sedimentation rate equation K value (ESRE K value), fibrinogen, and erythrocyte aggregation index (EA index).

2.4. Statistics. SPSS17.0 software package was used for statistical analysis of the data. Data are presented as the mean and standard deviation ($-x + s$) or percentage (%). Repeated-measure ANOVA was conducted to test the differences among changes in outcomes at baseline and at the end of week 2 and week 4 for both groups. Differences at baseline between the treatment group and control group were analyzed. A $p < 0.05$ was considered to indicate a statistically significant difference.

3. Results

No significant differences in age, sex, educational level, handedness, aphasia type, baseline WAB score, mRS score, or NIHSS score, or blood parameters of hemorheology were observed between the treatment and control groups (Tables 1 and 2). After two weeks of treatment, there was one death in the treatment group due to severe lung infection, while three subjects died in the control group (one due to acute heart failure, one due to cerebral herniation, and one due to severe pulmonary infection). After 4 weeks of treatment, contact with three subjects in the treatment group was lost after they left the hospital. In the control group, two patients died and contact with two subjects was lost. Fifty-four patients in the treatment group and 51 patients in the control group were ultimately included in the statistical analyses.

The WAB scores in both groups at the end of week 2 and week 4 were better than their baseline scores. The scores for comprehension, repetition, reading, and calculation at the end of week 2 and week 4 in the treatment group were significantly improved compared with before treatment (baseline) ($p < 0.05$ or $p < 0.01$). These scores were much better at the end of week 4 in the treatment group than in the control group ($p < 0.05$). At the end of week 4, the WAB scores for naming and writing were better in the treatment group compared with baseline ($p < 0.05$), while only the comprehension and reading scores in the control group were significantly improved at the end of week 4. The levels of improvement at the end of week 4 were worse in the control group than in the treatment group ($p < 0.05$, Table 2).

The mRS score was significantly improved at the end of week 2 and week 4 in the treatment group ($p < 0.05$ and $p < 0.01$) compared with baseline, and the improvements were markedly better than those in the control group at the end of week 4 ($p < 0.01$). The mRS score only improved at the end of week 4 in the control group ($p < 0.05$) compared with baseline (Figure 1, left). The number of patients with an mRS score in the 0-1 range increased in both groups at the end of week 2 and week 4 (Figure 1, right), although the change was significantly greater in the treatment group.

Table 3: Changes in hemorheology between before and after the additional treatments in the treatment and control groups.

	WBVLS (mPa·s)	WBVHS (mPa·s)	PV (mPa·s)	ESRE K value	Fibrinogen (g/L)	EA index
Treatment group (n = 54)						
Before	18.83 ± 4.36	3.82 ± 0.57	1.81 ± 0.52	68.27 ± 39.25	4.82 ± 1.25	4.72 ± 0.81
Week 2	17.96 ± 4.09	3.72 ± 0.35	1.68 ± 0.32	59.19 ± 41.62	4.19 ± 1.02	3.96 ± 0.63
Week 4	16.65 ± 3.74$^{*\#}$	3.53 ± 0.32$^{*\#}$	1.47 ± 0.44$^{**\#}$	53.56 ± 40.69$^{*\#}$	3.47 ± 0.72$^{*\#}$	3.25 ± 0.52$^{*\#}$
Control group (n = 51)						
Before	18.74 ± 5.05	3.82 ± 0.35	1.81 ± 0.37	67.82 ± 41.25	4.79 ± 1.46	4.70 ± 0.65
Week 2	18.38 ± 5.23	3.79 ± 0.62	1.76 ± 0.42	64.99 ± 39.02	4.02 ± 1.33	4.65 ± 0.92
Week 4	17.99 ± 4.59	3.77 ± 0.53	1.71 ± 0.38	63.47 ± 44.72	3.95 ± 1.49	3.97 ± 0.59

Note. WBVLS: whole blood viscosity low shear; WBVHS: whole blood viscosity high shear; PV: plasma viscosity; ESRE K value: erythrocyte sedimentation rate equation K value; and EA index: erythrocyte aggregation index. $^{*}p < 0.05$ and $^{**}p < 0.01$ compared with before for the same group; $^{\#}p < 0.05$ compared with control group at the same duration.

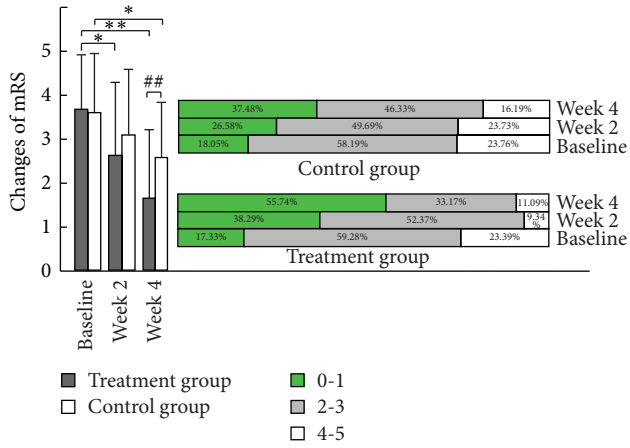

Figure 1: Changes in the modified Rankin score (mRS) between before and after the additional treatments in the treatment and control groups. Note: $^{*}p < 0.05$ and $^{**}p < 0.01$ compared with before for the same group; $^{\#\#}p < 0.01$ compared with control group at the same time.

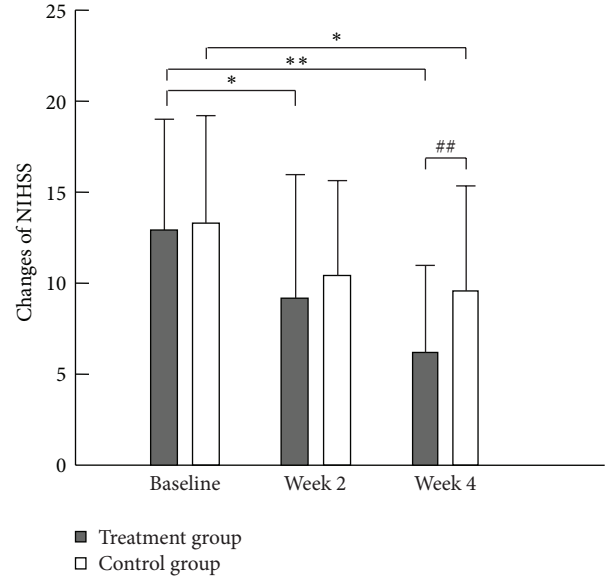

Figure 2: Changes in the National Institutes of Health Stroke Scale (NIHSS) scores between before and after the additional treatments in the treatment and control groups. Note: $^{*}p < 0.05$ and $^{**}p < 0.01$ compared with before for the same group; $^{\#\#}p < 0.01$ compared with control group at the same duration.

The NIHSS scores were improved at the end of week 2 and week 4 in both groups compared with their respective baselines, although the levels were markedly better in the treatment group than in the control group at the end of week 2 and week 4 (Figure 2).

The changes in most parameters in the blood hemorheology index in the treatment group at the end of week 4 were significantly different compared with baseline. The changes observed in all six parameters of the index in the treatment group were different compared with the control group at the end of week 4 (Table 3).

4. Discussion

There were more dropouts and deaths in the control group compared to the treatment group at the end of the study. Our results indicate that compared with baseline the treatment group (*Nao-Xue-Shu* oral liquid) had improved comprehension, repetition, reading, and calculating scores for aphasia parameters at the end of week 2 and the scores for these factors all had improved significantly at the end of week 4 compared with the control group and their baselines (Table 2). The treatment group exhibited improvements not only in the aphasia parameters but also in limb function, indicating that *Nao-Xue-Shu* oral liquid also can be used for treating patients with mixed stroke. After 4 weeks of treatment, the hemodynamic level of the treatment group improved compared with the control group, making it more close to the normal range (Table 3).

Mixed stroke is a common clinical cerebrovascular disease, and the patients experience acute onset and rapid progression. The cause of the disease is often an arterial lesion in the carotid artery system of the brain region, and the infarction area is large and often accompanied by damage to advanced brain function as the result of coma, aphasia, dementia, and epilepsy [15]. These have a serious impact on the quality of life and safety of the patient. Explaining the

mechanism of action of *Nao-Xue-Shu* oral liquid in terms of traditional Chinese medicine (TCM) theory may be difficult to understand for most Western doctors. Mixed stroke in TCM is explained as "apoplexia" and an "attack on the viscera and bowels" [16], caused by a *Qi* deficiency, blood stasis, and phlegm. Due to the *Qi* deficiency, the blood stasis and phlegm obstruct the internal structure of blood vessel then intertwist each other, causing the blood stasis with phlegm to insert the vessel in the brain, leading to infarction. The abnormal blood causes intervessel high blood pressure, and forcing the blood stasis with phlegm out of the blood vessel may break the vessel, leading to hemorrhage [17, 18]. In TCM theory, if blood stasis is accompanied by phlegm, it can lead to a more significantly damaged lesion in the brain [19]. This is the mechanism that explains why mixed stroke patients often also have advanced neuronal damage, including aphasia, and the two pathological phenomenons of infarction and hemorrhage can be caused simultaneously. Physiologically, cleaning and powerful *Qi* (*Qing-yang Qi*) can supply energy to the brain to maintain its function and collect and modulate the blood and force it to circulate in correct way in brain blood vessels [17, 18]. If the circulation has been obstructed by the blood stasis with phlegm, the occlusion of blood vessel orifices will occur and the power of *Qi* will decrease; *Qing-yang Qi* is also like nutrition for the brain; if it cannot rise, it can lead to the brain lack of power to speak and understand the language and then can cause dysarthria and dysphagia. When treating this disease, we should consider three TCM pathogenic matters: *Qi*, blood stasis, and phlegm. First, we should eliminate *Qing-yang Qi*, which can modulate blood circulation and control or decrease bleeding. A*stragalus root* as a major component in *Nao-Xue-Shu* oral liquid can provide a stronger *Qing-yang Qi* [19]. The *Qi* also provides energy to raise the nutrient level in blood to the brain when treating the infarction and improves the aphasia. In TCM, *Qi* can improve circulation throughout the entire system and excrete metabolin. The other main component in the oral liquid is *hirudo,* a type of earthworm that has been used for more than one thousand years in China, which can rapidly eliminate blood stasis and treat the second pathogenic condition, that of blood stasis [20, 21], without side effect as bleeding. Other than these two components, the *Nao-Xue-Shu* oral liquid formulation contains 5 other TCM herbs that can help increase *Qi*, remove blood stasis and phlegm, and assist the body to excrete the pathogenic metabolites of blood stasis and phlegm. In fact, *Nao-Xue-Shu* oral liquid contains two famous prescriptions of TCM; one is *Bu-Yang-Huan-Wu decoction*, which originated in the Qing Dynasty (about 185 years ago) and has been used frequently to treat stroke in China and Asia [22, 23]. The other is *Da-Huang-Shu-Chong pill*, which comes from the very famous TCM text *Jin-Gui-Yao-Lue* (By Zhang Zhongjing, about 1700 years ago) and has been used to remove blood stasis from the body [24]. The combination of these 2 prescriptions is the most effective treatments in treating for mixed stroke with aphasia. Clinical pharmacological studies have confirmed that *Nao-Xue-Shu* oral liquid accelerates the absorption of hematoma in the brain of rats, reduces edema around the hematoma accelerating fibrinolysis and inhibiting thrombosis, increases cerebral blood flow, and improves brain blood and oxygen supply, thereby improving blood circulation and promoting the absorption of hematoma [25].

In this study on treating mixed stroke with aphasia, we believe the disease is caused by 3 pathogenetic mechanisms: a deficiency of *Qi,* blood stasis, and phlegm. The sample size of this study is relatively small and a single blind random method was used, so the treatment group might have experienced placebo effects and we therefore cannot draw any definite conclusion. In TCM theory, each Chinese medicine has its own function to modulate the body or deal with diseases, including treating brain problems, but doctors in China are still unable to demonstrate how the medicine passes through the blood brain barrier (BBB). Including TCM herbs [26, 27], many integrative medicines such as Ayurveda medicine [28], electric stimulation [29], and Tai Chi quan [30] cannot confirm that they influence the nerve system directly by Western medical technology, but they have been used in many countries for treating many diseases [5]. *Nao-Xue-Shu* oral liquid contains a type of worm and this is another problem since, according to ethics, it is difficult to introduce such a treatment into foreign countries, although worms are frequently used in TCM treatments and TCM researchers in China have demonstrated they are harmless and safe. In order to validate the causes of the disease based on clinical data, large-scale, multicenter, double-blind randomized control studies will be needed to verify the effectiveness of *Nao-Xue-Shu* oral liquid in the treatment of mixed stroke aphasia.

Conflict of Interests

The authors declare that there is no conflict of interests regarding the publication of this paper.

Acknowledgment

This study was sponsored and supported by the National Natural Science Foundation of China (81373619).

References

[1] T. Ogawa and K. Uemura, "CT and MRI diagnosis of hemorrhagic infarction," *Nippon Rinsho*, vol. 51, supplement, pp. 800–805, 1993 (Japanese).

[2] B. R. Ott, A. Zamani, J. Kleefield, and H. H. Funkenstein, "The clinical spectrum of hemorrhagic infarction," *Stroke*, vol. 17, no. 4, pp. 630–637, 1986.

[3] P. F. Finelli and F. J. DiMario Jr., "Hemorrhagic infarction in white matter following acute carbon monoxide poisoning," *Neurology*, vol. 63, no. 6, pp. 1102–1104, 2004.

[4] M. S. Pessin, C. J. Estol, F. Lafranchise, and L. R. Caplan, "Safety of anticoagulation after hemorrhagic infarction," *Neurology*, vol. 43, no. 7, pp. 1298–1303, 1993.

[5] W. Pan and H. Zhou, "Inclusion of integrative medicine in clinical practice," *Integrative Medicine International*, vol. 1, no. 1, pp. 1–4, 2014.

[6] D. Xue, B. Suo, Y. Sun et al., "Nao-Xue-Shu liquid for hemorrhagic stroke," *Zhong Xi Yi Jie He Xin Nao Xue Guan Bing Za Zhi*, vol. 5, no. 8, pp. 690–691, 2007.

[7] S. Wang, R. Song, Z. Wang et al., "The clinical study for Nao-Xue-Shu liquid absorb hematoma of hemorrhagic stroke," *Zhong Xi Yi Jie He Xin Nao Xue Guan Bing Za Zhi*, vol. 12, no. 4, pp. 452–453, 2014.

[8] E. C. Jauch, J. L. Saver, H. P. Adams et al., "Guidelines for the early management of patients with acute ischemic stroke: a guideline for healthcare professionals from the American Heart Association/American Stroke Association," *Stroke*, vol. 44, no. 3, pp. 870–947, 2013.

[9] J. L. Saver and L. B. Goldstein, "The new standing guideline committee policy of the american stroke association stroke council," *Stroke*, vol. 37, no. 3, p. 753, 2006.

[10] L. Xiaoping, "The laboratory research and clinical study of Nao-Xue-Shu oral liquid," *China Journal of Pharmaceutical Economics*, vol. 6, pp. 128–130, 2012.

[11] C. M. Shewan and A. Kertesz, "Reliability and validity characteristics of the Western Aphasia Battery (WAB)," *Journal of Speech and Hearing Disorders*, vol. 45, no. 3, pp. 308–324, 1980.

[12] J. Horner, D. V. Dawson, A. Heyman, and A. M. Fish, "The usefulness of the Western Aphasia Battery for differential diagnosis of Alzheimer dementia and focal stroke syndromes: preliminary evidence," *Brain and Language*, vol. 42, no. 1, pp. 77–88, 1992.

[13] G. Sulter, C. Steen, and J. De Keyser, "Use of the Barthel index and modified Rankin scale in acute stroke trials," *Stroke*, vol. 30, no. 8, pp. 1538–1541, 1999.

[14] T. Brott, H. P. Adams Jr., C. P. Olinger et al., "Measurements of acute cerebral infarction: a clinical examination scale," *Stroke*, vol. 20, no. 7, pp. 864–870, 1989.

[15] P. M. Pedersen, H. S. Jørgensen, H. Nakayama, H. O. Raaschou, and T. S. Olsen, "Aphasia in acute stroke: incidence, determinants, and recovery," *Annals of Neurology*, vol. 38, no. 4, pp. 659–666, 1995.

[16] D. H. Yi, Y. Li, S. X. Shao, Y. M. Xie, and Y. Yuwen, "Evaluation of the conjoint efficacy in Chinese medicine with the longitudinal latent variable linear mixed model," *Chinese Journal of Integrative Medicine*, vol. 19, no. 8, pp. 629–635, 2013.

[17] L. M. Yang, "[Medico-psychology in Huang di nei jing (Yellow Emperor's Inner Canon)]," *Zhonghua Yi Shi Za Zhi*, vol. 34, no. 1, pp. 21–26, 2004 (Chinese).

[18] J. Zhu, "Textual research and explanation of "Qi-Huang"," *Zhonghua Yi Shi Za Zhi*, vol. 32, no. 4, pp. 200–204, 2002.

[19] Z. Chen, L. Yuan, and G. Zhang, "The clinical and laboratory research of Nao-Xue-Shu liquid in treating for vascular diseases," *Zhong Xi Yi Jie He Xin Nao Xue Guan Bing Za Zhi*, vol. 12, no. 8, pp. 1005–1006, 2014.

[20] F. von Rheinbaben, O. Riebe, J. Koehnlein, and S. Werner, "Viral infection risks for patients using the finished product *Hirudo verbana* (medicinal leech)," *Parasitology Research*, vol. 113, no. 11, pp. 4199–4205, 2014.

[21] F. Le Marrec-Croq, A. Bocquet-Garcon, J. Vizioli et al., "Calreticulin contributes to C1q-dependent recruitment of microglia in the leech Hirudo medicinalis following a CNS injury," *Medical Science Monitor*, vol. 20, pp. 644–653, 2014.

[22] L. H. Shaw, L. C. Lin, and T. H. Tsai, "HPLC-MS/MS analysis of a traditional Chinese medical formulation of Bu-Yang-Huan-Wu-Tang and its pharmacokinetics after oral administration to rats," *PLoS ONE*, vol. 7, no. 8, Article ID e43848, 2012.

[23] Z. Lai, S. Y. Wang, X. Y. Geng, C. Q. Deng, and R. Z. Zhang, "Effects of bu yang huan wu decoction on astrocytes after cerebral ischemia and reperfusion," *Zhongguo Zhong Yao Za Zhi*, vol. 27, no. 10, pp. 763–765, 2002 (Chinese).

[24] T. Jiang and H. Fu, "Progress of experimental studies on prescriptions designed by Zhang Zhongjing," *Journal of Traditional Chinese Medicine*, vol. 16, no. 1, pp. 55–64, 1996.

[25] X. Ai and C. Liu, "The study of cleaning volume of hematoma and protecting neuron function of hemorrhagic rat model by Nao-Xue-Shu liquid," *Zhong Guo Zhong Xi Yi Jie He Xin Nao Xue Guan Bing Za Zhi*, vol. 11, no. 7, pp. 859–861, 2014.

[26] W. Pan, Q. Wang, S. Kwak et al., "Shen-zhi-ling oral liquid improves behavioral and psychological symptoms of dementia in Alzheimer's disease," *Evidence-Based Complementary and Alternative Medicine*, vol. 2014, Article ID 913687, 6 pages, 2014.

[27] J. Shen, X. Chen, X. Chen, and R. Deng, "Targeting neurogenesis: a promising therapeutic strategy for post-stroke treatment with Chinese herbal medicine," *Integrative Medicine International*, vol. 1, no. 1, pp. 5–18, 2014.

[28] P. Santiago Lloret, M. Verónica Rey, and O. Rascol, "Ayurveda medicine for the treatment of Parkinson's disease," *International Journal of Integrative Medicine*, vol. 1, article 6, 2013.

[29] J. Lee, J. Y. Cho, and K. W. Kim, "Rapid treatment of waist pain by nanoscale electric stimulation," *Integrative Medicine International*, vol. 1, no. 1, pp. 19–24, 2014.

[30] F. Li, "Tai Ji Quan exercise for people with Parkinson's disease and other neurodegenerative movement disorders," *International Journal of Integrative Medicine*, vol. 1, no. 4, 2013.

Hindawi Publishing Corporation
Evidence-Based Complementary and Alternative Medicine
Volume 2015, Article ID 428106, 9 pages
http://dx.doi.org/10.1155/2015/428106

Research Article

The Renal Protective Effect of Jiangya Tongluo Formula, through Regulation of Adrenomedullin and Angiotensin II, in Rats with Hypertensive Nephrosclerosis

Lin Han,[1] Yan Ma,[2] Jian-guo Qin,[3] Li-na Li,[1] Yu-shan Gao,[1] Xiao-yu Zhang,[3] Yi Guo,[3] Lin-mei Song,[1] Yan-ni Luo,[3] and Xiao-yi Chi[3]

[1]*College of Basic Medicine, Beijing University of Chinese Medicine, Beijing 100029, China*
[2]*Molecular Research in Traditional Chinese Medicine Group, Department of Pathophysiology and Allergy Research, Center of Pathophysiology, Infectiology & Immunology, Vienna General Hospital, Medical University of Vienna, Waehringer Guertel 18-20, 1090 Vienna, Austria*
[3]*Department of Nephrology, Dongfang Hospital, The Second Clinical Medical College of Beijing University of Chinese Medicine, Beijing 100078, China*

Correspondence should be addressed to Jian-guo Qin; qindoctor@163.com

Received 13 December 2014; Revised 23 February 2015; Accepted 12 March 2015

Academic Editor: Zhang Tan

We investigated the effect of Jiangya Tongluo (JYTL) formula on renal function in rats with hypertensive nephrosclerosis. A total of 21 spontaneously hypertensive rats (SHRs) were randomized into 3 groups: valsartan (10 mg/kg/d valsartan), JYTL (14.2 g/kg/d JYTL), and a model group (5 mL/kg/d distilled water); Wistar Kyoto rats comprised the control group ($n = 7$, 5 mL/kg/d distilled water). Treatments were administered by gavage every day for 8 weeks. Blood pressure, 24-h urine protein, pathological changes in the kidney, serum creatinine, and blood urea nitrogen (BUN) levels were estimated. The contents of adrenomedullin (ADM) and angiotensin II (Ang II) in both the kidney and plasma were evaluated. JYTL lowered BP, 24-h urine protein, serum creatinine, and BUN. ADM content in kidneys increased and negatively correlated with BP, while Ang II decreased and negatively correlated with ADM, but there was no statistically significant difference of plasma ADM between the model and the treatment groups. Possibly, activated intrarenal renin-angiotensin system (RAS) plays an important role in hypertensive nephrosclerosis and the protective function of ADM via local paracrine. JYTL may upregulate endogenous ADM level in the kidneys and antagonize Ang II during vascular injury by dilating renal blood vessels.

1. Introduction

Hypertensive nephrosclerosis is one of the most common and serious chronic complications in primary hypertension. It is an independent risk factor for end-stage renal disease (ESRD) [1]; approximately 25% of patients with hypertensive nephrosclerosis require a kidney transplant [2]. Data from the United States Renal Data System suggest that hypertension is the second cause of ESRD and the multiple risk factor intervention study revealed that approximately 49% of ESRD cases are caused by hypertension. By 2002, there were 160 million patients with hypertension in China and approximately 9.6% of patients were on dialysis as a result of renal artery sclerosis due to hypertension. Improvements in the early prevention and treatment of hypertension have resulted in significant reductions in mortality from cardiovascular complications caused by hypertension; however, for hypertensive nephrosclerosis, the mortality rates have not significantly improved [2]. Therefore, research efforts are now being focused on the mechanism and prevention of hypertensive nephrosclerosis. Currently, the treatment of hypertensive nephrosclerosis involves controlling blood pressure and preglomerular arteriolar resistance, reducing intraglomerular pressure, and improving renal ischemia. However, this approach has failed to show a curative effect in approximately 50% of patients and the application of angiotensin-converting

enzyme inhibitor (ACEI) drugs is limited when renal function is impaired beyond a specific threshold (serum creatinine >3 mg/dL). Therefore, further research on new drugs and treatment approaches to delay the progression of hypertensive nephrosclerosis towards end-stage renal failure is required.

Adrenomedullin (ADM) is a vasodilator peptide that was originally isolated from the extract of human pheochromocytoma in 1993. It has numerous biological effects and is present in a variety of tissues and organs, particularly in the heart, kidney, and lungs [3]. ADM is mainly produced by vascular endothelial and smooth muscle cells, while mesangial and epithelial cells also secrete ADM [4]. When combined with calcitonin receptor-like receptors (CRLR) and receptor activity-modifying proteins 2 and 3 (RAMP2 and RAMP3), ADM has a strong vasodilator effect [5]; it increases renal blood flow and glomerular filtration via the expansion of efferent and afferent arterioles [4]. ADM exerts important vascular and renal protective effects through its interaction with Ang II and other vasoconstrictive substances [6]. Therefore, ADM is considered important in preventing high blood pressure and hypertension-induced organ damage. Consequently, investigation of the potential renal protective effects of ADM has become a research focus in the field of hypertension nephrosclerosis.

We routinely use Jiangya Tongluo (JYTL) at our daily clinic to treat hypertensive nephrosclerosis and we have observed good clinical curative effect. To gain insight into the mechanisms of regulation of JYTL in hypertensive nephrosclerosis, we investigated the effects of JYTL on blood pressure, renal function, and the expression of ADM and Ang II in kidney and plasma using a spontaneous hypertensive rat (SHR) experimental model to explore its decompression and protective effects on kidney.

2. Materials and Methods

2.1. Animal Models and Drugs. Sixteen-week-old, male SHRs (mean weight = 200 ± 10 g) were purchased from Vital River Laboratories (Beijing, China; number SCXK, 2002-2003). The animals were housed in the Central Laboratory at Beijing University of Chinese Medicine, with a 12-h light/dark cycle and free access to food and water. The SHRs were fed a normal diet for a week and were then randomized to one of 3 groups: model (5 mL/kg/d distilled water by gavage), valsartan (10 mg/kg/d valsartan by gavage), and JYTL (14.2 g/kg/d JYTL by gavage). The control group comprised Wistar Kyoto rats (5 mL/kg/d distilled water by gavage). These doses were determined from a previous pharmacodynamic experimental study [7]. Each group was then sacrificed after an 8-week treatment period. All experimental procedures were conducted in accordance with the guidelines for the use of experimental animals and approval was granted by the Institutional Review Committee on Animal Care and Use at the Experimental Animal Centre at Beijing University of Chinese Medicine (Certificate of Conformity: SCXK, Beijing, 2012-0001).

2.1.1. Preparation of JYTL Decoction. JYTL is frequently used in clinical practice for treatment of hypertension and is composed of 30 g *Nacre* (Zhen Zhu Mu, ZZM), 15 g *Cassia occidentalis* (Cao Jue Ming, CJM), 12 g *Safflower* (Hong Hua, HH), 20 g *Salvia miltiorrhiza* (danshen, DS), and 15 g *Chrysanthemum* (juhua, JH). The medicinal herbs were provided by Pharmacy Department at Dongfang Hospital, Beijing, China. The herbs were first cut and boiled together in 6x volume of water for 0.5 h (first extraction). Residue from the first extraction was boiled in 8x volume of water for 25 min. Finally, the filtered solutions were combined and concentrated into an aqueous extract containing 1.2 g/mL raw herbs. Valsartan was purchased from Novartis Pharma Ltd (Beijing, China).

2.2. Blood Pressure Detection. Systolic blood pressure (BP) was monitored prior to treatment (0 weeks) and after 2, 4, 6, and 8 weeks of treatment using a noninvasive, computerized, tail-cuff system (BESN-II, Desai Production Biotechnology Co, Nanjing, China) and performed by specifically assigned investigators at regular intervals in order to minimize error. The mean value from 3 measurements of BP was taken for each rate, representing the sample systolic pressure.

2.3. Pathological Examination of Renal Tissue. After 8 weeks of treatment, rats were sacrificed under chloral hydrate anesthesia (3.5 g/kg administered via intraperitoneal injection). Blood was rapidly sampled by abdominal aorta puncture and the serum was stored at −80°C prior to analysis. Renal tissue was excised, washed in physiological saline, snap-frozen in liquid nitrogen, and then stored at −80°C. Kidney tissues were fixed with 4% paraformaldehyde, embedded in paraffin, and cut into 3-μm thick sections. Hematoxylin-eosin (HE) staining was performed in order to assess glomerular and vascular injuries and perivascular lesions such as fibrosis under an electronic scanner (SIP NO. MIC 01579, Zeiss Co, Germany).

2.4. Determination of Urinary Protein over 24 Hours. Prior to and after 8 weeks of treatment, the rats were placed in metabolic cages where food was not provided (but water was available). Urine samples were collected over 24 h to calculate the total urinary output and 5 mL was collected for centrifugation; the supernatant was stored at −20°C. A commercial radioimmunoassay (RIA) kit (PLA Institute of RIA, Beijing, China) was used to estimate urine protein over 24 h, in accordance with the manufacturer's protocol.

2.5. Determination of Serum Creatinine and Blood Urea Nitrogen Levels. After 8 weeks of treatment, blood was collected from the abdominal aorta and serum was separated by centrifugation (1500 ×g) at 4°C for 10 min and stored in Eppendorf tubes. Blood urea nitrogen (BUN) and creatinine levels were determined by the Jaffe and diacetyl-oxime methods, in accordance with the manufacturer protocol.

2.6. Determination of Ang II and ADM Content in the Kidney and Plasma. After 8 weeks of treatment, rats were sacrificed and blood was sampled from the abdominal aorta. Fresh kidney tissues were collected, weighed, quickly ground with

normal saline, and boiled in water at 100°C for 10 min. The homogenate was centrifuged (1500 ×g) at 4°C for 15 min and the supernatant was preserved at −20°C. Ang II and ADM content in the renal tissue and plasma was determined using an RIA Kit (PLA Institute of RIA, Beijing, China) in accordance with the manufacturer's protocol. The protein content of the supernatant was also simultaneously determined for correction.

2.7. Statistical Analysis. All data were analyzed using SPSS 16.0 software (SPSS Inc., Chicago, USA). Statistical significance was analyzed using a one-way analysis of variance, followed by the post hoc Student-Newman-Keuls multiple comparison test. All data are expressed as mean ± standard error of the mean (SEM) and $P < 0.05$ was considered statistically significant.

3. Results

3.1. Effect of JYTL on Blood Pressure. Animal models in this study comprised SHRs with knocked out genes. Prior to treatment, the BP of rats in the model group and both treatment groups was significantly higher than in the control group ($P < 0.01$) (Figure 1(a)); the model and treatment groups were comparable indicating that the model was successfully established. No decrease in BP of rats was observed in the valsartan and JYTL groups compared with the model group after 2 weeks of treatment (Figure 1(b)). However, at 4, 6, and 8 weeks of treatment, the BP of rats in the JYTL and valsartan groups was significantly lower than that in the model group ($P < 0.01$ and $P < 0.05$). Furthermore, at 4 weeks, the BP of rats in the valsartan group was lower than that in the JYTL group (Figure 1(c)), while at 6 and 8 weeks, there was no statistically significant differences between the two groups (Figures 1(d) and 1(e)).

3.2. Effects of JYTL on Renal Pathological Morphology. We observed severely pathological lesion in SHRs by hematoxylin-eosin staining. It comprised glomerular ischemia and sclerosis, tubular atrophy and hyaline degeneration, and interstitial fibrosis with inflammatory cells hyperplasia, and the interlobular arteries show intimal thickening (Figure 2(b)). Such lesions were considerably diminished by JYTL and valsartan; the pathological change represented interlobular artery mild-thickening with tubular vacuolar degeneration (Figure 2(c)) and tubular ectasia with hyaline degeneration (Figure 2(d)). Furthermore, the renal structure of Wistar Kyoto rats appeared normal (Figure 2(a)). This indicated that JYTL and valsartan could significantly protect the kidney from hypertension-induced lesions. This result strongly supported the therapeutic potential of JYTL against hypertensive nephrosclerosis.

3.3. Effects of JYTL on Urinary Protein Quantity over 24 Hours. The quantity of urinary protein over 24 h was statistically significantly higher in the model group and both treatment groups compared with the control group ($P < 0.01$); there was no statistically significant difference between model and treatment groups, indicating a successful model. After 8 weeks of treatment, the 24-h urine protein level was significantly reduced in both the model and treatment groups ($P < 0.01$); it was slightly lower in the JYTL group than in the valsartan group; however, these differences were not statistically significant (Figures 3(a) and 3(b)).

3.4. Effects of JYTL on Renal Function. Following 8 weeks of treatment, serum creatinine levels were significantly reduced in both JYTL and valsartan groups ($P < 0.01$); serum creatinine levels in JYTL group were slightly lower than in the valsartan group; however there was no statistically significant difference between the two groups ($P > 0.05$). The blood urea nitrogen content was significantly reduced in both JYTL and valsartan groups after the 8-week treatment period ($P < 0.01$). While BUN was lower in the JYTL group than in the valsartan group, this difference was statistically significant ($P < 0.05$) (Figures 4(a) and 4(b)).

3.5. Effects of JYTL on the Expression of Ang II and ADM in the Kidneys and ADM in Plasma. The results of RIA showed that kidney Ang II expression in the model, JYTL, and valsartan groups was statistically significantly higher than that in the control group ($P < 0.01$). Ang II expression was statistically significantly lower in the valsartan and JYTL groups than in the model group ($P < 0.01$). While Ang II expression in valsartan group was slightly higher than the JYTL group, these differences were not statistically significantly different (Figure 5(a)). Levels of ADM in the model, JYTL, and valsartan kidneys were statistically significantly lower than the control ($P < 0.01$) and significantly higher in the valsartan group compared with the model ($P < 0.01$). While the level of ADM in the valsartan group was slightly higher than that in the JYTL group, this difference was not statistically significant (Figure 5(b)). After 8 weeks of treatment, the content of Ang II in plasma in the model group was statistically significantly higher than that in the control group ($P < 0.01$). In treatment groups though the levels of Ang II were higher than that of control group, but there was no statistically significant difference between them and also there was no statistically significant difference between the model and treatment groups (Figure 5(c)). Meanwhile, the content of ADM in the plasma in the model group and both treatment groups was statistically significantly lower than that in the control group ($P < 0.01$ and $P < 0.05$, resp.), but there was no statistically significant difference between the model and treatment groups (Figure 5(d)).

3.6. Correlation of ADM with Ang II and BP. There was a statistically significant negative correlation between ADM and Ang II and between ADM and BP in the kidneys (Figures 6(a) and 6(b)).

4. Discussion

Hypertensive nephrosclerosis is a form of hypertension-induced arteriolar nephrosclerosis and it results from benign arteriolar nephrosclerosis. Pathological changes indicative of

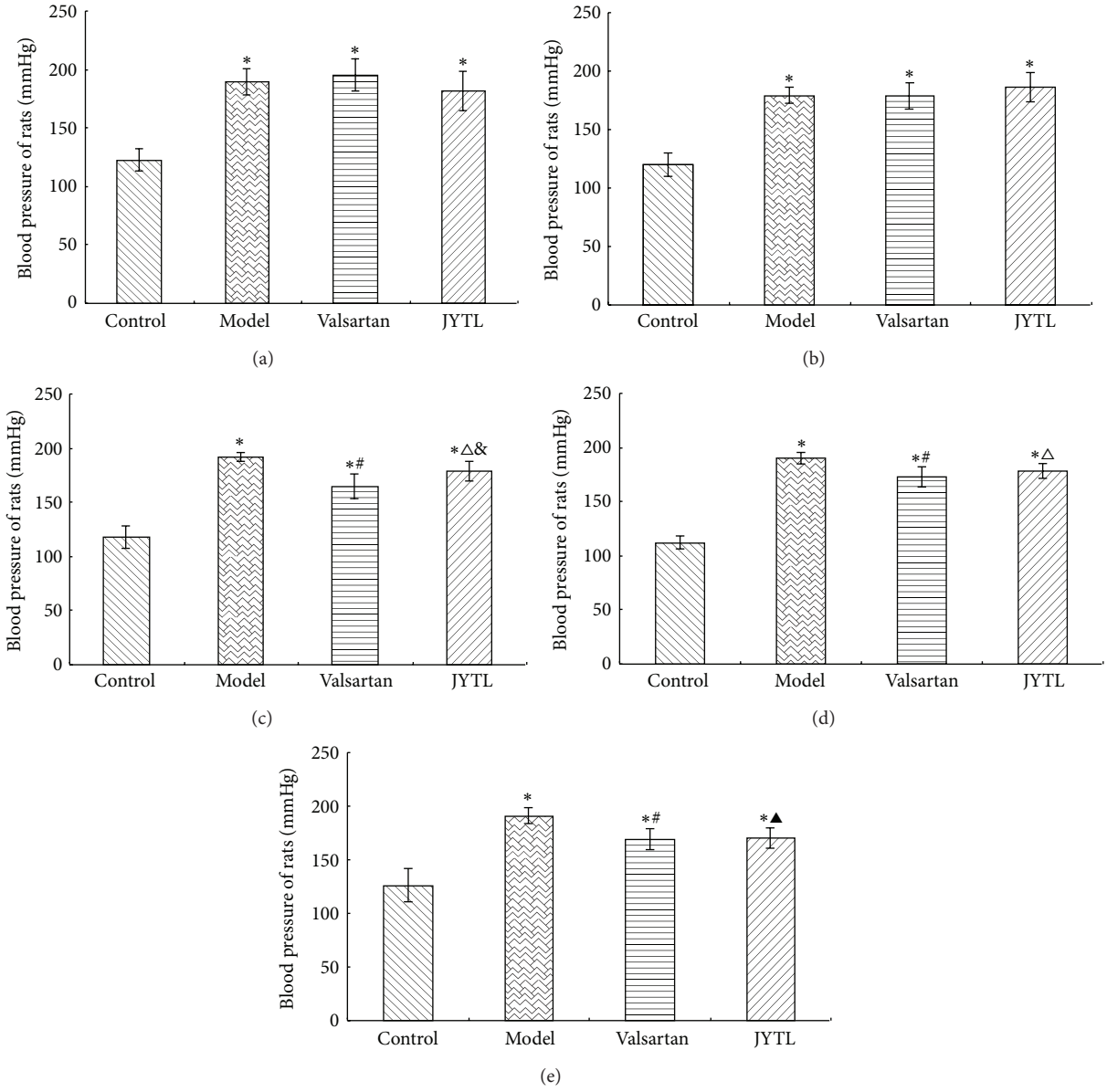

Figure 1: Effect of JYTL on mean ± SEM blood pressure ($n = 7$ per study group). (a) Before treatment. (b) After 2 weeks of treatment. (c) After 4 weeks of treatment. (d) After 6 weeks of treatment. (e) After 8 weeks of treatment. $^{*}P < 0.01$, model, valsartan, and JYTL rats versus control rats. $^{\#}P < 0.01$, rats in the valsartan group versus model rats. $^{\triangle}P < 0.05$ and $^{\blacktriangle}P < 0.01$, rats in the JYTL group versus model rats. $^{\&}P < 0.05$, rats in the JYTL group versus valsartan group.

the condition include renal afferent arteriole hyaline degeneration and myointimal hypertrophy in the arteria interlobulares and arteria arcuata [8, 9]. These lead to ischemic changes in the glomeruli and interstitium and consequently compromise renal function [10].

Decompression is the modern, universally accepted form of hypertensive nephrosclerosis therapy. Studies have demonstrated a significant contribution of ACE I and Ang II type 1 receptor blockers (ARB) in the prevention of renal and cardiovascular damage [11, 12]. However, this form of treatment has failed to demonstrate an obvious curative effect in approximately 50% of patients. Furthermore, the vasodilator effect of ACEI and ARB on efferent arterioles is superior to afferent arterioles that impacts the compensatory mechanisms of intraglomerular pressure, hypertransfusion, and hyperfiltration and accelerates renal function aggravation. For those patients with renal insufficiency, administering ACEI frequently predisposes them to hyperkalemia. Therefore, when renal functional impairment crosses a specific threshold (serum creatinine >3 mg/dL), the application of ACE I and ARB is limited. Consequently, it has become important to explore new therapeutic methods to delay the progression of hypertensive nephrosclerosis towards end-stage renal disease.

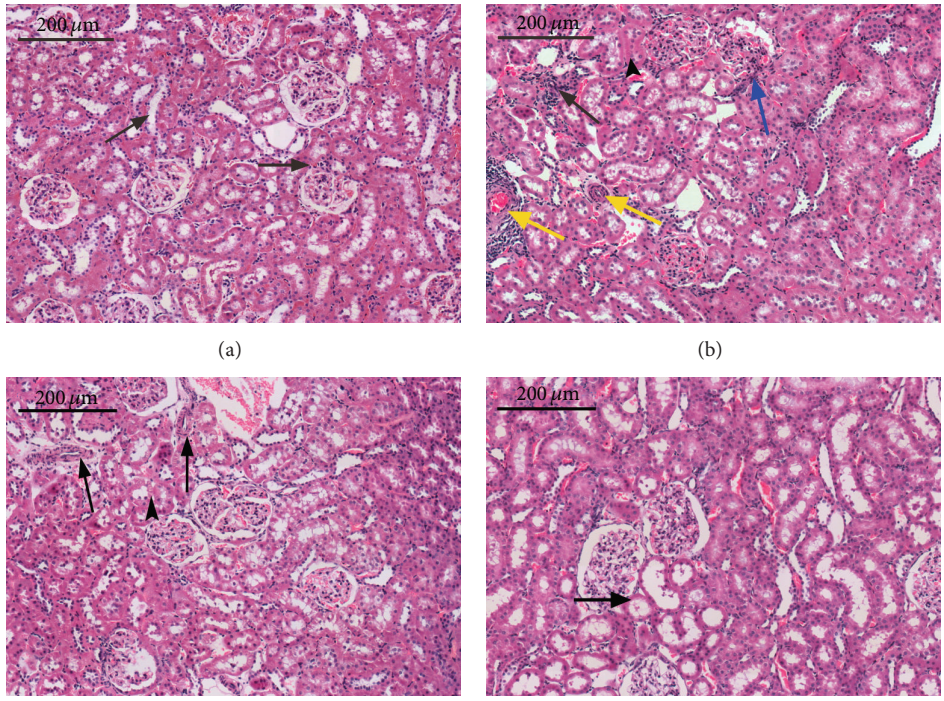

Figure 2: Histologic studies of JYTL in hypertensive nephrosclerosis rats after HE staining. (a) Control group. (b) Model group. (c) Valsartan group. (d) JYTL group. Bar = 200 μm; same magnification for all panels. (a) The arrows point to the glomerular and the lined epithelia of renal tubules in normal condition. (b) Glomerular ischemia and sclerosis (blue arrow), interlobular artery with marked myointimal proliferation (yellow arrows), tubular atrophy and hyaline degeneration (little black arrow), and interstitial fibrosis with inflammatory cells hyperplasia (black arrow). (c) Interlobular artery mild-thickening with tubular vacuolar degeneration. (d) Tubular ectasia with hyaline degeneration. HE in 3-μm thick sections, 200.

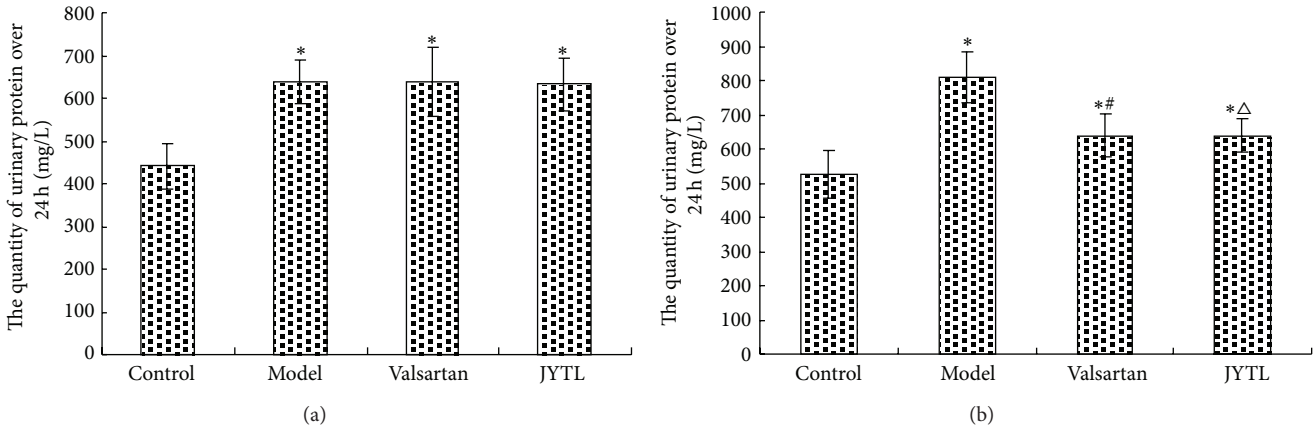

Figure 3: Effect of JYTL on the mean ± SEM urine protein content over 24 h ($n = 7$ per study group). (a) Before treatment. (b) After 8 weeks of treatment with JYTL. $^{*}P < 0.01$, model, valsartan, and JYTL rats versus control rats. $^{\#}P < 0.01$, rats in the valsartan group versus model rats. $^{\triangle}P < 0.01$, rats in the JYTL group versus model rats.

The pathogenesis and etiology of hypertensive nephrosclerosis are complex. The mechanism behind the condition is as follows. (1) Glomeruli hypertension results in vascular endothelial cell damage and increases vasoconstrictor (Ang II, ET-1) and platelet derived growth factors and the synthesis and secretion of extracellular matrix [11, 12]. (2) Elevations in the glomerular capillary pressure lead to an increase in some of the transforming growth factors such as TGF-β1; this procession stimulates collagen deposition and the proliferation of mesangial cells and increases the extracellular matrix, eventually leading to kidney sclerosis [13]. (3) The glomerular ischemia inflammatory response causes increases in vascular injury, vasoactive substances, chemical chemokines, and mitogenic factors and can aggravate kidney damage [14].

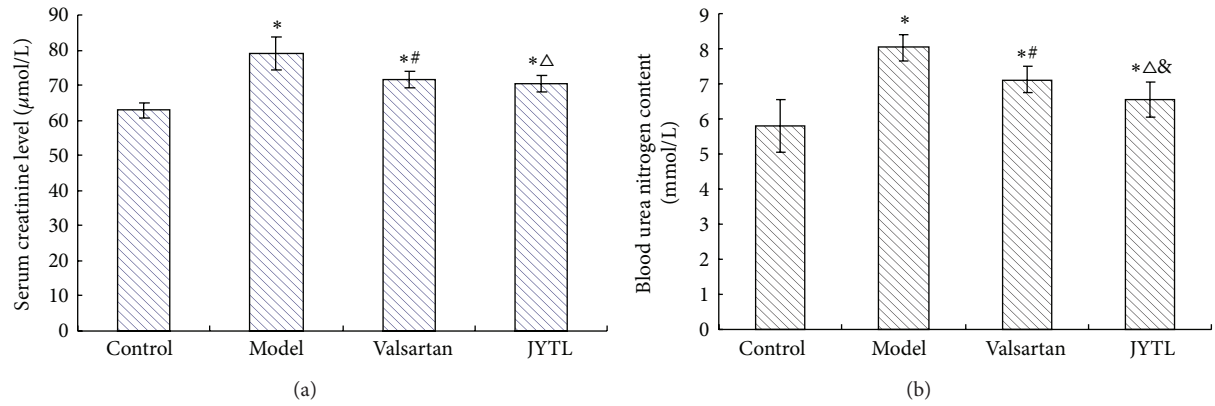

Figure 4: Effect of JYTL on mean ± SEM renal function ($n = 7$ in each group). (a) Serum creatinine. (b) Blood urea nitrogen. $^{*}P < 0.01$, model, valsartan, and JYTL rats versus control rats. $^{\#}P < 0.01$, rats in the valsartan group versus model rats. $^{\triangle}P < 0.01$, rats in the JYTL group versus model rats. $^{\&}P < 0.05$, JYTL versus valsartan group.

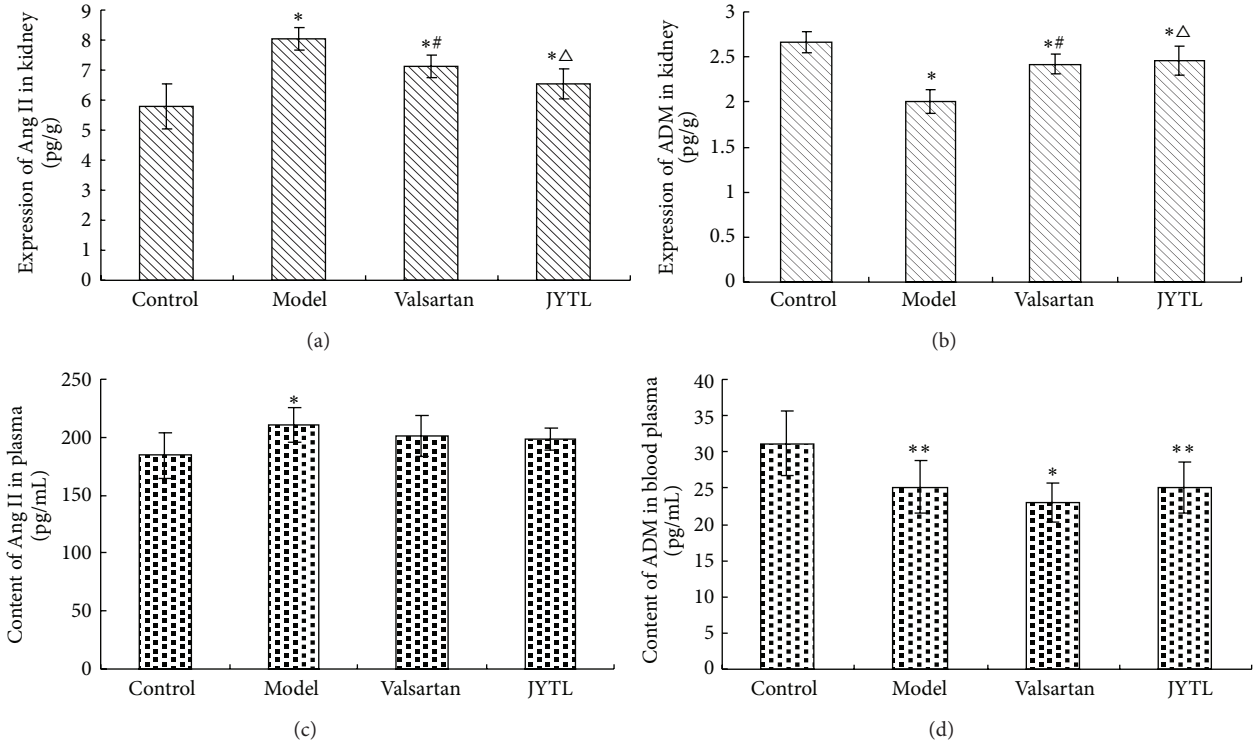

Figure 5: Effect of JYTL on mean ± SEM ADM and Ang II content ($n = 7$ per group). (a) Ang II in kidney. (b) ADM in kidney. (c) Ang II in plasma. (d) ADM in plasma. $^{*}P < 0.01$ and $^{**}P < 0.05$, model, valsartan, and JYTL rats versus control rats. $^{\#}P < 0.01$, rats in the valsartan group versus model rats. $^{\triangle}P < 0.01$, JYTL group versus model group.

Reactive oxygen species can stimulate enzymes which have oxidative stress sensitivity and nuclear transcription factors (NF-κB and AP-1) and can increase the expression levels of cytokine and chemotactic and adhesion factors. The final stages of the mechanism of hypertensive nephrosclerosis include triggering renal interstitial inflammation, renal fibroblasts proliferation and conversion, and the formation of renal fibrosis [15].

The functional impairment of vascular endothelial cells therefore plays a critical role in the pathogenesis of hypertensive nephrosclerosis. Apoptosis of microvascular endothelial cells induces microvessel rarefaction and increases peripheral resistance, which in turn increases BP, decreases the ability of substance and energy metabolism, and reduces reserve capacity and material exchange ability, resulting in the injury of target organs. This present study found that Ang II promoted

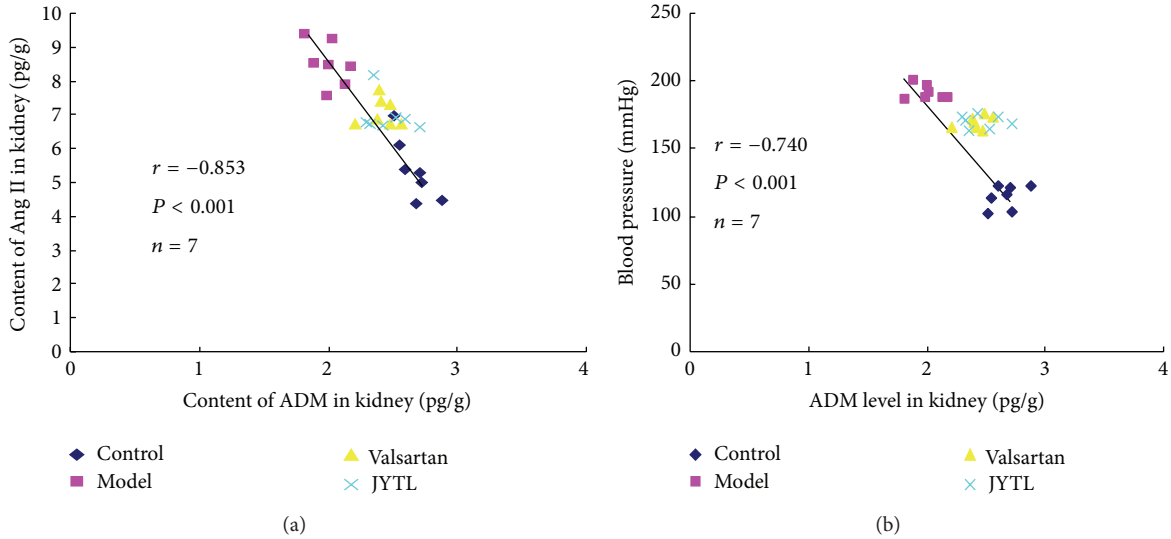

Figure 6: (a) Correlation between ADM and Ang II levels in the kidney. (b) Correlation between BP and ADM levels in the kidney.

endothelial cell apoptosis in a concentration-dependent manner. Endothelial cell apoptosis induces an imbalance of proliferation versus apoptosis of smooth muscle cells. This procession eventually results in changes to the structure and function of blood vessels and target organ damage [16–18]. Therefore, inhibition of blood vessel injuries by Ang II is key to the treatment of hypertension-induced organ injury.

AMD is a novel vasorelaxant peptide. It is critical for both vascular remodeling and blood pressure regulation and plays an important role in the protection of kidneys and blood vessels [5]. It dilates the blood vessels in two ways: endothelium-dependent dilation and endothelium-independent dilation [19–21]. ADM can increase blood flow and glomerular filtration rate through the dilation of the afferent and efferent arterioles [4]. It can also block the action of Ang II-induced mitogen-activated protein kinase, resulting in the prohibition of overproliferation of smooth muscle cells [4, 22] and the inhibition of endothelial cell apoptosis through a NO-dependent mechanism [23]. ADM promotes impaired endothelial cells reendothelialization through the cyclic adenosine monophosphate and phosphatidylinositol 3-kinase pathways, consequently playing a role in vascular endothelial growth and the promotion of angiogenesis [24, 25].

Collagen and elastin, which are secreted by fibroblasts and inhibit vascular sclerosis through the regulation of matrix metalloproteinase-2 activity and protein expression, are reduced by ADM [26]. Therefore, ADM is regarded as a crucial factor not only for preventing an increase in BP but also for preventing target organ damage. Consequently, studies of ADM have become a research focus in the field of hypertension nephrosclerosis. ADM is an endogenic substance involved in a variety of bodily functions in an autocrine and paracrine manner; however, it is expensive and therefore unsuitable for long-term therapy. Therefore, the development of drugs that promote the generation of endogenous ADM and improve its bioactivity has become an urgent requirement.

Traditional Chinese medicine (TCM) has been used since a long time and positive treatment effects have been observed in hypertensive nephrosclerosis [27, 28]. JYTL formula used in this study is composed of *Nacre, Cassia occidentalis, Safflower, Salvia miltiorrhiza, and Chrysanthemum*. This preparation was derived from the JYTM formula invented by Shikui Guo (one of the most prestigious TCM cardiovascular specialists) and it has obvious therapeutic effects on cardiovascular disease [29]. Modern pharmacological research has shown that *Nacre* exerts an anti-inflammatory effect in the treatment of vascular headache. *Cassia occidentalis* depresses blood pressure, reduces the extracellular matrix, inhibits mesangial cell proliferation, reduces proteinuria, and improves renal function. *Safflower and Salvia miltiorrhiza* have antioxidant and anti-inflammatory effects; clinical validation confirms their curative effect in terms of promoting blood circulation to remove blood stasis. They are also known to play a major role in renal interstitial fibrosis, vascular endothelial injury, and oxidative stress [29–33]. *Chrysanthemum* can cause significant dilation of the coronary artery, increase in coronary blood flow, and improvement of myocardial cells for hypoxia tolerance. It also plays an important role in decompression and often synergizes with other drugs to reduce hypertension [34]. In this study, we used JYTL to treat hypertensive nephrosclerosis in a rat model and explore the mechanisms underlying its decompression and protective effects on kidney function.

The results demonstrated that after 4 weeks of treatment with JYTL, the BP of rats decreased, though valsartan group showed better results than the JYTL group at this time. However, with prolonged JYTL treatment, at 6 and 8 weeks, JYTL group showed similar antihypertensive effect as valsartan. Since there are no obvious medical contraindications to TCM, JYTL also can be used when renal functional impairment crosses a specific threshold (serum creatinine >3 mg/dL). On the other hand, valsartan causes reduced glomerular filtration rate (GFR), aggravates renal injury, and is not recommended to use under such conditions.

Our results also showed that JYTL reduced albuminuria, improved renal function, and alleviated renal pathological damage in SHR. To further explore the mechanism of action of JYTL, we estimated the content of Ang II and ADM in the kidneys and plasma. We observed that the plasma ADM content decreased rapidly in the 24-week-old SHR which is different from previous research [35, 36]. This may be due to progressive endothelial cell injury and the self-regulation function in a state of decompensation. However, valsartan and JYTL showed no effect on the level of ADM and Ang II in plasma, which is generally comparable to previous studies [37, 38]. Some authors have described high levels of Ang II in kidney tissue [39] and locally generated Ang II has been implicated in paracrine regulatory mechanisms, leading to altered proliferative and synthetic responses of cells [40]. Therefore, we speculated that the renal protective effect of ADM is not associated with circulating ADM and perhaps renal local RAS plays a more important role in the process of hypertensive nephrosclerosis. We explored the correlation between ADM and Ang II in the kidneys. The data showed that ADM content in SHR kidneys decreased significantly as compared to that in control rats, while Ang II increased. ADM protein content showed a statistically significant, negative correlation between BP and Ang II levels. JYTL and valsartan upregulated the level of ADM and downregulated Ang II level in the kidney. Thus, it can be concluded that ADM may act as a paracrine factor affecting renal function during hypertensive nephrosclerosis and the renal protective effect of JYTL may occur via upregulation of endogenous ADM levels in the kidney and antagonism of vascular injury by Ang II. Further research is required to address the effect of JYTL on receptor systems and the signal transduction pathway of ADM. In addition, further investigations on the molecular mechanism of hypertensive nephrosclerosis may provide alternative therapy and new drug screening approaches.

5. Conclusion

JYTL has renal protective effect in SHRs that may be related to the upregulation of ADM levels in the kidney and the inhibition of vascular injury.

Conflict of Interests

The authors declare that they have no conflict of interests regarding the publication of this paper.

Authors' Contribution

Lin Han and Yan Ma equally contributed to this paper. Jianguo Qin obtained funding and supervised this study. Lin Han conducted the experiments, conceived and designed the experiments, and wrote the draft of the paper. Yan Ma designed this study and participated in writing of the paper. Li-na Li and Yu-shan Gao provided technical support. Xiaoyu Zhang, Yi Guo, Lin-mei Song, Yan-ni Luo, and Xiao-yi Chi helped perform the animal experiments and Lin Han and Jian-guo Qin analyzed the data.

Acknowledgments

This study was supported by the National Natural Science Foundation of China (Grant no. 81173407) and the Administration of Traditional Chinese Medicine of Beijing for the Shikui Guo Famous Doctor Research Lab Project to Jianguo Qin (no. 2011-SZ-A-27).

References

[1] A. J. Collins, R. N. Foley, B. Chavers et al., "United States Renal Data System 2011 Annual Data Report: atlas of chronic kidney disease & end-stage renal disease in the United States," *American Journal of Kidney Diseases*, vol. 59, no. 1, supplement 1, p. A7, 2012.

[2] B. Tomas, "American Society of Nephrology renal research report," *Journal of the American Society of Nephrology*, vol. 16, no. 7, pp. 1886–1903, 2005.

[3] A. Cases and J. Mora-Macía, "Adrenomedullin: a new vasoactive peptide," *Nefrologia*, vol. 21, no. 1, pp. 16–25, 2001.

[4] J. Kato, T. Tsuruda, T. Kita, K. Kitamura, and T. Eto, "Adrenomedullin: a protective factor for blood vessels," *Arteriosclerosis, Thrombosis, and Vascular Biology*, vol. 25, no. 12, pp. 2480–2487, 2005.

[5] J. Bełtowski and A. Jamroz, "Adrenomedullin—what do we know 10 years since its discovery?" *Pharmacology*, vol. 56, no. 1, pp. 5–27, 2004.

[6] C.-Y. Ma, T.-G. Cui, and C.-S. Tang, "Protective effect of adrenomedullin on human renal tubulointerstitial lesion," *Basic Medical Sciences and Clinics*, vol. 21, no. 2, pp. 151–153, 2001.

[7] J.-G. Qin, L. Han, Y.-H. Wang et al., "Action mechanism of Tongmai Yishen Fang in antagonism of renal interstitial fibrosis," *Journal of Beijing University of Traditional Chinese Medicine*, vol. 35, no. 11, pp. 739–742, 2012.

[8] S.-Q. Li, X.-M. Liu, and W.-Z. Wang, "The research study of *Salvia miltiorrhiza* effects on hypertension nephrosclerosis rats," *Chinese Archives of Traditional Chinese Medicine*, vol. 24, no. 2, pp. 224–225, 2006.

[9] W.-Z. Zou, "Instruction on pathologic diagnostic criteria of renal biopsy," *Chinese Journal of Nephrology*, vol. 17, no. 4, pp. 270–275, 2001.

[10] I. Mimura and M. Nangaku, "The suffocating kidney: tubulointerstitial hypoxia in end-stage renal disease," *Nature Reviews Nephrology*, vol. 6, no. 11, pp. 667–678, 2010.

[11] "Effect of enalapril on mortality and the development of heart failure in asymptomatic patients with reduced left ventricular ejection fractions," *The New England Journal of Medicine*, vol. 327, no. 10, pp. 685–691, 1992.

[12] B. M. Brenner, M. E. Cooper, D. de Zeeuw et al., "Effects of losartan on renal and cardiovascular outcomes in patients with type 2 diabetes and nephropathy," *The New England Journal of Medicine*, vol. 345, no. 12, pp. 861–869, 2001.

[13] D. Fliser, "Perspectives in renal disease progression: the endothelium as a treatment target in chronic kidney disease," *Journal of Nephrology*, vol. 23, no. 4, pp. 369–376, 2010.

[14] H.-T. Kuo, S.-J. Shin, M.-C. Kuo, and H.-C. Chen, "Effects of specific endothelin-1 receptor antagonists on proliferation and fibronectin production of glomerular mesangial cells stimulated with angiotensin II," *Kaohsiung Journal of Medical Sciences*, vol. 22, no. 8, pp. 371–376, 2006.

[15] H. T. Tang, D. S. Cheng, Y. T. Jia et al., "Angiotensin II induces type I collagen gene expression in human dermal fibrovlasts through an AP-1 /TCF-β1-dependent pathway," *Biochemical and Biophysical Research Communications*, vol. 385, no. 3, pp. 418–423, 2009.

[16] P. Minuz, P. Patrignani, S. Gaino et al., "Increased oxidative stress and platelet activation in patients with hypertension and renovascular disease," *Circulation*, vol. 106, no. 22, pp. 2800–2805, 2002.

[17] A. J. Polichnowski, C. Jin, C. Yang, and A. W. Cowley, "Role of renal perfusion pressure versus angiotensin II on renal oxidative stress in angiotensin II-induced hypertensive rats," *Hypertension*, vol. 55, no. 6, pp. 1425–1430, 2010.

[18] N. Bouvier, J. P. Flinois, J. Gilleron et al., "Cyclosporine triggers endoplasmic reticulum stress in endothelial cells: a role for endothelial phenotypic changes and death," *The American Journal of Physiology—Renal Physiology*, vol. 296, no. 1, pp. F160–F169, 2009.

[19] P.-X. Xu, H. Li, and Z.-Y. Sun, "Expression of vascular endothelial growth factor in myocardium of spontaneously hypertensive rats," *Medical Journal of the Chinese People's*, vol. 16, no. 7, pp. 491–493, 2005.

[20] S.-L. Wang and Z.-B. Zhang, "Apoptosis of vascular endothelial cells," *Journal of Liaoning University of TCM*, vol. 13, no. 3, pp. 50–53, 2011.

[21] F. Yoshihara, S.-I. Suga, N. Yasui et al., "Chronic administration of adrenomedullin attenuates the hypertension and increases renal nitric oxide synthase in Dahl salt-sensitive rats," *Regulatory Peptides*, vol. 128, no. 1, pp. 7–13, 2005.

[22] Y. Shimekake, K. Nagata, S. Ohta et al., "Adrenomedullin stimulates two signal transduction pathways, cAMP accumulation and Ca^{2+} mobilization, in bovine aortic endothelial cells," *The Journal of Biological Chemistry*, vol. 270, no. 9, pp. 4412–4417, 1995.

[23] T. Horio, M. Kohno, H. Kano et al., "Adrenomedullin as a novel antimigration factor of vascular smooth muscle cells," *Circulation Research*, vol. 77, no. 4, pp. 660–664, 1995.

[24] M. Kohno, K. Yokokawa, H. Kano et al., "Adrenomedullin is a potent inhibitor of angiotensin II-induced migration of human coronary artery smooth muscle cells," *Hypertension*, vol. 29, no. 6, pp. 1309–1313, 1997.

[25] H. K. Wong, T. T. Cheung, and B. M. Y. Cheung, "Adrenomedullin and cardiovascular diseases," *JRSM Cardiovascular Disease*, vol. 1, no. 5, article 14, 7 pages, 2012.

[26] K. Miyashita, H. Itoh, N. Sawada et al., "Adrenomedullin provokes endothelial Akt activation and promotes vascular regeneration both in vitro and in vivo," *FEBS Letters*, vol. 544, no. 1–3, pp. 86–92, 2003.

[27] S. E. Hermansen, T. Lund, T. Kalstad, K. Ytrehus, and T. Myrmel, "Adrenomedullin augments the angiogenic potential of late outgrowth endothelial progenitor cells," *American Journal of Cell Physiology*, vol. 300, no. 4, pp. C783–C791, 2011.

[28] T. Tsuruda, J. Kato, Y.-N. Cao et al., "Adrenomedullin induces matrix metalloproteinase-2 activity in rat aortic adventitial fibroblasts," *Biochemical and Biophysical Research Communications*, vol. 325, no. 1, pp. 80–84, 2004.

[29] X.-X. Zhu, D. Yan, S.-H. Yan et al., "Empirical study of Jiang ya Yi shen particles on ET-1 and TGF-β_1 expression in spontaneously hypertensive rats (SHR)," *Chinese Archives of Traditional Chinese Medicine*, vol. 28, no. 9, pp. 1805–1806, 2010.

[30] I. J. Cho, C. Lee, and T. Y. Ha, "Hypolipidemic effect of soluble fiber isolated from seeds of cassia tora Linn. In rats fed a high-cholesterol diet," *Journal of Agricultural and Food Chemistry*, vol. 55, no. 4, pp. 1592–1596, 2007.

[31] J. Ma, Z. Chen, and Y. Wang, "The clinical observation of treatment of hypertensive renal injury edema by combination of fangjihuangqi decoction and western medicine," *Chinese Journal of Basic Medicine in Traditional Chinese Medicine*, vol. 18, no. 8, pp. 879–880, 2012.

[32] H.-Q. Tao, J. Li, J. Zhang et al., "The curative effect observation of treatment of early stage in hypertensive renal injury by combination of Liuwei Dihuang Wan and western medicine," *Shaanxi Journal of Traditional Chinese Medicine*, vol. 33, no. 4, pp. 411–412, 2012.

[33] W. Zheng and S.-Q. Li, "The effect of tongxinluo on blood vessel endothelium in spontaneously hypertension rat," *Chinese Journal of Integrative Medicine on Cardio-/Cerebrovascular Disease*, vol. 7, no. 2, pp. 179–180, 2009.

[34] Z. Jan, Y.-B. Li, D.-W. Qian et al., "Chrysanthemum chemical components and pharmacological activity research progress," *Lishizhen Medicine and Materia Medica Research*, vol. 17, no. 10, pp. 1941–1942, 2006.

[35] R. Tang, Q.-L. Zhou, P. Veeraragoo, Z. Xiao, and Z. Liu, "Effects of cordyceps sinensis on renal Klotho expression and oxidative stress in spontaneously hypertensive rats," *Chinese Journal of Nephrology Dialysis & Transplantation*, vol. 19, no. 4, pp. 338–343, 2010.

[36] J.-G. Qin, Y.-H. Wang, J.-P. Liang et al., "Weiqin Guo's treatment experience about hypertension," *Journal of Traditional Chinese Medicine*, vol. 48, no. 7, pp. 586–589, 2007.

[37] T. Ishimitsu, T. Nishikimi, Y. Saito et al., "Plasma levels of adrenomedullin, a newly identified hypotensive peptide, in patients with hypertension and renal failure," *Journal of Clinical Investigation*, vol. 94, no. 5, pp. 2158–2161, 1994.

[38] M. Kohno, T. Hanehira, H. Kano et al., "Plasma adrenomedullin concentrations in essential hypertension," *Hypertension*, vol. 27, no. 1, pp. 102–107, 1996.

[39] B. Braam, K. D. Mitchell, J. Fox, and L. G. Navar, "Proximal tubular secretion of angiotensin II in rats," *The American Journal of Physiology—Renal Fluid and Electrolyte Physiology*, vol. 264, no. 5, part 2, pp. F891–F898, 1993.

[40] M. Bader, J. Peters, O. Baltatu, D. N. Müller, F. C. Luft, and D. Ganten, "Tissue renin-angiotensin systems: new insights from experimental animal models in hypertension research," *Journal of Molecular Medicine*, vol. 79, no. 2, pp. 76–102, 2001.

Hindawi Publishing Corporation
Evidence-Based Complementary and Alternative Medicine
Volume 2015, Article ID 864597, 6 pages
http://dx.doi.org/10.1155/2015/864597

Research Article

Qing Re Liang Xue Decoction Alleviates Hypercoagulability in Kawasaki Disease

Jiao-yang Chen,[1] Ji-ming Yin,[2] Zhong-dong Du,[1] Jing Hao,[1] and Hui-min Yan[1]

[1]*Department of Pediatrics, Beijing Children's Hospital, Capital Medical University, Beijing 100045, China*
[2]*Research Department Beijing Institute of Hepatology, Beijing Youan Hospital, Capital Medical University, Beijing 100045, China*

Correspondence should be addressed to Hui-min Yan; huiminyan@sina.com

Received 29 December 2014; Revised 7 March 2015; Accepted 14 March 2015

Academic Editor: Zhang Tan

Objective. Kawasaki disease (KD) is a multisystemic autoimmune vasculitis. Intravenous immunoglobulin (IVIG) is the first-line treatment for KD. It is unclear whether traditional Chinese medicine (TCM) has an effect on KD. We aimed to observe the clinical efficacy of TCM on acute KD via serum interleukin-33 (IL-33) and tumor necrosis factor alpha (TNF-α) measurements. *Methods*. Thirty-one KD patients were treated with Qing Re Liang Xue decoction and Western medicine (integrative medicine treatment group), while 28 KD patients were treated with Western medicine only (Western medicine treatment group). Thirty patients were included in a febrile group and 28 healthy children were included in the control group. Clinical characteristics and laboratory findings were gathered and compared. Serum IL-33 and TNF-α levels were measured by multiplex Luminex assay. *Results*. The platelet count in the integrative medicine treatment group was significantly lower than that in the Western medicine treatment group. The integrative medicine group had a shorter fever duration and lower IL-33 and TNF-α levels than those in the Western medicine group, but there were no significant differences between the two KD groups after treatment. *Conclusion*. Qing Re Liang Xue decoction improved the hypercoagulable state of KD patients. Potential myocardial protective effects require further research.

1. Introduction

Kawasaki disease (KD) is an acute, self-limiting multisystem inflammatory vasculitis that occurs in children. More than 85% of patients are younger than 5 years old. Although children are treated with large doses of intravenous immunoglobulin (IVIG), as many as 3–5% suffer coronary artery lesions (CAL) [1]. The etiology of KD is unknown, but the most widely proposed theories include environmental toxin exposure, autoimmune pathogenesis, and infectious diseases [2].

Cytokines like tumor necrosis factor alpha (TNF-α), an inflammatory mediator, are believed to be involved in the vascular lesions of KD. TNF-α expression is increased in the peripheral blood of KD patients during the acute phase [3] and upregulates the expression and activities of matrix metalloproteinases [4]. Interleukin-33 (IL-33), a novel member of the IL-1 family, has recently been implicated in several inflammatory and autoimmune diseases, including atherosclerosis, sepsis, asthma, allergy, Crohn's disease, ankylosing spondylitis, arthritis, and systemic lupus erythematosus [5, 6]. IL-33 is widely expressed in many tissues such as the lung, liver, central nervous system, and multiple types of cells including epithelial cells, endothelial cells, smooth muscle cells, macrophages, and fibroblasts [6–8]. IL-33 is stimulated by signals like inflammation and is secreted into the extracellular milieu [9]. IL-33 induces cytokine synthesis and mediates inflammatory responses through its receptor, ST2 [7]. KD may be induced by one or more known or unknown microbes, monocytes, macrophages, or T and B cells, which generate a systemic inflammatory response mediated by cytokines and chemical factors.

The first-line treatment of KD is IVIG and oral aspirin. IVIG reduces the prevalence of coronary artery abnormalities by reducing tissue inflammation and immune activation [10]. However, IVIG is expensive, and it can cause Qi and Yin deficiency in later stage of KD. Chinese herbs have a significant effect on some pediatric diseases. Therefore, traditional

Table 1: Clinical characteristics of KD patients, febrile patients, and healthy children.

	IG ($n = 31$)	WG ($n = 28$)	Febrile group ($n = 30$)	Healthy group ($n = 28$)
Male/female	22/9	25/3	24/6	22/6
Age onset (years)	2.1 ± 1.3	2.1 ± 1.8	3.4 ± 1.7	3.6 ± 1.1
<1 year	8	8	2	3
1–5 years	23	19	24	21
>5 years	0	1	4	4

Note: IG: integrative medicine treatment group (treated with Qing Re Liang Xue decoction and Western medicine); WG: Western medicine treatment group (treated with IVIG and/or aspirin); febrile group: children who had a fever with pneumonia or bronchitis; healthy group: healthy children without any diseases; KD: Kawasaki disease.

Chinese treatment might provide a new therapy for KD. We aimed to observe the clinical efficacy of Qing Re Liang Xue decoction on serum IL-33 and TNF-α levels in KD patients to observe whether Chinese herbs could alleviate inflammation.

2. Materials and Methods

2.1. Patients and Sample Preparations. Fifty-nine patients diagnosed with KD, 28 healthy children, and 30 febrile children (including bronchitis and pneumonia) were enrolled in the study at Beijing Children's Hospital, China. KD patients were divided into two groups with the random number table method: integrative medicine treatment group (IG) ($n = 31$) and Western medicine treatment group (WG) ($n = 28$). All KD patients met the Diagnostic Guidelines established by the Kawasaki Disease Research Committee in Japan [11]. All 59 KD patients were also diagnosed with flaring heat in qifen and yingfen, according to traditional Chinese medicine (TCM) diagnostic criteria. Exclusion criteria included incomplete KD, fever time exceeding 7 days, treatment with IVIG before hospitalization, and not having flaring heat in qifen and yingfen syndrome.

All KD patients received both IVIG (2 g/kg) and aspirin (30 mg/kg/day). The aspirin dosage was decreased to 5 mg/kg per day after normalization of C-reactive protein (CRP) values. The IG also received Qing Re Liang Xue decoction. No response to initial treatment with IVIG was defined as a fever ($T > 38^{\circ}$C) lasting more than 36 hours after the end of the IVIG infusion or recurring fever after fever abatement with at least one of the clinical features of KD. Patients not responding to IVIG received additional IVIG (1 g/kg) or prednisone (1 mg/kg).

Serum was obtained from patients in the acute phase of KD before IVIG administration and in the recovery phase (7 days after fever abatement). Serum samples from healthy children and febrile patients were also collected. Patients in the febrile group had a fever before treatment. All serum samples were stored at −80°C until the assay was performed.

2.2. Syndrome Differentiation Treatment. The IG was treated with Qing Re Liang Xue decoction. The decoction is composed of Shengshigao (gypsum fibrosum) 15 g, Zhimu (*Rhizoma Anemarrhenae*) 9 g, Jinyinhua (*Flos Lonicerae*) 6 g, Lianqiao (*Fructus Forsythiae Suspensae*) 6 g, Huangqin (*Radix Scutellariae Baicalensis*) 9 g, Danshen (*Radix Salviae Miltiorrhizae*) 9 g, Zhuye (*Folium Phyllostachydis Henonis*) 3 g, Mudanpi (*Cortex Moutan Radicis*) 9 g, Dihuang (*Radix Rehmanniae*) 8 g, Zhizi (*Fructus Gardeniae*) 6 g, and Lingyangjiao (*Cornu Saigae Tataricae*) 0.15 g. All Chinese herbs were decocted in water and administered orally twice a day, with 7 days in a course.

2.3. Assay for Serum IL-33 and TNF-α Level. The levels of serum cytokines IL-33 and TNF-α were measured with a multiplex Luminex assay (EMD Millipore Co., Billerica, MA, USA), following the manufacturer's instructions. All samples were measured in duplicate as previously described.

2.4. Statistical Analysis. All data were analyzed using SPSS 17.0 (IBM Institute, Armonk, NY, USA) software. All data are expressed as mean ± SD. KD patients, febrile patients, and healthy children were compared using the Mann-Whitney U test for numerical data. Changes in serum IL-33 and TNF-α levels before and after IVIG treatment were compared with the paired Student's t-test. All P values were two-tailed. A P value less than 0.05 was considered statistically significant for all tests.

3. Results

3.1. Clinical Characteristics of KD Patients, Febrile Patients, and Healthy Children. In this study, 31 KD patients treated with integrative medicine (aged 7 months to 5 years), 28 KD patients treated with Western medicine (aged 4 months to 8 years), 30 febrile patients (aged 6 months to 7 years), and 28 healthy children (aged 5 months to 6 years) were evaluated. The clinical characteristics of all study subjects are shown in Table 1.

3.2. Changes in Clinical Manifestations of Different Treatment Groups. Temperature recovery time in the IG was 1.55 ± 1.16 days, which was shorter than that of the WG (1.79±1.44 days). However, there was no significant difference between the two groups ($P = 0.657$) (Figure 1). Changes in lips and oral cavity appearance, hyperemia bulbar, polymorphous exanthema, changes in extremities, and cervical lymphadenopathy are the main symptoms of KD. The occurrence of these symptoms was obviously decreased after treatment in both IG and WG, but there was no significant difference between the two groups (Figure 2).

Table 2: Comparison of laboratory tests in different treatment groups before and after treatment.

	Integrative medicine treatment group		Western medicine treatment group	
	Before treatment	After treatment	Before treatment	After treatment
WBC ($\times 10^9$/L)	13.5 ± 6.3	8.7 ± 2.7[a]	14.1 ± 6.7	8.5 ± 3.1[b]
PLT ($\times 10^9$/L)	374.9 ± 110.9	478.9 ± 138.3[a]	371.3 ± 130.2	541.5 ± 138.4[bc]
CRP (mg/L)	71.7 ± 48.2	9.0 ± 2.4[a]	67.4 ± 45.7	8.3 ± 1.2[b]
ESR (mm/h)	42.4 ± 25.6	33.7 ± 18.4	51.0 ± 30.0	35.9 ± 20.2

Note: WBC: white blood cell; PLT: platelets; CRP: C-reactive protein; ESR: erythrocyte sedimentation rate. Compared with the integrative medicine group before treatment, [a]$P < 0.05$; compared with Western medicine treatment group before treatment, [b]$P < 0.05$; compared with the integrative medicine treatment group after treatment, [c]$P < 0.05$.

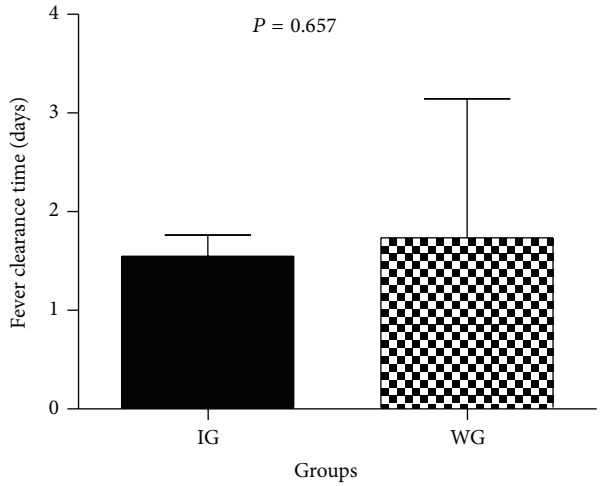

Figure 1: Fever clearance time in the integrative medicine group and Western medicine group. IG: integrative medicine treatment group (treated with Qing Re Liang Xue decoction and Western medicine); WG: Western medicine treatment group (treated with IVIG and/or aspirin). Data are presented as the mean ± SEM. No significant difference was observed between the two groups ($P > 0.05$).

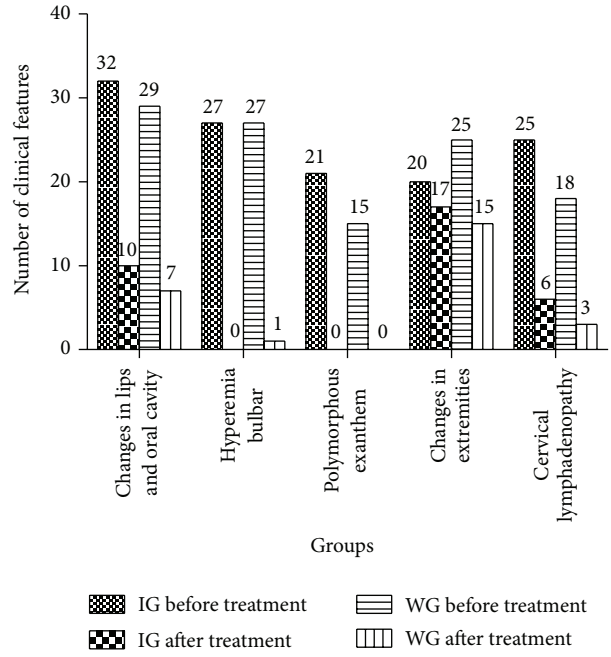

Figure 2: Comparison of numbers of clinical symptoms between the integrative medicine group and Western medicine group before and after therapy. IG: integrative medicine group (treated with Qing Re Liang Xue decoction and Western medicine); WG: Western medicine treatment group (treated with IVIG and/or aspirin).

3.3. Laboratory Examination of IG and WG before and after Therapy. White blood cells (WBC), platelets (PLT), C-reactive protein (CRP), and erythrocyte sedimentation rate (ESR) were evaluated in all patients. WBC, ESR, and CRP were lower after treatment, and PLT was higher in both the IG and WG. There were significant differences in WBC, PLT, and CRP between before and after treatment in each group. After treatment, PLT in the IG was significantly lower than that in the WG ($P = 0.048$) (Table 2).

3.4. Comparison of Serum IL-33 and TNF-α Levels among Groups. Levels of IL-33 and TNF-α in serum were detected in healthy children, febrile children without KD, and KD patients before and after treatment. Figure 3 shows that the serum levels of IL-33 in healthy controls (28.1 ± 56.0 pg/mL) were significantly lower than those in IG before therapy (43.4 ± 29.0 pg/mL) and after therapy (47.3 ± 36.6 pg/mL) and WG after IVIG (78.0 ± 143.7 pg/mL) ($P < 0.05$) (Figure 3(a)). There were no significant differences in IL-33 levels between the KD groups and the febrile group.

TNF-α levels in the WG before therapy (42.3 ± 21.1 pg/mL) were significantly higher than those of healthy controls (29.0 ± 11.3) and febrile children (27.8 ± 9.3 pg/mL). After therapy, TNF-α level increased in the WG (47.0 ± 57.8 pg/mL). TNF-α levels were significantly higher in the WG than those in the febrile group (27.8 ± 9.3 pg/mL) (Figure 3(b)). No significant differences were observed in TNF-α level between the IG before and after treatment and healthy group or febrile patients.

IL-33 and TNF-α in the IG were lower than those in the WG (47.3 ± 36.5 pg/mL versus 78.0 ± 143.7 pg/mL and 36.5 ± 18.4 pg/mL versus 47.0 ± 57.8 pg/mL, resp.), but the differences were not significant (Figures 3(a) and 3(b)).

4. Discussion

In this study, we found that treatment with Qing Re Liang Xue decoction plus Western medicine resulted in a significantly lower increase in PLT levels than in the Western medicine

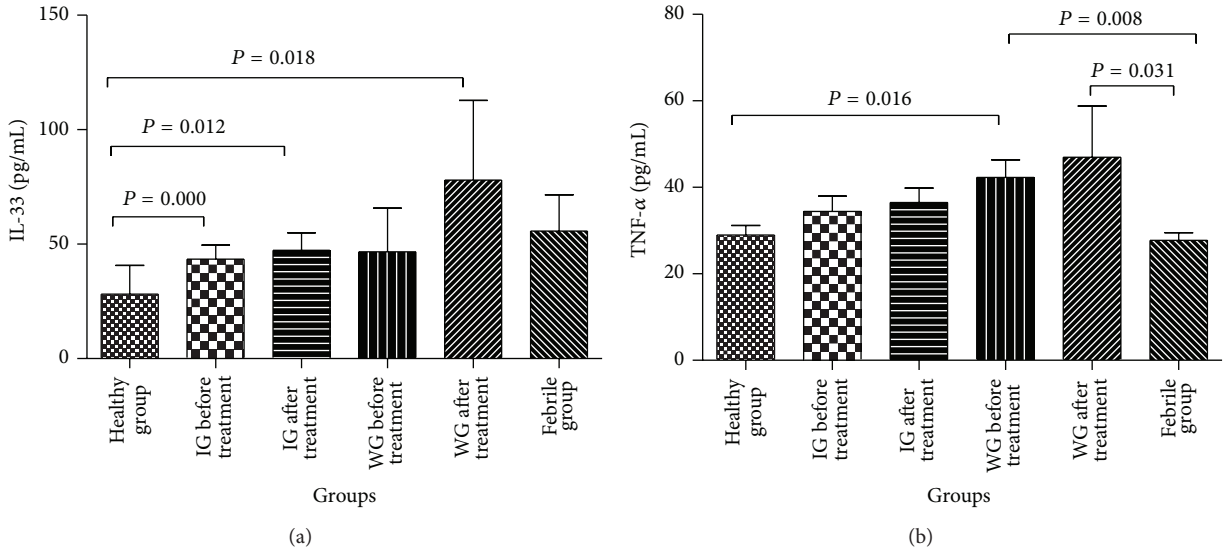

Figure 3: Serum IL-33 and TNF-α levels among groups. IL: interleukin; TNF: tumor necrosis factor; IG: integrative medicine treatment group (treated with Qing Re Liang Xue decoction and Western medicine); WG: Western medicine treatment group (treated with IVIG and/or aspirin). Data are presented as the mean ± SEM. Significant differences comparing IL-33 level in the healthy group with the IG before and after treatment and the WG after treatment are marked as $P < 0.05$. Significant differences comparing TNF-α levels in the WG before treatment with the healthy and febrile groups and the WG after treatment with the febrile group are marked as $P < 0.05$.

group. Moreover, inflammatory cytokines were lower in KD patients treated with integrative medicine compared with Western medicine, although the differences were not significant. We used multiplex Luminex assay because it offers a highly sensitive and accurate method of determining serum levels in samples and uses small quantities.

KD patients treated with integrative medicine had a normal temperature more quickly than those in the Western medicine group, although the difference was not significant. Therefore, Chinese medicine could possibly abate the fever in KD patients. In Qing Re Liang Xue decoction, *Cornu Saigae Tataricae*, gypsum fibrosum, *Radix Rehmanniae*, and *Cortex Moutan Radicis* have cold properties according to TCM theory, which might have a role in removing heat to cool the blood and drop temperature.

In the laboratory tests after treatment, only the PLT level was significantly different between the two KD groups. Platelet counts are usually evaluated after day 7 of an illness [12], which makes the patients hypercoagulable. Coronary artery lesions (CAL) are the most common and worst complication of KD and are related to cardiac disease progression in adults who have a KD history. One risk factor for predicting aneurysms is platelet count. The smaller increase in PLT levels in the IG compared with the WG might be caused by the *Radix Salviae Miltiorrhizae* and *Cortex Moutan Radicis*. These two herbs can activate circulation to remove blood stasis, according to TCM. *Radix Salviae Miltiorrhizae* can act as an antiarrhythmic, antiplatelet aggregate and has myocardial protective effects [13]. Qingying decoction and Qingwenbaidu decoction are classical Chinese medicine formulae to clear heat. Qingying decoction is supposed to clear heat and cool blood and can act as an antipyretic, sedative, anti-inflammatory, and antibiotic and can repair myocardial cells [14]. Modern pharmacological study indicates that heat-clearing and blood-activating Chinese medicines could improve microcirculation, increase hemodynamics, reduce platelet aggregation, and prevent thrombus formation. Qing Re Liang Xue decoction gathered the advantages of many prescriptions; therefore, we hypothesize that Qing Re Liang Xue decoction could relieve hypercoagulability and decrease CAL incidence, but more research is required.

IL-33 expression was significantly higher in KD patients compared with healthy control patients, but there was no significant difference between the two KD groups and febrile group. TNF-α in the WG before treatment was significantly higher than that in the healthy and febrile groups. TNF-α, either alone or in cooperation with other cytokines, regulates the production of chemokines on endothelial cells [3]. IL-33 is a newly reported cytokine in the IL-1 family and can be produced by various types of tissues and cells. It has been reported to participate in the development and progression of many diseases like rheumatoid arthritis, systemic lupus erythematosus, ankylosing spondylitis, Behçet's disease, systemic sclerosis, and coronary artery disease [6, 15]. IL-33 functions by binding to its receptor ST2 as a proinflammatory cytokine [16] and shares the IL-1R accessory protein (IL-1RAcP) and subsequent IL-1RAcP-dependent signaling pathway activation with other members of the IL-1 family [17]. In our study, serum IL-33 levels were higher in the IG and WG after treatment, although the differences were not significant. Nevertheless, this slight effect might suggest that an inflammatory response was present. Immune disorder and inflammatory cytokine activity increase in the middle stages of KD, from the 3rd to 5th weeks. During this period, patients are at high risk of CAL development. Therefore, inhibiting this acute inflammation is important for reducing the CAL

risk. Serum IL-33 levels in the IG were lower than the WG after treatment, and fever duration in the IG was shorter than that in the WG, although these differences were not significant. These results indicate that Chinese herbs might help prevent the progression of KD and possibly protect the myocardium.

Many studies have focused on the relationship between IL-33 and TNF-α. Previous studies reported that TNF-α could stimulate the production of IL-33 [18]. In the synovial fibroblasts of patients with rheumatoid arthritis, IL-33 was detected and was markedly upregulated by the addition of TNF-α and IL-1β [19]. Matsuyama et al. also found that IL-33 expression was induced by IL-1β, and IL-33 expression was enhanced by costimulation with IL-1β and TNF-α [20].

Recent studies have shown that the inflammatory factors IL-6, TNF-α, C-reactive protein, adhesion molecules, and Endothelin-1 participate in the formation of blood stasis directly or indirectly [21]. Some studies have previously reported that TNF-α is closely linked to inflammatory responses and the development and maintenance of arterial remodeling through the release of cytokines [22]. TNF-α appears to be critical during the evolution of coronary artery damage in a murine model of KD [3], and chronic overexpression of TNF-α in the heart resulted in dilated cardiomyopathy and increased mortality [23]. Xie et al. found that the expressions of apolipoprotein A-I and α_1-antitrypsin were different in patients with blood stasis syndrome and coronary heart disease (CHD) with unstable angina pectoris. This result indicated that inflammation may be one of the mechanisms of blood stasis syndrome in CHD [24]. *Radix Salviae Miltiorrhizae* can improve blood stasis and reduce IL-6 levels [25]. KD patients have severe inflammation, which can cause myocardial damage. However, some Chinese herbal medicines can activate blood and remove stasis to treat inflammation and myocardial injury. This mechanism could explain why IL-33 and TNF-α did not decrease after treatment in the two KD groups.

Our study has some limitations. The small sample size was not adequate for reliable assessment. The prevalence of KD has regional and ethnic differences, so a larger sample size from different populations is required to replicate the results. Furthermore, we did not detect cellular IL-33 and TNF-α levels. Serum IL-33 and TNF-α levels are relatively low and were occasionally out of range for measurement. Measuring cellular cytokine expression could contribute more to the role and origin of IL-33 and TNF-α during KD progression. In this study, we collected serum from KD patients on the 1st and 7th days to observe changes in serology. There was no significant difference from before to after treatment in serum IL-33 or TNF-α levels in either treatment group. This could be because of the short surveillance time. KD requires a long rehabilitation and the cytokine levels could change over time. A follow-up evaluation might be important in patients with KD. Finally, the decoction has an unfavorable taste for younger children, so compliance in the study was poor. Innovation in Chinese traditional drug agents could help improve this issue, but further study is required.

5. Conclusion

Qing Re Liang Xue decoction reduced platelet count, which indicates that the decoction could alleviate hypercoagulability in KD patients. Serum IL-33 and TNF-α levels were remarkably elevated in KD patients, which indicates that KD development involves inflammation. Qing Re Liang Xue decoction could decrease serum IL-33 and TNF-α levels. Therefore, the traditional Chinese medicine might have an effect on alleviating inflammation and protecting the myocardium in KD patients.

Ethical Approval

All procedures performed in this study were in accordance with the ethical standards of the institutional and national research committee and with the 1964 Helsinki declaration and its later amendments or comparable ethical standards.

Consent

All patients gave informed consent.

Disclosure

The funding agencies had no role in the design or conduct of the study, no role in data collection or analysis, and no role in the preparation or review of the paper.

Conflict of Interests

The authors declare that they have no conflict of interests.

Authors' Contribution

All the authors listed have read through the paper, approved for publication.

Acknowledgments

This study was supported by the grants from National Natural Science Foundation of China (nos. 81274109 and 30973238), Key Research Project of Beijing Natural Science Foundation (B)/Beijing Education Committee (no. KZ 201010025024), and Project for Science and Technology Innovation, Beijing Education Committee (no. PXM2011_014226_07_000085).

References

[1] J. C. Burns and M. P. Glodé, "Kawasaki syndrome," *The Lancet*, vol. 364, no. 9433, pp. 533–544, 2004.

[2] A. H. Rowley, "Kawasaki disease: novel insights into etiology and genetic susceptibility," *Annual Review of Medicine*, vol. 62, pp. 69–77, 2011.

[3] J. S. Hui-Yuen, T. T. Duong, and R. S. M. Yeung, "TNF-α is necessary for induction of coronary artery inflammation and aneurysm formation in an animal model of Kawasaki disease," *The Journal of Immunology*, vol. 176, no. 10, pp. 6294–6301, 2006.

[4] H. Xue, K. Sun, W.-P. Xie et al., "Etanercept attenuates short-term cigarette-smoke-exposure-induced pulmonary arterial remodelling in rats by suppressing the activation of TNF-α/NF-κB signal and the activities of MMP-2 and MMP-9," *Pulmonary Pharmacology & Therapeutics*, vol. 25, no. 3, pp. 208–215, 2012.

[5] C. J. Beltrán, L. E. Núñez, D. Díaz-Jiménez et al., "Characterization of the novel ST2/IL-33 system in patients with inflammatory bowel disease," *Inflammatory Bowel Diseases*, vol. 16, no. 7, pp. 1097–1107, 2010.

[6] L. Duan, J. Chen, F. Gong, and G. Shi, "The role of IL-33 in rheumatic diseases," *Clinical and Developmental Immunology*, vol. 2013, Article ID 924363, 5 pages, 2013.

[7] J. Schmitz, A. Owyang, E. Oldham et al., "IL-33, an interleukin-1-like cytokine that signals via the IL-1 receptor-related protein ST2 and induces T helper type 2-associated cytokines," *Immunity*, vol. 23, no. 5, pp. 479–490, 2005.

[8] D. Préfontaine, S. Lajoie-Kadoch, S. Foley et al., "Increased expression of IL-33 in severe asthma: evidence of expression by airway smooth muscle cells," *The Journal of Immunology*, vol. 183, no. 8, pp. 5094–5103, 2009.

[9] G. Haraldsen, J. Balogh, J. Pollheimer, J. Sponheim, and A. M. Küchler, "Interleukin-33—cytokine of dual function or novel alarmin?" *Trends in Immunology*, vol. 30, no. 5, pp. 227–233, 2009.

[10] C. Galeotti, J. Bayry, I. Kone-Paut, and S. V. Kaveri, "Kawasaki disease: aetiopathogenesis and therapeutic utility of intravenous immunoglobulin," *Autoimmunity Reviews*, vol. 9, no. 6, pp. 441–448, 2010.

[11] M. Ayusawa, T. Sonobe, S. Uemura et al., "Revision of diagnostic guidelines for Kawasaki disease (the 5th revised edition)," *Pediatrics International*, vol. 47, no. 2, pp. 232–234, 2005.

[12] J. W. Newburger, M. Takahashi, M. A. Gerber et al., "Diagnosis, treatment, and long-term management of Kawasaki disease: a statement for health professionals from the Committee on Rheumatic Fever, Endocarditis and Kawasaki Disease, Council on Cardiovascular Disease in the Young, American Heart Association," *Circulation*, vol. 110, no. 17, pp. 2747–2771, 2004.

[13] M. Zhang, H. Zhang, P. Xu, and R.-Y. Su, "Research progress of Tanshinone II A pharmacological activity," *Yi Yao Dao Bao*, vol. 28, no. 10, pp. 1237–1239, 2008.

[14] B.-G. Zhang, T.-F. Cheng, and Q.-F. Liu, "Efficacy and modern clinical application of Qingying decoction," *Chinese Traditional Patent Medicine*, vol. 31, no. 11, pp. 1741–1744, 2009.

[15] X. Tu, S. Nie, Y. Liao et al., "The IL-33-ST2L pathway is associated with coronary artery disease in a Chinese Han population," *The American Journal of Human Genetics*, vol. 93, no. 4, pp. 652–660, 2013.

[16] D. Xu, H.-R. Jiang, P. Kewin et al., "IL-33 exacerbates antigen-induced arthritis by activating mast cells," *Proceedings of the National Academy of Sciences of the United States of America*, vol. 105, no. 31, pp. 10913–10918, 2008.

[17] J. Seltmann, T. Werfel, and M. Wittmann, "Evidence for a regulatory loop between IFN-γ and IL-33 in skin inflammation," *Experimental Dermatology*, vol. 22, no. 2, pp. 102–107, 2013.

[18] I. S. Wood, B. Wang, and P. Trayhurn, "IL-33, a recently identified interleukin-1 gene family member, is expressed in human adipocytes," *Biochemical and Biophysical Research Communications*, vol. 384, no. 1, pp. 105–109, 2009.

[19] G. Palmer, D. Talabot-Ayer, C. Lamacchia et al., "Inhibition of interleukin-33 signaling attenuates the severity of experimental arthritis," *Arthritis and Rheumatism*, vol. 60, no. 3, pp. 738–749, 2009.

[20] Y. Matsuyama, H. Okazaki, M. Hoshino et al., "Sustained elevation of interleukin-33 in sera and synovial fluids from patients with rheumatoid arthritis non-responsive to anti-tumor necrosis factor: possible association with persistent IL-1β signaling and a poor clinical response," *Rheumatology International*, vol. 32, no. 5, pp. 1397–1401, 2012.

[21] X.-J. Ma, H.-J. Yin, and K.-J. Chen, "Research progress of correlation between blood-stasis syndrome and inflammation," *Chinese Journal of Integrative Medicine*, vol. 27, no. 7, pp. 669–672, 2007.

[22] J. L. Wright, H. Tai, R. Wang, X. Wang, and A. Churg, "Cigarette smoke upregulates pulmonary vascular matrix metalloproteinases via TNF-α signaling," *American Journal of Physiology—Lung Cellular and Molecular Physiology*, vol. 292, no. 1, pp. L125–L133, 2007.

[23] T. Kuhota, C. F. McTiernan, C. S. Frye et al., "Dilated cardiomyopathy in transgenic mice with cardiac-specific overexpression of tumor necrosis factor-alpha," *Circulation Research*, vol. 81, no. 4, pp. 627–635, 1997.

[24] H. Xie, W. Wang, H.-H. Zhao, and S.-Z. Guo, "Relationgship between plasma ApoA-I, α1-AT and inflammation in blood stasis syndrome of coronary heart disease," *Journal of Beijing University of Traditional Chinese Medicine*, vol. 33, no. 4, pp. 253–256, 2010.

[25] Y. Lv, Y.-P. Wang, W.-J. Li, and L. Zhang, "Clinical researches that the serum NOfbfh ETfbfh IL-6 varieties of chronic renal failure patients with blood stasis symptom and effect of Lei's Danshen tablets," *Chinese Traditional Patent Medicine*, vol. 28, no. 1, pp. 63–67, 2006.

Hindawi Publishing Corporation
Evidence-Based Complementary and Alternative Medicine
Volume 2015, Article ID 358352, 11 pages
http://dx.doi.org/10.1155/2015/358352

Research Article

Enhanced Protective Effect of the Combination of *Uncaria* and *Semen Raphani* on Vascular Endothelium in Spontaneously Hypertensive Rats

Yun-lun Li,[1] Yue-Hua Jiang,[1] Chuan-Hua Yang,[1] Jing-Chang Sun,[2] Miao-Miao Wang,[2] and Wen-Qing Yang[2]

[1]*Affiliated Hospital of Shandong University of Traditional Chinese Medicine, Jinan, Shandong 250011, China*
[2]*Shandong University of Traditional Chinese Medicine, Jinan, Shandong 250355, China*

Correspondence should be addressed to Yun-lun Li; yunlun.lee@hotmail.com

Received 13 February 2015; Revised 20 May 2015; Accepted 28 May 2015

Academic Editor: Zhang Tan

Endothelial dysfunction and low-grade inflammation are closely associated with hypertension and other cardiovascular diseases. The combination of *Uncaria (U)* and *Semen Raphani (R)* is common in traditional Chinese medicine for the treatment of hypertension and heart diseases. We aimed to investigate the therapeutic effect of the combination of *Uncaria* and *Semen Raphani* on spontaneously hypertensive rats (SHRs), and valsartan was used as a positive control. In the present study, all extracts decreased systolic pressure, diastolic pressure, and mean arterial pressure. *U* alone showed antihypertensive efficacy and effectively decreased CECs count, while *R* alone showed efficacy in relieving inflammatory level. The combination of *U* and *R* showed enhanced effectiveness at lowering activated CECs and improving endothelial integrity of thoracic aorta and mesenteric artery and normalized the level of plasma biomarkers of endothelial damage. The combination of *U* and *R* decreased the mRNA level of VCAM-1, Sel-L, TFPI, and Sel-P, while it elevated mRNA expression of FGF-1 and THBD of the thoracic aorta, which may be, at least in part, involved in the mechanism of protective effect on hypertensive endothelial injury.

1. Introduction

Hypertension is a very common disease and an important risk factor in cardiovascular events, which are characterized by functional and structural vascular abnormalities. Vascular endothelium plays a fundamental role in modulating vascular tone and structure, and the endothelial dysfunction and resulting structural changes may be responsible for the adverse outcomes of hypertension [1]. Well-maintained endothelial function and integrity is of importance in numerous conditions, such as hypertension and inflammatory and cardiovascular disease and their risk factors [2, 3]. The damage of vascular endothelium leads to hypercoagulation, vascular inflammation, and an imbalance of oxidative and antioxidative systems. These pathological changes increase the risk of cardiovascular events and one of the pathological changes of hypertension is to convert mural endothelial cells into circulating endothelial cells (CECs). The amount of peripheral CECs correlates to disease intensity and functions as a valuable damage marker, and these cells are thought to originate from the sloughing-off of the vessel wall, following some form of pathological insult [4]. Increased CECs number in the blood is the product of a disease process that irreversibly damages the endothelium [5].

Uncaria (U) is a rubiaceous plant growing in South China. Total *Uncaria* alkaloids are the alcohol extract of the stems of *Uncaria*. *Rhynchophylline* and *Isorhynchophylline* are main pharmacological components in total *Uncaria* alkaloids. We know that *Rhynchophylline* and *Isorhynchophylline* have pharmacological effects similar to calcium channel antagonist, blood pressure lowering, antimyocardial structure, and antivascular smooth muscle cell and fibroblast proliferation [6, 7]. *Semen Raphani* (R) is the mature seed of radish, helping digestive, antibacterial, and antiexotoxin effects. *Sinapine thiocyanate* is the main effective ingredient of *Semen Raphani*. In recent years, the focus of TCM research on this herb has

been on its vascular dilation and antihypertensive functions. One of the advantages of TCM is the combination of several compatible herbs which may demonstrate dramatic efficacy.

What we are interested in is whether there is enhanced efficacy combining *Uncaria* and *Semen Raphani* to treat hypertensive disease. In the present study, we aimed to investigate the therapeutic effect of the combination of *Uncaria* and *Semen Raphani* on SHR, through the assessment of blood pressure, heart rate, the degree of endothelial damage, and overall inflammatory level, and then explored the possible pharmacological mechanism preliminarily by microarray analysis and quantitative real-time PCR.

2. Materials and Methods

2.1. Drugs and Reagents. *Total Uncaria alkaloids* and soluble *Semen Raphani alkaloid*, the two extracts, both of 50% purity, were provided by Pharmacological Department, Shandong University of Traditional Chinese Medicine. The content of *total Uncaria alkaloids* was determined by the acid dye staining method, and content of *Rhynchophylline* was determined by high performance liquid chromatography (HPLC). The fingerprint of *total Uncaria alkaloids* was established by HPLC and the content of *Rhynchophylline* accounted for more than 5.5% of *total Uncaria alkaloids*. The HPLC method was employed to ensure that the content of sinapine thiocyanate accounted for more than 42.53% in the soluble *Semen Raphani alkaloids*. After the dose screening experiments, the extracts were dissolved in saline before use and kept at 4°C. The final concentration of *total Uncaria alkaloids* solution is 3.853 mg/mL, and that of *Semen Raphani alkaloids* solutionis4.623 mg/mL. Valsartan was purchased from Beijing Novartis Pharma Ltd., Lot # x1417, dissolved in saline to a concentration of 1.335 mg/mL, and kept at 4°C.

Rat lymphocyte separation medium was purchased from Solarbio (Beijing, China, Lot # 20120516); FACS lysing solution was from BD (USA, Lot # 34543); Monensin Solution, Cell Stimulation Cocktail (500X), Anti-Rat CD54 (ICAM-1) PerCP-eFluor 710, Anti-Rat CD3PE, and TNF-α were from eBioscience (USA, Lot # E00020-1630, E13495-102, E14752-101, E00983-1634, and E00877-321); the improved RPMI-1640 culture medium was from Tianzhu Biochemical Products Co., Ltd. (Beijing, China, Lot # NYB0813); mouse serum was from Ding Guo Technology Co. Ltd. (Beijing, Lot # 23U00130); Triton X-100 was from Solarbio (Beijing, China, Cat. # T8200); CD31 (TLD-3A12) FITC and rabbit monoclonal antibody [EPR3208] to CD146 (ab75769) were from Abcam (UK, Lot # GR79311-3); goat anti-rabbit IgG-PerCP (sc-45090) and CD62P (P-selectin) [CTB201] PerCP were from Santa Cruz Biotechnology (USA, Lot # A3009).

2.2. Animals. 200 male spontaneously hypertensive rats (SHRs), VAH/SPF level, 5-week-old, 94–120 g, and 40 age-matched normotensive Wistar Kyoto (WKY) rats were purchased from Beijing Weitong Lihua Experimental Animal Technology Co., Ltd. (certificate: SCXK (Beijing) 20120001). SHRs were randomly divided into 5 groups and intragastrically administrated for 6 days per week for the duration of 8 weeks: valsartan group (13.350 mg valsartan/kg body weight/d), *total Uncaria alkaloids* group (U group, 38.525 mg *total Uncaria alkaloids*/kg body weight/d), soluble *Semen Raphani alkaloids* group (R group, 46.230 mg soluble *Semen Raphani alkaloids*/kg body weight/d), 5 : 6 component compatibility of *total Uncaria alkaloids* group and soluble *Semen Raphani alkaloids* group (U-R group, combination of 38.525 mg *total Uncaria alkaloids* and 46.230 mg soluble *Semen Raphani alkaloids*/kg body weight/d), and hypertension model rats group. 20 SHRs and 20 WKY rats which were intragastrically given the same volume of saline for the same duration were used as control. The animals, housed under a 12 : 12 light-dark cycle, were allowed food and water *ad libitum* with normal salt intake. Ethical approval for the project was granted by the Faculty of Medicine & Health Sciences Ethics Committee for Animal Research, Affiliated Hospital of Shandong University of Traditional Chinese Medicine.

2.3. Detection of Blood Pressure and Heart Rate. Systolic pressure, diastolic pressure, mean arterial pressure, and heart rate were detected daily by the noninvasive rat tail method. Rats were collected and put in the ALC-HTP animal system, heated to dilate rat tail artery, and data were measured with ALC-NIBP noninvasive blood pressure analysis system [8]. All rats were measured 3 times in parallel, and data was shown as mean ± SD.

2.4. Ultrastructural Observation of Vascular Endothelium. Eight SHRs of each group were sacrificed at the end of the 1st, 2nd, 4th, 6th, and 8th week by overdose anesthesia with sodium pentobarbital (60 mg/kg, i.p.). After blood was collected by venipuncture, the thoracic aorta and mesenteric artery were taken immediately. The thoracic aorta was cut into two parts, one part for endothelial morphology observation by scanning electron microscope (SEM) and the other part for gene chip analysis and quantitive real-time PCR assay. For endothelial morphology observation, the thoracic aorta and mesenteric artery were isolated gently, washed, and fixed in 2.5% glutaraldehyde solution and then observed under SEM.

2.5. Measurement of the Number of Peripheral Circulating Endothelial Cells (CECs). CECs in the peripheral blood can be considered an indicator of endothelial injury and vascular integrity [3]. CD31 is a constitutive marker expressed on endothelial cells (EC). CD146 is the key cell surface antigen on quantifying blood-borne endothelial cells.

The number of peripheral circulating endothelial cells was measured by indirect FACS-fluorescence labeled antibody by flow cytometry. Mononuclear cells were isolated from 2 mL hemolysin-treated EDTA-anticoagulant peripheral blood by centrifugation. The isolated mononuclear cells were labeled with CD146-PerCP 20 μL, CD3-PE 0.25 μg, and CD31-FITC 10 μL and then detected by flow cytometry. $CD3^-CD31^+CD146^+$ cells were regarded as peripheral circulating endothelial cells [5, 9]. The absolute value of WBC was counted with hemocytometer under microscopy. The amount of circulating endothelial cells was calculated by multiplying the absolute value of WBC by the percentage of peripheral circulating endothelial cells in WBC.

2.6. Observation of the Activity of Circulating Endothelial Cells. ICAM-1 (CD54) and P-selectin (CD62P) were taken as markers of CECs with activity and adhesive ability. The mean fluorescence intensity of CD54 and CD62P of $CD3^{-}CD31^{+}$ cells was detected by flow cytometry. Mononuclear cells were isolated from 1 mL lymphocyte separation medium treated with EDTA-anticoagulant peripheral blood by centrifugation. After being blocked with 20 μL mouse serum, cells were triple-stained with anti-CD3-PE, anti-CD31-FITC, and anti-CD54-PerCP or with anti-CD3-PE, anti-CD31-FITC, and CD62P-PerCP. Fluorescence intensity was determined in a FACSCalibur flow cytometer.

2.7. Determination of the Level of Biomarkers of Endothelial Damage in Plasma. The contents of plasma nitric oxide (NO), endothelin-1 (ET-1), P-selectin (P-S), von Willebrand factor (vWF), intercellular adhesion molecule-1 (ICAM-1), and vascular cellular adhesion molecule-1 (VCAM-1) were assayed using ELISA kits (R&D Systems, USA, Lot # 20120718). All assays were performed according to the manufacturer's instructions. Wells were developed with tetramethylbenzidine in the dark and the well absorbance was measured at 450 nm. The protein content was quantified against a standard curve calibrated with known amounts of bovine serum albumin. All samples were assayed in triplicate and measurements were expressed as mean ± SD.

2.8. Assessment of TNF-α Secretion of T Cells Subsets in Spleen. Inflammation is one of the factors closely related to hypertension. The content of TNF-α in plasma associated with the spleen can reflect overall inflammatory state. The content of plasma TNF-α was assayed using ELISA kit (R&D Systems, USA, Lot # 20150320). The spleen was dissected under sterile conditions and ground gently through 200-mesh strainers. Thereafter, cells were collected by centrifugation and the sediment was resuspended in PBS. After T cell subsets were collected using lymphocytes separation medium, they were adjusted to a concentration of 5×10^6 cells/mL and then stimulated with PMA plus ionomycin and monensin, for 4 hours. After that, cells were collected and fixed with 4% polyformaldehyde solution. Fc receptors on the cell surface were blocked with mouse serums, and cells were stained with anti-TNF-α-FITC antibodies; then the fluorescence intensity of the cells was detected in a FACSCalibur flow cytometer. All the data was analyzed with the software FACSDiva Version 6.13.

2.9. Microarray Analysis. In order to explore the mechanism of the protective effect of the combination of *Uncaria* and *Semen Raphani* on vascular endothelium, RT-PCR chip for biological function of endothelium was performed to observe mRNA expression of the thoracic aorta [10]. The total RNA of the thoracic aorta was isolated using the TRIzol method and then reverse-transcribed into cDNA with the PrimeScript RT reagent kit (RR047A, TaKaRa, Dalian, China). Following quantitative detection, the cDNA was hybridized in an Affymetrix Hybridization Oven 640, with subsequent elution inside a clean workstation (GeneChip Fluidics Station 450, Affymetrix). The chips were then scanned with a Gene Array Scanner 3000 7G (Affymetrix) to trace the detection signal. A GeneSpring GX 7.3.1 was used for the gene expression analysis and transcripts with low expression levels (<25% of the median gene expression value) and frequently missed hybridizations (>2 absent flags among the samples) were not analyzed further. Transcripts that showed a >2-fold expression reduction in tissue from drug-treatment groups relative to SHR groups were extracted. The transcript list contained 84 transcripts. Both the test group and control group included three biological replicates [11].

2.10. Quantitative Real-Time PCR. According to the results of the microarray analysis, key genes (fibroblast growth factor-1 (FGF-1), L-selectin (Sel-L), P-selectin (Sel-P), tissue factor pathway inhibitor (TFPI), thrombomodulin (THBD), and vascular cell adhesion molecule-1 (VCAM-1)) were chosen for quantitative real-time PCR to verify the gene expression results. The specific forward/reverse primer sequences (Sangon Biotech, Shanghai, China) were as follows: FGF-1 (5′-ACAGCAGCAGGAATGCATTGAG-3′/5′-AACTGTCGATGGTGCGTTCAAG-3′), Sel-L (5′-CCCTGAGCTGGGTACCATGAA-3′/5′-GCTGCTAGAGGCATGCACTGA-3′), TFPI (5′-CAGCAACAACTTTGAGACCTTGGA-3′/5′-GCGCTTTGGTAGCCTGAGGA-3′), THBD (5′- ACATATCTGAGACGGATGGATGGAA-3′/5′-TGGGACTACAAATGGCAAACACA-3′), VCAM-1 (5′-CGGTCATGGTCAAGTGTTTG-3′/5′-GAGATCCAGGGG AGA TGT CA-3′), and β-actin (5′-CGTTGACATCCGTAAAGA-3′/5′-AGCCACCAATCCACACAG-3′). Total RNA of vascular endothelium was isolated using the TRIzol method and reverse-transcribed into cDNA with the PrimeScript RT reagent kit. Real-time PCR was performed with a SYBR Premix Ex Taq kit (RR420A, TaKaRa, Dalian, China). The reaction mixture contained SYBR Green Premix Ex Taq, cDNA, and the forward/reverse primers. Reaction mixture and amplification conditions were maintained according to the manufacturer's instructions. Each RNA sample was tested in triplicate, and the threshold cycle values were normalized to β-actin and were presented as the mean ± SD. The relative gene expressions (fold change) of WKY rats, SHRs, valsartan group, U group, R group, and U-R group were calculated with the $2^{-\Delta\Delta CT}$ method [12, 13].

2.11. Statistics. Statistical analyses were performed using SPSS 17.0. Values were presented as mean ± SEM. Unless stated otherwise, statistical comparisons were made using two-factor analysis of variance (ANOVA). P values of less than 0.05 were considered significant.

3. Results

3.1. Blood Pressure and Heart Rate. Blood pressure of untreated SHRs kept increasing gradually during the study process and then began to decrease after being treated with drugs for a week ($P < 0.05$). The antihypertensive effect reached the highest point at the end of the 8 weeks, significantly different compared with that of untreated SHRs ($P < 0.05$). Systolic blood pressure decreased by about 30 mmHg

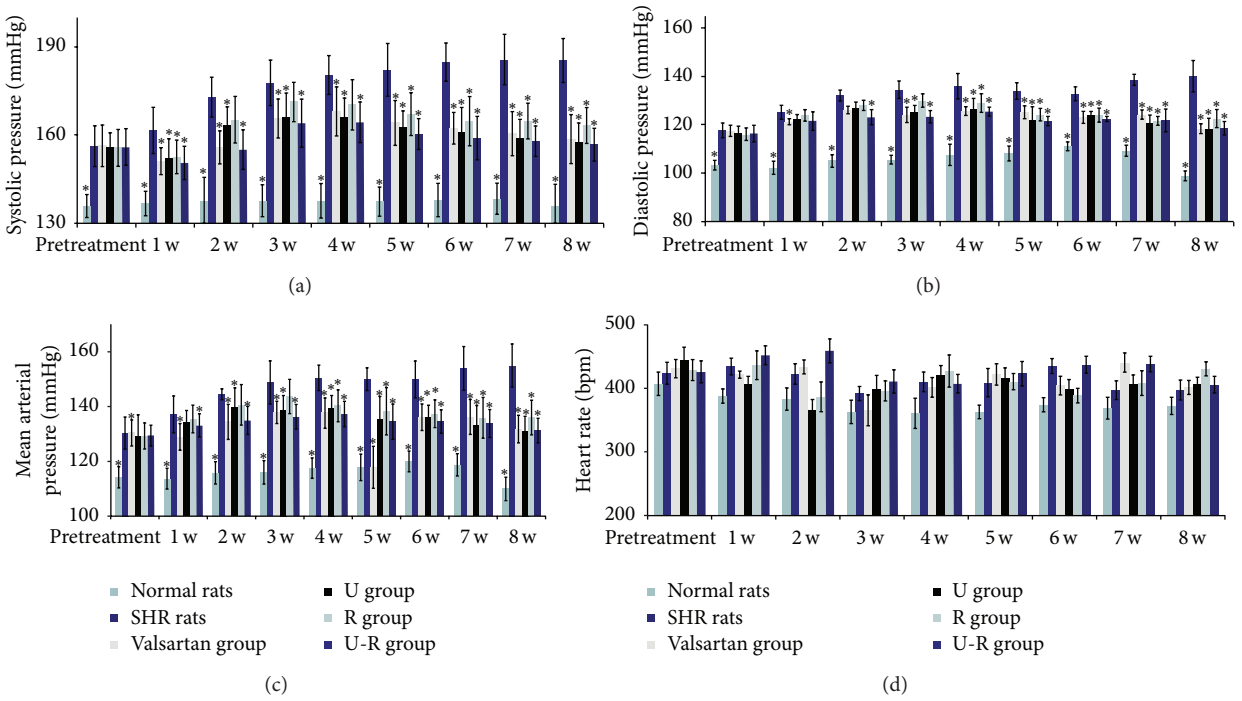

Figure 1: The changes of blood pressure and heart rate were detected by noninvasive rat tail method. Systolic pressure (a), diastolic pressure (b), and mean arterial pressure (c) of SHRs kept increasing gradually during the 8-week study. In the period of the first 4 weeks of drug treatment, systolic pressure, diastolic pressure, and mean arterial pressure of SHRs still increased and then decreased significantly. Heart rate (d) of SHRs changed slightly but there was no significance between groups. $^{*}P < 0.05$ versus SHRs.

in valsartan group, U group, and U-R group, while that in R group was less significant (20 mmHg) at the end of the 8-week treatment (Figure 1(a)). Diastolic pressure decreased by about 20 mmHg in all treatment groups (Figure 1(b)). Mean arterial pressure decreased by 19–24 mmHg in treatment groups at the end of the 8-week treatment (Figure 1(c)). Heart rates of the rats slightly decreased with advancing age, but there was no significant difference between groups during the 8-week study process (Figure 1(d)).

3.2. Endothelial Morphology Change. The SEM study directly revealed the morphological change of vascular endothelium directly as shown in Figure 2; both large elastic arteries (thoracic aorta) and resistance vessels (mesenteric artery) were damaged seriously in SHRs. The vascular cord of WKY rats was arranged in neat rows, maintaining structural integrity and intercellular connection integrity, and mucosa was smooth, with no obvious fibre or plaque attached. The vascular endothelium of SHRs had shed significantly and aggregated, the cable was partly disordered, and cell connection was lost, with a "hole" or "honeycomb" shaped endometrium and with attachments adhering to the membrane. Endometrial integrity and shedding state of endothelial cells improved notably after drug treatment. U alone showed a significant protective effect on endothelium, which was better in U-R combination. The improvement effects of the drugs were U-R > valsartan > U > R. The best improvement groups were the valsartan group and U-R group.

3.3. The Amount and Activity of Peripheral Circulating Endothelial Cells. Compared with the WKY rats, CECs number of SHRs increased significantly and kept rising with advancing age ($P < 0.05$). When treated with *total Uncaria alkaloids* or soluble *Semen Raphani alkaloids*, respectively, the count of CECs decreased at different degrees (U group: 25%; R group: 23%) during 8 weeks ($P > 0.05$). The amount of CECs was decreased notably ($P < 0.05$; 37% at 2 weeks' end; 42% at 8 weeks' end) after administration of U-R for 2 weeks. The combination of U-R demonstrated the most powerful effect on decreasing the amount of CECs (Figures 3(a) and 3(b)).

Compared with the WKY rats, CD54 and CD62P expression on CECs of SHRs was increased significantly ($P < 0.05$). When treated with drugs, CD54 expression on CECs decreased in different degrees over the 8 weeks. U-R group showed the best efficacy (decreased by 20% at the end of the second week and 15.7% at the end of the eighth week), while the efficacy of other groups was not stable (Figures 3(c) and 3(d)). All groups showed a significantly low level of CD62P expression in CECs ($P < 0.05$), suggesting that all drugs had beneficial effects on decreasing activity of CECs (Figures 3(e) and 3(f)).

3.4. The Change of the Level of Biomarkers of Endothelial Damage in Plasma. The plasma level of NO decreased; meanwhile, vWF, ET-1, ICAM-1, VCAM-1, and P-S increased significantly ($P < 0.05$) in SHR compared with the WKY rats. The level

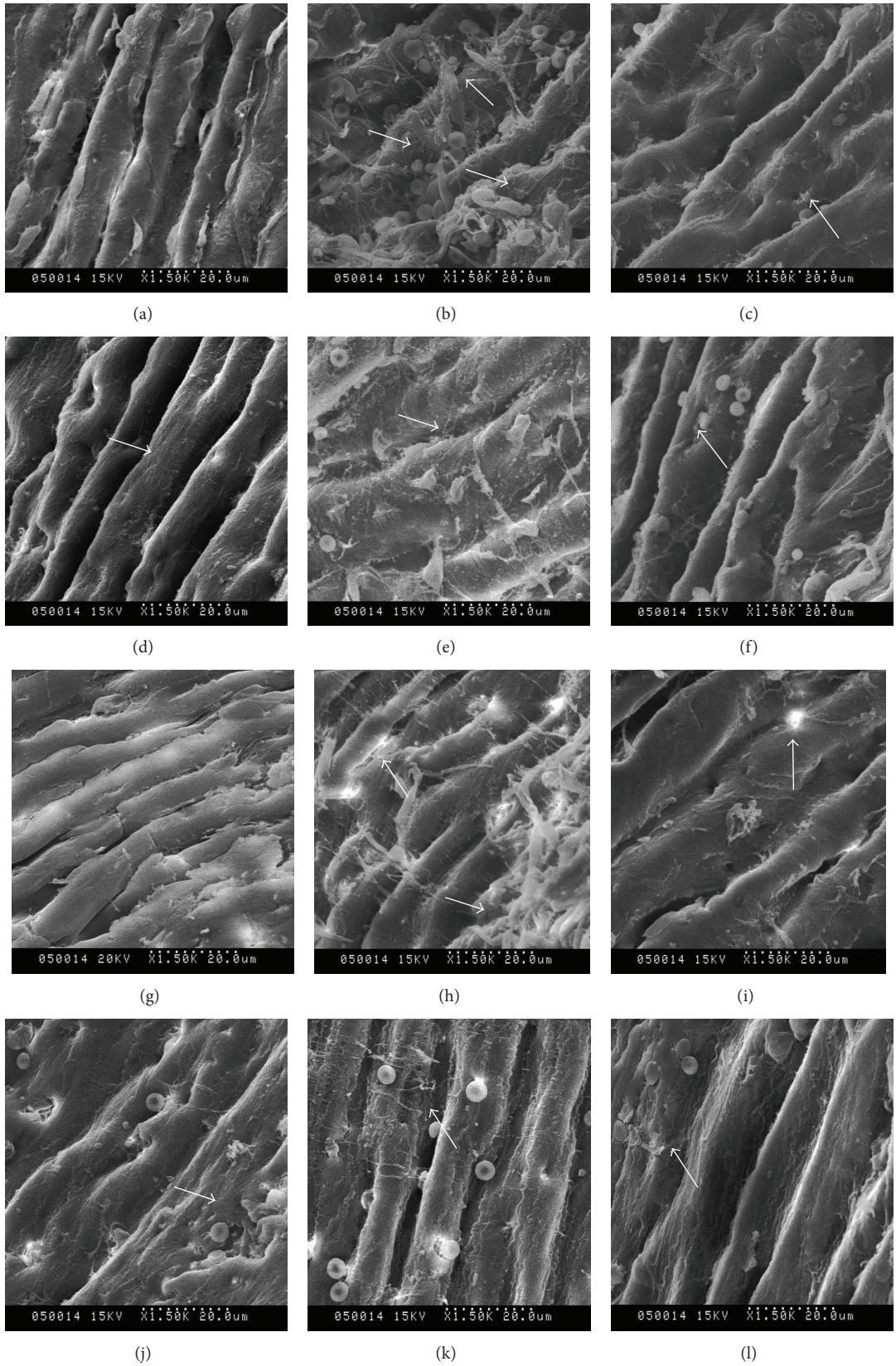

Figure 2: Endothelial morphologies of thoracic aorta and mesenteric artery were observed by scanning electron microscope after 8 weeks of drug treatment. (a)–(f) Endothelial morphology of thoracic aorta; (g)–(l) endothelial morphology of mesenteric artery. ((a) and (g)) WKY rats; ((b) and (h)) SHRs; ((c) and (i)) valsartan group; ((d) and (j)) U (*Uncaria*) group; ((e) and (k)) R (*Semen Raphani*) group; ((f) and (l)) U-R (effective components of *Uncaria* and *Semen Raphani*) group. The arrows point to the endothelial damage and the change of endothelial morphology.

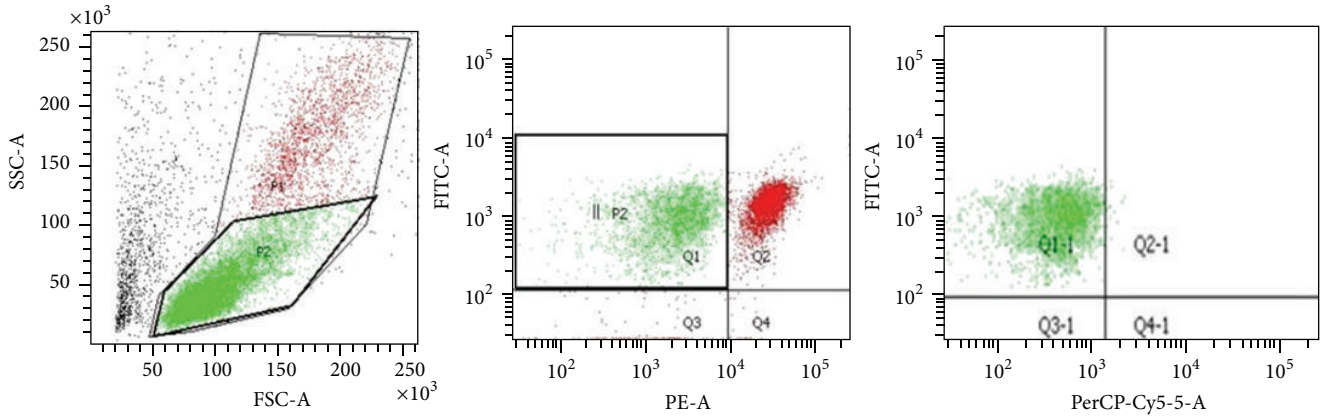

(a)

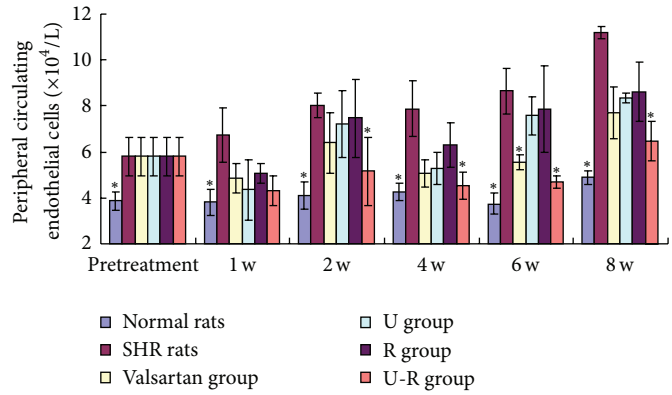

(b)

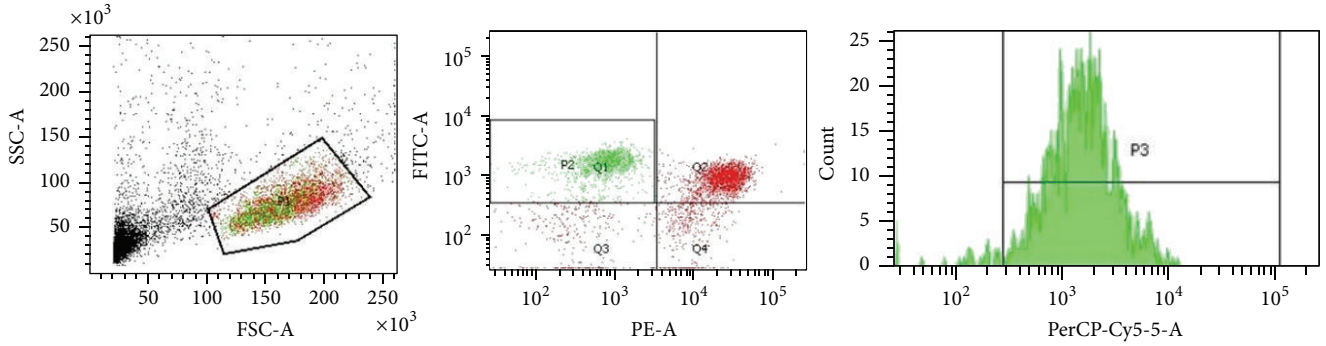

(c)

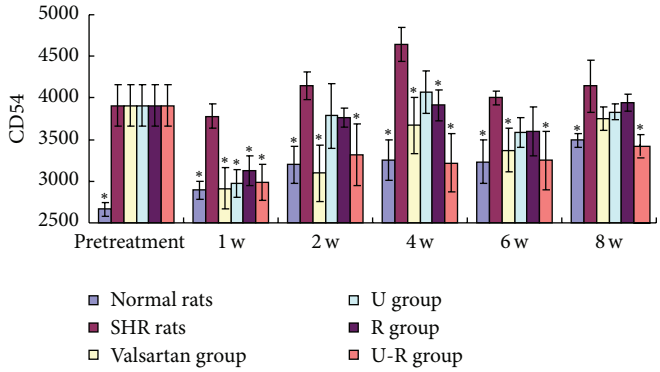

(d)

Figure 3: Continued.

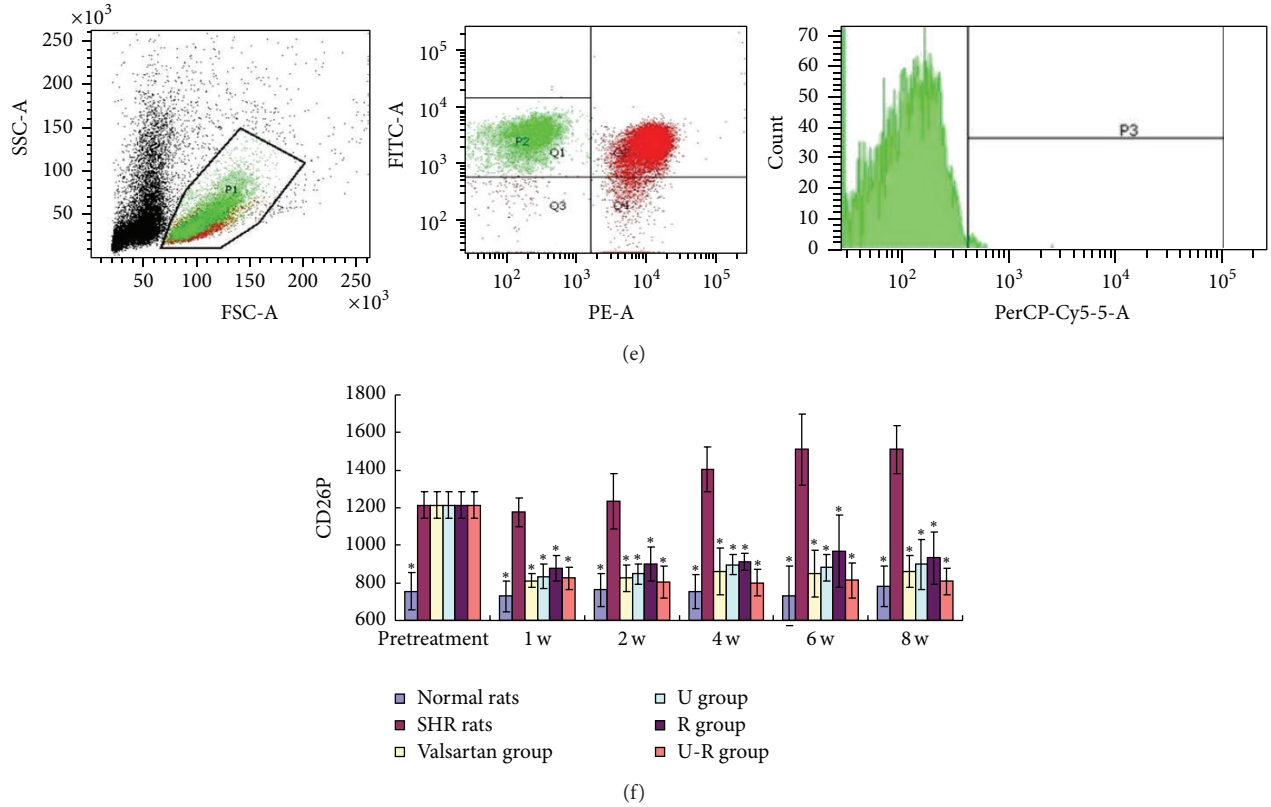

Figure 3: The amount and activity of peripheral CECs by flow cytometry. Identification of $CD3^-CD31^+CD146^+$ cells as peripheral circulating endothelial cells (CECs) in the mononuclear cells by flow cytometry ((a) and (b)). Observation of activated CECs by $CD3^-CD31^+CD54^+$ ((c) and (d)) and $CD3^-CD31^+CD62P^+$ ((e) and (f)) by flow cytometry. $^*P < 0.05$ versus SHRs.

of all the biomarkers of endothelial damage normalized in different degrees with the treatments (Figure 4). Valsartan demonstrated excellent efficacy on regulation of ET-1, ICAM-1, and VCAM-1; U showed good efficacy in regulation of ET-1, vWF, VCAM-1, and P-S; R demonstrated good efficacy in regulation of vWF and P-S, while U-R had excellent efficacy in regulation of all the factors.

3.5. Assessment of the Overall Inflammatory Level. The plasma level of TNF-α was increased ($P < 0.05$) in SHR compared with the WKY rats. The plasma level of TNF-α decreased in different degrees after drug administration (Figure 5(a)). The mean fluorescence intensity of TNF-α in T cell subsets of SHR's spleens was much higher than that of WKY rats ($P < 0.05$). TNF-α decreased to varying degrees after treatment, especially in R and U-R groups ($P < 0.05$). We speculated that this was one of the mechanisms of U-R of protecting vascular endothelium against hypertension (Figures 5(b) and 5(c)).

3.6. Expression of Key Genes. Changes of gene expression in microarray analysis were listed in Table 1. QRT-PCR was then performed to confirm the microarray findings. Consistent with the gene chip data, the mRNA expression of VCAM-1, Sel-L, Sel-P, and TFPI was elevated and that of FGF-1 and THBD was decreased in vascular endothelium of SHRs. After drug treatment, the mRNA levels of these cytokines were normalized in different degrees (Figure 6).

4. Discussion

Hypertension, to some extent, is a vascular disease. Alteration of the vascular endothelium is a primary event in the pathogenesis of vascular diseases, such as atherosclerosis and systemic hypertension [14]. Hypertension and vascular endothelial dysfunction are a reciprocal causation. The abnormal hemodynamics and the change of shear force of hypertension may cause endothelial dysfunction, which is one of the initiating factors of endothelial injury. The injury of vascular endothelial cells often leads to the development of hypertension. Damaged endothelial cells tend to detach from the vessel wall, leaving a thrombogenic and proinflammatory subendothelial surface, and simultaneously release many active substances, such as thrombin, 5 HT, and endothelin, resulting in the disordered regulation of vascular tone and elevation of blood pressure [15]. Elevated blood pressure further aggravates the vascular endothelial injury and dysfunction. Therefore, it is vital to study the pathology of endothelial dysfunction and damage [16].

In the present study, we observed the vascular endothelial injury process of SHRs to speculate the pathophysiology in hypertension patients, as well as U-R's targets and

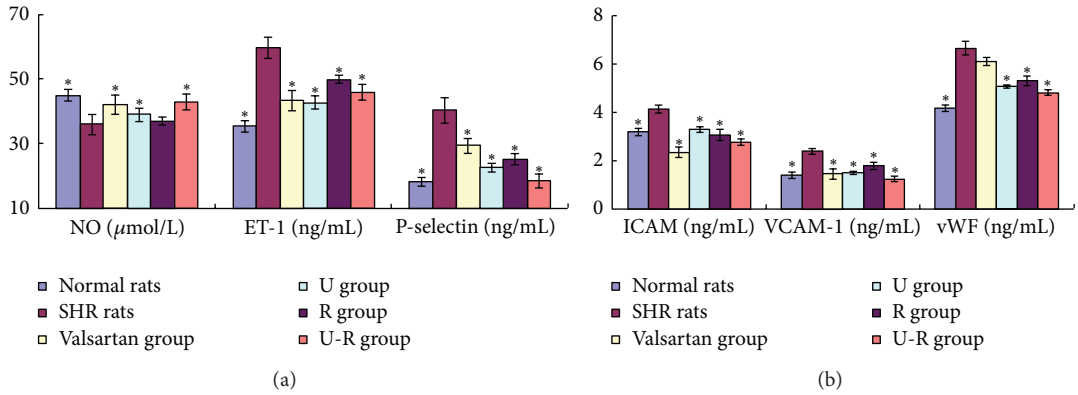

Figure 4: Assessment of the level of biomarkers of endothelial damage in plasma. The plasma level of NO, vWF, ET-1, ICAM-1, VCAM-1, and P-S was determined by ELISA to assess the degree of endothelial damage. $^{*}P < 0.05$ versus SHRs.

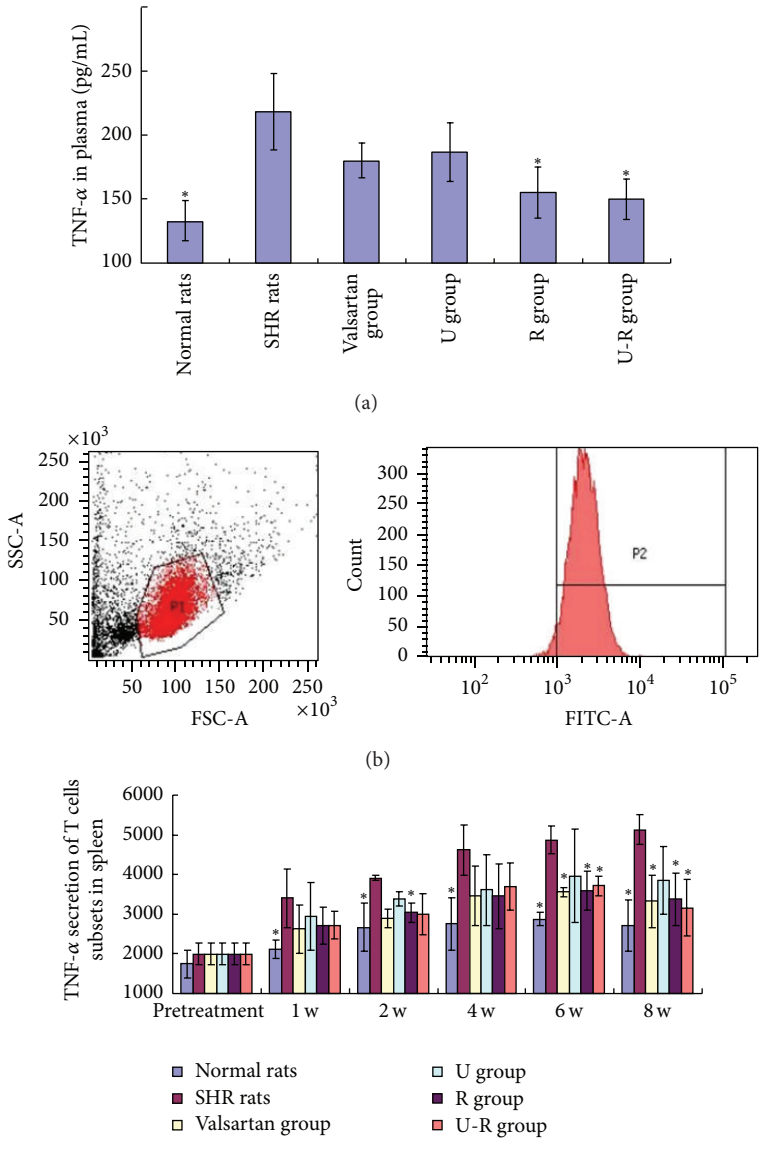

Figure 5: Assessment of the overall inflammatory level. The level of plasma TNF-α (a) was measured by ELISA. TNF-α secretion in spleen (b) was measured by flow cytometry. The level of plasma TNF-α and the mean fluorescence intensity of TNF-α on SHRs were much higher than those of WKY rats ($P < 0.05$). TNF-α was decreased after drug treatment, except in U group ($P < 0.05$). $^{*}P < 0.05$ versus SHRs.

Table 1: Changes in gene expression (fold Change, $2^{-\Delta\Delta Ct}$).

	WKY rats/SHRs	Valsartan group/SHRs	U group/SHRs	R group/SHRs	U-R group/SHRs
VCAM-1	0.55	0.41	0.60	0.69	0.29
FGF-1	6.00	3.27	2.82	2.97	6.64
Sel-L	0.53	0.23	0.24	0.30	0.35
THBD	5.89	3.33	3.34	3.46	3.96
TFPI	0.26	0.32	0.23	0.21	0.31
Sel-P	0.24	0.30	0.17	0.24	0.18

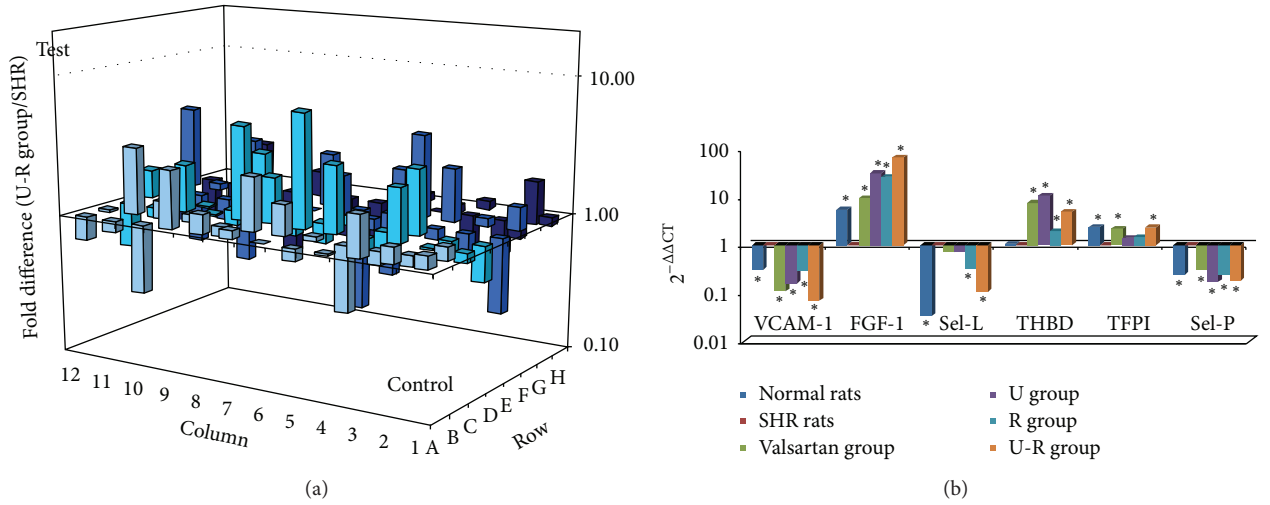

Figure 6: Changes of gene expression of the antithrombotic actions related genes. The pharmacological mechanism of U-R was speculated by microarray analysis (a), and the microarray results were verified and antithrombotic action related genes were determined by and quantitive RT-PCR (b). $^{*}P < 0.05$ versus SHRs.

pharmacological processes. The combined use of U and R effectively decreased systolic pressure, diastolic pressure, and mean arterial pressure. The efficacy of combination of U-R was better than that of U or R alone, demonstrating similar efficacy to valsartan. U-R showed particularly prominent efficacy on lowering systolic blood pressure, which provided the premise for U-R as vascular protective agents. U-R improved endothelial morphology of both large elastic arteries (thoracic aorta) and resistance vessels (mesenteric artery). As the morphology of elastic arteries improved, which helped cushion the shear force, systolic pressure was lowered. Accompanied by the improved morphology of resistance vessel, the passive expansion capability of peripheral resistance vessels was increased and diastolic pressure was reduced. U-R increased the plasma level of NO and decreased the level of vWF, ET-1, ICAM-1, VCAM-1, and P-S, suggesting the recovery of vascular function. The improvement of endothelial integrity and elastic vascular and resistance vascular function may be attributed to the antihypertensive effect.

Vascular endothelial cells (ECs) provide a nonthrombogenic and nonadhesive surface in healthy subjects, but under pathologic conditions they become proadhesive and procoagulant [17]. In normal steady-state conditions, the amount of mature CECs in the bloodstream is very low, due to the fact that endothelial turnover is a very slow process in the absence of pathological stimuli and that nonviable CECs are likely rapidly cleared by the reticuloendothelial system. The level of peripheral CECs is expected to increase as a consequence of any type of damage to the vessel wall [18, 19]. In this study, the amount of CECs of SHRs was much higher than that of WKY rats. During the 8-week study, the peripheral CECs count of SHRs kept increasing, while that of WKY rats stayed stable. The count of CECs in treatment groups also increased but was much lower than that of SHRs, especially in valsartan and U-R groups. The combination of U-R demonstrated even better efficacy (41.8%) on lowering CECs count of valsartan (30.3%). Not only the amount but also the cell status of CECs has valuable significance [20]. We take ICAM-1 (CD54) and P-selectin (CD62P) as markers of activated CECs. Endothelial adhesion molecule CD54 (ICAM-1) mediates cellular adhesion and transcellular migration. CD62P is expressed appreciably in inflammatory conditions and participates in a variety of pathological changes [21]. All drugs showed beneficial efficacy on decreasing CD62P expression. But only the combination of *Uncaria* and *Semen Raphani* could effectively decrease CD54 to approximate level in WKY rats, which may effectively reduce the risk of vascular injury and thrombosis.

Inflammation contributes to the pathophysiology of hypertension. We observed TNF-α level in both plasma and T cell subsets of SHR's spleens to assess overall inflammatory level [22]. TNF-α promotes inflammatory responses and

activates the adhesion molecules, which leads to the injury of endothelial cells resulting in endothelium dysfunction, vasomotor strengthening, diastolic weakening, and systemic small artery spasm; thus, blood pressure is elevated [23]. Both *Semen Raphani* alone and combination of U-R showed good efficacy in relieving inflammation. Effectively reducing the low-grade inflammation may be one of the pharmacological ways in which *Semen Raphani* is antihypertensive. U alone showed antihypertensive efficacy and effectively decreased CECs count, while R alone showed efficacy in relieving inflammatory level. The combination of U and R proved the enhanced endothelial protective effects.

According to the results of microarray and qRT-PCR, we believe that the expression and regulation of antithrombotic actions and adhesion related genes are closely related to endothelial dysfunction. A common function of the endothelium is to maintain blood in a fluid state and to limit clot formation when there is a breach in the integrity of the vascular wall. On the anticoagulant side, ECs express tissue factor pathway inhibitor (TFPI), heparan, thrombomodulin, endothelial protein C receptor (EPCR), tissue-type plasminogen activator (t-PA), ecto-ADPase, prostacyclin, and nitric oxide. On the procoagulant side, ECs synthesize tissue factor, plasminogen activator inhibitor- (PAI-) 1, von Willebrand factor (vWF), and protease activated receptors [24]. Regulation of coagulation action and inhibition of the inflammatory cytokine and adhesion molecules may alleviate endothelial injury and relieve vascular wall inflammation, to slow the progress of hypertension. The results of the present study suggested that combination of U-R decreased the mRNA level of VCAM-1, Sel-L, TFPI, and Sel-P, while elevating mRNA expression of FGF-1 and THBD of the thoracic aorta. The regulation of extracts of U-R on antithrombotic actions and adhesion related genes may contribute to the mechanism of the regulation on hypertension and endothelium injury.

5. Conclusions

The combination of extracts of *Uncaria* and *Semen Raphani* (*total Uncaria alkaloids* and soluble *Semen Raphani alkaloid*) demonstrated good antihypertensive effect and vascular endothelium protective effect. The possible mechanism of this protective effect on vascular endothelium may be attributed to the regulation of antithrombotic actions related genes (FGF-1, Sel-L, Sel-P, TFPI, THBD, and VCAM-1) and relieving the overall low-grade inflammation.

Conflict of Interests

The authors declare that they have no competing interests.

Authors' Contribution

Yun-lun Li and Chuan-Hua Yang designed experiments, contributed to discussion, and were responsible for critical revision and approval of the paper. Yue-Hua Jiang and Jing-Chang Sun performed experiments and data analysis and drafted the paper. Miao-Miao Wang and Wen-Qing Yang were responsible for animal care and data collection. All authors read and approved the final paper. Yun-lun Li and Yue-Hua Jiang contributed equally to this work and should be considered as co-first authors.

Acknowledgments

This work was funded by the Natural Science Foundation of China (no. 81072794) and Modernization of Traditional Chinese Medicine in Science and Technology Funding of Shandong Province (no. 2008GG2NS02011).

References

[1] M. Juonala, J. S. A. Viikari, T. Rönnemaa, H. Helenius, L. Taittonen, and O. T. Raitakari, "Elevated blood pressure in adolescent boys predicts endothelial dysfunction: the cardiovascular risk in young finns study," *Hypertension*, vol. 48, no. 3, pp. 424–430, 2006.

[2] N. Sattar, D. W. McCarey, H. Capell, and I. B. McInnes, "Explaining how "high-grade" systemic inflammation accelerates vascular risk in rheumatoid arthritis," *Circulation*, vol. 108, no. 24, pp. 2957–2963, 2003.

[3] R. M. Touyz and E. L. Schiffrin, "Reactive oxygen species in vascular biology: implications in hypertension," *Histochemistry and Cell Biology*, vol. 122, no. 4, pp. 339–352, 2004.

[4] D. A. Ingram, N. M. Caplice, and M. C. Yoder, "Unresolved questions, changing definitions, and novel paradigms for defining endothelial progenitor cells," *Blood*, vol. 106, no. 5, pp. 1525–1531, 2005.

[5] A. D. Blann, A. Woywodt, F. Bertolini et al., "Circulating endothelial cells. Biomarker of vascular disease," *Thrombosis and Haemostasis*, vol. 93, no. 2, pp. 228–235, 2005.

[6] Y.-L. Li, "Effect of rhynchophylline and isorhynchophylline on the proliferation of rat vascular smooth muscle cell induced by angiotensin II," *Chinese Pharmacological Bulletin*, vol. 24, no. 1, pp. 53–58, 2008.

[7] X. J. Xiong, X. C. Yang, Y. M. Liu, Y. Zhang, P. Q. Wang, and J. Wang, "Chinese herbal formulas for treating hypertension in traditional Chinese medicine: perspective of modern science," *Hypertension Research*, vol. 36, no. 7, pp. 570–579, 2013.

[8] X. Kong, M. Z. Ma, L. Qin et al., "Pioglitazone enhances the blood pressure-lowering effect of losartan via synergistic attenuation of angiotensin II-induced vasoconstriction," *Journal of the Renin-Angiotensin-Aldosterone System*, vol. 15, no. 3, pp. 259–270, 2014.

[9] N. Bardin, F. Anfosso, J.-M. Massé et al., "Identification of CD146 as a component of the endothelial junction involved in the control of cell-cell cohesion," *Blood*, vol. 98, no. 13, pp. 3677–3684, 2001.

[10] H. Takase, K. Matsumoto, R. Yamadera et al., "Genome-wide identification of endothelial cell-enriched genes in the mouse embryo," *Blood*, vol. 120, no. 4, pp. 914–923, 2012.

[11] F. Bedoya, M. M. Medveczky, T. C. Lund et al., "Identification of mitochondrial genome concatemers in AIDS-associated lymphomas and lymphoid cell lines," *Leukemia Research*, vol. 33, no. 11, pp. 1499–1504, 2009.

[12] L. Chang and M. Karin, "Mammalian MAP kinase signalling cascades," *Nature*, vol. 410, no. 6824, pp. 37–40, 2001.

[13] K. Yamamoto, H. Hamada, H. Shinkai, Y. Kohno, H. Koseki, and T. Aoe, "The KDEL receptor modulates the endoplasmic

reticulum stress response through mitogen-activated protein kinase signaling cascades," *Journal of Biological Chemistry*, vol. 278, no. 36, pp. 34525–34532, 2003.

[14] E. G. Lakatta and D. Levy, "Arterial and cardiac aging: major shareholders in cardiovascular disease enterprises: part I: aging arteries: a "set up" for vascular disease," *Circulation*, vol. 107, no. 1, pp. 139–146, 2003.

[15] H. Cai, "Hydrogen peroxide regulation of endothelial function: origins, mechanisms, and consequences," *Cardiovascular Research*, vol. 68, no. 1, pp. 26–36, 2005.

[16] F. Dignat-George and J. Sampol, "Circulating endothelial cells in vascular disorders: new insights into an old concept," *European Journal of Haematology*, vol. 65, no. 4, pp. 215–220, 2000.

[17] T. Bombeli, M. Mueller, and A. Haeberli, "Anticoagulant properties of the vascular endothelium," *Thrombosis and Haemostasis*, vol. 77, no. 3, pp. 408–423, 1997.

[18] C. J. Boos, G. Y. H. Lip, and A. D. Blann, "Circulating endothelial cells in cardiovascular disease," *Journal of the American College of Cardiology*, vol. 48, no. 8, pp. 1538–1547, 2006.

[19] G. P. Fadini and A. Avogaro, "Cell-based methods for ex vivo evaluation of human endothelial biology," *Cardiovascular Research*, vol. 87, no. 1, pp. 12–21, 2010.

[20] A. Solovey, Y. Lin, P. Browne, S. Choong, E. Wayner, and R. P. Hebbel, "Circulating activated endothelial cells in sickle cell anemia," *The New England Journal of Medicine*, vol. 337, no. 22, pp. 1584–1590, 1997.

[21] C. Pericleous, I. Giles, and A. Rahman, "Are endothelial microparticles potential markers of vascular dysfunction in the antiphospholipid syndrome?" *Lupus*, vol. 18, no. 8, pp. 671–675, 2009.

[22] C. Sutton, C. Brereton, B. Keogh, K. H. Mills, and C. L. Ed, "A crucial role for interleukin (IL)-1 in the induction of IL-17–producing T cells that mediate autoimmune encephalomyelitis," *Thrombosis and Haemostasis*, vol. 93, pp. 228–235, 2005.

[23] R. Rabbani and E. J. Topol, "Strategies to achieve coronary arterial plaque stabilization," *Cardiovascular Research*, vol. 41, no. 2, pp. 402–417, 1999.

[24] W. C. Aird, "Phenotypic heterogeneity of the endothelium. I. Structure, function, and mechanisms," *Circulation Research*, vol. 100, no. 2, pp. 158–173, 2007.

Hindawi Publishing Corporation
Evidence-Based Complementary and Alternative Medicine
Volume 2015, Article ID 929012, 9 pages
http://dx.doi.org/10.1155/2015/929012

Research Article

Tongxinluo Prevents Endothelial Dysfunction Induced by Homocysteine Thiolactone *In Vivo* via Suppression of Oxidative Stress

Yi Zhang,[1] Tiecheng Pan,[2] Xiaoxuan Zhong,[1] and Cai Cheng[2]

[1]*Department of Surgery, The Third Affiliated Hospital of Jianghan University, Wuhan 430300, China*
[2]*Division of Cardiothoracic Surgery, Tongji Hospital of Tongji Medical College, Huazhong University of Science and Technology, Wuhan 430030, China*

Correspondence should be addressed to Cai Cheng; cai20122013@163.com

Received 9 February 2015; Revised 7 March 2015; Accepted 26 May 2015

Academic Editor: Dan Hu

Aim. To explore whether Chinese traditional medicine, tongxinluo (TXL), exerts beneficial effects on endothelial dysfunction induced by homocysteine thiolactone (HTL) and to investigate the potential mechanisms. *Methods and Results*. Incubation of cultured human umbilical vein endothelial cells with HTL (1 mM) for 24 hours significantly reduced cell viabilities assayed by MTT, and enhanced productions of reactive oxygen species. Pretreatment of cells with TXL (100, 200, and 400 μg/mL) for 1 hour reversed these effects induced by HTL. Further, coincubation with GW9662 (0.01, 0.1 mM) abolished the protective effects of TXL on HTL-treated cells. In *ex vivo* experiments, exposure of isolated aortic rings from rats to HTL (1 mM) for 1 hour dramatically impaired acetylcholine-induced endothelium-dependent relaxation, reduced SOD activity, and increased malondialdehyde content in aortic tissues. Preincubation of aortic rings with TXL (100, 200, and 400 μg/mL) normalized the disorders induced by HTL. Importantly, all effects induced by TXL were reversed by GW9662. *In vivo* analysis indicated that the administration of TXL (1.0 g/kg/d) remarkably suppressed oxidative stress and prevented endothelial dysfunction in rats fed with HTL (50 mg/kg/d) for 8 weeks. *Conclusions*. TXL improves endothelial functions in rats fed with HTL, which is related to PPARγ-dependent suppression of oxidative stress.

1. Introduction

Hyperhomocysteinemia might play a role in the pathogenesis of vascular disorders and it is considered as an independent risk factor for atherosclerosis in 1969 [1]. Homocysteine occurs in human blood plasma in several forms, including the most reactive one which is HTL of a cyclic thioester, and represents up to 0.29% of total plasma homocysteine [2]. HTL reacts with proteins by acylation of free basic amino groups. In particular, the epsilon-amino group of lysine residues forms adducts and induces structural and functional changes in plasma proteins [3]. High levels of homocysteine impair endothelial function and cause endothelial damage in humans and in animal models [4, 5], indicating that the endothelial monolayer is very sensitive to changes in plasma homocysteine levels.

Tongxinluo (TXL) is a traditional Chinese compound prescription and has been approved by the State Food and Drug Administration of China in 1996 for the treatment of angina pectoris and ischemic stroke. Increasing evidence has indicated that the TXL has cardioprotective functions. Treatment with TXL is effective in lowering serum lipid levels, inhibiting plaque inflammation, and enhancing stability of vulnerable plaques [6]. It can also reduce myocardial no-reflow and ischemia-reperfusion injury and modulate vascular endothelial function [7]. Based on the aforementioned studies, we tested the hypothesis that TXL may produce protective effects on endothelial dysfunction induced by high homocysteine via suppression of oxidative stress. Here, we reported that pharmacological activation of peroxisome proliferator-activated receptor gamma (PPARγ)

by TXL improves endothelial function in rats with hyperhomocysteinemia.

2. Materials and Methods

2.1. Materials. TXL was from Shijiazhuang Yiling Pharmaceutical Company, China. GW9662 (2-Chloro-5-nitro-N-phenylbenzamide, Cat.: M6191, purity >98%), pyrrolidine dithiocarbamate (PDTC), dihydroethidium (DHE), apocynin, acetylcholine (Ach), sodium nitroprusside (SNP), and phenylephrine (PE) were purchased from Sigma Company. Commercial kits for determinations of malondialdehyde (MDA) and superoxide dismutase (SOD) activity were from Cayman Company.

2.2. Components, Preparation, and Chemical Analysis of TXL. The herbal drugs of TXL were authenticated and standardized on marker compounds according to the Chinese Pharmacopoeia 2005 as described previously [8]. TXL contains 12 medicinal components: *Panax ginseng* C.A. Mey, 1.677%; *Ziziphus jujube Mill.* var. *spinosa*, 1.173%; *Paeonia lactiflora Pall.*, 1.558%; *Santalum album L.*, 0.354%; *Dalbergia odorifera T. Chen*, 4.005%; *Boswellia carteri Birdw.*, 5.927%; *Borneolum syntheticum*, 3.626%; *Scolopendra subspinipes mutilans L. Koch*, 3.623%; *Buthus martensii Karsch*, 18.111%; *Steleophage plancyi*, 18.111%; *Hirudo nipponica*, 27.330%; *Cryptotympana pustulata Fabricius*, 18.111%. They were ground to superfine powder with the diameter of 10 μm or less by a Micronizer and prepared as capsules. To reduce the dose variability of TXL capsule among different batches, the species, origin, harvest time, medicinal parts, and concocted methods for each component were strictly standardized. Moreover, high performance liquid chromatography was applied to quantitate the components of the TXL capsule. Five major components of the aqueous extract of tongxinluo capsule included *paeoniflorin* (6.142 mg/g), *ginsenoside Rg1* (0.884 mg/g), *ginsenoside Rb1* (0.730 mg/g), *jujuboside A* (0.661 mg/g), and *jujuboside B* (0.646 mg/g). Besides, another two peaks on the gas chromatogram fingerprint of TXL capsule were identified, which are *isoborneol* and *borneol*.

2.3. Animals. Male Sprague-Dawley rats (8 ± 2 weeks old, 180 ± 20 g) were purchased from the Center of Experiment Animals, Central South University (Changsha, China). Rats were housed in temperature-controlled cages with a 12-hour light-dark cycle. The animal protocol was reviewed and approved by Jianghan University and Huazhong University of Science and Technology.

2.4. Cell Culture. Human umbilical vascular endothelial cells (HUVECs) from America Type Collection Center (ATCC) were grown in endothelial cells basal medium (Clonetics Inc., Walkersville, MD) supplemented with 2% FBS, penicillin (100 U/mL), and streptomycin (100 μg/mL). In all experiments, cells were between passages 3 and 8. All cells were incubated at 37°C in a humidified atmosphere of 5% CO_2 and 95% air. Cells were grown to 70–80% confluency before being treated with different agents.

2.5. Organ Chamber. Organ chamber study was performed as described previously [9]. Rats were sacrificed under anesthesia by intravenous injection with pentobarbital sodium (30 mg/kg). The descending aorta isolated by removing the adhering perivascular tissue carefully was cut into rings (3-4 mm in length). Aortic rings were suspended and mounted to organ chamber by using two stainless clips. The rings were placed in organ baths filled with Krebs buffer of the following compositions (in mM): NaCl, 118.3; KCl, 4.7; $MgSO_4$, 0.6; KH_2PO_4, 1.2; $CaCl_2$, 2.5; $NaHCO_3$, 25.0; EDTA, 0.026; pH 7.4 at 37°C and gassed with 95% O_2 plus 5% CO_2. Before contraction, a tension of 2 g was given to the aorta ring for 90 minutes. During this period, Krebs solution was changed every 15 min. After the equilibration, aortic rings were challenged with 60 mM KCl. After washing and another 30 minutes equilibration period, contractile response was elicited by PE (1 μM). At the plateau of contraction, accumulative Ach (0.01, 0.03, 0.1, 0.3, 1, and 3 μM) or SNP (0.01, 0.03, 0.1, 0.3, 1, 3, and 10 μM) was added into the organ bath to induce endothelium-dependent or -independent relaxation.

For *ex vivo* experiments, the rings were contracted by PE (1 μM) and then dilated with cumulative concentrations of Ach (0.01–3 μM) to assess the integrity of the endothelium. The ring whose maximal relaxation induced by Ach (3 μM) is over 80% was considered to have intact endothelium and was used in the following study. Then, the rings were pretreated with TXL (100, 200, 400 μg/mL) for 30 minutes followed by addition of HTL (1 mM) for 90 minutes. After washing, Ach-induced endothelium-dependent relaxation and SNP-induced endothelium-independent relaxation were assayed, respectively. At the end of the experiments, the aortic rings were collected in liquid nitrogen for measurements of NO and MDA after homogenization.

2.6. Measurements of MDA Content, SOD Activity, and Nitric Oxide (NO) Level. The contents of MDA content, SOD activity, and NO level in aortic tissues or blood were assayed by using commercial kits following the recommended protocol.

2.7. Evaluation of Cell Viability. Cell viability was assayed by using 3-(4,5)-dimethylthiahiazo(-z-y1)-3,5-di-phenytetrazoliumromide (MTT) as described previously [10]. Cells were seeded into 96-well plate at the density of 10000/mL and incubated for 24 hours. After treatment, 10 μL MTT (5 mg/mL) was added into cultured medium in each well for 2–4 hours until purple precipitate is visible. After the removal of culture medium, 75 μL dimethyl sulphoxide was added to each well, leaving the cells at room temperature in the dark for 2 hours. The absorbance at 570 nm was recorded.

2.8. Detection of ROS. ROS productions in cultured cells were assayed by measuring the DHE fluorescence as described previously [11]. Briefly, before the end of the treatment, 10 μM DHE was added to the medium, incubated for 30 min at 37°C, and then washed with PBS twice. The image was taken by fluorescent microscope. The DHE fluorescent intensity was recorded by fluorescent reader at the wave of excitation (485 nm) and emission (545 nm). Control was set up as 100%.

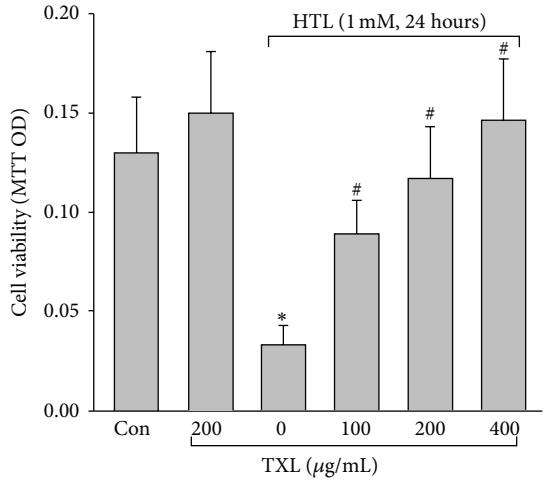

(a)

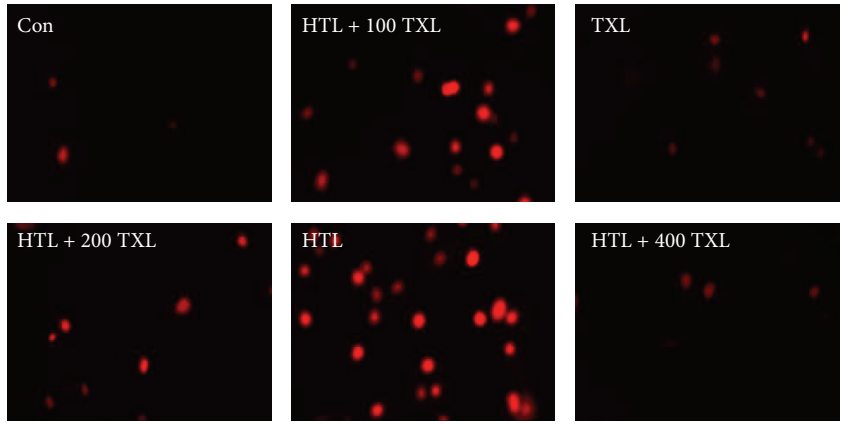

(b)

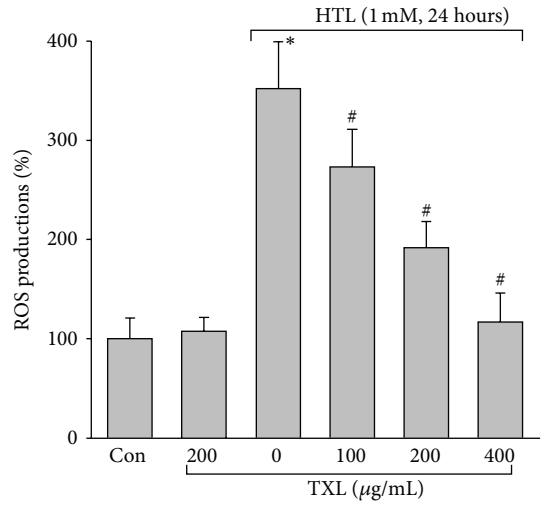

(c)

Figure 1: TXL dose-dependently suppresses HTL-induced oxidative stress and improves cell viabilities in cultured HUVECs. Cultured HUVECs were pretreated with TXL (100, 200, and 400 μg/mL) for 1 hour and then incubated with HTL (1 mM) for 24 hours. (a) Cell viability was measured by MTT. (b) Intracellular ROS productions were detected by DHE fluorescence. (c) Quantitative analysis of ROS productions. All data were expressed as mean ± SEM. N is 3 in each group. $^{*}P < 0.05$ versus Con, $^{\#}P < 0.05$ versus HTL alone.

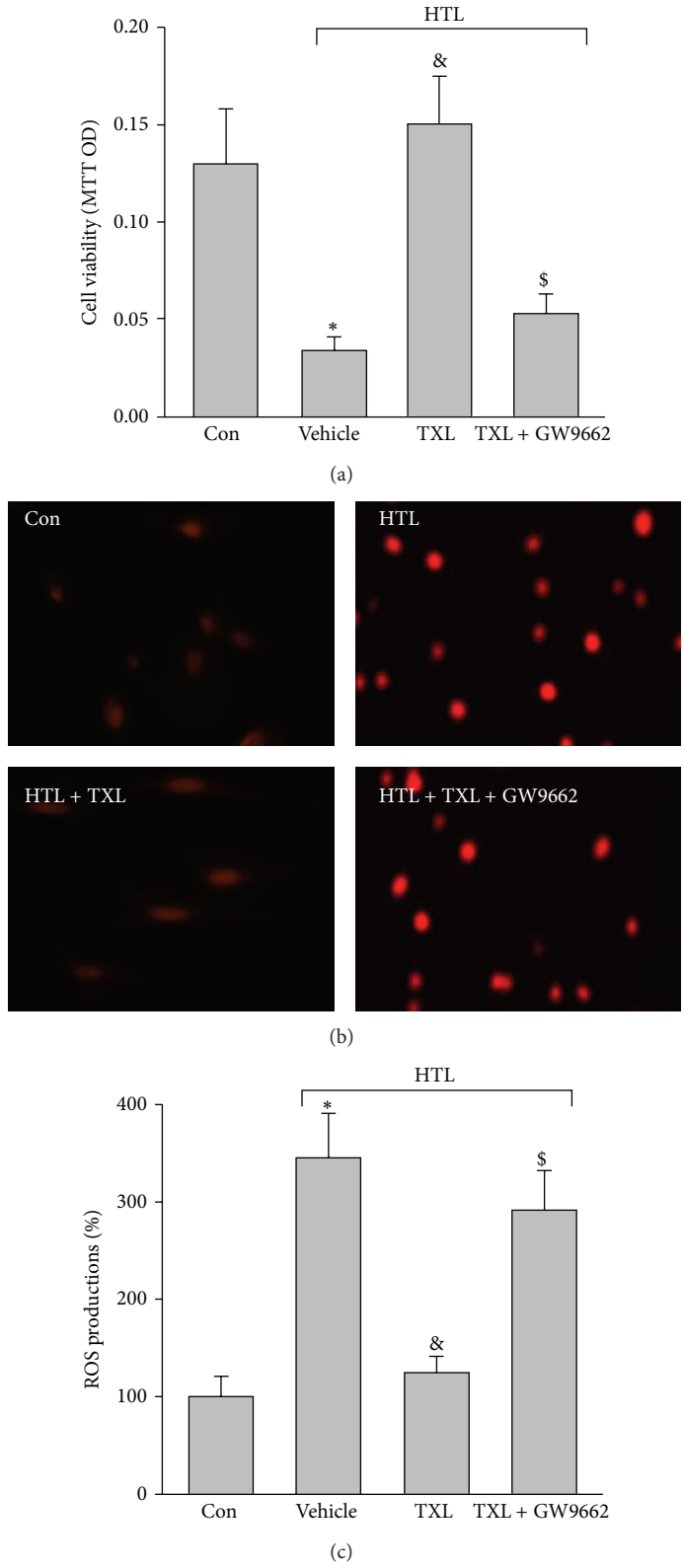

Figure 2: Inhibition of PPARγ abolished TXL-suppressed oxidative stress and maintains cell viability in HTL-treated cells. Cultured HUVECs were pretreated with TXL (200 μg/mL) for 1 hour and then incubated with HTL (1 mM) for 24 hours in presence of GW9662 (0.01 mM). Cell was subjected to assay: (a) cell viability by MTT and (b) intracellular ROS productions by DHE fluorescence. (c) Quantitative analysis of ROS productions. All data were expressed as mean ± SEM. N is 3 in each group. $^{*}P < 0.05$ versus Con, $^{\&}P < 0.05$ versus HTL alone, and $^{\$}P < 0.05$ versus HTL + TXL.

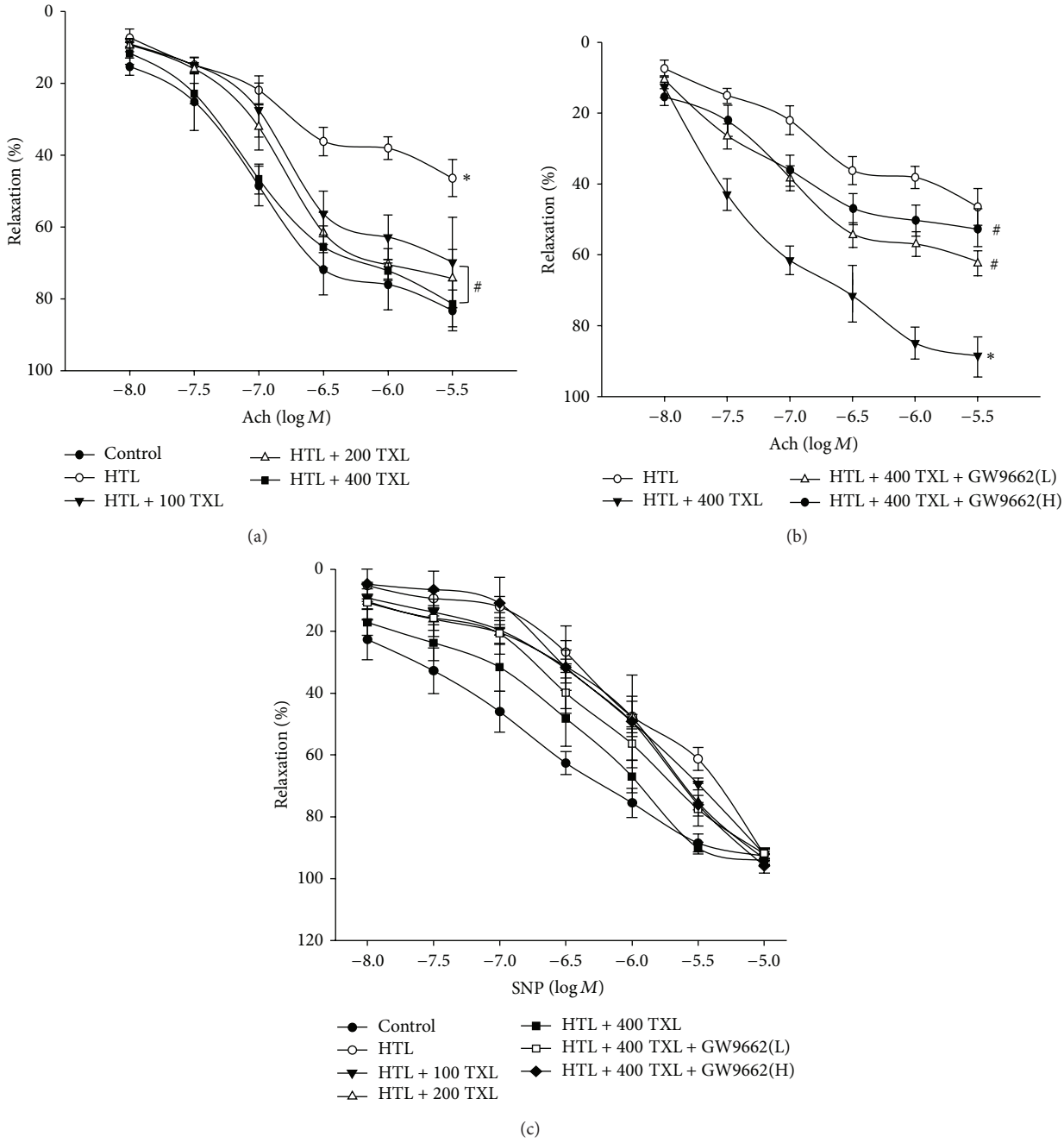

Figure 3: TXL via PPARγ prevents from the impairment of endothelium-dependent relaxation induced by HTL in isolated rat aortas. (a) The isolated rat aortic rings were exposed to HTL (1 mM) for 1 hour after preincubation with TXL (100, 200, and 400 μg/mL) for 30 minutes. The endothelium-dependent relaxation induced by acetylcholine (Ach) was assayed by organ chamber. All data were expressed as mean ± SEM. N is 5 in each group. $^{*}P < 0.05$ versus Control and $^{\#}P < 0.05$ versus HTL alone. (b) The isolated rat aortic rings were exposed to HTL (1 mM) for 1 hour after preincubation with TXL (400 μg/mL) for 30 minutes with GW9662 (0.01, 0.1 mM). The endothelium-dependent relaxation induced by acetylcholine (Ach) was assayed by organ chamber. All data were expressed as mean ± SEM. N is 5 in each group. $^{*}P < 0.05$ versus HTL alone, $^{\#}P < 0.05$ versus HTL + TXL. (c) Endothelium-independent relaxation was assayed in all groups by using sodium nitroprusside (SNP).

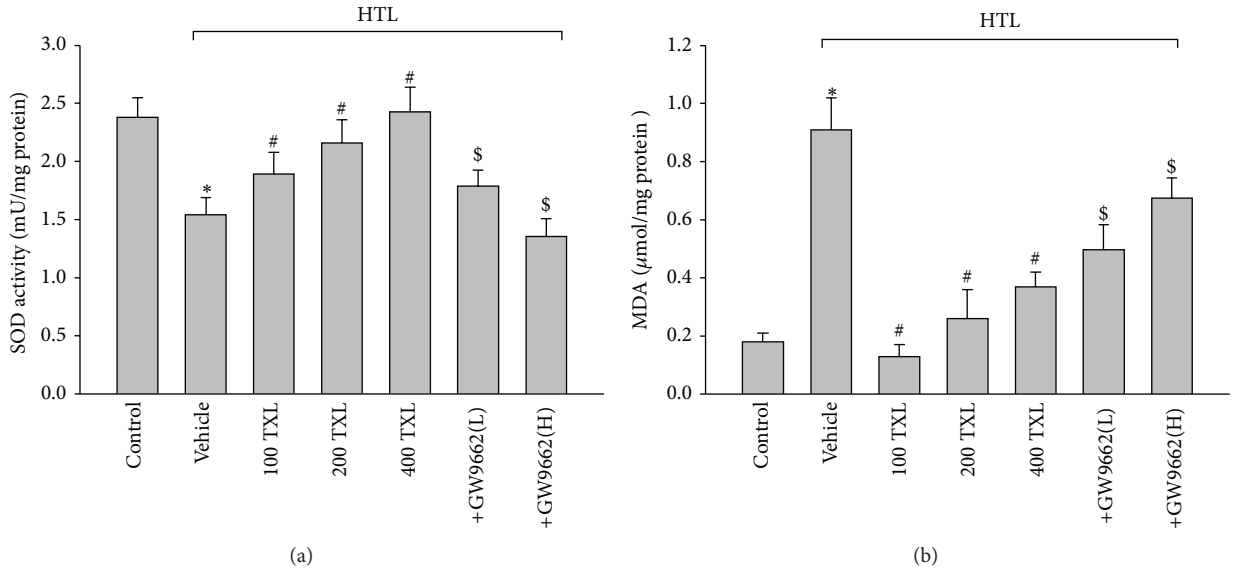

Figure 4: TXL via activation of PPARγ suppresses oxidative stress in isolated rat aortas. The isolated rat aortic rings were exposed to HTL (1 mM) for 1 hour after preincubation with TXL (100, 200, and 400 μg/mL) for 30 minutes. Aortas treated with 400 μg/mL TXL were in the presence of GW9662 (0.01, 0.1 mM). Homogenates of aortic tissues were subjected to assay (a) SOD activity and (b) MDA content by commercial kits. All data were expressed as mean ± SEM. N is 5 in each group. $^{*}P < 0.05$ versus Control and $^{\#}P < 0.05$ versus HTL alone, and $^{\$}P < 0.05$ versus HTL + 400 TXL.

2.9. Statistical Analysis. Data are reported as mean ± SEM. All data were analyzed with the use of 1- or 2-way ANOVA followed by multiple t-tests, and $P < 0.05$ were considered statistically significant.

3. Results

3.1. TXL Dose-Dependently Normalizes Cell Viabilities in HTL-Treated Endothelial Cells. We firstly investigated whether HTL, which is the most reactive one of homocysteine, affected cell viabilities in cultured HUVECs. As shown in Figure 1(a), incubation of HUVECs with HTL (1 mM) for 24 hours dramatically reduced cell viabilities detected by MTT assay, indicating that detrimental effects of homocysteine are related to the high reactivity of HTL. We next examined whether TXL protected endothelial cells against HTL. As depicted in Figure 1(a), TXL alone did not affect endothelial cell viabilities but dose-dependently reversed cell viabilities reduced by HTL.

3.2. TXL Dose-Dependently Suppresses HTL-Induced Oxidative Stress in Cultured Endothelial Cells. We then investigated that TXL via suppression of oxidative stress maintains the normal phenotypes of vascular endothelial cells. As expected in Figures 1(b) and 1(c), incubation of HUVECs with HTL (1 mM) for 24 hours remarkably increased ROS productions in cultured cells. However, preincubation of these cells with TXL inhibited the enhancements of ROS productions induced by HTL in a dose-dependent manner. Taking these together, it indicates that TXL protects cell viabilities reduced by HTL, which is possibly related to suppression of oxidative stress.

3.3. TXL via PPARγ Protects HTL-Treated Endothelial Cells. Activation of PPARγ by agonists has been reported to produce protective effects on oxidative stress in endothelial cells [12, 13]. We next determined whether TXL via activation of PPARγ provided beneficial effects in endothelial cells by using GW9662 which is a specific antagonist of PPARγ to disrupt PPARγ signaling [14]. As expected, inhibition of PPARγ by GW9662 significantly abolished the protective effects of TXL on the improvement of cell viabilities (Figure 2(a)) and reductions of ROS productions (Figures 2(b) and 2(c)) in dose-dependent manner. Taking these data together, it indicates that TXL via PPARγ activation suppresses oxidative stress and protects cell viabilities.

3.4. TXL via PPARγ Preserves Endothelium-Dependent Relaxation Impaired by HTL in Mice Isolated Aortic Rings. We then performed *ex vivo* experiments to test whether TXL protected vascular endothelial functions by incubating isolated mice aortic rings with HTL. Exposure of aortic ring to HTL dramatically impaired Ach-induced endothelium-dependent relaxation (Figure 3(a)). Similar to *in vitro* observations from cultured cells, TXL dose-dependently reversed Ach-induced endothelium-dependent relaxation in aortic rings incubated with HTL (Figure 3(a)), suggesting TXL functions as a protector on vascular endothelium.

We next determined whether TXL via activation of PPARγ provided beneficial effects in endothelial cells by using GW9662 [14]. As expected, inhibition of PPARγ by GW9662 significantly abolished the protective effects of TXL on Ach-induced endothelium-dependent relaxation (Figure 3(b)), indicating that TXL via PPARγ activation protects endothelial function. In addition, SNP-induced

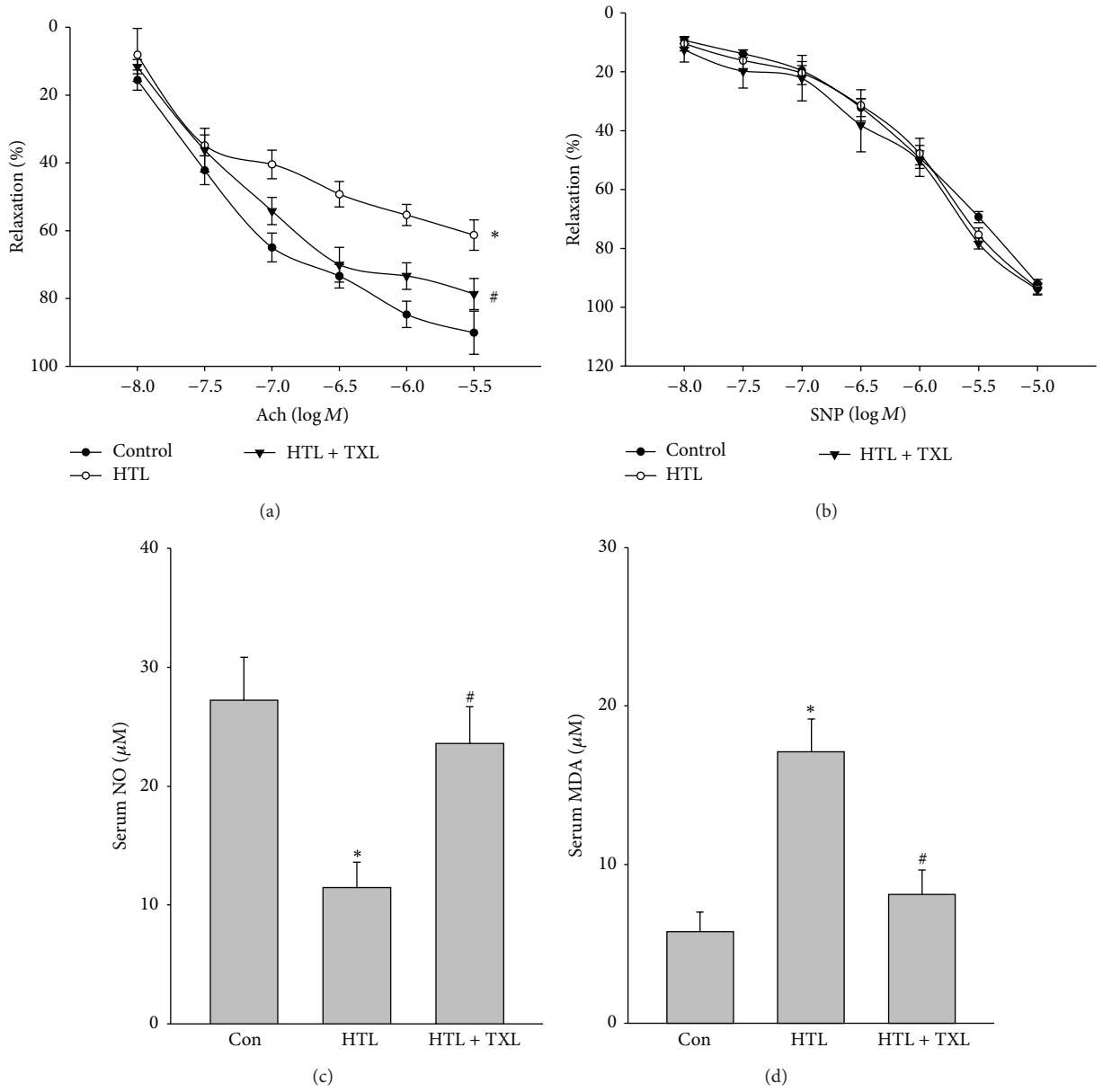

Figure 5: TXL suppresses oxidative stress and improves endothelial functions in rats fed with HTL *in vivo*. The rats were intragastric gavage HTL (50 mg/kg/d) and received administration of TXL (1.0 g/kg/d) for 8 weeks. At the end of experiments, rats were sacrificed under anesthesia. Artery from descending aorta was subjected to assay (a) endothelium-dependent relaxation induced by acetylcholine (Ach) and (b) endothelium-independent relaxation induced by sodium nitroprusside (SNP) in organ chamber. Blood was collected to assay serum level of (c) NO by Griess method and (d) MDA by TBA method. All data were expressed as mean ± SEM, 5–10 rats in each group. $^{*}P < 0.05$ versus Con and $^{\#}P < 0.05$ versus HTL alone.

endothelium-independent relaxation was not altered in all groups (Figure 3(c)), suggesting that the protective effects produced by TXL on vascular function are limited to endothelium but not to vascular smooth muscle.

3.5. TXL via PPARγ Reserves Redox State in Aortas, Which Is Disturbed by HTL. Decreased NO bioavailability, which is due to the decreased NO production or aberrant conversion of NO to $ONOO^{-}$ by ROS, contributes to impairment of Ach-induced endothelium-dependent relaxation in cardiovascular system [15]. We then examined whether HTL maintains normal redox state in rat isolated aortic rings. We found that HTL dramatically decreased SOD activity (Figure 4(a)) and increased the content of MDA (Figure 4(b)), which is formed when ROS reacts with polyunsaturated fatty acid chain in membrane lipids [16]. However, pretreatment of cells with GW9662 significantly abolished TXL-rescued abnormalities in HTL-incubated aortas, suggesting that TXL via

PPARγ/SOD-MDA reserves the normal balance of antioxidative system.

3.6. Administration of TXL Improves Endothelial Function in Rats Fed with HTL. We then performed *in vivo* experiments to confirm whether TXL improves vascular endothelial functions in rats with hyperhomocysteinemia. Homocysteine circulates as different species, mostly protein bound, with approximately 1% as its reduced form and the cyclic thioester HTL. Despite the fact that the level of plasma thiolactone is being markedly low, detrimental effects of homocysteine are related to the high reactivity of HTL [17]. We fed rats with HTL (50 mg/kg/day) for 13 weeks to mimic the model of hyperhomocysteinemia-induced endothelial dysfunction. Endothelial function was determined by measuring the vascular dilation induced by Ach. As shown in Figure 5(a), HTL significantly inhibited Ach-induced vascular relaxation. Importantly, the reduction of Ach-induced vascular relaxation was reversed by the administration of TXL. Both HTL and TXL did not change SNP-induced vessel relaxation (Figure 5(b)), suggesting that the improvement of TXL on vascular bioactivity in HTL-fed rats is due to maintaining endothelial function.

3.7. Administration of TXL Suppresses Oxidative Stress in Rats Fed with HTL. We finally determined whether TXL preserves the normal redox state in HTL-fed rats. As expected, HTL induced the alternations, such as decreased serum NO level (Figure 5(c)), and increased serum levels of MAD (Figure 5(d)). All these defects induced by HTL were normalized by the administration of TXL. This evidence indicates that the *in vivo* protective effects of TXL may be related to suppression of oxidative stress.

4. Discussions

The present study firstly demonstrates that HTL *in vitro* or *in vivo* causes accelerated oxidative stress and endothelial dysfunction, all of which are abrogated by TXL. Mechanistically, the protective effect of TXL on vascular function is attributable to PPARγ activation, resulting in suppressions of oxidative stress. In this way, TXL normalizes the redox state in endothelial cells and protects endothelial function in hyperhomocysteinemic rats.

The major finding in this paper is that TXL prevents HTL-induced endothelial dysfunctions. Recent studies have found that the conversion of homocysteine into HTL plays a critical role in the progress of cardiovascular diseases in patients with hyperhomocysteinemia. In this present study, we used HTL to treat isolated aortic ring *ex vivo* or rats *in vivo*, by which both impaired Ach-induced endothelium-dependent relaxation, which is consistent with our previous study [18]. This supports the observation that detrimental effects of homocysteine are related to the high reactivity of HTL, though the level of plasma thiolactone is very low. Most importantly, HTL-induced endothelial dysfunction both *ex vivo* and *in vivo* was reversed by TXL, which is in dose-dependent manner. Collectively, our results suggest that TXL functions as a protector of endothelial cells. This discovery is also supported by several published studies done in cultured endothelial cells [19, 20] or animals [21, 22], which have shown that TXL protects endothelial function. However, a recent study on human reported that TXL caused endothelial dysfunction in normal volunteers. Of course, the reason for this discrepancy between healthy and hyperhomocysteinemia needs further investigations.

In summary, these studies support a novel function of TXL which activates PPARγ to suppress NF-κB -dependent nicotinamide-adenine dinucleotide phosphate hydrogenase NAD(P)H oxidase. This, in turn, inhibits oxidative stress in endothelial cells, leading to improvement of endothelia function. The finding that TXL attenuates endothelial dysfunction induced by HTL through suppression of oxidative stress may have broad applications for cardiovascular diseases, since endothelial dysfunction is a common character at the beginning and in the progress in a number of vascular diseases including atherosclerosis [23, 24] and diabetes [25]. Thus, TXL may be a useful drug for more effective treatment of atherosclerosis and hypertension.

Conflict of Interests

The authors declare that there is no conflict of interests regarding the publication of this paper.

Authors' Contribution

Yi Zhang designed and conducted the experiments, analyzed data, and wrote the paper. Tiecheng Pan, Xiaoxuan Zhong, and Cai Cheng partially performed some experiments.

Acknowledgment

This project was supported financially by the longitudinal support project by Science and Technology Department of Hubei Province, China (2012FFB03401).

References

[1] K. S. McCully, "Vascular pathology of homocysteinemia: implications for the pathogenesis of arteriosclerosis," *The American Journal of Pathology*, vol. 56, no. 1, pp. 111–128, 1969.

[2] J. Malinowska, J. Kolodziejczyk, and B. Olas, "The disturbance of hemostasis induced by hyperhomocysteinemia; the role of antioxidants," *Acta Biochimica Polonica*, vol. 59, no. 2, pp. 185–194, 2012.

[3] V. Genoud, A. M. Lauricella, L. C. Kordich, and I. Quintana, "Impact of homocysteine-thiolactone on plasma fibrin networks," *Journal of Thrombosis and Thrombolysis*, vol. 38, no. 4, pp. 540–545, 2014.

[4] J. Kolodziejczyk-Czepas, B. Talar, P. Nowak, B. Olas, and B. Wachowicz, "Homocysteine and its thiolactone impair plasmin activity induced by urokinase or streptokinase in vitro," *International Journal of Biological Macromolecules*, vol. 50, no. 3, pp. 754–758, 2012.

[5] Y. Liu, T. Tian, H. Zhang, L. Gao, and X. Zhou, "The effect of homocysteine-lowering therapy with folic acid on flow-mediated vasodilation in patients with coronary artery disease: a meta-analysis of randomized controlled trials," *Atherosclerosis*, vol. 235, no. 1, pp. 31–35, 2014.

[6] L. Zhang, Y. Liu, X. T. Lu et al., "Traditional Chinese medication Tongxinluo dose-dependently enhances stability of vulnerable plaques: a comparison with a high-dose simvastatin therapy," *The American Journal of Physiology—Heart and Circulatory Physiology*, vol. 297, no. 6, pp. H2004–H2014, 2009.

[7] W.-W. Bai, Y.-F. Xing, B. Wang et al., "Tongxinluo improves cardiac function and ameliorates ventricular remodeling in mice model of myocardial infarction through enhancing angiogenesis," *Evidence-based Complementary and Alternative Medicine*, vol. 2013, Article ID 813247, 9 pages, 2013.

[8] W. Q. Chen, L. Zhong, L. Zhang et al., "Chinese medicine tongxinluo significantly lowers serum lipid levels and stabilizes vulnerable plaques in a rabbit model," *Journal of Ethnopharmacology*, vol. 124, no. 1, pp. 103–110, 2009.

[9] S. Wang, Q. Peng, J. Zhang, and L. Liu, "Na^+/H^+ exchanger is required for hyperglycaemia- induced endothelial dysfunction via calcium-dependent calpain," *Cardiovascular Research*, vol. 80, no. 2, pp. 255–262, 2008.

[10] J. Yi, Y. Zheng, C. Miao, J. Tang, and B. Zhu, "Desflurane preconditioning induces oscillation of NF-κB in human umbilical vein endothelial cells," *PLoS ONE*, vol. 8, no. 6, Article ID e66576, 2013.

[11] S. Wang, M. Zhang, B. Liang et al., "AMPKα2 deletion causes aberrant expression and activation of NAD(P)H oxidase and consequent endothelial dysfunction in vivo: role of 26S proteasomes," *Circulation Research*, vol. 106, no. 6, pp. 1117–1128, 2010.

[12] A. T. Reddy, S. P. Lakshmi, J. M. Kleinhenz, R. L. Sutliff, C. M. Hart, and R. C. Reddy, "Endothelial cell peroxisome proliferator-activated receptor gamma reduces endotoxemic pulmonary inflammation and injury," *Journal of Immunology*, vol. 189, no. 11, pp. 5411–5420, 2012.

[13] T. Zhang, F. Wang, H.-X. Xu et al., "Activation of nuclear factor erythroid 2-related factor 2 and PPARγ plays a role in the genistein-mediated attenuation of oxidative stress-induced endothelial cell injury," *British Journal of Nutrition*, vol. 109, no. 2, pp. 223–235, 2013.

[14] S. Sharma, J. Barton, R. Rafikov et al., "Chronic inhibition of PPAR-γ signaling induces endothelial dysfunction in the juvenile lamb," *Pulmonary Pharmacology and Therapeutics*, vol. 26, no. 2, pp. 271–280, 2013.

[15] S. Wang, J. Xu, P. Song et al., "Acute inhibition of guanosine triphosphate cyclohydrolase 1 uncouples endothelial nitric oxide synthase and elevates blood pressure," *Hypertension*, vol. 52, no. 3, pp. 484–490, 2008.

[16] S.-X. Wang, L.-Y. Liu, and Y.-H. Liu, "Na^+/H^+ exchanger inhibitor prevented endothelial dysfunction induced by high glucose," *Journal of Cardiovascular Pharmacology*, vol. 45, no. 6, pp. 586–590, 2005.

[17] H. Jakubowski and E. Goldman, "Synthesis of homocysteine thiolactone by methionyl-tRNA synthetase in cultured mammalian cells," *FEBS Letters*, vol. 317, no. 3, pp. 237–240, 1993.

[18] Y.-H. Liu, Y. You, T. Song, S.-J. Wu, and L.-Y. Liu, "Impairment of endothelium-dependent relaxation of rat aortas by homocysteine thiolactone and attenuation by captopril," *Journal of Cardiovascular Pharmacology*, vol. 50, no. 2, pp. 155–161, 2007.

[19] H. Cui, X. Li, N. Li et al., "Induction of autophagy by tongxinluo via the MEK/ERK pathway protects human cardiac microvascular endothelial cells from hypoxia/reoxygenation injury," *Journal of Cardiovascular Pharmacology*, vol. 64, no. 2, pp. 180–190, 2014.

[20] X.-C. Wu, J. Lai, X.-F. Wu, Z.-H. Jia, C. Wei, and H.-T. Wang, "Effects of Tongxinluo on neuron ultrastructure and endothelial cell self-repairing ability in hypoxia preconditioning mice," *Zhongguo Ying Yong Sheng Li Xue Za Zhi*, vol. 27, no. 4, pp. 396–399, 2011.

[21] Y.-H. Yu, X.-Q. Xu, Y. Wang, S.-Z. Sun, and Y. Chen-, "Intervention of Tongxinluo capsule against vascular lesion of atherosclerosis and its effect on lectin-like oxidized low density lipoprotein receptor-1 expression in rabbits," *Chinese Journal of Integrative Medicine*, vol. 12, no. 1, pp. 32–36, 2006.

[22] X.-C. Wu, J. Lai, and X.-F. Wu, "Effect of chronic psychological stress on vascular endothelial dysfunction rats and intervention tongxinluo on it," *Zhongguo Zhong Xi Yi Jie He Za Zhi*, vol. 31, no. 5, pp. 680–683, 2011.

[23] C. Antoniades, C. Shirodaria, N. Warrick et al., "5-Methyltetrahydrofolate rapidly improves endothelial function and decreases superoxide production in human vessels: effects on vascular tetrahydrobiopterin availability and endothelial nitric oxide synthase coupling," *Circulation*, vol. 114, no. 11, pp. 1193–1201, 2006.

[24] S. Kawashima and M. Yokoyama, "Dysfunction of endothelial nitric oxide synthase and atherosclerosis," *Arteriosclerosis, Thrombosis, and Vascular Biology*, vol. 24, no. 6, pp. 998–1005, 2004.

[25] N. J. Alp, S. Mussa, J. Khoo et al., "Tetrahydrobiopterin-dependent preservation of nitric oxide-mediated endothelial function in diabetes by targeted transgenic GTP-cyclohydrolase I overexpression," *The Journal of Clinical Investigation*, vol. 112, no. 5, pp. 725–735, 2003.

Hindawi Publishing Corporation
Evidence-Based Complementary and Alternative Medicine
Volume 2015, Article ID 802368, 7 pages
http://dx.doi.org/10.1155/2015/802368

Research Article

Antihypertensive Effect of the GaMiSamHwangSaSimTang in Spontaneous Hypertensive Rats

Kyungjin Lee, Bumjung Kim, Heseung Hur, Khanita Suman Chinannai, Inhye Ham, and Ho-Young Choi

Department of Herbology, College of Korean Medicine, Kyung Hee University, 26 Kyungheedae-ro, Dongdaemun-gu, Seoul 130-701, Republic of Korea

Correspondence should be addressed to Ho-Young Choi; hychoi@khu.ac.kr

Received 10 March 2015; Revised 29 April 2015; Accepted 4 May 2015

Academic Editor: Yanwei Xing

The present study was designed to evaluate the antihypertensive effect of GaMiSamHwangSaSimTang (HVC1), a 30% ethanol extract of a mixture comprising Pruni Cortex, Scutellariae Radix, Coptidis Rhizoma, and Rhei Rhizoma, on spontaneous hypertensive rats (SHRs). The systolic blood pressure (SBP) was measured every 4 or 7 days using the noninvasive tail cuff system. The vasorelaxant effects on isolated aortic rings were evaluated. Aortic rings were contracted using phenylephrine (PE) or KCl, and the changes in tension were recorded via isometric transducers connected to a data acquisition system. In this study, oral administration of HVC1 decreased the SBP of SHRs over the experimental period. HVC1 induced concentration-dependent relaxation in the aortic rings that had been precontracted using PE or KCl. The vasorelaxant effects of HVC1 on endothelium-intact aortic rings were inhibited by pretreatment with *N*ω-Nitro-L-arginine methyl ester (L-NAME) or methylene blue. HVC1 inhibited the contraction induced by extracellular Ca^{2+} in endothelium-denuded rat aortic rings that had been precontracted using PE or KCl. In conclusion, HVC1 reduced the SBP of SHR and relaxed isolated SHR aortic rings by upregulating NO formation and the NO-cGMP pathway and blocking the entry of extracellular Ca^{2+} via receptor-operative Ca^{2+} channel and voltage-dependent Ca^{2+} channel.

1. Introduction

Hypertension is a global public health issue and is associated with increased risk of cardiovascular disease, stroke, and kidney disease [1]. The disease is regarded as a "silent killer" as it rarely produces symptoms in its early stages and as a result many people go undiagnosed [1]. In 2008, the worldwide prevalence of high blood pressure was reported to be approximately 40% of adults aged 25 or older; every year, about 9.4 million deaths are estimated to be caused by hypertension, which accounts for 12.8% of the worldwide total [1]. Hypertension has a huge economic impact, and in higher-income countries, including those in Eastern Europe and Central Asia, the disease accounts for almost 23% of health care expenditure [2].

In 2013, in Korea, the prevalence of hypertension in men and women over 30 years of age was 32.4 and 22.2%, respectively; the prevalence increased with age and in adults over 70 years of age, the prevalence of hypertension in men was 59% and in women was 64.3% [3]. The number of hypertensive patients is constantly increasing, and the cost of hypertension treatment is also steadily increasing in Korea. According to the National Health Insurance Statistical Yearbook 2013, the costs paid by national health insurance for the treatment of hypertension ($1.9 billion) formed a larger proportion of total medical costs ($46.3 billion) than any other disease, and—among 13.7 million patients—hypertension was the most common disease (5.5 million people) [4]. However, traditional medicines have not been widely used for the treatment of hypertension in Korea. There are several useful traditional medicines for the treatment of hypertension [5–7], but few patients choose to use them, and health insurance does not pay for them. This is because the herbal medicines for hypertension have not yet been developed throughout efficacy and safety studies in Korea.

Scutellariae Radix (SR), Coptidis Rhizoma (CR), and Rhizoma Rhei (RR) have been commonly used traditional medicines for cardiovascular diseases in China, Japan, and

Korea. A herbal prescription SanHuangXieXinTang (SamHwangSaSimTang in Korean) composed of SR, CR, and RR was reported to decrease U46619-induced increase in pulmonary arterial blood pressure [8]. And we found that Pruni Cortex (PC) has potent vasorelaxant activities in the previous study [9]. Therefore, these herbal materials are expected to be useful for the treatment of spontaneous hypertension. For the development of new antihypertensive herbal medicine, a new prescription GaMiSamHwangSaSimTang (HVC1) which consists of four kinds of traditional medicine including Pruni Cortex, Scutellariae Radix, Coptidis Rhizoma, and Rhei Rhizoma was developed based on SamHwangSaSimTang. In the previous animal study, we found that vasorelaxant effect of HVC1 was better than SamHwangSaSimTang (data not shown).

In this study, we aimed to demonstrate the hypotensive effect and mechanisms of action of a HVC1 on spontaneous hypertensive rats and we performed standardization of HVC1.

2. Materials and Methods

2.1. Preparation of GaMiSamHwangSaSimTang. The extract was prepared from a mixture of dried PC (200 g), SR (100 g), CR (100 g), and RR (200 g). PC and RR were purchased from Dongwoodang Co., Ltd. (Yeongcheon, Kyungpook, Republic of Korea). CR and SR were purchased from Dong Yang Herb Co., Ltd. (Seoul, Republic of Korea). Professor Hocheol Kim of Kyung Hee University identified these herbal medicines. The mixture was extracted with 30% ethanol for 2 h in a reflux apparatus. After reflux and filtration, the extract was evaporated using a rotary vacuum evaporator (N-N series, EYELA, Japan) at 60°C and lyophilized to yield 159.9 g of crude extract.

2.2. Chemicals and Drugs. Phenylephrine (PE), KCl, acetylcholine, *Nω*-Nitro-L-arginine methyl ester (L-NAME), methylene blue (MB), atropine, indomethacin, and ethylene glycol-bis-(2-aminoethylether)-N,N,N′,N′-tetraacetic acid were purchased from Sigma Aldrich (St. Louis, MO, USA). Amlodipine besylate was purchased from Kolmar Korea Co., Ltd. (Yeongi-gun, Chungnam, Republic of Korea). All other reagents were of analytical purity.

2.3. Animals. Spontaneous hypertensive rats (SHR/lzm; male; weight: 200–250 g; age: 8 weeks) were purchased from Japan SLC Inc. (Hamamatsu, Shizuoka Prefecture, Japan). All procedures involving animals were conducted according to the animal welfare guidelines issued by the National Veterinary Research & Quarantine Service and World Organization for Animal Health (OIE), and this study was approved (KHUASP(SE)-13-018) by the Kyung Hee University Institutional Animal Care and Use Committee. The rats were housed under controlled conditions (22 ± 2°C; lighting, 07:00–19:00), and food and water were available *ad libitum*.

2.4. Measurement of Blood Pressure. The systolic blood pressure of SHRs was evaluated using the noninvasive tail cuff system (CODA 8-Channel High Throughput Non-Invasive Blood Pressure system, Kent Scientific Co. Ltd., Torrington, CT, USA) [10]. We randomly divided SHRs into four groups of six animals each. For 50 days, they were orally administered either distilled water, amlodipine, or HVC1. Amlodipine and HVC1 were dissolved in distilled water. Amlodipine was not completely soluble in distilled water; therefore, an aqueous suspension of amlodipine was used in this experiment. Control rats were treated with distilled water ($1\,mL \cdot kg^{-1} \cdot day^{-1}$), positive control rats were treated with amlodipine ($10\,mg \cdot kg^{-1} \cdot day^{-1}$), and the rats of the two experimental groups were treated with HVC1 (50 or $300\,mg \cdot kg^{-1} \cdot day^{-1}$).

2.5. Vasoactivity Measurement. Spontaneous hypertensive rat aortic rings were isolated and placed in organ chambers containing Krebs-Henseleit solution (K-H solution; 10 mL) at 37°C, and then the vasoactivity of HVC1 was evaluated using previously described methods [9]. HVC1 was dissolved in K-H solution. The endothelium-intact and endothelium-denuded aortic rings were contracted using PE (1 μM) or KCl (60 mM) treatment. Endothelium-intact aortic rings were also preincubated with L-NAME (10 μM), MB (10 μM), indomethacin (10 μM), or atropine (1 μM) for 20 min before contraction with PE (1 μM) treatment to investigate the vasorelaxant mechanisms of HVC1 action. The presence of functional endothelium was verified by the ability of ACh (10 μM) to induce more than 80% relaxation in rings that were precontracted by PE (1 μM). The relaxant effect of HVC1 on the aortic rings was calculated as a percentage of the contraction in response to PE or KCl.

2.6. High Performance Liquid Chromatography (HPLC) Analysis of HVC1. Precisely weighed HVC1 (100 mg) was dissolved in methanol (10 mL; HPLC grade; J. T. Baker Co. Ltd., USA) and the solution was filtered through a 0.45 μm syringe filter (poly(vinylidene difluoride), Milford, USA). The analytical standards used for the HPLC analysis of HVC1 were as follows: sennoside A and sennoside B (Rhei Rhizoma standards, Sigma, USA), coptisine, berberine, wogonin (Rhizoma Coptidis standards, Sigma, USA), baicalin, baicalein (Coptidis Rhizoma standards, Sigma, USA), prunetin (Pruni Cortex standards, Sigma, USA), genistein-7-glucose, and prunetin-5-glucose (Pruni Cortex standards, isolated according to a previously published procedure [11]). Each standard (1 mg) was dissolved in 100 μg/mL 50% methanol. Equal amounts of each standard mixture were combined and a HPLC chromatogram was obtained. The HPLC apparatus was a Gilson System equipped with a 234 Autosampler, a UV/VIS-155 detector, and a 321 HPLC Pump (Gilson, Seoul, Korea). A Luna 4.60 × 264 mm C18 reverse-phase column with 5 μm particles (Phenomenex, CA, USA) was used. The mobile phase consisted of 0.1% formic acid (A) and acetonitrile (HPLC grade, J. T. Baker Co. LTD., USA) (B) in a ratio specified by the following binary gradient with linear interpolation: 0 min, 20% B; 60 min, 30% B; 70 min, 60% B; 100 min, 70% B. The column eluent was monitored at 250 nm, and all solvents were degassed with a micro-membrane filter (poly(tetrafluoroethylene), Advantec, Tokyo, Japan). Chromatography was performed at room

temperature at a flow rate of 0.5 mL/min, using 10 μL analyte, for 100 min.

2.7. Statistical Analysis. Data are expressed as mean ± standard error of the mean (SEM). Statistical comparisons were made using Student's t-test or one-way analysis of variance (ANOVA) followed by Tukey's post hoc test. All statistical analyses were performed using SPSS v.13.0 statistical analysis software (SPSS Inc., USA). P values less than 0.05 were considered statistically significant.

3. Results

3.1. Effect of HVC1 on Blood Pressure in SHRs. Before the experiment commenced (day 0), the systolic blood pressure (SBP) of the control group (198.8 ± 4.6 mmHg), the amlodipine 10 mg·kg^{-1}·day^{-1} treated group (197.5 ± 1.4 mmHg), the HVC1 50 mg·kg^{-1}·day^{-1} treated group (201.7 ± 1.5 mmHg), and the HVC1 300 mg·kg^{-1}·day^{-1} treated group (203.3 ± 4.8 mmHg) were measured using the noninvasive tail cuff system. At the end of the experiment (day 50), the SBP of the control group had increased to 225.2 ± 1.9 mmHg. The SBP of the positive control group (i.e., the amlodipine-treated group) continuously decreased during the experimental period and thus this experiment was considered to be reliable.

Orally administered HVC1 doses of 50 and 300 mg·kg^{-1}·day^{-1} also continuously decreased the SBP of SHRs during the experimental period. On average, orally administered HVC1 doses of 50 and 300 mg·kg^{-1}·day^{-1} decreased the SBP of SHRs to 191.1 ± 2.5 and 186.6 ± 2.9 mmHg, respectively. The maximal hypotensive effect was recorded on day 36 and SBP was 179.8 ± 10.8 and 172.2 ± 5.8 mmHg for the 50 and 300 mg·kg^{-1}·day^{-1} dose-treated groups, respectively (Figure 1).

3.2. Effects of HVC1 on PE- or KCl-Induced Contraction of Endothelium-Intact or Endothelium-Denuded Aortic Rings. HVC1 (3, 10, 30, 100, and 300 μg/mL) caused concentration-dependent relaxation in both endothelium-intact and endothelium-denuded aortic rings that had been precontracted using PE (1 μM) treatment. However, endothelium-intact aortic rings were more relaxed than endothelium-denuded aortic rings (Figure 2(a)). HVC1 (3, 10, 30, 100, and 300 μg/mL) also caused concentration-dependent relaxation in endothelium-intact and endothelium-denuded aortic rings that had been precontracted using KCl (60 mM) treatment. But there were no significantly differences between endothelium-intact and endothelium-denuded aortic rings (Figure 2(b)).

3.3. Effect of HVC1 on Endothelium-Intact Aortic Rings Preincubated with L-NAME or MB. Incubation with L-NAME (10 μM) or MB (10 μM) significantly decreased HVC1-induced relaxation of endothelium-intact aortic rings that had been precontracted using PE (1 μM) treatment. However, the vasorelaxant effect of HVC1 300 μg/mL was not affected by preincubation with MB (Figure 3).

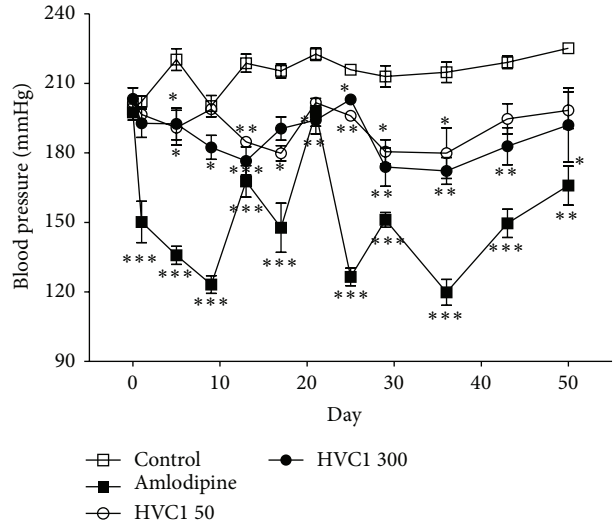

Figure 1: Hypotensive effect of HVC1 on the arterial systolic blood pressure of spontaneous hypertensive rats. Arterial systolic blood pressure was measured using the noninvasive tail cuff system. Values are expressed as mean ± SEM ($n = 6$). $^{*}P < 0.05$; $^{**}P < 0.01$; $^{***}P < 0.001$ versus control. Amlodipine = amlodipine 10 mg·kg^{-1}·day^{-1} oral administration; HVC1 50 = HVC1 50 mg·kg^{-1}·day^{-1} oral administration; HVC1 300 = HVC1 300 mg·kg^{-1}·day^{-1} oral administration.

3.4. Effect of HVC1 on Endothelium-Intact Aortic Rings Preincubated with Indomethacin or Atropine. Incubation with indomethacin (10 μM) or atropine (1 μM) did not affect HVC1-induced relaxation of endothelium-intact aortic rings that had been precontracted using PE (1 μM) treatment (Figure 4).

3.5. Effect of HVC1 on Extracellular Ca^{2+}-Induced Contraction. In Ca^{2+}-free K–H solution, the cumulative addition of $CaCl_2$ (0.3–10 mM) induced progressively increased tension in rat aortic rings that had been precontracted using PE (1 μM; Figure 5(a)) or KCl (60 mM; Figure 5(b)) treatment. As shown in Figure 5, preincubation with HVC1 (300 μg/mL) for 20 min significantly inhibited the contraction induced by extracellular Ca^{2+}.

3.6. Standard Material Analysis. The retention times of the standards in the sample mixture were as follows: sennoside A, 3.49 min; genistein-7-glucose, 4.98 min; coptisine, 9.61 min; baicalin, 13.78 min; prunetin-5-glucose, 17.18 min; berberine, 21.22 min; baicalein, 59.76 min; wogonin, 72.53 min; prunetin, 74.12 min (Figure 6(a)). In the HPLC chromatogram of HVC1, the peaks for the standards were observed (Figure 6(b)).

4. Discussion

In this study, HVC1, a herbal prescription containing extracts of PC, SR, CR, and RR, decreased the SBP of SHRs and relaxed aortic rings that had been contracted by treatment with PE or KCl.

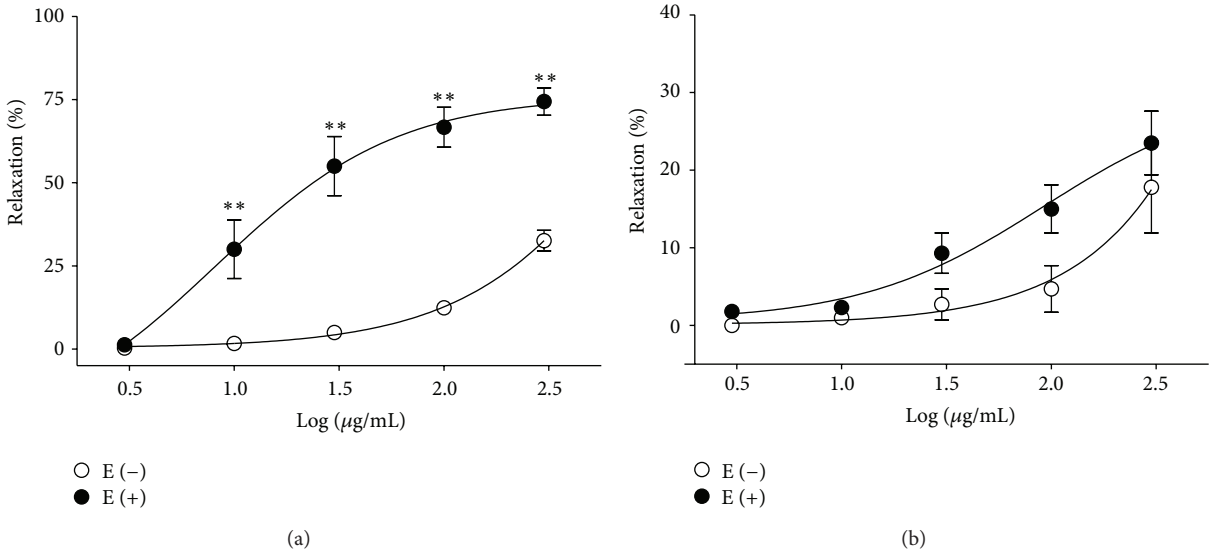

Figure 2: Concentration-dependent relaxant effects of HVC1 on precontracted spontaneous hypertensive rat aortic rings. Endothelium-intact [E (+)] or endothelium-denuded [E (−)] aortic rings were precontracted by phenylephrine (PE, 1 μM) (a) or KCl (60 mM) (b). Values are expressed as mean ± SEM ($n = 8$). $^{**}P < 0.01$ versus E (−).

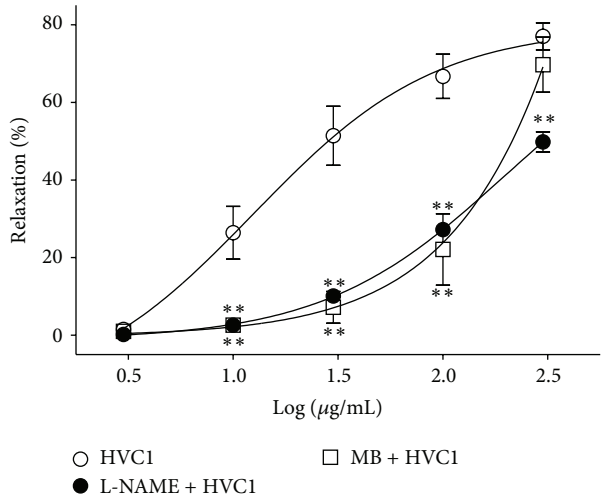

Figure 3: Effect of HVC1 on endothelium-intact aortic rings preincubated with *N*ω-Nitro-L-arginine methyl ester (L-NAME, 10 μM) or methylene blue (MB, 10 μM). The graph shows the relaxation responses induced by HVC1 in endothelium-intact spontaneous hypertensive rat aortic rings that had been precontracted with phenylephrine (PE, 1 μM) in the presence or absence of L-NAME or MB in Krebs-Henseleit solution. The relaxant effects of HVC1 on isolated spontaneous hypertensive rat aortic rings were calculated as a percentage of the contraction in response to PE. Values are expressed as mean ± SEM ($n = 4$). $^{*}P < 0.05$ and $^{**}P < 0.01$ versus HVC1.

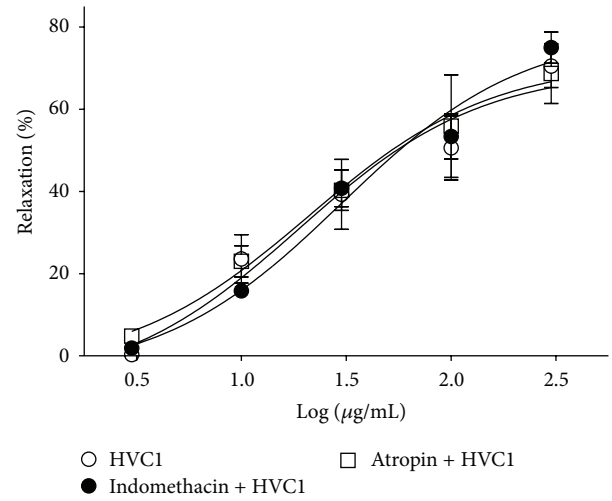

Figure 4: Effect of HVC1 on endothelium-intact aortic rings preincubated with indomethacin or atropine. Graph showing relaxation responses induced by HVC1 in endothelium-intact spontaneous hypertensive rat aortic rings that had been precontracted with phenylephrine (PE, 1 μM) in Krebs-Henseleit solution in the presence or absence of indomethacin (10 μM) or atropine (1 μM). The relaxant effects of HVC1 on isolated spontaneous hypertensive rat aortic rings were calculated as a percentage of the contraction in response to PE. Values are expressed as mean ± SEM ($n = 4$).

Over the 50-day long experimental period, the SBP of the control group (orally administrated distilled water) increased from 198.8 ± 4.6 mmHg on day 0 to 225.2 ± 1.9 mmHg on day 50. On the other hand, the SBP of the HVC1 50 and 300 mg·kg^{-1}·day^{-1} treated groups significantly decreased during the experimental period. These results suggest that HVC1 has an antihypertensive effect.

Vascular tone is important for the regulation of blood pressure. In blood vessels, the vascular endothelium and smooth muscle play an important role in vasorelaxation. The

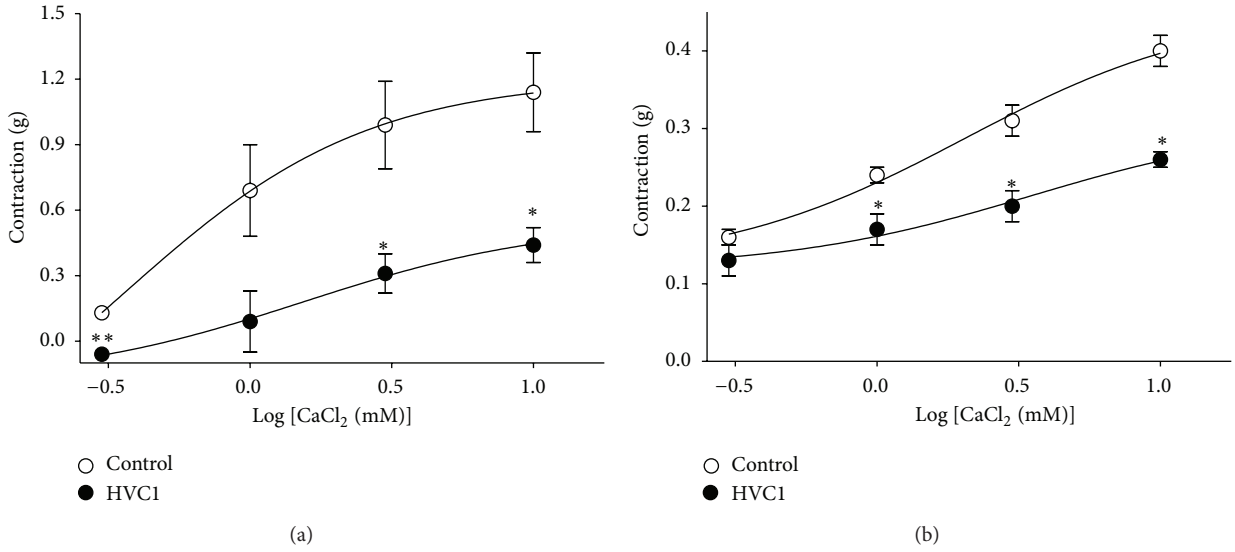

Figure 5: Effect of HVC1 on Ca^{2+}-induced aortic ring contraction. Graph showing the inhibitory effect of HVC1 (300 μg/mL) on the contraction induced by extracellular Ca^{2+} addition (0.3–10 mM) in endothelium-denuded spontaneous hypertensive rat aortic rings that had been precontracted using phenylephrine (PE, 1 μM) (a) or KCl (60 mM) (b) treatment in Ca^{2+}-free Krebs-Henseleit solution. Values are expressed as mean ± SEM ($n = 4$). $^{*}P < 0.05$ and $^{**}P < 0.01$ versus control.

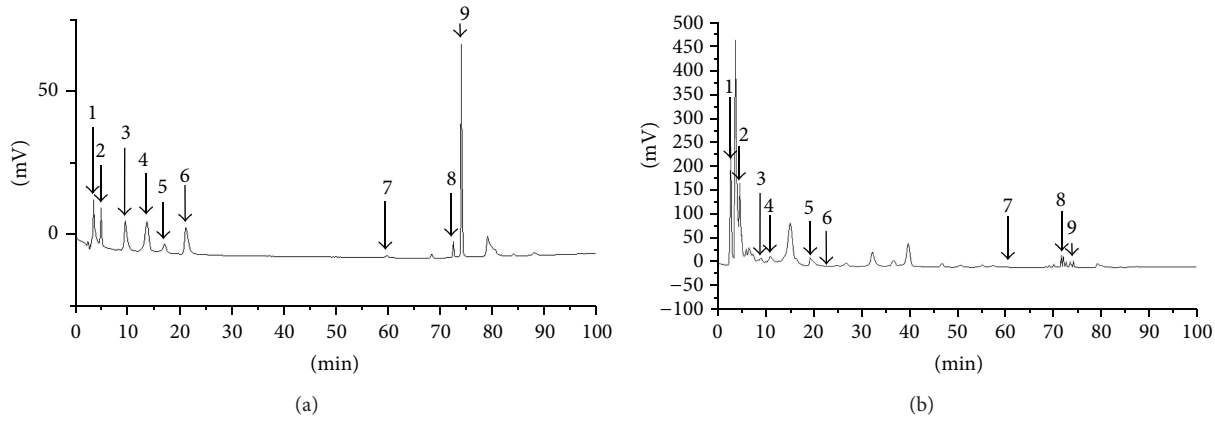

Figure 6: HPLC chromatogram of HVC1 standard mixtures (a) and HVC1 (b). 1: sennoside A; 2: genistein-7-O-β-glucopyranoside; 3: coptisine; 4: baicalin; 5: prunetin-5-O-β-glucopyranoside; 6: berberine; 7: baicalein; 8: wogonin; 9: prunetin.

vascular endothelium releases potent vasodilators such as nitric oxide (NO) and prostacyclin (PGI_2) [12].

NO is synthesized from L-arginine and when released from the vascular endothelium, it activates cyclic guanidine monophosphate (cGMP), which leads to relaxation of vascular smooth muscles [12]. Thus, NO synthesis and the cGMP pathway are important factors in hypertension. In this study, preincubation with L-NAME (10 μM), an inhibitor of NO synthase, significantly decreased the HVC1-induced relaxation of endothelium-intact aortic rings that had been contracted using PE treatment. Preincubation with MB (10 μM), a soluble guanylate cyclase inhibitor, also significantly decreased HVC1-induced relaxation. These results suggested that the antihypertensive and vasorelaxant effects of HVC1 are partly related to NO synthesis and the NO-cGMP pathway.

PGI_2 is synthesized by cyclooxygenase and when released from the vascular endothelium, it activates adenyl cyclase (AC). Activated AC increases the intracellular concentration of cyclic adenosine monophosphate (cAMP), which relaxes vascular smooth muscle by decreasing the intracellular calcium concentration [12]. In this study, preincubation with indomethacin (10 μM) did not affect the HVC1-induced relaxation of endothelium-intact aortic rings that had been contracted using PE treatment. These results suggested that PGI_2 might not be involved in the antihypertensive and vasorelaxant effect of HVC1.

Muscarinic receptors located on endothelial or smooth muscle cells also play an important role in vasorelaxation [13]. In this work, preincubation with atropine (1 μM), a nonselective muscarinic receptor antagonist, did not affect HVC1-induced relaxation of endothelium-intact aortic rings

that had been contracted using PE treatment. This result suggested that the muscarinic receptor might not contribute to the antihypertensive and vasorelaxant effects of HVC1.

The contraction and relaxation of vascular smooth muscle can be regulated by extracellular Ca^{2+} influx via the receptor-operative Ca^{2+} channel (ROCC) or the voltage-dependent Ca^{2+} channel (VDCC) without endothelial derived factors [14]. In the present study, preincubation with HVC1 (300 μg/mL) for 20 min significantly inhibited the contraction induced by extracellular Ca^{2+} supplementation in endothelium-denuded aortic rings that had been contracted using PE or KCl treatment in Ca^{2+}-free K–H solution. These results suggested that the antihypertensive and vasorelaxant effects of HVC1 are partly related to blockage of extracellular Ca^{2} entry via the ROCC and VDCC.

Furthermore, HVC1 (300 μg/mL) inhibited the PE-induced contractions to a greater extent than high K^+-induced contractions (Figure 5). Several reports have described that the involvement of the contractile elements is more related to agonist-induced contractions than high K^+. Phosphorylation of myosin light chain (MLC) is induced to a greater extent by receptor agonist like phenylephrine than by high K^+ [15]. Moreover, drugs such as forskolin [16] and sodium nitroprusside [17] decrease the agonist-induced contractions to a greater extent than high K^+-induced contractions owing to the involvement of the contractile elements. The agonists like phenylephrine cause an initial spike in Ca^{2+} followed by small sustained rise in Ca^{2+} above the basal levels, thus increasing the Ca^{2+} sensitivity of MLC phosphorylation and leading to increased contraction. However, high K^+ depolarization results in a maintained increase in the Ca^{2+}-induced contractions [18]. These findings suggest that HVC1 involves the contractile elements of the aortic smooth muscle cells suggesting one of the possible mechanisms that HVC1 selectively inhibits the receptor-linked Ca^{2+} channel or that it decreases the Ca^{2+} influx or Ca^{2+} sensitivity.

HVC1 is a herbal prescription consisting of PC, SR, CR, and RR extracts. Sennoside A is a known standard component of RR, baicalin, baicalein, and wogonin are known standard components of SR, and berberine is a known standard component of CR [19]. However, the standard components of PC have not yet been established. In a previous study, we isolated genistein-7-*O*-β-glucopyranoside and prunetin-5-*O*-β-glucopyranoside from *Prunus* bark [11]. Prunetin is known as one of the major components of the *Prunus* species [20]. Therefore, we used these compounds as standards in the HPLC analysis of HVC1. Among these compounds, coptisine [21], baicalin [22, 23], berberine [24, 25], and wogonin [26] showed vasorelaxant activities and we found that prunetin also has vasorelaxant activities (data not shown). Therefore, these compounds might be the active compounds in HVC1 that help treat hypertension.

5. Conclusions

In this study, HVC1 reduced the SBP of SHRs and relaxed isolated SHR aortic rings by upregulating NO formation and the NO-cGMP pathway and blocking the entry of extracellular Ca^{2+} via ROCC and VDCC. Therefore, HVC1 could be a useful herbal medicine for the prevention and treatment of hypertension.

Conflict of Interests

The authors declare that they have no conflict of interests.

Acknowledgment

This study was supported by a Grant from the Korea Healthcare Technology R&D Project, Ministry of Health & Welfare, Republic of Korea (B110081).

References

[1] World Health Organization, *A Global Brief on Hypertension; Silent Killer, Global Public Health Crisis*, World Health Organization, 2013.

[2] T. A. Gaziano, A. Bitton, S. Anand, and M. C. Weinstein, "The global cost of nonoptimal blood pressure," *Journal of Hypertension*, vol. 27, no. 7, pp. 1472–1477, 2009.

[3] Korea Centers for Disease Control and Prevention, *The Sixth Korea National Health and Nutrition Examination Survey (KNHANES VI-1)*, Korea Centers for Disease Control and Prevention, Daejeon, South Korea, 2013.

[4] National Health Insurance Service, *National Health Insurance Statistical Yearbook 2013*, National Health Insurance Service, 2013.

[5] Z. Chen, L. Wang, G. Yang, H. Xu, and J. Liu, "Chinese herbal medicine combined with conventional therapy for blood pressure variability in hypertension patients: a systematic review of randomized controlled trials," *Evidence-Based Complementary and Alternative Medicine*. In press.

[6] X. Xiong, X. Yang, W. Liu, F. Chu, P. Wang, and J. Wang, "Trends in the treatment of hypertension from the perspective of traditional chinese medicine," *Evidence-Based Complementary and Alternative Medicine*, vol. 2013, Article ID 275279, 13 pages, 2013.

[7] J. Wang and X. Xiong, "Evidence-based Chinese medicine for hypertension," *Evidence-Based Complementary and Alternative Medicine*, vol. 2013, Article ID 978398, 12 pages, 2013.

[8] H.-H. Tsai, I.-J. Chen, and Y.-C. Lo, "Effects of San-Huang-Xie-Xin-Tang on U46619-induced increase in pulmonary arterial blood pressure," *Journal of Ethnopharmacology*, vol. 117, no. 3, pp. 457–462, 2008.

[9] K. Lee, I. Ham, G. Yang et al., "Vasorelaxant effect of *Prunus yedoensis* bark," *BMC Complementary and Alternative Medicine*, vol. 13, article 31, 2013.

[10] A. Daugherty, D. Rateri, L. Hong, and A. Balakrishnan, "Measuring blood pressure in mice using volume pressure recording, a tail-cuff method," *Journal of Visualized Experiments*, vol. 2009, no. 27, p. 1291, 2009.

[11] J. Lee, G. Yang, K. Lee et al., "Anti-inflammatory effect of *Prunus yedoensis* through inhibition of nuclear factor-κB in macrophages," *BMC Complementary and Alternative Medicine*, vol. 13, article 92, 2013.

[12] E. Stankevicius, E. Kevelaitis, E. Vainorius, and U. Simonsen, "Role of nitric oxide and other endothelium-derived factors," *Medicina*, vol. 39, no. 4, pp. 333–341, 2003.

[13] L. Walch, C. Brink, and X. Norel, "The muscarinic receptor subtypes in human blood vessels," *Therapie*, vol. 56, no. 3, pp. 223–226, 2001.

[14] H. Karaki, H. Ozaki, M. Hori et al., "Calcium movements, distribution, and functions in smooth muscle," *Pharmacological Reviews*, vol. 49, no. 2, pp. 157–230, 1997.

[15] P. H. Ratz, "Receptor activation induces short-term modulation of arterial contractions: Memory in vascular smooth muscle," *The American Journal of Physiology—Cell Physiology*, vol. 269, no. 2, pp. C417–C423, 1995.

[16] K. H. Han, G. J. Cheon, D. S. Yeon, and S. C. Kwon, "Forskolin changes the relationship between cytosolic Ca^{2+} and contraction in guinea pig ileum," *The Korean Journal of Physiology & Pharmacology*, vol. 13, no. 3, pp. 189–194, 2009.

[17] H. Ozaki, T. Ohyama, K. Sato, and H. Karaki, "Ca^{2+}-dependent and independent mechanisms of sustained contraction in vascular smooth muscle of rat aorta," *Japanese Journal of Pharmacology*, vol. 52, no. 3, pp. 509–512, 1990.

[18] R. A. Khalil, *Regulation of Vascular Smooth Muscle Function*, Morgan & Claypool Publishers, San Francisco, Calif, USA, 2010.

[19] Ministry of Food and Drug Safety, *The Korean Pharmacopoeia*, Ministry of Food and Drug Safety, 10th edition, 2012.

[20] H. A. Jung, A. R. Kim, H. Y. Chung, and J. S. Choi, "*In vitro* antioxidant activity of some selected *Prunus* species in Korea," *Archives of Pharmacal Research*, vol. 25, no. 6, pp. 865–872, 2002.

[21] L.-L. Gong, L.-H. Fang, H.-L. Qin, Y. Lv, and G.-H. Du, "Analysis of the mechanisms underlying the vasorelaxant action of coptisine in rat aortic rings," *The American Journal of Chinese Medicine*, vol. 40, no. 2, pp. 309–320, 2012.

[22] Y.-L. Lin, Z.-K. Dai, R.-J. Lin et al., "Baicalin, a flavonoid from *Scutellaria baicalensis* Georgi, activates large-conductance Ca^{2+}-activated K^+ channels via cyclic nucleotide-dependent protein kinases in mesenteric artery," *Phytomedicine*, vol. 17, no. 10, pp. 760–770, 2010.

[23] Y. Huang, S. Y. Tsang, X. Yao, C. W. Lau, Y. L. Su, and Z. Y. Chen, "Baicalin-induced vascular response in rat mesenteric artery: role of endothelial nitric oxide," *Clinical and Experimental Pharmacology & Physiology*, vol. 29, no. 8, pp. 721–724, 2002.

[24] D. G. Kang, E. J. Sohn, E. K. Kwon, J. H. Han, H. Oh, and H. S. Lee, "Effects of berberine on angiotensin-converting enzyme and NO/cGMP system in vessels," *Vascular Pharmacology*, vol. 39, no. 6, pp. 281–286, 2002.

[25] W. H. Ko, X. Q. Yao, C. W. Lau et al., "Vasorelaxant and antiproliferative effects of berberine," *European Journal of Pharmacology*, vol. 399, no. 2-3, pp. 187–196, 2000.

[26] M. Akinyi, X. M. Gao, Y. H. Li et al., "Vascular relaxation induced by *Eucommiae Ulmoides Oliv*. and its compounds Oroxylin A and wogonin: implications on their cytoprotection action," *International Journal of Clinical and Experimental Medicine*, vol. 7, no. 10, pp. 3164–3180, 2014.

Hindawi Publishing Corporation
Evidence-Based Complementary and Alternative Medicine
Volume 2015, Article ID 584596, 9 pages
http://dx.doi.org/10.1155/2015/584596

Research Article

Effect of Compound Chuanxiong Capsule on Inflammatory Reaction and PI3K/Akt/NF-κB Signaling Pathway in Atherosclerosis

Qunfu Kang,[1] Weihong Liu,[1,2] Hongxu Liu,[1] and Mingxue Zhou[1,2]

[1]*Beijing Hospital of Traditional Chinese Medicine, Capital Medical University, Beijing 100010, China*
[2]*Beijing Institute of Traditional Chinese Medicine, Beijing 100010, China*

Correspondence should be addressed to Weihong Liu; wh.l-007@163.com and Mingxue Zhou; mingxue78@163.com

Received 1 April 2015; Revised 31 May 2015; Accepted 11 June 2015

Academic Editor: Zhang Tan

Compound Chuanxiong Capsule (CCC), a Chinese herbal compound, can exhibit antiatherosclerotic effect; however, its mechanism is still unclear. This study is designed to study the mechanism of CCC on atherosclerosis in the ApoE-knockout ($ApoE^{-/-}$) mice fed with a high-fat diet. After 6 weeks of high-fat feeding, 40 $ApoE^{-/-}$ mice were randomized ($n = 10$) and treated with lipitor, high-dose or low-dose CCC, or distilled water ($ApoE^{-/-}$ group) for 7 weeks. The blood lipids in serum and the plaque areas of the mice were measured and the mRNA expressions of phosphatidylinositol-3-kinases (PI3K), Akt, nuclear factor-kappa B (NF-κB), tumor necrosis factor-α (TNF-α), and interleukin-6 (IL-6) of the aortae were determined. The data showed that CCC can significantly decrease the levels of blood lipids, atherosclerosis index, and plaque areas and increase collagen proportion in plaques as compared with the untreated mice ($p < 0.05$, $p < 0.01$). In addition, CCC can significantly reduce the mRNA expressions of PI3K, Akt, NF-κB, IL-6, and TNF-α in the mice fed with a high-fat diet ($p < 0.001$). Thus, we concluded that CCC can inhibit inflammatory reaction in the $ApoE^{-/-}$ mice fed with a high-fat diet. This mechanism may be attributed to regulating PI3K/Akt/NF-κB signaling pathway.

1. Introduction

Atherosclerosis, a chronic inflammatory disease, plays a key role in the occurrence and development of the cardiovascular diseases, which has become as the most chronic cause of death worldwide [1]. The data from the report of Cardiovascular Disease in China 2013 showed that cardiovascular disease resulted in 41.1% deaths in the city and 38.7% in the rural areas [2]. Therefore, it is essential to prevent and treat atherosclerosis for the better prognosis of the patients with cardiovascular diseases.

In the inflammatory mechanism of initiating the occurrence of atherosclerosis, NF-κB plays one of the most important roles as multifunctional transcription regulators. Once activated, it exerts crucial effects on inflammatory reaction, immune reaction, cell proliferation, and apoptosis by regulating gene expressions of inflammatory cytokines and chemokines, such as IL-6 and TNF-α [3]. The expressions of NF-κB and its cascade genes can be regulated by PI3K/Akt signaling pathway, which plays a vital role in the process of cell proliferation, apoptosis, and inflammatory reaction [4, 5].

CCC, one of the typical Chinese herbal compounds with the potential of activating blood circulation, is composed of Chuanxiong (*Ligusticum*) and Danggui (*Angelica sinensis*). Zhao and Niu showed that CCC can decrease the level of blood lipids in the patients with coronary heart disease [6] and can reduce the risk of heart failure, for example, the frequency and severity, and improve clinical symptoms of cardiac insufficiency [7]. In rat atherosclerosis model, it was found that CCC could increase the coronary blood flow, inhibit platelet adhesion and aggregation, reduce blood viscosity, and improve the state of blood stasis in blood vessels [8].

The mechanism of action of CCC, in TCM, is attributed to the potential of Chuanxiong and Danggui in activating blood circulation. Chuanxiong and Danggui have been widely used

in the diseases with blood stasis syndrome [9]. It was reported that CCC can inhibit the aggregation of platelets and lower the viscosity of the blood [10]. However, the mechanism of action of CCC on atherosclerosis is still unclear.

Considering the role of PI3K/Akt/NF-κB signaling pathway and its downstream inflammatory cytokines in atherosclerosis, this study was designed to investigate the inflammatory mechanism of CCC on atherosclerosis in the ApoE-knockout (ApoE$^{-/-}$) mice fed with a high-fat diet by detecting the expressions of TNF-α, IL-6, PI3K, Akt, and NF-κB.

2. Materials and Methods

2.1. Animals and Treatment. Eight-week-old male ApoE$^{-/-}$ mice (n = 40, 18–20 g) on a C57BL/6J background and 10 C57BL mice introduced and bred by the Animal Unit of Peking University Health Science Center were used in the study. The housing and care of the animals and all the procedures were performed in accordance with the guidelines and regulations of the University of Bristol and the United Kingdom Home Office.

2.2. Ethics Statement. This study was approved by the Institutional Animal Care and Use Committee (IACUC) from Peking University Health Science Center.

2.3. Materials and Reagents. A TRIzol kit was purchased from Invitrogen Company (California, USA), PCR primers were synthesized by Sangon Biotech Co., Ltd. (Shanghai, China), and an M-MLV RT kit and a real-time (RT)-PCR kit were purchased from Takara Company (Otsu, Shiga, Japan). The blood lipid kits were purchased from Zhongsheng Beikong Biotechnology Co., Ltd. (Beijing, China) to measure total cholesterol (TC), triglycerides (TGs), low-density lipoprotein (LDL), and high-density lipoprotein (HDL-C). Van Gieson (VG) staining kit was purchased from MAIXIN-BIO (Fuzhou, China). CCC was purchased from Shandong Phoenix Pharmaceutical Co., Ltd., (Shandong, China; Batch number: Z20000035) and lipitor (atorvastatin) was purchased from Pfizer Pharmaceutical Co., Ltd. (Dalian, China; Batch number: H20051408).

2.4. Establishment of Atherosclerosis Model. All the ApoE$^{-/-}$ mice were fed with a high-fat diet containing 21% (wt/wt) fat from lard supplemented with 0.15% (wt/wt) cholesterol [11] and obtained from Beijing Ke'ao Xieli Feed Co. Ltd. (Beijing, China) for 13 weeks. Additionally, 10 C57BL mice fed a standard chow diet containing 4% fat were used as normal control group. All the mice were inspected at least once every 24 h.

2.5. Drug Treatment. After 6 weeks of high-fat diet, the ApoE$^{-/-}$ mice were randomized into ApoE$^{-/-}$ (n = 10), ApoE$^{-/-}$ + lipotor (n = 10), ApoE$^{-/-}$ + CCC low (n = 10), and ApoE$^{-/-}$ + CCC high (n = 10) and were treated with 2.973 mg/kg/d lipitor (positive-control drug) by intragastric administration, high dose of CCC (1333.48 mg/kg per day), low dose of CCC (333.37 mg/kg per day), or distilled water (control group) for an additional 7 weeks. The feeding of the mice in all the groups was accompanied by a high-fat diet. The choice of medical doses was based on the clinically relevant doses in humans (the conversion coefficient between human and mice is 9.01, and the medical doses in mice are 9.01 × the clinically medical doses in humans [12]). Distilled water was used to dilute the medicine. Distilled water consumption was monitored twice weekly, and drug concentration was adjusted as required.

2.6. Histology. All the mice in the five groups were euthanized with 0.1% pentobarbital sodium. The heart from each mouse was removed and the one-third of the apical heart, including the aortic sinus, was fixed in 10% formaldehyde, embedded, and sectioned to determine the morphology of any atherosclerotic plaque by hematoxylin and eosin (HE) and VG staining.

2.7. Evaluation of Atherosclerotic Lesions. To quantitatively evaluate atherosclerotic lesions, eight sections (5 μm-thick) per group were selected and the sections in the same segment were quantified according to Suzuki et al. [13]. Ten slides per group were examined for morphometric analysis. The average of the measured four sections per sample was recorded. The plaque morphology and the collagen content of atherosclerotic plaque were evaluated by HE and VG staining. A morphometric analysis was performed using Image Pro Plus (Media Cybernetics, Rockville, MD, USA). The plaque area was measured directly and was subtracted from the area enclosed by the internal elastic lamina to derive the patent lumen area [14], but the plaque area should be corrected by dividing the internal elastic lamina surrounding area.

2.8. Determination of Plasma Lipid Concentration. Blood samples were drawn from the left ventricle of a cohort of all male ApoE$^{-/-}$ mice that received a high-fat diet for 13 weeks. TC and TGs were determined by enzyme studies in serum. LDL-C and HDL-C levels were determined by immunoturbidimetry. Finally, all the indices were determined using the RX-2000 radiometer (Technicon Instruments Company, Tarrytown, NY, USA), and the atherosclerosis index (AI) was calculated using the formula [15]:

$$\text{AI} = \frac{\text{non-HDL-C}}{\text{HDL-C}}. \quad (1)$$

2.9. Real-Time Quantitative PCR. The aortic root from each mouse from all the groups was removed and stored in −80°C to examine the mRNA expressions of PI3K, Akt, NF-κB, IL-6, and TNF-α. The total RNA from aortae was extracted using TRIzol kit according to the manufacturer's instructions. The primers of PI3K, Akt, NF-κB, IL-6, and TNF-α are shown in Table 1. The protocol used for RT-PCR was similar to the previously described method [16]. The model of qPCR machine was ABI 7500 (America) and the program used was SDS 1.3 version. The data was analyzed by $2^{-\Delta\Delta CT}$ method,

Table 1

Genes	Forward	Reverse
GAPDH	5′-GCAAGTTCAACGGCACAG-3′	5′-CGCCAGTAGACTCCACGAC-3′
PI3K	5′-TCCAAATACCAGCAGGATCA-3′	5′-ATGCTTCGATAGCCGTTCTT-3′
Akt	5′-TACTCATTCCAGACCCACGA-3′	5′-GAGGTTCTCCAGCTTCAGGT-3′
NF-κB	5′-GGAGAAGGCTGGAGAAGATG-3′	5′-GCTCATACGGTTTCCCATTT-3′
IL-6	5′-GGACCAAGACCATCCAATTC-3′	5′-ACCACAGTGAGGAATGTCCA-3′
TNF-α	5′-CTAGCCAGGAGGGAGAACAG-3′	5′-GCTTTCTGTGCTCATGGTGT-3′

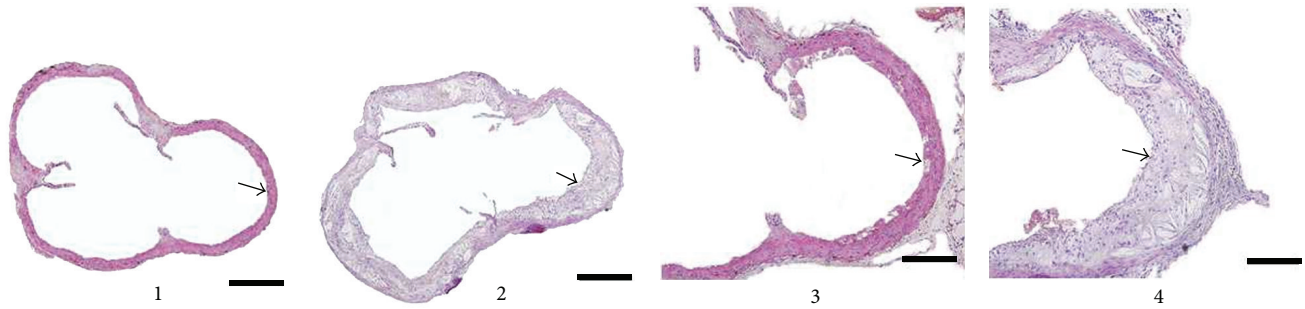

Figure 1: Comparison of pathological morphology of the aorta of the C57BL/6J mice and the ApoE$^{-/-}$ mice under different magnification at 13 weeks after being fed with different diets. (a) The pathological morphology of the aortae of the C57BL/6J and ApoE$^{-/-}$ mice under ×100 magnification at 13 weeks after being fed with different kinds of diets (scale bars = 500 μm). (b) The pathological morphology of the aortae of the C57BL/6J and ApoE$^{-/-}$ mice under ×200 magnification at 13 weeks after being fed with different kinds of diets (scale bars = 200 μm). Hematoxylin and eosin (HE) staining: the black arrow indicates the aorta of the mice.

and the internal reference gene used was glyceraldehyde 3-phosphate dehydrogenase (GAPDH).

2.10. Statistical Analysis. Mean values and standard deviations (mean ± S.D.) were calculated for each of the variables. All the statistical procedures were performed using Statistical Package for the Social Sciences (SPSS) 11.5. Normally distributed data was analyzed using one-way analysis of variance (ANOVA), while the statistical significance of intergroup differences in all the tested variables was evaluated using Bonferroni post hoc test. In all the cases, $p < 0.05$ was as statistically significant.

3. Results

3.1. High-Fat Diet Induced Atherosclerosis in ApoE$^{-/-}$ Mice Model. After the ApoE$^{-/-}$ mice were fed with high-fat diet for 13 weeks, the atherosclerotic plaques in the aortic valves attachment sites, including cholesterol crystal and foam cells, were observed in the aortic roots of the ApoE$^{-/-}$ mice, whereas no plaques were observed in the aortic roots of the C57 mice (Figure 1).

3.2. Effects of CCC on Blood Lipids. The results showed that, in comparison with the ApoE$^{-/-}$ group mice, the levels of TGs, TC, and LDL-C in serum of the ApoE$^{-/-}$ mice in the high-dose and low-dose CCC groups were significantly decreased ($p < 0.05$), but the level of HDL-C in serum was not significantly altered ($p > 0.05$) (Figures 2(a)–2(d)).

3.3. Effects of CCC on Atherosclerotic Index. The atherosclerotic indexes of mice in the ApoE$^{-/-}$ + lipitor group and the ApoE$^{-/-}$ + CCC low and ApoE$^{-/-}$ + CCC high groups were significantly decreased as compared with the ApoE$^{-/-}$ group mice ($p < 0.05$) (Figure 2(e)).

3.4. Effects of CCC on the Atherosclerotic Plaques and Its Compositions. The corrected areas of atherosclerotic plaque in the mice of the ApoE$^{-/-}$ + lipitor and the ApoE$^{-/-}$ + CCC low groups were significantly decreased ($p < 0.01$). Moreover, the area percentage of collagen in the atherosclerotic plaques of the mice in ApoE$^{-/-}$ + CCC high group was significantly increased ($p < 0.01$) as compared to the mice in ApoE$^{-/-}$ group, while the area percentage of extracellular lipid of the two ApoE$^{-/-}$ + CCC groups was decreased, but not significantly changed ($p > 0.05$) (Figure 3).

3.5. Effects of CCC on mRNA Expressions of IL-6 and TNF-α. As shown in Figure 4, the mRNA expression of IL-6 in mice in the ApoE$^{-/-}$ + CCC high group was more significantly decreased than in mice in the ApoE$^{-/-}$ group ($p < 0.0001$). Additionally, the mRNA expression of TNF-α in mice in the ApoE$^{-/-}$ + CCC low group was significantly decreased ($p < 0.0001$).

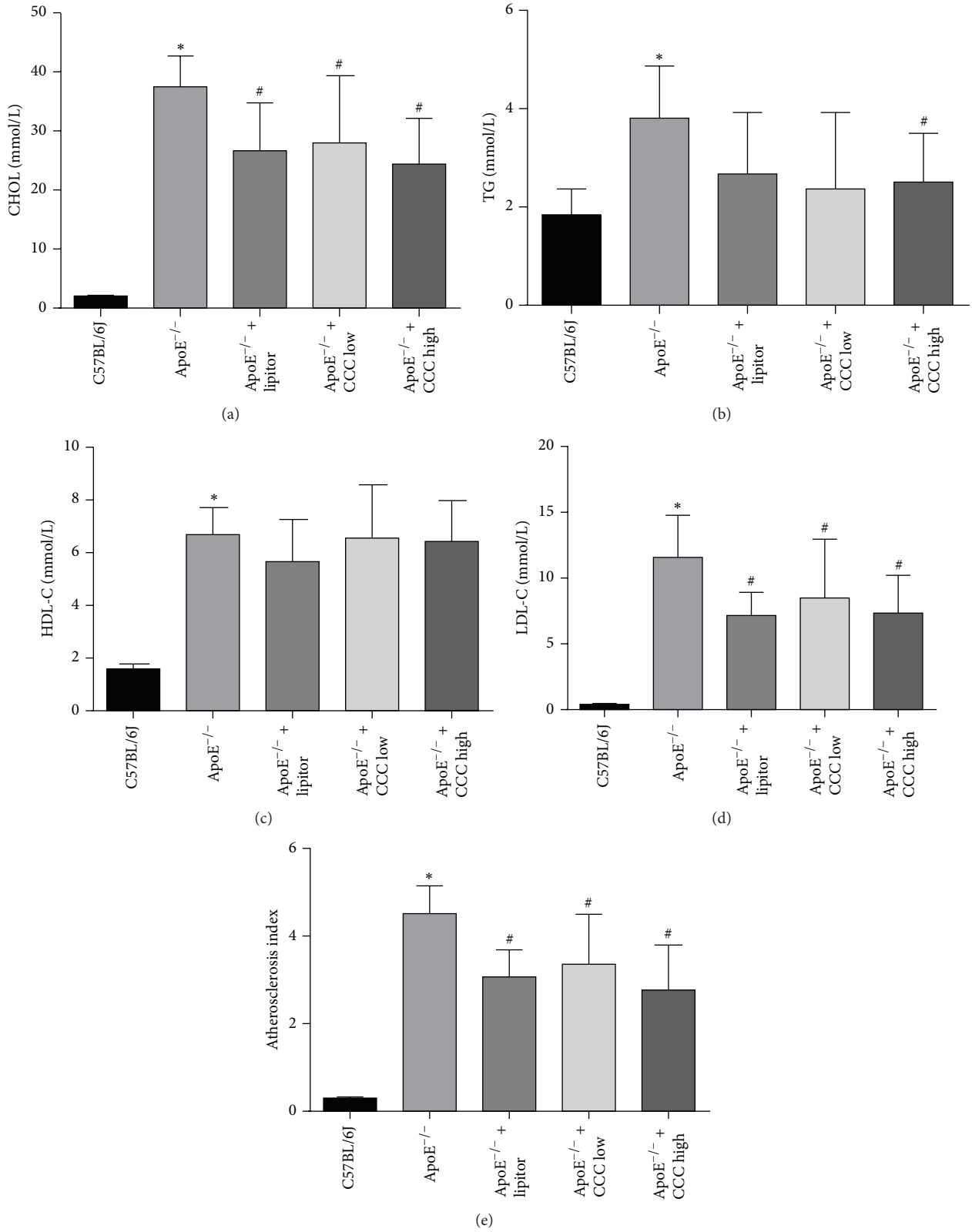

Figure 2: Effects of Compound Chuanxiong Capsule (CCC) on blood lipids in serum of ApoE$^{-/-}$ mice fed with high-fat diet. (a) Total cholesterol (CHOL). (b) Triglyceride (TG). (c) Low-density lipoprotein cholesterol (LDL-C). (d) High-density lipoprotein cholesterol (HDL-C). (e) Atherosclerotic index (AI, AI = non-HDL-C/HDL). $^{*}p < 0.05$ versus C57BL/6J group; $^{\#}p < 0.05$ versus ApoE$^{-/-}$ group (C57BL/6J: $n = 10$; ApoE$^{-/-}$: $n = 10$; ApoE$^{-/-}$ + lipitor: $n = 10$; ApoE$^{-/-}$ + CCC low: $n = 10$; ApoE$^{-/-}$ + CCC high: $n = 10$).

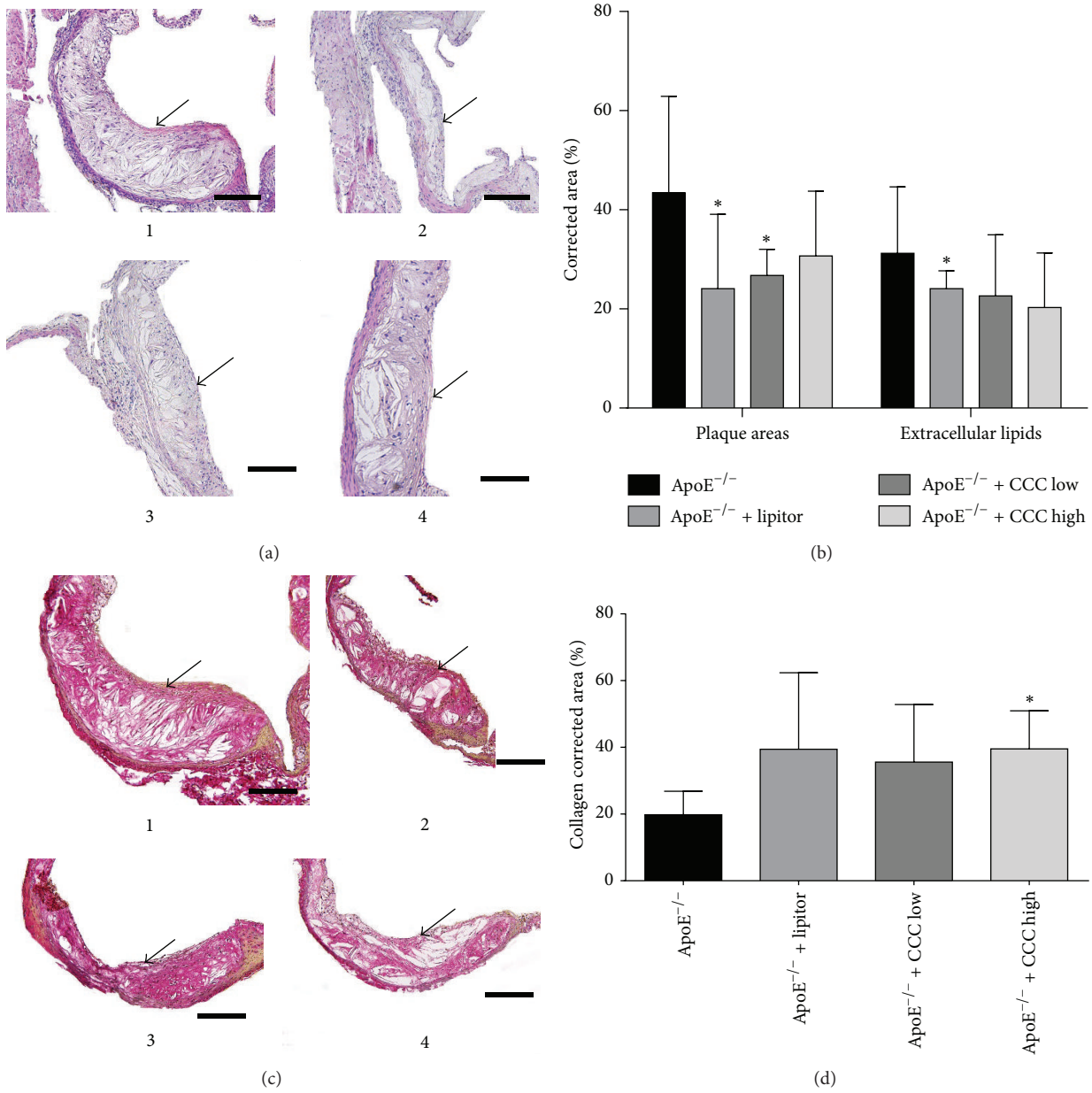

Figure 3: Effect of Compound Chuanxiong Capsule (CCC) on atherosclerotic plaque. (a) Hematoxylin and eosin (HE) staining showing the pathological morphology change of the atherosclerotic plaque in aorta of the ApoE$^{-/-}$ mice after the treatment of CCC. 1: ApoE$^{-/-}$ group; 2: ApoE$^{-/-}$ + lipitor group; 3: ApoE$^{-/-}$ + CCC low group; 4: ApoE$^{-/-}$ + CCC high group. Scale bars = 200 μm, and the black arrow indicates the atherosclerotic plaque in aorta. (b) The statistical analysis of the corrected area of atherosclerotic plaque and extracellular lipids content in plaque of the ApoE$^{-/-}$ mice after the treatment of CCC. $^{*}p < 0.01$ versus ApoE$^{-/-}$ group. (c) Van Gieson (VG) staining showing the pathological morphology change of content in atherosclerotic plaque in aorta of the ApoE$^{-/-}$ mice after the treatment of CCC. 1: ApoE$^{-/-}$ group; 2: ApoE$^{-/-}$ + lipitor group; 3: ApoE$^{-/-}$ + CCC low group; 4: ApoE$^{-/-}$ + CCC high group. Scale bars = 200 μm, and the black arrow indicates the collagen content in plaque. (d) The statistical analysis of the corrected area of collagen in atherosclerotic plaque of the ApoE$^{-/-}$ mice after the treatment of CCC. $^{*}p < 0.01$ versus ApoE$^{-/-}$ group (ApoE$^{-/-}$: $n = 10$; ApoE$^{-/-}$ + lipitor: $n = 10$; ApoE$^{-/-}$ + CCC low: $n = 10$; ApoE$^{-/-}$ + CCC high: $n = 10$).

3.6. Effects of CCC on mRNA Expressions of PI3K, Akt, and NF-κB. As shown in Figure 5, the mRNA expressions of PI3K, Akt, and NF-κB in mice in the ApoE$^{-/-}$ + CCC group were significantly decreased as compared to the mice in the ApoE$^{-/-}$ group ($p < 0.0001$), while the mRNA expressions of PI3K and Akt in mice in the ApoE$^{-/-}$ + CCC low were decreased, but not significantly changed ($p > 0.05$).

3.7. Effects of CCC on Protein Expressions of PI3K and p-Akt. As shown in Figure 6, the protein expression of PI3K in mice

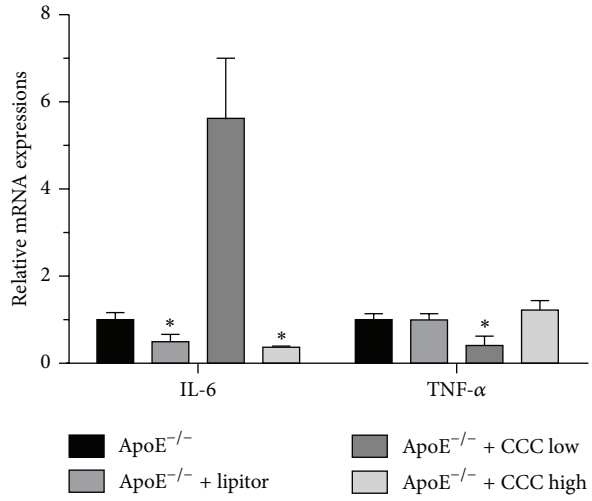

Figure 4: Effect of Compound Chuanxiong Capsule (CCC) on mRNA expressions of IL-6 and TNF-α in ApoE$^{-/-}$ mice fed with high-fat diet. $^{*}p < 0.001$ versus ApoE$^{-/-}$ group. mRNA indicates messenger RNA (ApoE$^{-/-}$: $n = 10$; ApoE$^{-/-}$ + lipitor: $n = 10$; ApoE$^{-/-}$ + CCC low: $n = 10$; ApoE$^{-/-}$ + CCC high: $n = 10$).

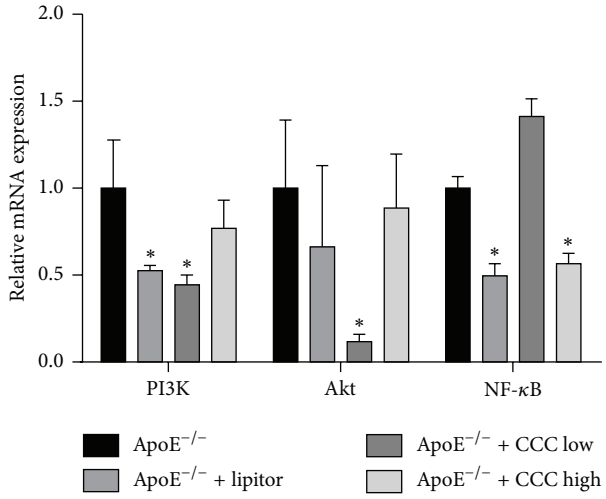

Figure 5: Effect of Compound Chuanxiong Capsule (CCC) on mRNA expressions of PI3K, Akt and NF-κB. $^{*}p < 0.001$ versus ApoE$^{-/-}$ group. mRNA indicates messenger RNA (ApoE$^{-/-}$: $n = 10$; ApoE$^{-/-}$ + lipitor: $n = 10$; ApoE$^{-/-}$ + CCC low: $n = 10$; ApoE$^{-/-}$ + CCC high: $n = 10$).

in the ApoE$^{-/-}$ + CCC low and high group was significantly decreased as compared to the mice in the ApoE$^{-/-}$ group ($p < 0.01$). The protein expression of p-Akt in the ApoE$^{-/-}$ + CCC low group was decreased, but not significantly changed, as compared to the mice in the ApoE$^{-/-}$ group ($p > 0.05$).

4. Discussion

In this study, we have demonstrated that CCC can dramatically ameliorate atherosclerosis in the ApoE$^{-/-}$ mice fed with high-fat diet by improving the blood lipid levels and reducing the plaque areas, which is consistent with the results of the previous studies [7, 10, 17]. In addition, we showed that CCC may inhibit the expression of IL-6 and TNF-α by regulating PI3K/Akt/NF-κB signaling pathway in transcriptional level, which may be the main mechanism of CCC exerting the antiatherosclerotic effect.

CCC is one of the typical Chinese herbal compounds, which has been widely used in clinical practices at the physiological relevance dosage of 4T and Tid (666.7 mg/kg per day). It was shown that CCC, at the dosage of 666.7 mg/kg per day, could decrease the blood lipids and C-reactive protein significantly [18] and improves the symptoms of cardiac insufficiency [7, 19]. In this study, the results showed that CCC inhibited atherosclerosis by regulating PI3K/Akt/NF-κB signaling pathway. The potential active ingredients of CCC, we supposed, might be ligustrazine, the main active ingredient of Chuanxiong, and ferulic acid, the main active ingredients of both Chuanxiong and Danggui. Previous studies showed that ligustrazine exhibited protective effects by reducing the levels of TNF-α [20] and ox-LDL [21] and others Ferulic acid could significantly decrease TC and the ratio of apo B to apo A and prevent the formation of aortic fatty plaques [22]. However, Xu et al. [23] reported that the contents of ligustrazine in the mixture of Chuanxiong and Danggui were higher than it in the Chuanxiong alone, while Danggui was devoid of ligustrazine. Thus, the inhibitory effect of CCC on atherosclerosis may not be contributed to the individual pharmacological effect of Chuanxiong or Danggui, but the overall effect of CCC, which was consistent with the holistic concept of TCM.

In the present study, the data showed that CCC can significantly decrease the blood lipid, especially TC and LDL-C, in the mice. CCC is composed of Chuanxiong (*Ligusticum*) and Danggui (*Angelica sinensis*); thus its action was attributed to the effects of ligustrazine, the main ingredients of Chuanxiong, or ferulic acid, the main ingredient of both Chuanxiong and Danggui, since the data from the previous studies showed that ligustrazine and ferulic acid can decrease blood lipids and produce a tangible protection in atherosclerosis.

The extracellular lipids and collagen in atherosclerotic plaque were responsible for its stability of atherosclerotic plaque. The data showed that CCC can decrease the percentage of extracellular lipids and increase the percentage of collagen in atherosclerotic plaque. This finding was suggestive that CCC may have the potential effect of promoting the stability of atherosclerotic plaque.

Atherosclerosis has been considered as a chronic inflammatory disease since 1999 [24] and inflammatory factors play an important role in its occurrence and development of atherosclerosis [25–27]. IL-6, an intense inflammatory cytokine, plays a critical role in cardiovascular disease [28], and it can activate endothelial cells and regulate the extracellular lipids [29]. Moreover, IL-6 can induce the synthesis of matrix metalloproteinases and regulate their function to make the atherosclerotic plaques vulnerable [30, 31]. TNF-α is a vital cytokine involved in the progress of atherosclerosis [32]. Kivirikko et al. showed that TNF-α can inhibit the expression of P4H, which promotes the formation of collagen

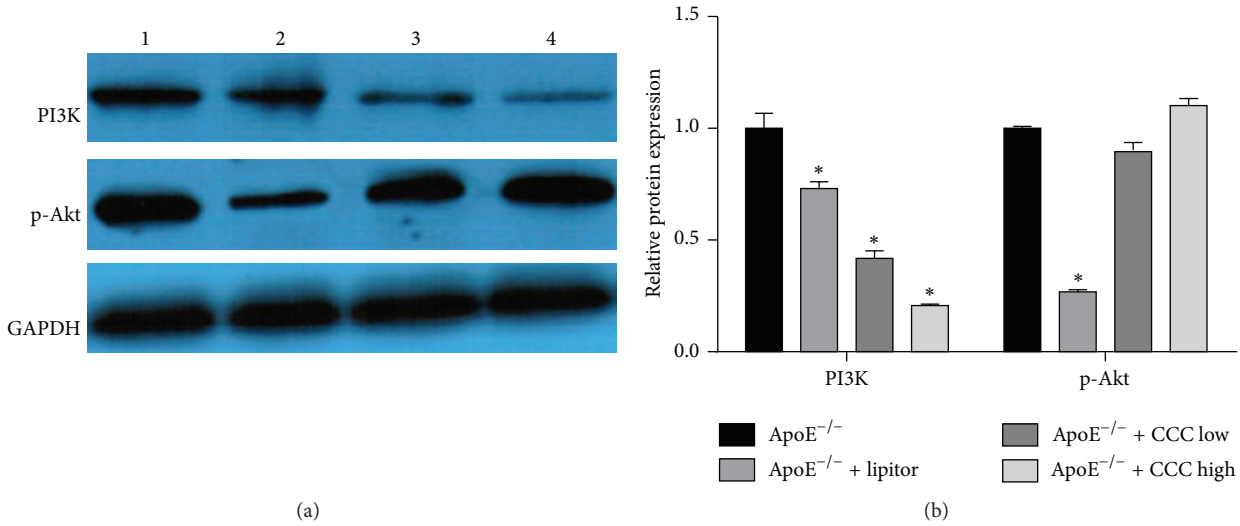

Figure 6: Effect of of Compound Chuanxiong Capsule (CCC) on protein expressions of PI3K and p-Akt. (a) Western blotting (WB) results of PI3K and p-Akt levels in mouse aorta. (b) Quantitative analysis (column diagram) of PI3K and p-Akt levels in mouse aorta based on WB results. $^{*}p < 0.05$ versus ApoE$^{-/-}$ group (ApoE$^{-/-}$: $n = 6$; ApoE$^{-/-}$ + lipitor: $n = 6$; ApoE$^{-/-}$ + CCC low: $n = 6$; ApoE$^{-/-}$ + CCC high: $n = 6$).

that makes the atherosclerotic plaques vulnerable [33, 34], and it can inhibit the endothelial cells' function, induce lipid deposition, and promote the generation of inflammatory cytokines to aggravate atherosclerosis [25, 35]. In this study, the data showed that CCC can inhibit the mRNA expression of IL-6 and TNF-α in the aorta in the ApoE$^{-/-}$ mice fed with high-fat diet. Based on the effects of IL-6 and TNF-α in inflammatory reaction and atherosclerosis, the role of CCC in preventing atherosclerosis may be related to inhibiting the inflammation reaction.

NF-κB is one of the crucial multifunctional transcription regulators. Once activated, it exerts effects on inflammatory reaction, immune reaction, cell proliferation, and apoptosis by regulating the gene expressions of inflammatory cytokines, and chemokines, such as IL-6 and TNF-α [3]. Kuang and Wang reported that, in ApoE$^{-/-}$ atherosclerosis mice model fed with high-fat diet, the level of NF-κB was significantly increased and exhibited a positive correlation with inflammation [36], and the results in our study showed that the expression of NF-κB was significantly decreased in the ApoE$^{-/-}$ + lipitor group and ApoE$^{-/-}$ + CCC high group as compared with the model group. In addition, several studies showed that both IL-6 and TNF-α were under the influence of NF-κB [37–39] and, in turn, IL-6 and TNF-α could promote the activation of NF-κB to result in an inflammatory response [40–42]. In this study, our results showed that CCC can inhibit the expressions of NF-κB in the aorta in mice fed with high-fat diet. These findings suggest that CCC may inhibit inflammatory reaction in atherosclerosis by regulating the expression of NF-κB.

PI3K signaling pathway and its main downstream effector protein kinase B (PKB/Akt) participate in glucose metabolism, differentiation, proliferation, apoptosis, and migration of cells and inflammatory response, and NF-κB is one-key transcription factors in regulating inflammation [43]. PI3K/Akt signaling pathway can enable the NF-κB transcription factors to increase the activity of inflammatory medium gene, which results in the generation of many cytokines. Luo et al. reported that the activation of PI3K/Akt signaling pathway could decrease the levels of reactive oxygen species and lipid deposits that can restrain the formation of plaques to reverse the progress of atherosclerosis [44]. However, it is well known that the activation of PI3K/Akt signaling pathway could induce the aggregation of inflammatory cells to promote the inflammation and accelerate the development of atherosclerosis [45, 46]. Therefore, the inhibitory effect on the PI3K/Akt signaling pathway can inhibit the expression of NF-κB to ameliorate the progress of atherosclerosis [47–49]. Our results showed that both the high-dose and low-dose CCC can inhibit the mRNA expressions of PI3K and Akt, and high-dose CCC can significantly inhibit the mRNA expression of NF-κB in aortae of the ApoE$^{-/-}$ mice fed with high-fat diet. Thus, CCC may suppress the mRNA expression of IL-6 and TNF-α by regulating PI3K/Akt/NF-κB signaling pathway in transcriptional level. The results also showed that CCC can significantly inhibit the protein expression of PI3K, but not significantly inhibit the protein expression of p-Akt in aortae of the ApoE$^{-/-}$ mice fed with high-fat diet. The possible explanation is that the dose of CCC did not exert the corresponding effect. Therefore, further investigation is required to explain the possible mechanism of CCC on PI3K/Akt/NF-κB signaling pathway more explicitly.

5. Conclusion

The results from the study showed that CCC can dramatically ameliorate atherosclerosis in the ApoE$^{-/-}$ mice fed with high-fat diet. The possible mechanism was attributed to the inhibition of the expression of IL-6 and TNF-α by regulating PI3K/Akt/NF-κB signaling pathway. Therefore, it is necessary

to further investigate the potential effect and mechanism of CCC preventing the occurrence of atherosclerosis.

Conflict of Interests

The authors declare that there is no conflict of interests regarding the publication of this paper.

Acknowledgments

This work was supported by Grants from the National Natural Science Foundation of China (no. 81303086), Beijing Natural Science Foundation (no. 7133233), Beijing Nova Program (no. Z131107000413026), and Beijing Health System-High Level Health Technology Talent Cultivation Plan (2014-3-100).

References

[1] M. Lehrke and C. Lebherz, "AAV-mediated gene therapy for atherosclerosis," *Current Atherosclerosis Reports*, vol. 16, no. 9, p. 434, 2014.

[2] W.-W. Chen, R.-L. Gao, L.-S. Liu et al., "China cardiovascular summary report 2013," *Chinese Circulation Journal*, vol. 7, pp. 487–491, 2014.

[3] M. S. Hayden and S. Ghosh, "Shared principles in NF-κB signaling," *Cell*, vol. 132, no. 3, pp. 344–362, 2008.

[4] S. Liu, H. Shen, M. Xu et al., "FRP inhibits ox-LDL-induced endothelial cell apoptosis through an Akt-NF-κB-Bcl-2 pathway and inhibits endothelial cell apoptosis in an apoE-knockout mouse model," *The American Journal of Physiology—Endocrinology and Metabolism*, vol. 299, no. 3, pp. E351–E363, 2010.

[5] J. Sun and S.-Q. Huang, "The effect of NF-κB signaling pathway in the formation of atherosclerosis," *Modern Journal of Integrated of Traditional Chinese and Western Medicine*, vol. 16, no. 15, pp. 2158–2162, 2007.

[6] Z.-B. Zhao and Y.-Y. Niu, "The effect of compound Chuanxiong capsules on the blood lipids of CHD patients," *Medical Aesthetics and Cosmetology*, no. 2, p. 222, 2015.

[7] H. Li, "Compound Chuanxiong Capsule treating coronary heart disease in 50 cases with mild heart failure," *Shanxi Journal of Traditional Chinese Medicine*, vol. 34, no. 6, pp. 647–648, 2013.

[8] Y. Huo, T.-M. Yao, Z. Liang, J. Li, Y. You, and Y.-L. Han, "Effects of Guanxin Shutong capsule on lipid metabolism and hemorrheology in rat model with experimental atherosclerosis," *Journal of Liaoning University of Traditional Chinese Medicine*, vol. 13, no. 11, pp. 248–250, 2013.

[9] S.-F. Huang, R.-Y. Hou, S.-S. Gao, and T.-F. Du, "Study about the frequency of the Chinese medicine used in coronary heart disease," *Traditional Chinese Drug Research & Clinical Pharmacology*, vol. 20, no. 4, pp. 395–396, 2009.

[10] S.-B. Sun, Z. Lei, H.-J. Jiang, K. Fang, and F. Chen, "The research of active blood of compound Chuanxiong capsules," *Herald of Medicine*, vol. 28, no. 2, pp. 189–190, 2009.

[11] J. Johnson, K. Carson, H. Williams et al., "Plaque rupture after short periods of fat feeding in the apolipoprotein E-knockout mouse: model characterization and effects of pravastatin treatment," *Circulation*, vol. 111, no. 11, pp. 1422–1430, 2005.

[12] M.-X. Zhou, H. Xu, L. Pan, J.-Y. Wen, W.-Q. Liao, and K.-J. Chen, "Rosiglitazone promotes atherosclerotic plaque stability in fat-fed ApoE-knockout mice," *European Journal of Pharmacology*, vol. 590, no. 1–3, pp. 297–302, 2008.

[13] H. Suzuki, Y. Kurihara, M. Takeya et al., "A role for macrophage scavenger receptors in atherosclerosis and susceptibility to infection," *Nature*, vol. 386, no. 6622, pp. 292–296, 1997.

[14] J. L. Johnson, R. Fritsche-Danielson, M. Behrendt et al., "Effect of broad-spectrum matrix metalloproteinase inhibition on atherosclerotic plaque stability," *Cardiovascular Research*, vol. 71, no. 3, pp. 586–595, 2006.

[15] S.-K. Yan, "Several important calculated parameters of blood lipids and its clinical significance," in *Proceedings of the 4th National Symposium about Lipid Analysis and 9th National Clinical Lipoprotein Conference Papers Series*, vol. 4, 2008.

[16] S.-L. Qi, Y.-F. Wang, M. X. Zhou et al., "A mitochondria-localized glutamic acid-rich protein (MGARP/OSAP) is highly expressed in retina that exhibits a large area of intrinsic disorder," *Molecular Biology Reports*, vol. 38, no. 5, pp. 2869–2877, 2011.

[17] D.-Z. Shi, X.-C. Ma, and X.-A. Gao, "The overview of blood circulation herbs on the prevention of atherosclerosis," *Journal of Traditional Chinese Medicine*, vol. 36, no. 7, pp. 433–435, 1995.

[18] Y. Hu, "Clinical observation of compound Chuanxiong capsule in the treatment of carotid atherosclerotic vertigo," *Practical Clinical Journal of Integrated Traditional Chinese and Western Medicine*, vol. 11, no. 1, pp. 8–23, 2011.

[19] Q.-T. Feng and X.-J. Qian, "The curative effect of compound Chuanxiong combined with bisoprolol treatment of right heart function insufficiency observation," *Modern Diagnosis and Treatment*, no. 18, pp. 4174–4175, 2014.

[20] H.-J. Wu, J. Hao, S.-Q. Wang, B.-L. Jin, and X.-B. Chen, "Protective effects of ligustrazine on TNF-α-induced endothelial dysfunction," *European Journal of Pharmacology*, vol. 674, no. 2-3, pp. 365–369, 2012.

[21] G.-F. Wang, C.-G. Shi, M.-Z. Sun et al., "Tetramethylpyrazine attenuates atherosclerosis development and protects endothelial cells from ox-LDL," *Cardiovascular Drugs and Therapy*, vol. 27, no. 3, pp. 199–210, 2013.

[22] E. Y. Kwon, G. M. Do, Y. Y. Cho, Y. B. Park, S. M. Jeon, and M. S. Choi, "Anti-atherogenic property of ferulic acid in apolipoprotein E-deficient mice fed Western diet: comparison with clofibrate," *Food and Chemical Toxicology*, vol. 48, no. 8-9, pp. 2298–2303, 2010.

[23] C.-J. Xu, Y. Kong, G.-Y. Zheng, and J.-Z. Shentu, "Content of tetramethylpyrazine in the decoction of Chuanxiong rhizome and that of Chuanxiong rhizome together with Chinese angelica root," *Herald of Medicine*, vol. 26, no. 10, pp. 1207–1211, 2007.

[24] R. Ross, "Atherosclerosis—an inflammatory disease," *The New England Journal of Medicine*, vol. 340, no. 2, pp. 115–126, 1999.

[25] R. Kleemann, S. Zadelaar, and T. Kooistra, "Cytokines and atherosclerosis: a comprehensive review of studies in mice," *Cardiovascular Research*, vol. 79, no. 3, pp. 360–376, 2008.

[26] E. L. Gautier, T. Huby, J. L. Witztum et al., "Macrophage apoptosis exerts divergent effects on atherogenesis as a function of lesion stage," *Circulation*, vol. 119, no. 13, pp. 1795–1804, 2009.

[27] P. Libby, P. M. Ridker, and A. Maseri, "Inflammation and atherosclerosis," *Circulation*, vol. 105, no. 9, pp. 1135–1143, 2002.

[28] P. Libby, "Role of inflammation in atherosclerosis associated with rheumatoidarthritis," *The American Journal of Medicine*, vol. 121, supplement 1, pp. S21–S31, 2008.

[29] M. Hibi, K. Nakajima, and T. Hirano, "IL-6 cytokine family and signal transduction: a model of the cytokine system," *Journal of Molecular Medicine*, vol. 74, no. 1, pp. 1–12, 1996.

[30] K. P. Sundararaj, D. J. Samuvel, Y. Li, J. J. Sanders, M. F. Lopes-Virella, and Y. Huang, "Interleukin-6 released from fibroblasts is essential for up-regulation of matrix metalloproteinase-1 expression by U937 macrophages in coculture: cross-talking between fibroblasts and U937 macrophages exposed to high glucose," *The Journal of Biological Chemistry*, vol. 284, no. 20, pp. 13714–13724, 2009.

[31] L. R. Luckett and R. M. Gallucci, "Interleukin-6 (IL-6) modulates migration and matrix metalloproteinase function in dermal fibroblasts from IL-6KO mice," *British Journal of Dermatology*, vol. 156, no. 6, pp. 1163–1171, 2007.

[32] A. Ozeren, M. Aydin, M. Tokac et al., "Levels of serum IL-1β, IL-2, IL-8 and tumor necrosis factor-α in patients with unstable angina pectoris," *Mediators of Inflammation*, vol. 12, no. 6, pp. 361–365, 2003.

[33] K. I. Kivirikko, T. Helaakoski, K. Tasanen et al., "Molecular biology of prolyl 4-hydroxylase," *Annals of the New York Academy of Sciences*, vol. 580, pp. 132–142, 1990.

[34] R. Nissi, H. Autio-Harmainen, P. Marttila, R. Sormunen, and K. I. Kivirikko, "Prolyl 4-hydroxylase isoenzymes I and II have different expression patterns in several human tissues," *The Journal of Histochemistry and Cytochemistry*, vol. 49, no. 9, pp. 1143–1153, 2001.

[35] H. Zhang, Y. Park, J. Wu et al., "Role of TNF-α in vascular dysfunction," *Clinical Science*, vol. 116, no. 3, pp. 219–230, 2009.

[36] J. Kuang and W. Wang, "Effects of nuciferine on vascular inflammation and matrix metalloproteinases in mouse with atherosclerosis," *Journal of Clinical Cardiology*, vol. 35, no. 1, pp. 97–100, 2015.

[37] A. R. Brasier, "The nuclear factor-kappaB-interleukin-6 signalling pathway mediating vascular inflammation," *Cardiovascular Research*, vol. 86, no. 2, pp. 211–218, 2010.

[38] S. Fujioka, J. Niu, C. Schmidt et al., "NF-κB and AP-1 connection: Mechanism of NF-κB-dependent regulation of AP-1 activity," *Molecular and Cellular Biology*, vol. 24, no. 17, pp. 7806–7819, 2004.

[39] Y.-H. Son, Y.-T. Jeong, K.-A. Lee et al., "Roles of MAPK and NF-κB in interleukin-6 induction by lipopolysaccharide in vascular smooth muscle cells," *Journal of Cardiovascular Pharmacology*, vol. 51, no. 1, pp. 71–77, 2008.

[40] F. Chen and X. Shi, "NF-κB, a pivotal transcription factor in silica-induced diseases," *Molecular and Cellular Biochemistry*, vol. 234-235, pp. 169–176, 2002.

[41] P. Storz and A. Toker, "NF-kappaB signaling: an alternate pathway for oxidative stress responses," *Cell Cycle*, vol. 2, no. 1, pp. 9–10, 2003.

[42] K. E. de Visser, A. Eichten, and L. M. Coussens, "Paradoxical roles of the immune system during cancer development," *Nature Reviews Cancer*, vol. 6, no. 1, pp. 24–37, 2006.

[43] Y. Hattori, S. Hattori, and K. Kasai, "Lipopolysaccharide activates Akt in vascular smooth muscle cells resulting in induction of inducible nitric oxide synthase through nuclear factor-kappa B activation," *European Journal of Pharmacology*, vol. 481, no. 2-3, pp. 153–158, 2003.

[44] Y. Luo, G.-B. Sun, M. Wang et al., "Isorhamnetin inhibit macrophage apoptosis induced atherosclerosis by activating PI3K/AKT and induce the production of HO-1," in *Proceedings of the 1st Session of the Conference of Chinese Medicine Information*, vol. 8, 2014.

[45] T. J. Cremer, P. Shah, E. Cormet-Boyaka, M. A. Valvano, J. P. Butchar, and S. Tridandapani, "Akt-mediated proinflammatory response of mononuclear phagocytes infected with *Burkholderia cenocepacia* occurs by a novel GSK3β-dependent, IκB kinase-independent mechanism," *The Journal of Immunology*, vol. 187, no. 2, pp. 635–643, 2011.

[46] F. Morello, A. Perino, and E. Hirsch, "Phosphoinositide 3-kinase signalling in the vascular system," *Cardiovascular Research*, vol. 82, no. 2, pp. 261–271, 2009.

[47] P. M. Mourani, P. J. Garl, J. M. Wenzlau, T. C. Carpenter, K. R. Stenmark, and M. C. M. Weiser-Evans, "Unique, highly proliferative growth phenotype expressed by embryonic and neointimal smooth muscle cells is driven by constitutive Akt, mTOR, and p70S6K signaling and is actively repressed by PTEN," *Circulation*, vol. 109, no. 10, pp. 1299–1306, 2004.

[48] J. E. Sousa, M. A. Costa, A. Abizaid et al., "Lack of neointimal proliferation after implantation of sirolimus-coated stents in human coronary arteries: a quantitative coronary angiography and three-dimensional intravascular ultrasound study," *Circulation*, vol. 103, no. 2, pp. 192–195, 2001.

[49] M. Poon, J. J. Badimon, and V. Fuster, "Overcoming restenosis with sirolimus: from alphabet soup to clinical reality," *The Lancet*, vol. 359, no. 9306, pp. 619–622, 2002.

Hindawi Publishing Corporation
Evidence-Based Complementary and Alternative Medicine
Volume 2015, Article ID 574169, 12 pages
http://dx.doi.org/10.1155/2015/574169

Research Article

Tang-Tong-Fang Confers Protection against Experimental Diabetic Peripheral Neuropathy by Reducing Inflammation

Mingdi Li, Da Huang, Xiaoxing Liu, and Lan Lin

Guang'anmen Hospital, Chinese Academy of Chinese Medical Sciences, Beijing 100053, China

Correspondence should be addressed to Mingdi Li; mdlee2009@126.com and Lan Lin; linlan05@163.com

Received 5 May 2015; Revised 19 July 2015; Accepted 4 August 2015

Academic Editor: Dan Hu

Tang-tong-fang (TTF) is a Chinese herbal formula that has been shown to be beneficial in diabetic peripheral neuropathy (DPN), a common complication secondary to diabetic microvascular injury. However, the underlying mechanism of protection in nerve ischemia provided by TTF is still unclear. We hypothesized that TTF alleviates DPN via inhibition of ICAM-1 expression. Therefore, we tested the effect of TTF in a previously established DPN model, in which nerve injury was induced by ischemia/reperfusion in streptozotocin-induced diabetic rats. We found that the conduction velocity and amplitude of action potentials of sciatic nerve conduction were reduced in the DPN model group but were rescued by TTF treatment. In addition, TTF treatment also attenuated the effect of DPN on other parameters including histology and ultrastructural changes, expression of ICAM-1, MPO, and TNF-α in rat sciatic nerves, and plasma sICAM-1 and MPO levels. Together, our data suggest that TTF treatment may alleviate DPN via ICAM-1 inhibition.

1. Introduction

Diabetes mellitus is one of the most morbid diseases worldwide and, according to projections by the World Health Organization, the adult diabetic population is expected to grow by 170% between 1995 and 2025 [1]. Diabetic peripheral neuropathy (DPN) is the most common complication of diabetes, affecting almost half of patients with diabetes [2]. A myriad of therapeutic modalities, including several currently in clinical trials, have been used to treat DPN with limited efficacy. The only known prevention strategy for DPN remains tight glucose control [3].

Diabetic medical experts have recently turned their attention towards complementary and alternative medicine as possible avenues to identify new therapeutic strategies for diabetic complications [4]. Specifically, it has been reported that traditional Chinese medicine or natural medicine has had some success in the treatment of DPN. Existing studies focus on nerve repair and regeneration, Schwann cell survival signaling pathways, neurotrophic factor, free radicals, NF-κB, TNF-α, and IL-1 [4–9]. However, though previous studies suggest that plasma cell adhesion molecules (CAMs) play an important role in the development and progression of peripheral neuropathy in diabetes mellitus, the role of adhesion factor in nerve microvasculature during the development of neuropathy has not been explored.

Cross-sectional studies have shown plasma cell adhesion molecules to be increased in patients with diabetic complications [10]. Plasma CAM expression may even predict the development of diabetic neuropathy. Specifically, intercellular adhesion molecule-1 (ICAM-1) is an important CAM produced by vascular endothelial cells, which mediates the interaction of polymorphonuclear neutrophils (PMN) with vascular endothelial cells and may serve as an independent factor in the pathogenesis and progression of DPN [10]. ICAM-1 has an important role in the regulation of neutrophil adhesion to the endothelium and capillary wall permeability [11]. Under normal conditions, the expression of ICAM-1 is low or absent. However, recent studies have shown that the expression of ICAM-1 in the nerve tissue microvasculature of ischemia-reperfusion DPN model rats is increased and aggravates axonal degeneration [12]. A previous study has

demonstrated that the circulating levels of ICAM-1 are elevated in DPN rats [13]. Blocking intracellular adhesion molecule-1 (ICAM-1) prevents leukostasis and retinal vascular leakage [14].

Tang-tong-fang (TTF) is a Chinese herbal formula developed by Professor Lin from Guang'anmen Hospital. The main ingredients of TTF consist of *Astragalus*, *Ligusticum wallichii*, Ramulus Cinnamomi, Radix Paeoniae Alba, *Eupolyphaga*, *Curcuma*, and Asiasarum. In traditional Chinese medicine, this formula has been used to improve circulation. Clinically, TTF has been shown to be effective in the treatment of DPN [15]. Past clinical trials have confirmed that TTF can increase nerve conduction velocity and ameliorate lower extremity sensory changes [15]. However, no research exists exploring the mechanism of the therapeutic benefit provided by TTF.

We, therefore, hypothesized that TTF may improve DPN-related nerve injury through the inhibition of ICAM-1 expression. We examined nerve conduction velocity of DPN rats as well as histopathology and ultrastructural changes of sciatic nerve tissue. In order to further characterize the mechanism of TTF in improving DPN, we also measured the expression of ICAM-1, myeloperoxidase (MPO), and TNF-α in sciatic nerve tissue, as well as plasma levels of ICAM-1 and MPO.

2. Materials and Methods

2.1. Animals. One hundred and ten male Sprague-Dawley (SD) rats (body weight = 180 ± 10 g) (Beijing HFK bioscience Co. Ltd., license number: SYXK (E) 2009-0007, Beijing, China) were randomly divided into a control and a diabetic model group. Controls (n = 18) were injected with citrate buffer alone. In the model group (n = 92), diabetes was induced by intraperitoneal injection of STZ in 0.1 mol/L citrate buffer at pH 4.2 (20 mg/mL; dose 60 mg/kg). Successful induction of diabetes was confirmed when fasting blood glucose exceeded 16.7 mmol/L three days after injection of STZ and remained >16.7 mmol/L throughout the study. All of the following experiments conformed to the Guiding Principles for the Care and Use of Laboratory Animals issued by the National Committee of Science and Technology of China.

2.2. Drugs and Solutions. TTF was provided by the Guang'anmen Hospital. The medicine was boiled, vacuum-packaged, preserved under 4°C, and diluted before use, according to standard protocols.

2.3. Creation of the DPN Model. The DPN model was established by inducing ischemia-reperfusion (IR) in diabetic animals as previously described [16, 17]. After a four-week induction period, the STZ-diabetic rats were anesthetized with intraperitoneal pentobarbital. Ischemia was produced by occlusion of the abdominal aorta, right common iliac, and femoral artery with artery clips, which were removed after three hours. Sixty-seven rats were included in the final study, as twenty-five rats were excluded either for death during surgery (n = 18) or due to an insufficient increase in fasting blood glucose (<16.7 mmol/L) (n = 7).

2.4. Animal Groups and Treatment. The sixty-seven IR rats were initially divided into four groups: model (n = 18), low-dose TTF (n = 16), medium-dose TTF (n = 17), and high-dose TTF (n = 16). Respectively, the three TTF groups were dosed with TTF 3.5 times (5.15 g/kg/d), 7 times (10.30 g/kg/d), or 14 times (20.60 g/kg/d) for eight weeks. The control group and model groups were treated with distilled water (10 mL/kg/day) for eight weeks.

2.5. Plasma Biochemical Parameters Measurement. Plasma soluble ICAM-1 (sICAM-1) was measured by the STAT FAX 2100 automatic enzyme immunoassay instrument (Awareness Technology Inc., USA) using rat sICAM-1/CD54 ELISA Kit (R&D Systems Inc., USA). Plasma MPO was measured by UV-2000 UV Spectrophotometry (Unico Instrument Co. Ltd., China) using a commercially available MPO Kit (Nanjing Jiancheng Bioengineering Institute, China).

2.6. Electrophysiology. The conduction velocity (CV) and amplitude of nerve action potentials (NAP) were measured by the BL-420F biological function experimental system (ChengDu Technology & Market Co. Ltd., China) using stimulating and recording electrodes. After anesthesia with intraperitoneal pentobarbital, the right sciatic nerves were exposed by blunt dissection. The nerve was stimulated proximally and the electric signal recorded from the distal digital nerve. The CV of tails were measured in a similar manner with single needle stimulating electrodes inserted into the proximal tail and recording electrodes inserted distally. The time (T) and distance (S) between the stimulating electrodes and recording electrodes were used to calculate CV using the equation CV = S/T.

2.7. Neuropathology. Following electrophysiological testing, the right sciatic nerves were excised and portions fixed with 3% glutaraldehyde for one week, followed by 1% osmium tetroxide fixation for 1.5 hours and dehydration in a stepwise manner with 50%–100% alcohol, soaked in epoxy resin and acetone mixture for two hours, embedded in epoxy resin, and then cut into semithin sections (1–3 μm) and ultrathin sections (50–70 nm) by an EM UC7 ultrathin slicing machine (Leica Ltd., Germany). The semithin sections were stained with 1% toluidine blue and observed with a DM-3000 biological microscope (Leica Ltd., Germany) under 200x magnification. The ultrathin sections were stained with uranium-lead staining and observed with a JEM-1400 transmission electron microscope (JEOL Ltd., Japan) under 8000x magnification.

2.8. Immunohistochemistry. Portions of right sciatic nerve were also fixed by 10% formalin phosphate buffer, dehydrated by alcohol, infiltrated and embedded in liquid paraffin, and cut into paraffin sections by a RM2255 rotary slicing machine (Leica Ltd., Germany). The following reagents were used: ICAM-1 antibody (Santa Cruz, USA), anti-TNF alpha antibody (Abcam, Britain), and ultrasensitive two-step immunohistochemical detection reagent (OriGene-Your Gene Company, China). Paraffin sections were dewaxed,

incubated in 3% H_2O_2 deionized water for ten minutes, repaired by microwave antigen, incubated in ICAM-1/Anti-TNF alpha antibody overnight at 4°C and ultrasensitive two-step immunohistochemical detection reagent for twenty minutes at room temperature, stained with diaminobenzidine (DAB), and then examined by microscope with 200x magnification. The integral optical densities (IOD) were measured using Image-Pro Plus 6.0 software.

2.9. Western Blot Analysis. Portions of the right sciatic nerves were also immediately harvested for Western blot analyses. The following reagents were used: ICAM-1 antibody (1 : 300, Santa Cruz, USA), MPO heavy chain antibody (1 : 300, Santa Cruz, USA), Beta actin antibody (1 : 1000 OriGene-Your Gene Company, China), goat anti-mouse IgG (H + L), HRP (1 : 10000 Jackson ImmunoResearch Laboratories Inc.), BCA Protein Assay Kit (CW Biotech, China), and PVDF membrane (Merck Millipore, China). Western blot analyses were performed using standard methods. Briefly, the tissues were homogenized by RIPA buffer, and extracted proteins were separated by 10% SDS-PAGE and transferred onto PVDF membranes, which were then incubated with the indicated antibodies overnight at 4°C. The membranes were further incubated with horseradish peroxidase-conjugated goat anti-mouse IgG for one hour at room temperature. Bands were visualized by chemiluminescence.

2.10. Real-Time PCR Detection. Total RNA was extracted from fresh-frozen neural tissue using an Ultrapure RNA Kit (CWbio Co. Ltd., China) and then reverse-transcribed with a HiFi-MMLV cDNA Kit (CWbio Co. Ltd., China). Real time PCR was performed on a Bioer line gene PCR instrument (BIOER, China) using Invitrogen primers. The PCR amplification procedure includes 95°C for 10 min, followed by 45 cycles of 95°C for 15 s and 59°C for 60 s. Data were normalized to Beta actin.

2.11. Statistical Analysis. Statistics were performed using SPSS 18.0. Significant differences between means were calculated by one-way analysis of variance (ANOVA), followed by multiple comparisons with least significant difference (LSD) test (equal variances) or Dunnett T3 test (unequal variances). Statistical significance was defined by $p < 0.05$.

3. Results

3.1. Effects of TTF on the Nerve Conduction Velocity of DPN Rats. In order to determine the potential therapeutic effect of TTF on DPN, we first measured the effect of TTF on the nerve conduction velocity of DPN rats. Compared with the control (N) group, the sciatic nerve conduction velocity, action potential (AP) amplitude, and tail nerve conduction velocity were significantly reduced in the non-TTF diabetic model (M) group (N versus M; sciatic nerve conduction velocity (m/s): 48.12 ± 6.9 versus 23.47 ± 4.43; AP amplitude: 10.97 ± 2.33 versus 6.11 ± 0.88; tail nerve conduction velocity: 30.03 ± 3.63 versus 15.89 ± 2.67; n = 16–18, $p < 0.01$). Treatment with TTF at different doses was found to increase the sciatic nerve conduction velocity, AP amplitude, and tail nerve conduction velocity compared with those detected in the control group (n = 15-16, $p < 0.01$) (Figure 1).

3.2. Sciatic Light Microscopy Structure. Since TTF treatment improves the nerve conduction velocity in DPN rats, we next hypothesized that TTF may protect the structure of nerve tissue against diabetic and ischemic insults. As shown in Figure 2, electron microscopy confirmed edematous and ischemic nerve myelin, atrophied and misshapen axons, and thrombus formation in capillaries in the DPN model group. Conversely, signs of clinical improvement in the TTF group were manifested by an observable decrease in abnormal nerve fibers.

3.3. Sciatic Nerve Ultrastructure. Ultrastructural studies demonstrated edema in control sciatic nerves, as well as swelling and disruption of the myelin sheath, axonal atrophy, and reduction in cellular organelles. These observations are consistent with the observations obtained from light microscope. After TTF treatment, pathological changes were reduced in comparison to the control group, including mitigation of edema and injury to myelin sheath and axons (Figure 3).

3.4. Effect of TTF on Expression Level of sICAM-1 and MPO in Plasma of DPN Rats. It was reported that sICAM-1 play an important role in the pathogenesis and progression of DPN [10]; whereas MPO is associated with various types of inflammation, its role in DPN has not been elucidated yet. Therefore, we measured the effect of TTF on expression levels of sICAM-1 and MPO in plasma of DPN rats. Compared with the control group, the levels of sICAM-1 and MPO in the model group were significantly increased ($p < 0.01$). After treatment with TTF, sICAM-1 and MPO levels in the TTF groups were reduced significantly compared with those in the model group ($p < 0.01$) in a dose-dependent manner ($p < 0.05$) (Figure 4).

3.5. Immunohistochemical Staining. ICAM-1 and TNF-α have been demonstrated to play a major role in the nerve inflammation associated with DPN [10, 18]. Therefore, we measured the expression of ICAM-1 and TNF-α in sciatic nerves using immunohistochemical staining. Compared with the control group, the expression levels of ICAM-1 and TNF-α in sciatic nerves from the diabetic model group were significantly increased ($p < 0.05$). After treatment with different doses of TTF, expression levels of ICAM-1 and TNF-α in sciatic nerve was decreased significantly in the TTF groups compared with those in the model group ($p < 0.05$), with a demonstrated dose-dependent change ($p < 0.05$) (Figure 5).

3.6. Sciatic rtPCR Test. To confirm the observations obtained from immunohistochemical staining experiment. We further measured the mRNA expression of ICAM-1. Compared with the control group, the expression level of ICAM-1 mRNA in sciatic nerve in the model group was significantly increased ($p < 0.01$). After treatment with different doses of TTF,

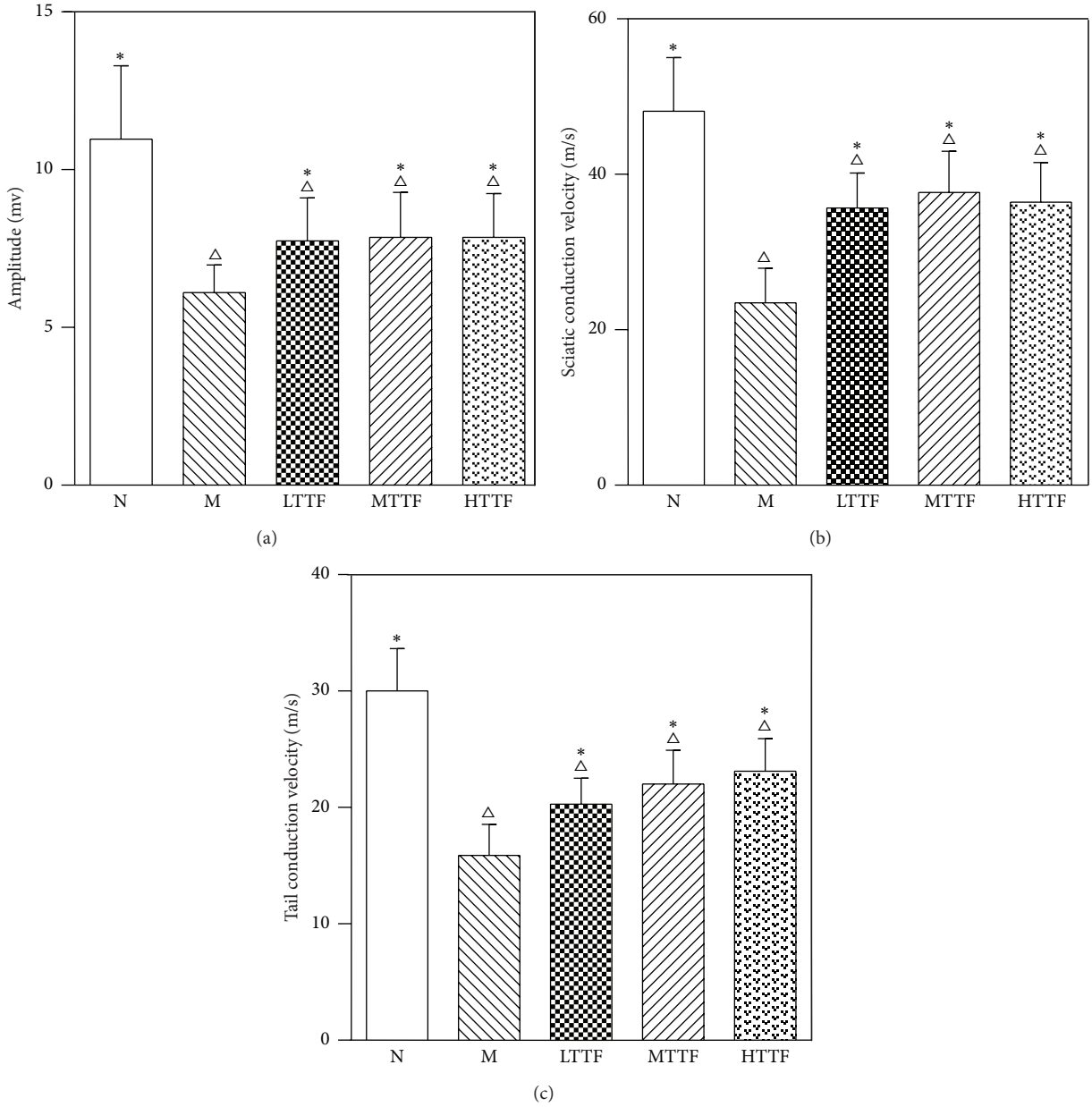

Figure 1: Action potential amplitude (a), sciatic nerve conduction velocity (b), and tail nerve conduction velocity (c) in N (control, $n = 18$), M (model, $n = 16$), LTTF (low-dose TTF, $n = 16$), MTTF (medium-dose TTF, $n = 15$), and HTTF (high-dose TTF, $n = 15$) groups ($^{\triangle}p < 0.05$ versus the control group and $^{*}p < 0.05$ versus the model group).

expression levels of ICAM-1 mRNA in sciatic nerve were significantly decreased in the TTF groups compared with the model group ($p < 0.01$) (Figure 6).

3.7. Western Blot of Sciatic Nerve. We further measured the protein expression of ICAM-1 and MPO in sciatic nerve to confirm the data obtained from previous experiments. Compared with the control group, expression levels of ICAM-1 and MPO in sciatic nerve from the diabetic model group were significantly increased ($n = 5$, $p < 0.01$). After treatment with different doses of TTF, the expression levels of ICAM-1 and MPO in sciatic nerve were significantly reduced in the TTF groups compared with the control group ($n = 5$, $p < 0.01$) (Figure 7).

4. Discussion

Diabetic peripheral neuropathy is characterized by symmetric sensory and motor dysfunction of peripheral nerves in distal extremities. DPN is one of the most serious comorbidities of diabetes and leads to significant morbidity and mortality due to sequelae such as ulceration, gangrene,

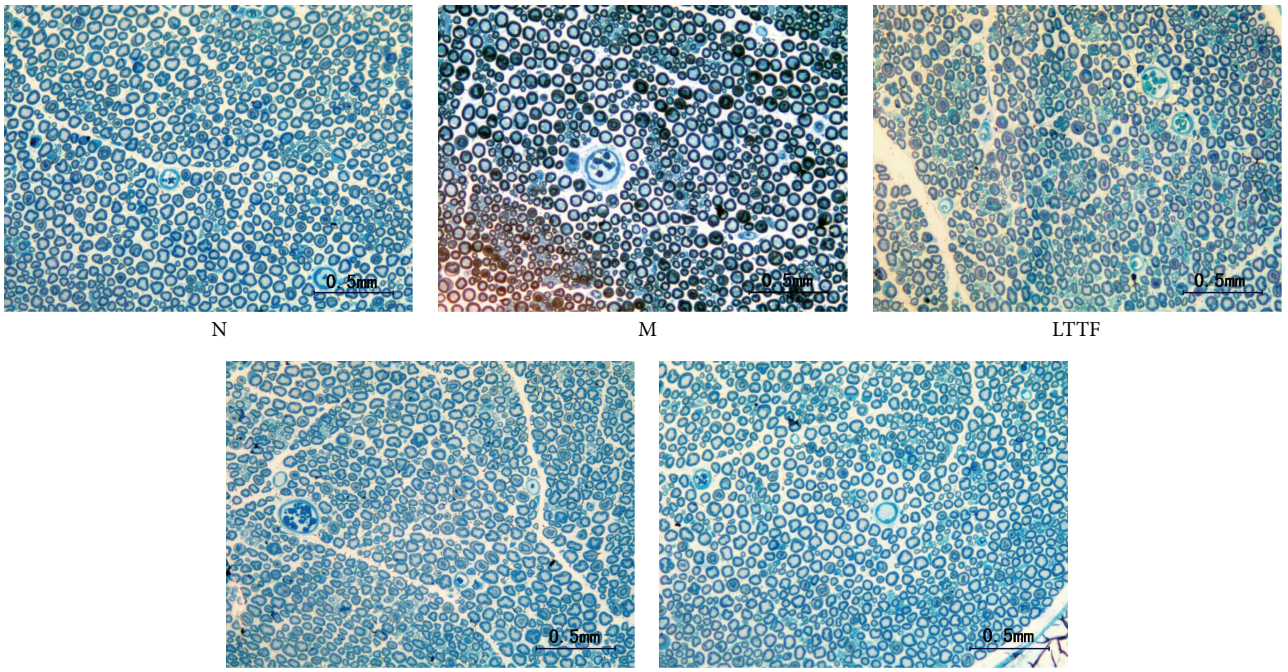

Figure 2: Sciatic light microscopy structure: semithin sections stained with toluidine blue. Control group (N): sciatic nerve fibers with full axons and even staining of myelin sheath. Model group (M): atrophied and misshapen axons with darkened and edematous myelin sheath. Low-dose TTF group (LTTF). Medium-dose TTF group (MTTF). High-dose TTF group (HTTF).

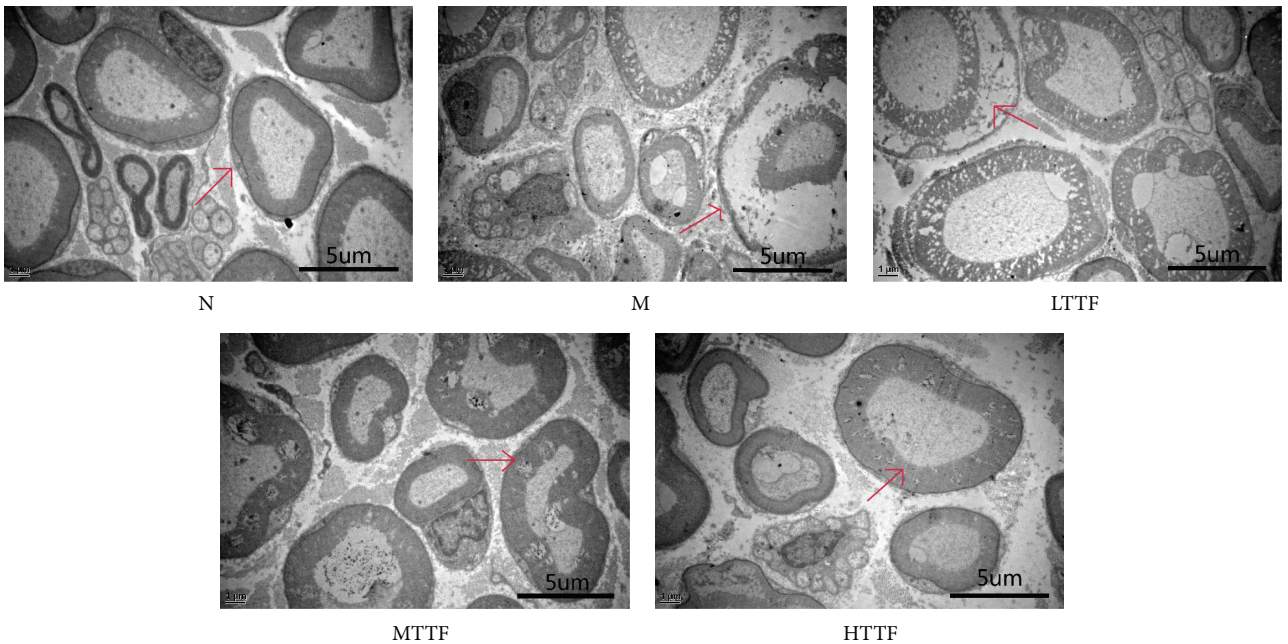

Figure 3: Sciatic nerve ultrastructure (uranium-lead staining). Control group (N): sciatic nerve with intact myelin sheaths, healthy axons with prolific cell organelles. Model group (M): the sciatic nerve with disrupted, tortuous myelin sheaths, axonal atrophy, and attenuation in cell organelles. LTTF: low-dose TTF group. MTTF: medium-dose TTF group. HTTH: high-dose TTF group.

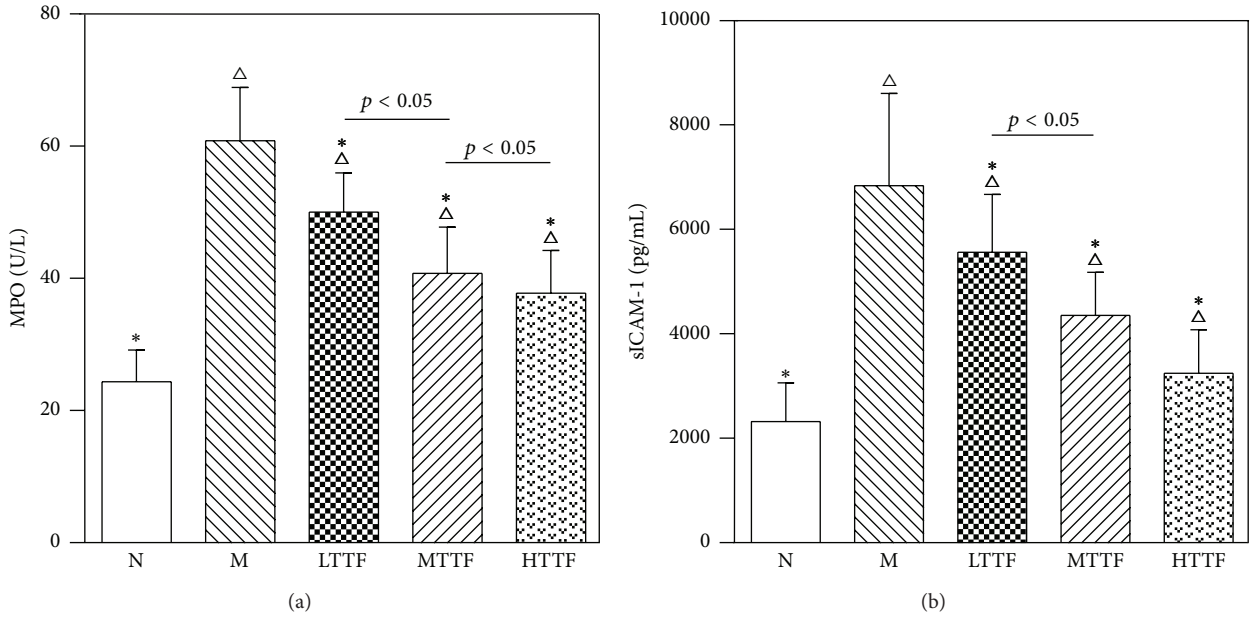

Figure 4: Expression level of MPO (a) and sICAM-1 (b) in plasma from N (control, $n = 17$), M (model, $n = 15$), LTTF (low-dose TTF, $n = 16$), MTTF (medium-dose TTF, $n = 12$), and HTTF (high-dose TTF, $n = 15$) groups ($^{\triangle}p < 0.05$ versus the control group, $^{*}p < 0.05$ versus the model group).

and even limb loss. Diagnosis involves careful history and physical examination, as well as adjunctive studies including nerve conduction velocity and EMG examination [19].

The pathogenesis of DPN is multifactorial and is yet to be fully elucidated, though it is considered to be secondary to both hyperglycemia-induced pathologic changes intrinsic to neurons and ischemia-induced neuronal damage through decreased neurovascular blood flow [20, 21]. It is currently believed that this microvascular dysfunction is due to the reduction in nerve blood flow by alterations in vasoregulation of nerve microvessels and increased blood viscosity caused by hyperglycemia. Additionally, changes in the endothelium itself have been shown to involve AGE-RAGE-NF-κB, cell adhesion molecules, nitric oxide, and peanut acid analogs [22].

Within the first week of development of diabetes, nerve blood flow is reduced by approximately 50% and hyperglycemia affects both sensory and sympathetic neuronal axons and cell bodies [23, 24]. Increased blood viscosity, increased platelet aggregation, and decreased red blood cell deformability together lead to decreased blood flow and tissue hypoxia [25]. Because of the vascular involvement, diabetic neuropathy is, therefore, considered a microvascular disease. Current diabetic animal models simulate human diabetic neuropathy in terms of nerve conduction velocities, blood flow, and biochemical abnormalities but tend to have less severe microangiopathy. Therefore, we induced diabetic neuropathy in our DPN model rats by combining two well-established models of both diabetes and of ischemia-reperfusion [12].

Our results showed that the sciatic and tail nerve conduction velocity and sciatic nerve action potential amplitude of the DPN rats were significantly slower than those of normal rats ($p < 0.01$). However, following treatment with increasing doses of TTF, tail nerve conduction velocity of the DPN model rats increased in a dose-dependent manner. Interestingly, the improvement in sciatic nerve conduction velocity and action potential amplitude was most efficacious in the medium-dose group; however, the reason for this remains unclear and requires further investigation.

Diabetes and hyperglycemia also lead to increased expression of E-selectin, VCAM-1, and ICAM-1 by endothelial cells [26–28]. Intercellular adhesion molecule- (ICAM-) 1 is an immunoglobulin- (Ig-) like cell adhesion molecule expressed by several cell types including leukocytes and endothelial cells. ICAM-1 plays an important role in both innate and adaptive immune responses. It is involved in the transendothelial migration of leukocytes to sites of inflammation, as well as interactions between antigen presenting cells (APC) and T cells during immunological synapse formation. Increased ICAM-1 expression in the endothelial cell surface attracts monocytes, neutrophils, and T lymphocytes and endothelial cells, resulting in direct endothelial cell injury by proteases and oxygen free radical release [29]. Previous studies have found that blocking ICAM-1 can prevent leukocytosis as well as retinal vascular leakage [14].

Tumor necrosis factor-α (TNF-α) is a 25 kD molecular weight membrane protein mainly produced by macrophages and monocytes. The expression of circulating TNF-α is elevated in both streptozotocin-induced diabetic rats as well

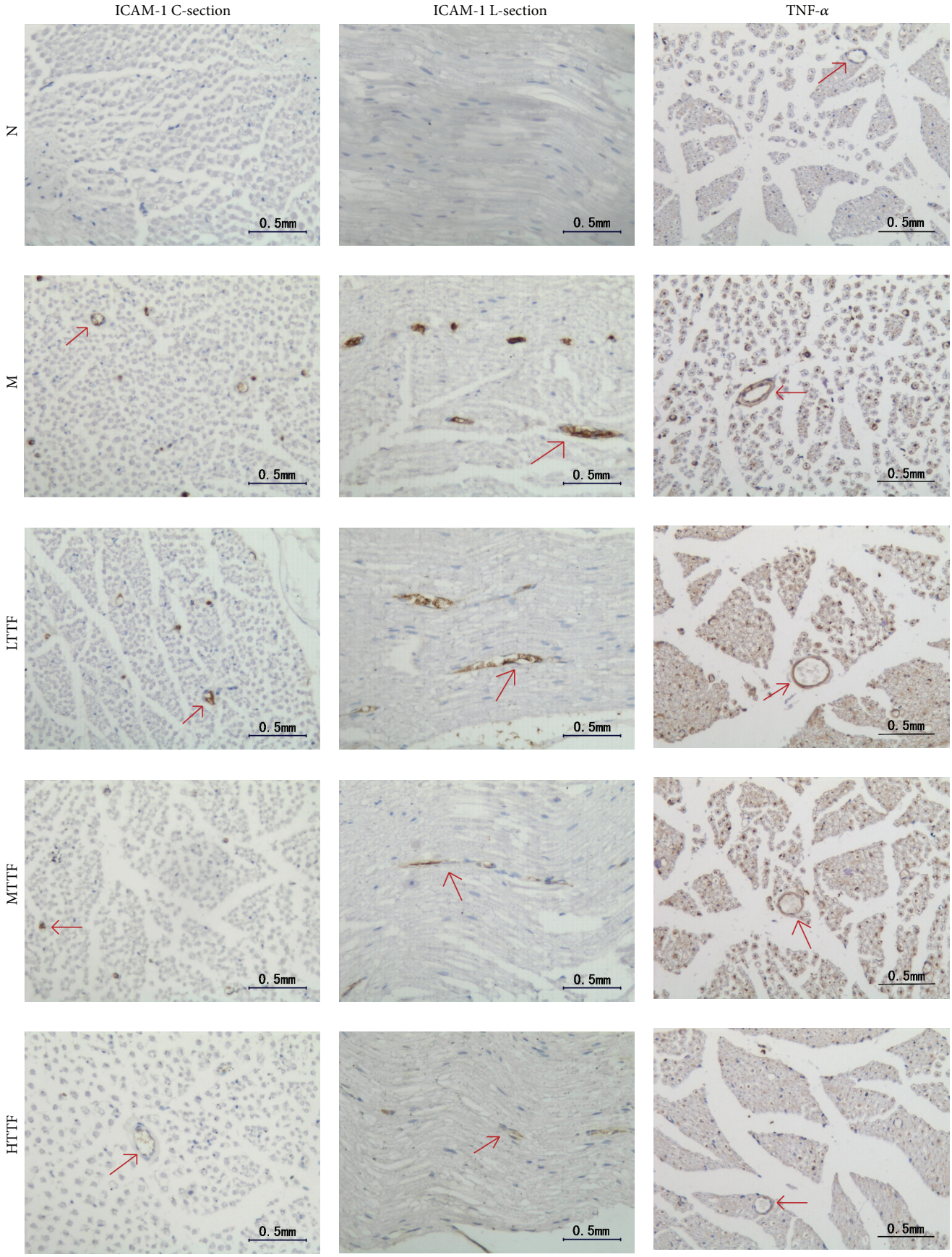

(a)

Figure 5: Continued.

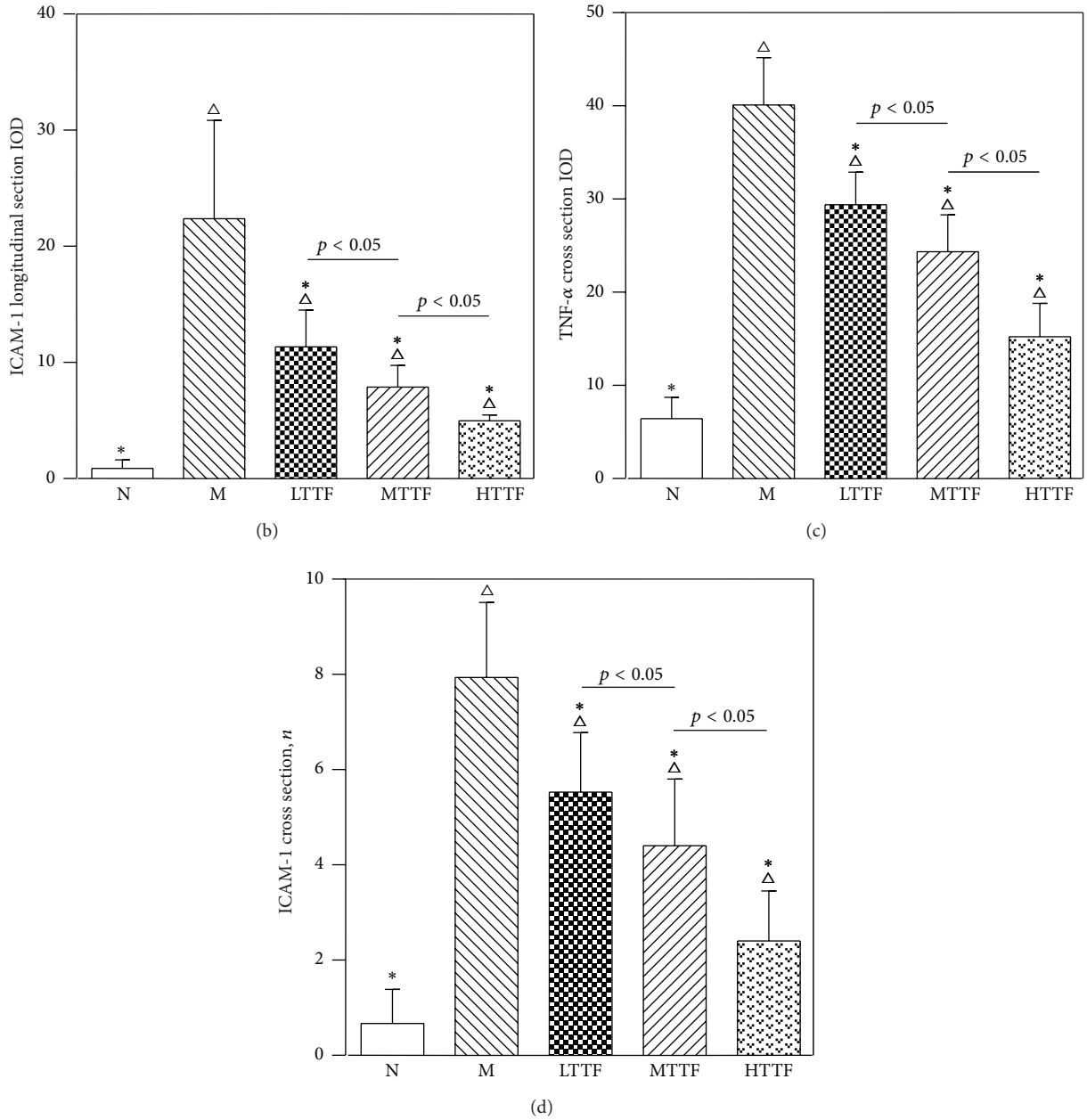

Figure 5: Immunohistochemical staining of ICAM-1/TNF-α in sciatic nerve. (a) Paraffin sections stained with ICAM-1/anti-TNF-α antibody. (b) The integral optical densities (IOD) of ICAM-1 staining in longitudinal section ($n = 15$ for each group). (c) The integral optical densities (IOD) of the TNF-α staining in cross section ($n = 15$ for each group). (d) The number of stained vessels by ICAM-1 in cross section ($n = 15$ for each group) ($^{\triangle}p < 0.05$ versus the control group, $^{*}p < 0.05$ versus the model group).

as diabetic patients [30]. Due to this association, this cytokine has potential to be a biomarker for DPN [31, 32]. Treatment of streptozotocin-induced diabetic rats with high-dose aspirin, the cyclooxygenase-2 inhibitor meloxicam, or etanercept, a competitive inhibitor of TNF-α, prevents increased ICAM-1 expression, leukostasis, capillary leakage, and upregulation of eNOS [14].

Myeloperoxidase (MPO), a neutrophil-specific reductase, is most abundantly expressed in the azurophilic granules of polymorphonuclear neutrophils (PMN). Analysis of MPO activity of nerve tissue may, therefore, reflect the extent of PMN extravasation from the microvasculature [33, 34]. Our results show that, compared with normal rats, ICAM-1 and TNF-α expression in sciatic nerve are significantly higher in DPN model rats. Additionally, increased MPO expression reflects the extent of PMN extravasation, and, indirectly, an increase in absolute number of neutrophils. This suggests that

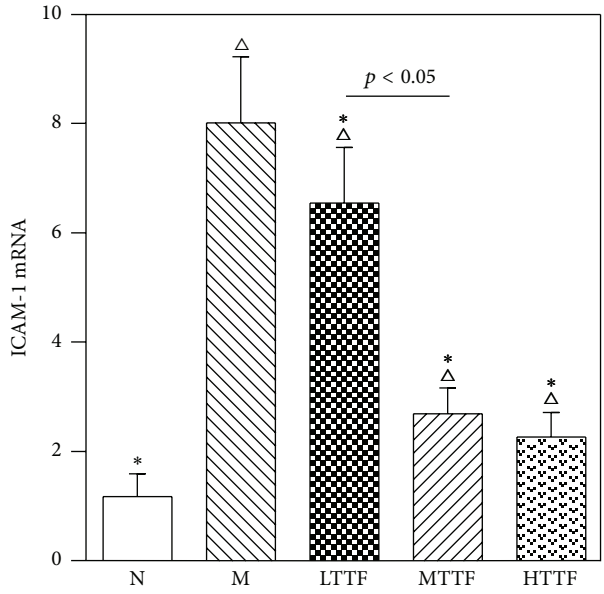

Figure 6: Real time PCR test of sciatic nerve from N (control, $n = 5$), M (diabetic, $n = 5$), LTTF (low-dose TTF, $n = 5$), MTTF (medium-dose TTF, $n = 5$), and HTTF (high-dose TTF, $n = 5$) groups ($^{\triangle}p < 0.05$ versus the control group, $^{*}p < 0.05$ versus the model group).

there is a series of inflammatory reactions *in vivo* caused by ischemia in the ischemia-reperfusion DPN model rats.

We also found that the plasma ICAM-1 and MPO expression levels in the DPN model rats are significantly higher than the control group ($p < 0.01$), further confirming the existence of ICAM-1-mediated inflammatory reaction *in vivo* of the DPN model rats. TTF treatment causes a significant dose-dependent decrease in both ICAM-1 expression and MPO and TNF-α expression ($p < 0.01$). These data show that the TTF can inhibit the plasma level of TNF-α and ICAM-1, thereby reducing the extent of the polymorphonuclear neutrophils tissue invasion from the microvasculature.

Previous studies have found that there are three major histopathological changes that affect the peripheral nerves in diabetic patients. First, thickening and proliferation of the endoneurium capillary wall and the stratum basale occur [35, 36]; second, capillary density and area decrease and become obstructed [35–37]; third, fiber loss is multifocal, suggesting an ischemic etiology [38, 39]. Of importance, similar histopathological changes were also present in the DPN model established in this study. Our results also showed sciatic capillary wall thickening, occlusion, and thrombosis in DPN model rats. Additionally, we observed that sciatic nerve fiber density decreased significantly, accompanied with uneven distribution, endoneurial edema, and axonal atrophy and deformity due to myelin extrusion. After TTF therapy, the occluded capillaries gradually returned to normal, and the number of abnormal nerve fibers and edema of the endoneurium decreased significantly.

Modern pharmacological studies have shown that the major components in TTF have significant antiplatelet aggregation and anti-inflammatory effects. For example, the total saponins of *Astragalus* (ASTs), the active constituent of *Astragalus*, can reduce whole blood viscosity and plasma viscosity, shorten erythrocyte electrophoresis time and erythrocytic specific volume [40], and have significant antithrombotic effects [41]. *Astragalus* extract also has a significant protective effect on vascular endothelial injury by reducing the content of ICAM-1 and propylene glycol (MDA) and increasing superoxide dismutase (SOD) content. This protective effect is attributed to inhibition of inflammatory cell infiltration, reduction of inflammation, and scavenging oxygen free radicals [42, 43]. Ligustrazine (LTZ), the active constituent of *Ligusticum wallichii*, and total glucosides of *Paeonia* (TGP) both inhibit platelet aggregation and also improve hemorheology [44]. Radix Paeoniae Alba extract can inhibit the division of pUC18 DNA induced by phenol, clear peroxide, and hydroxyl radicals [45]. Curcumin, the effective constituent of *Curcuma*, can inhibit platelet aggregation and has a protective effect on ischemia-reperfusion injury [46]. *Eupolyphaga* can effectively reduce blood viscosity and fibrinogen and inhibit thrombosis and platelet aggregation. Finally, *Eupolyphaga* water extract has an effect on antioxidation, serves as an anti-free radical, and protects vascular endothelial cells [47–49].

5. Conclusions

In the present study, we demonstrated that TTF treatment reduces the expression of ICAM-1, TNF-α, and MPO in the nerve tissue, which in turn reduces the blood viscosity and alleviates nerve ischemia, thereby improving peripheral nerve conduction velocity. In order to further understand the mechanism underlying the protective effect of TTF on DPN, future study is required to examine the effect of TTF on

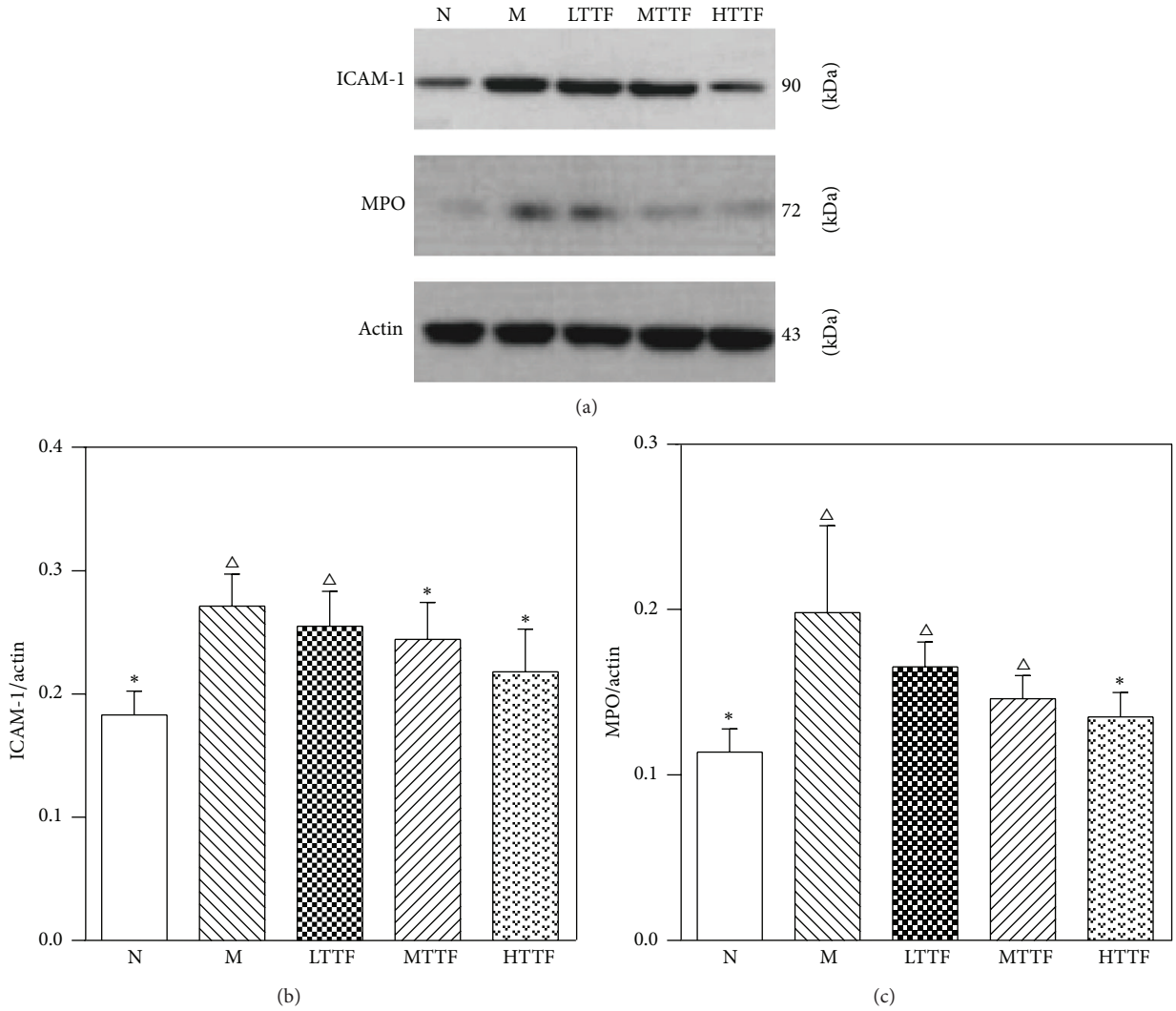

Figure 7: Western blot analysis of sciatic nerve. (a) Films of ICAM-1, MPO, and β-actin (control) bands. (b) Densitometric analysis of the ICAM-1 bands is expressed as integrated optical density (IOD), corrected for the corresponding β-actin ($n = 5$ for each group). (c) Densitometric analysis of the MPO bands ($n = 5$ for each group) ($^{\triangle}p < 0.05$ versus the control group, $^{*}p < 0.05$ versus the model group).

the signaling pathway upstream of ICAM-1, including levels oxidative stress and inflammatory cytokines.

Conflict of Interests

All authors declare that there is no conflict of interests regarding the publication of this paper.

Authors' Contribution

Mingdi Li, Da Huang, and Xiaoxing Liu contributed equally to this paper.

Acknowledgment

This work was supported by the National Natural Science Foundation of China (Grant no. 81173445).

References

[1] S. S. Sharma, A. Kumar, and R. K. Kaundal, "Protective effects of 4-amino1,8-napthalimide, a poly (ADP-ribose) polymerase inhibitor in experimental diabetic neuropathy," *Life Sciences*, vol. 82, no. 11-12, pp. 570–576, 2008.

[2] C. Figueroa-Romero, M. Sadidi, and E. L. Feldman, "Mechanisms of disease: the oxidative stress theory of diabetic neuropathy," *Reviews in Endocrine & Metabolic Disorders*, vol. 9, no. 4, pp. 301–314, 2008.

[3] H. Urabe, T. Terashima, F. Lin, H. Kojima, and L. Chan, "Bone marrow-derived TNF-α causes diabetic neuropathy in mice," *Diabetologia*, vol. 58, no. 2, pp. 402–410, 2015.

[4] J.-Y. Zhou and S.-W. Zhou, "Protection of trigonelline on experimental diabetic peripheral neuropathy," *Evidence-Based Complementary and Alternative Medicine*, vol. 2012, Article ID 164219, 8 pages, 2012.

[5] Y. L. Piao and X. C. Liang, "Chinese medicine in diabetic peripheral neuropathy: experimental research on nerve repair and regeneration," *Evidence-Based Complementary and Alternative Medicine*, vol. 2012, Article ID 191632, 13 pages, 2012.

[6] D.-W. Zou, Y.-B. Gao, Z.-Y. Zhu et al., "Traditional chinese medicine tang-luo-ning ameliorates sciatic nerve injuries in streptozotocin-induced diabetic rats," *Evidence-based Complementary and Alternative Medicine*, vol. 2013, Article ID 989670, 12 pages, 2013.

[7] Y. Wang, Z. Chen, R. Ye, Y. He, Y. Li, and X. Qiu, "Protective effect of Jiaweibugan decoction against diabetic peripheral neuropathy," *Neural Regeneration Research*, vol. 8, no. 12, pp. 1113–1121, 2013.

[8] B. S. Rao, K. E. Reddy, K. Parveen, B. L. Narendra, S. C. Shekhar, and L. Mangala, "Effects of *Cleome viscosa* on hyperalgesia, oxidative stress and lipid profile in STZ induced diabetic neuropathy in Wistar rats," *Pakistan Journal of Pharmaceutical Sciences*, vol. 27, no. 5, pp. 1137–1145, 2014.

[9] R. Ranjithkumar, S. Prathab Balaji, B. Balaji, R. V. Ramesh, and M. Ramanathan, "Standardized aqueous Tribulus terristris (Nerunjil) extract attenuates hyperalgesia in experimentally induced diabetic neuropathic pain model: role of oxidative stress and inflammatory mediators," *Phytotherapy Research*, vol. 27, no. 11, pp. 1646–1657, 2013.

[10] E. B. Jude, C. A. Abbott, M. J. Young, S. G. Anderson, J. T. Douglas, and A. J. M. Boulton, "The potential role of cell adhesion molecules in the pathogenesis of diabetic neuropathy," *Diabetologia*, vol. 41, no. 3, pp. 330–336, 1998.

[11] M. Ishikawa, D. Cooper, J. Russell et al., "Molecular determinants of the prothrombogenic and inflammatory phenotype assumed by the postischemic cerebral microcirculation," *Stroke*, vol. 34, no. 7, pp. 1777–1782, 2003.

[12] Y. Wang, A. M. Schmeichel, H. Iida, J. D. Schmelzer, and P. A. Low, "Enhanced inflammatory response via activation of NF-κB in acute experimental diabetic neuropathy subjected to ischemia-reperfusion injury," *Journal of the Neurological Sciences*, vol. 247, no. 1, pp. 47–52, 2006.

[13] A. Ceriello, E. Falleti, E. Motz et al., "Hyperglycemia-induced circulating ICAM-1 increase in diabetes mellitus: the possible role of oxidative stress," *Hormone and Metabolic Research*, vol. 30, no. 3, pp. 146–149, 1998.

[14] A. P. Adamis, "Is diabetic retinopathy an inflammatory disease?" *The British Journal of Ophthalmology*, vol. 86, no. 4, pp. 363–365, 2002.

[15] M. D. Li, L. Lin, S. C. Sun et al., "Clinical study of Chinese herb formula Tangtongfang by bathing the affected feet with diabetic peripheral neuropathy," *Chinese Journal of Rehabilitation Theory and Practice*, vol. 15, no. 6, pp. 553–555, 2009.

[16] M. Alipour, M. R. Gholami, I. Jafari Anarkooli et al., "Intraperitoneal aminoguani-dine improves sciatic nerve ischemia—reperfusion injury in male Sprague Dawley rats," *Cellular and Molecular Neurobiology*, vol. 31, no. 5, pp. 765–773, 2011.

[17] Y. Wang, A. M. Schmeichel, H. Iida, J. D. Schmelzer, and P. A. Low, "Ischemia-reperfusion injury causes oxidative stress and apoptosis of Schwann cell in acute and chronic experimental diabetic neuropathy," *Antioxidants & Redox Signaling*, vol. 7, no. 11-12, pp. 1513–1520, 2005.

[18] N. Kawamura, A. M. Schmeichel, Y. P. Wang, J. D. Schmelzer, and P. A. Low, "Multiple effects of hypothermia on inflammatory response following ischemia-reperfusion injury in experimental ischemic neuropathy," *Experimental Neurology*, vol. 202, no. 2, pp. 487–496, 2006.

[19] M. Y. Xu, G. H. Lu, and M. D. Chen, *Diabetes Mellitus*, Shanghai Science and Technology, Shanghai, China, 2010.

[20] J. Eichberg, "Protein kinase C changes in diabetes: is the concept relevant to neuropathy?" *International Review of Neurobiology*, vol. 50, pp. 61–82, 2002.

[21] K. Sugimoto, Y. Murakawa, and A. A. F. Sima, "Diabetic neuropathy—a continuing enigma," *Diabetes/Metabolism Research and Reviews*, vol. 16, no. 6, pp. 408–433, 2000.

[22] C. Ronald Kahn, G. L. King, A. C. Moses et al., *Joslin's Diabetes Mellitus*, Lippincott Williams & Wilkins, 14th edition, 2006.

[23] N. E. Cameron, M. A. Cotter, and P. A. Low, "Nerve blood flow in early experimental diabetes in rats: Relation to conduction deficits," *The American Journal of Physiology—Endocrinology and Metabolism*, vol. 261, no. 1, pp. E1–E8, 1991.

[24] R. R. Tuck, J. D. Schmelzer, and P. A. Low, "Endoneurial blood flow and oxygen tension in the sciatic nerves of rats with experimental diabetic neuropathy," *Brain*, vol. 107, no. 3, pp. 935–950, 1984.

[25] P. A. Low, T. D. Lagerlund, and P. G. McManis, "Nerve blood flow and oxygen delivery in normal, diabetic, and ischemic neuropathy," *International Review of Neurobiology*, vol. 31, pp. 355–438, 1989.

[26] J. A. Kim, J. A. Berliner, R. D. Natarajan, and J. L. Nadler, "Evidence that glucose increases monocyte binding to human aortic endothelial cells," *Diabetes*, vol. 43, no. 9, pp. 1103–1107, 1994.

[27] M. Richardson, S. J. Hadcock, M. DeReske, and M. I. Cybulsky, "Increased expression *in vivo* of VCAM-1 and E-selectin by the aortic endothelium of normolipemic and hyperlipemic diabetic rabbits," *Arteriosclerosis, Thrombosis, and Vascular Biology*, vol. 14, no. 5, pp. 760–769, 1994.

[28] M. Morigi, S. Angioletti, B. Imberti et al., "Leukocyte-endothelial interaction is augmented by high glucose concentrations and hyperglycemia in a NF-κB-dependent fashion," *The Journal of Clinical Investigation*, vol. 101, no. 9, pp. 1905–1915, 1998.

[29] L. Q. Zhu, S. R. Wang, and Y. Qin, "Effects of huoxue injection on the adherence of human monocytes to endothelial cells and expression of vascular cell adhesion molecules," *Chinese Journal of Integrated Traditional and Western Medicine*, vol. 29, no. 3, pp. 238–241, 2009.

[30] A. M. Joussen, V. Poulaki, N. Mitsiades et al., "Nonsteroidal anti-inflammatory drugs prevent early diabetic retinopathy via TNF-alpha suppression," *The FASEB Journal*, vol. 16, no. 3, pp. 438–440, 2002.

[31] G. Hussain, S. A. A. Rizvi, S. Singhal, M. Zubair, and J. Ahmad, "Serum levels of TNF-α in peripheral neuropathy patients and its correlation with nerve conduction velocity in type 2 diabetes mellitus," *Diabetes & Metabolic Syndrome: Clinical Research and Reviews*, vol. 7, no. 4, pp. 238–242, 2013.

[32] T. Zhu, Q. Meng, J. Ji, X. Lou, and L. Zhang, "Toll-like receptor 4 and tumor necrosis factor-alpha as diagnostic biomarkers for diabetic peripheral neuropathy," *Neuroscience Letters*, vol. 585, pp. 28–32, 2015.

[33] S. T. Yao, X. H. Liu, X. M. Tang et al., "Ischemic post-conditioning ameliorates pia mater microcirculation in rats subjected to cerebral ischemia reperfusion," *Chinese Journal of Pathophysiology*, vol. 25, no. 3, pp. 451–455, 2009.

[34] W. Zhang, Y. H. Wang, W. W. Li et al., "Effect of lipoic acid on expression of ICAM-1 of lung tissue following renal ischemia reperfusion in aged rats," *Journal of the Fourth Military Medical University*, vol. 30, no. 10, pp. 923–925, 2009.

[35] C. Giannini and P. J. Dyck, "Basement membrane reduplication and pericyte degeneration precede development of diabetic polyneuropathy and are associated with its severity," *Annals of Neurology*, vol. 37, no. 4, pp. 498–504, 1995.

[36] R. A. Malik, P. G. Newrick, A. K. Sharma et al., "Microangiopathy in human diabetic neuropathy: relationship between capillary abnormalities and the severity of neuropathy," *Diabetologia*, vol. 32, no. 2, pp. 92–102, 1989.

[37] P. J. Dyck, S. Hansen, J. Karnes et al., "Capillary number and percentage closed in human diabetic sural nerve," *Proceedings of the National Academy of Sciences of the United States of America*, vol. 82, no. 8, pp. 2513–2517, 1985.

[38] P. J. Dyck, J. L. Karnes, M. S. O'Brien, H. Okazaki, A. Lais, and J. Engelstad, "The spatial distribution of fiber loss in diabetic polyneuropathy suggests ischemia," *Annals of Neurology*, vol. 19, no. 5, pp. 440–449, 1986.

[39] P. J. Dyck, A. Lais, J. L. Karnes, P. O'Brien, and R. Rizza, "Fiber loss is primary and multifocal in sural nerves in diabetic polyneuropathy," *Annals of Neurology*, vol. 19, no. 5, pp. 425–439, 1986.

[40] D. F. Jiang, C. H. Yin, G. N. Yu et al., "Reserch on effect of total saponins of *Astragalus* on hemorrheology of old rats," *Primary Journal of Chinese Materia Medica*, vol. 16, no. 5, p. 15, 2002.

[41] J. Gao, X. X. Xu, X. J. Xu et al., "Research on antithrombotic effect of total saponins of Astragalus," *Chinese Traditional Patent Medicine*, vol. 24, no. 2, pp. 116–118, 2002.

[42] Y. H. Yin and J. L. Teng, "Progress of Astragalus active ingredients intervene diabetic vascular endothelial injury," *Shan Dong Zhong Yi Za Zhi*, vol. 32, no. 8, pp. 599–601, 2013.

[43] S. B. Duan, L. Yu, Y. Liu et al., "Influence of astragalus on vascular endothlial cells injury in rat models of multiple organ dysfunction syndrome," *China Journal of Modern Medicine*, vol. 22, no. 1, pp. 5–8, 2012.

[44] Y. Yang, W. W. Lv, Y. S. Song et al., "Antithrombotic effect of total glucosides of paeonia," *Chinese Traditional and Herbal Drugs*, vol. 37, no. 7, pp. 1066–1068, 2006.

[45] T. Okubo, F. Nagai, T. Seto, K. Satoh, K. Ushiyama, and I. Kano, "The inhibition of phenylhydroquinone-induced oxidative DNA cleavage by constituents of Moutan Cortex and Paeoniae Radix," *Biological & Pharmaceutical Bulletin*, vol. 23, no. 2, pp. 199–203, 2000.

[46] R. Motterlini, R. Foresti, R. Bassi, and C. J. Green, "Curcumin, an antioxidant and anti-inflammatory agent, induces heme oxygenase-1 and protects endothelial cells against oxidative stress," *Free Radical Biology and Medicine*, vol. 28, no. 8, pp. 1303–1312, 2000.

[47] Y. Yu, J. L. Liu, J. Y. Wang et al., "Protective effect of eupolyphaga sinesiswalker on endothelial cells in experimental hyperlipidemic rats," *Journal of Shandong University (Health Sciences)*, vol. 40, no. 5, pp. 398–400, 2002.

[48] Y. Yu, J. L. Liu, J. Y. Wang et al., "The effects of aqueous extract of Eupolyphaga sinesis walker on endothelium and endothelin of the hyperlipidemic rats," *Chinese Journal of Biochemical Pharmaceutics*, vol. 24, no. 1, pp. 15–17, 2003.

[49] C. F. Zhou, M. Lai, X. H. Wang et al., "Effects of ground beetle on blood rheology of rats," *Chinese Traditional and Herbal Drugs*, vol. 25, no. 1, pp. 28–29, 1994.

Hindawi Publishing Corporation
Evidence-Based Complementary and Alternative Medicine
Volume 2015, Article ID 162145, 6 pages
http://dx.doi.org/10.1155/2015/162145

Research Article

Panax notoginseng Saponins Attenuate Phenotype Switching of Vascular Smooth Muscle Cells Induced by Notch3 Silencing

Nan Liu,[1] Dazhi Shan,[2] Ying Li,[1] Hui Chen,[1] Yonghong Gao,[3] and Yonghua Huang[1]

[1]*Department of Neurology, Military General Hospital of Beijing PLA, Beijing 100700, China*
[2]*191 Clinical Department, 303 Hospital of People's Liberation Army, Guigang, Guangxi Zhuang Autonomous Region 537105, China*
[3]*Key Laboratory of Chinese Internal Medicine of Ministry of Education and Beijing Dongzhimen Hospital, Beijing University of Chinese Medicine, Beijing 100700, China*

Correspondence should be addressed to Yonghong Gao; gaoyh7088@hotmail.com and Yonghua Huang; huangyh@163.com

Received 16 April 2015; Revised 20 May 2015; Accepted 30 May 2015

Academic Editor: Dan Hu

Panax notoginseng saponins (PNS) could maintain vascular smooth muscle cells (VSMCs) in stable phenotypes so as to keep blood vessel elasticity as well as prevent failing in endovascular treatment with stent. Downregulation of Notch3 expression in VSMCs could influence the phenotype of VSMCs under pathologic status. However, whether PNS is able to attenuate the Notch3 silencing induced phenotype switching of VSMCs remains poorly understood. Primary human VSMCs were transfected with a plasmid containing a small interfering RNA (siRNA) against Notch3 and then exposed to different doses of PNS. The control groups included cells not receiving any treatment and cells transfected with a control siRNA. Phenotypic switching was evaluated by observing cell morphology with confocal microscopy, as well as examining α-SM-actin, SM22α, and OPN using Western blot. Downregulated Notch3 with a siRNA induced apparent phenotype switching, as reflected by morphologic changes, decreased expression of α-SM-actin and SM22α and increased expression of OPN. These changes were inhibited by PNS in a dose-dependent manner. The phenotype switching of VSMCs induced by Notch3 knockdown could be inhibited by PNS in a dose-dependent manner. Our study provided new evidence for searching effective drug for amending stability of atherosclerotic disease.

1. Introduction

With ageing population worldwide, atherosclerotic disease is responsible for nearly 50% of all deaths [1]. Atherosclerosis is a condition in which plaques build up inside the large and medium-sized arteries. Plaques may partially or totally block the blood flow through the artery system. Some of the diseases may develop as a result of atherosclerosis including stroke, coronary heart disease, and carotid artery disease. Medium-sized arteries may contain up to 40 layers of smooth muscle cells in the media, so they are also called muscular arteries. Phenotypic switching of the vascular smooth muscle cells (VSMCs) is a central pathologic feature in atherosclerosis lesion development, progression, and end-stage disease consequences such as plaque rupture with possible myocardial infarction or stroke. Plaque stability is highly dependent on the VSMCs phenotype, which may either undergo apoptosis or activate the production of matrix metalloproteinases or inflammatory mediators that in turn trigger plaque rupture and thrombosis [2].

Recently, saponins from *Panax notoginseng* (PNS) have been widely used in the treatment of atherosclerotic diseases like stroke and coronary heart disease in China. PNS, the root of *Panax notoginseng*, is a highly valued and important traditional Chinese medicine, which is mainly made up of ginsenoside Rg1, ginsenoside Rb1, notoginsenoside R1, and so forth [3], belonging to the Araliaceae family. Numerous studies have reported that PNS had the therapeutical effect in cardiovascular diseases because PNS could relax blood vessel [4], decrease platelet aggregation [5], and inhibit the inflammatory response in atherosclerotic lesion [6].

Similar to our study, many experiments had proven that PNS may have effect on abnormal proliferation VSMCs to prevent atherosclerosis and restenosis. Some research showed that PNS downregulated the expression of proliferating cell nuclear antigen (PCNA), fibronectin (FN), and

matrix metalloproteinase-9 (MMP-9) to inhibit the VSMCs proliferation [7, 8]. Other studies have been focusing on the mechanism of PNS therapeutical effect in the view of signal transduction pathway. For example, Yuan et al. [9] reported that PNS inhibits atherogenesis by suppressing FAK phosphorylation, integrins expression, and NF-κB translocation. Xu et al. [10] also found that PNS inhibits VSMCs proliferation and induces VSMCs apoptosis through upregulating p53, Bax, and caspase-3 expressions and downregulating Bcl-2 expression.

However, few studies described the effects of PNS on the morphology of VSMCs and proteins alteration in pathologic state.

Notch3 is predominantly expressed in adult VSMCs. Notch3 gene mutations cause the cerebral autosomal dominant arteriopathy with subcortical infarcts and leukoencephalopathy (CADASIL), an inherited early stroke syndrome, which results in dementia because of systemic vascular degeneration. This suggests that Notch3 plays a critical role in maintaining the phenotypic stability of vascular smooth muscle cells (VSMCs) [11].

Notch3 mutant VSMCs had marked alterations in shape and size [12]. Mutant VSMCs are thinner and often have thin elongated cytoplasmic processes, as well as phenotype change from "contractile" to "synthetic." This leads to obvious proliferation of VSMCs and increased secretion of extracellular matrix [13].

Contractile VSMCs are typically characterized by high expression of the genes for contractile elements, including α-smooth muscle actin (α-SM-actin), smooth muscle 22α (SM22α), SM myosin heavy chain (MHC), and smoothelin [14, 15], whereas synthetic VSMCs have high expression of osteopontin (OPN), a kind of extracellular matrix proteins secreted by synthetic VSMCs. Therefore, OPN is hardly expressed in contractile VSMCs [16]. Besides, there are some other markers expressed on synthetic VSMCs including epiregulin, tropoelastin, and thrombospondin.

Although these markers are specifically expressed in the fully contractile VSMCs, most of them may be expressed at least transiently in other cells during the tissue repair, or disease stage. Therefore, evidence of expression of a single contractile VSMCs marker gene alone is not sufficient for VSMCs identification and assessment. Thus, the rigorous identification of contractile VSMCs requires examination of multiple marker genes [17]. In order to identify VSMCs phenotype accurately, our study detected the expression of the α-SM-actin and SM22α markers of contractile VSMCs, as well as the expression of the OPN related to synthetic VSMCs.

In current study, we induced phenotype switching in VSMCs using a siRNA against Notch3 in primary culture of VSMCs. Effects of PNS on phenotype switching were examined by observing cell morphology and the expression of α-SM-actin, SM22α, and OPN.

2. Materials and Methods

2.1. Cells and Cell Culture. VSMCs were obtained from human aortic arteries from donors who died of traffic accidents, within 24 h of death, to establish primary culture in DMEM (Invitrogen, Grand Island, NY, USA) containing FBS (Invitrogen) in 5% CO_2 at 37°C. The acquisition of the samples was approved by the Ethical Board of the General Hospital of Beijing PLA, Beijing, China. All experiments were performed on cells at least 3 times.

2.2. Reagents and Antibodies. PureLink DNAse set and PureLink RNA mini kit were purchased from Invitrogen (Grand Island, NY, USA). High-Capacity cDNA Reverse Transcription kit and Power SYBR green Mastermix were purchased from Applied Biosystems (Foster City, CA, USA). Polyvinylidene difluoride (PVDF) membranes were purchased from Bio-Rad (Berkeley, CA, USA). Amersham ECL Plus Western Blotting Detection reagents were purchased from GE Healthcare (Rockford, IL, USA). Xuesaitong injection (containing 400 mg PNS per ampule) was obtained from the Kunming Pharmaceutical Group Co., Ltd. (Yun Nan province, China). Rabbit anti-Notch3, mouse anti-SM22α, and rabbit anti-OPN were purchased from Abcam (Cambridge, MA, USA). TRITR-phalloidin, FITC-phalloidin, and mouse anti-α-SM-actin were purchased from Sigma-Aldrich (St. Louis, MO, USA). Mouse anti-β-actin and mouse anti-β-tubulin were purchased from Sigma (St. Louis, MO, USA).

2.3. RNA Silencing. To generate adenovirus transfection particles, a set of 4pAd/CMV/V5-DEST vectors (Invitrogen) encoding siRNA targeting the Notch3 gene (Gen Bank accession number NM_000435.2, mRNA, 8089 bp) and a nontarget siRNA control vector (TRC1 library, Sigma-Aldrich, St. Louis, MO, USA) were used to cotransfect HEK293A cells (Invitrogen) using pDONR221 (Invitrogen). VSMCs were seeded onto 6-cm plates (6×10^5 cells per plate) 24 h before transfection. Viral transfection was carried out using a medium containing adenoviruses particles. The culture medium was replaced 24 h later. The transfected VSMCs were selected 48 h after transfection. Stable cell lines created with two vectors (referred to as pAD-EGFP-Notch3-1 and pAD-EGFP-Notch3-3, resp.) showed significant reduction of Notch3 protein expression. Subsequent experiments were performed using stable cell lines generated with the pAD-EGFP-Notch3-1 construct. Nontransfected VSMCs and control siRNA VSMCs had similar growth curves. The details were described in our earlier study and have proven that Notch3 gene decreased significantly [18].

2.4. Intervention. Primary culture of VSMCs was transfected with pAD-EGFP-Notch3-1 and treated with PNS (800, 400, or 200 mg/L) or vehicle control. Vehicle control cells, which were transfected with empty plasmid, exhibited no detectable fluorescence. VSMCs transfected with pAD-EGFP-Notch3-1 exhibited a transfection efficiency of more than 50% at 48 h after transfection, called control siRNA. These results had been proven in our earlier study [18]. The control conditions also include blank control and cells treated with the control siRNA only.

2.5. Cell Morphology and Immunocytochemistry. VSMCs were fixed with paraformaldehyde for analysis of cell

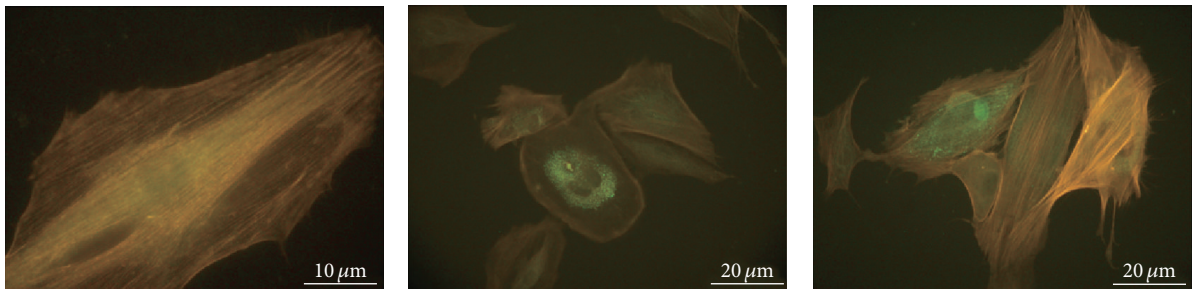

Figure 1: TRITC labeled phalloidin staining showing actin cytoskeleton of VSMCs. Under the excitation wavelength of 488 nm, the cytoskeletons of control and Notch3 siRNA VSMCs were reddish-yellow and the GFP dots were green in the cytoplasm. Notch3 siRNA VSMCs are more rounded and irregular and lack actin cytoskeleton. Upon treatment with PNS, VSMCs became regular.

morphology. Fixed cells were stained by FITC or TRITC labeled phalloidin to show actin. Cell images were analyzed and captured with a FluoView 1000 laser scanning confocal microscope (Olympus, Tokyo, Japan).

2.6. Western Blot Analysis. Samples of equal amounts of protein were separated by gel electrophoresis, transferred onto polyvinylidene difluoride (PVDF) membranes, and incubated with a primary antibody against one of the following: α-smooth muscle actin (α-SM-actin), smooth muscle 22α (SM22α), and osteopontin (OPN), followed by treatment with a secondary antibody. Amersham ECL Plus Western Blotting Detection reagents were used for chemiluminescence. Band intensity was analyzed using the ImageJ analysis software (NIMH, Bethesda, MD, USA) and normalized to β-actin and β-tubulin as internal control. Protein concentration was determined using a BCA assay (Pierce, Rockford, IL, USA).

2.7. Statistics. All experiments were repeated for a minimum of three times. Data were analyzed by one-way analysis of variance (ANOVA) followed by post hoc Dunnett's t-test for multiple comparisons. P values of < 0.05 were considered statistically significant.

3. Results

3.1. Morphology of VSMCs. Morphological characteristics of all VSMCs were tested. Compared to blank control, control siRNA did not affect the morphology or the cytoskeleton pattern. Actin-phalloidin staining revealed normal actin filament system and cell shape (Figure 1). Notch3 siRNA VSMCs with actin-phalloidin staining revealed abnormal nuclear configuration, a disorganized actin filament system, and polygonal cell shape. In addition to decreased cell size, some filaments of F-actin became shrunk and lost (Figure 1). PNS significantly decreased the number of polymorphous cells and increased intercellular gaps and cell size. These findings suggested that the PNS could maintain stable VSMCs phenotypes.

3.2. PNS Increased the Expression of α-SM-Actin and SM22α and Decreased the Expression of OPN in Notch3 siRNA VSMCs. The relative expression levels of α-SM-actin and SM22α protein in blank control group were 0.622 ± 0.088 and 0.381 ± 0.040, 0.620 ± 0.123 and 0.409 ± 0.043 in cells exposed to the control siRNA, and 0.233 ± 0.023 and 0.140 ± 0.025 in cells treated with Notch3 siRNA, respectively. PNA treatment of the cells transfected with Notch3 siRNA at 800, 400, and 200 mg/L increased relative expression levels of α-SM-actin and SM22α expression to 0.485 ± 0.044, 0.436 ± 0.040, 0.228 ± 0.048 and 0.335 ± 0.067, 0.265 ± 0.0341, 0.194 ± 0.024, respectively. The relative expression levels of α-SM-actin and SM22α protein of VSMCs were positively correlated with PNS concentration (Figures 2 and 3). In comparison to cells transfected with Notch3 siRNA, PNS at 400 and 800 mg/L, but not 200 mg/L, significantly upregulated protein expressions of α-SM-actin ($P < 0.0001$). Similar to α-SM-actin, PNS significantly upregulated protein expressions of SM22α in a dose-dependent manner ($P < 0.05$ or 0.01). These results suggested that PNS could maintain α-SM-actin and SM22α protein level and stabilize the VSMCs phenotype at high concentration.

OPN protein was not detectable in blank control group or transfected with the control siRNA group. Notch3 siRNA increased the OPN protein to 0.735 ± 0.107. PNS treatment decreased the OPN protein to 0.379 ± 0.069, 0.486 ± 0.048, and 0.691 ± 0.070 at 800, 400, and 200 g/mL. In comparison with cells transfected with Notch3 siRNA, PNS at 400 and 800 mg/L, but not 200 mg/L, significantly downregulated protein expressions of OPN ($P < 0.0001$).

PNS may inhibit OPN overexpression and stabilize the VSMCs phenotype too (Figure 4).

4. Discussion

Control of VSMCs phenotype is essential in the development and maintenance of a healthy vasculature. The contractile phenotype can be altered by phenotypic modulation leading to a high rate of proliferation and migration and extracellular matrix (ECM) accumulation while markers of VSMC contractility are downregulated. Notch3 protein, a large single

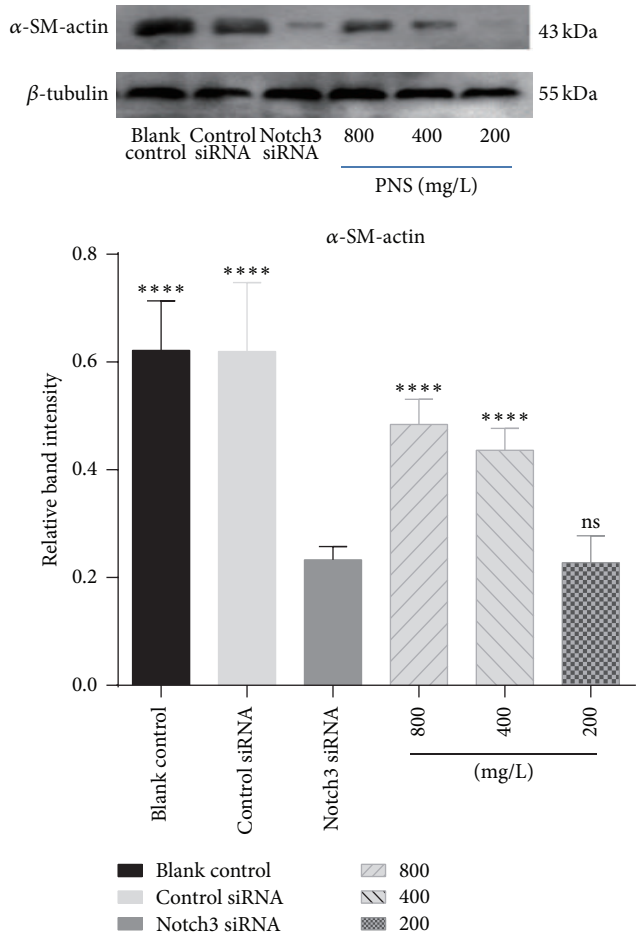

Figure 2: Effects of PNS on α-SM-actin in VSMCs transfected with a Notch3 siRNA. α-SM-actin was examined with Western blot. The data represent mean ± S.D. $^{****}P < 0.0001$ versus Notch3 siRNA VSMCs.

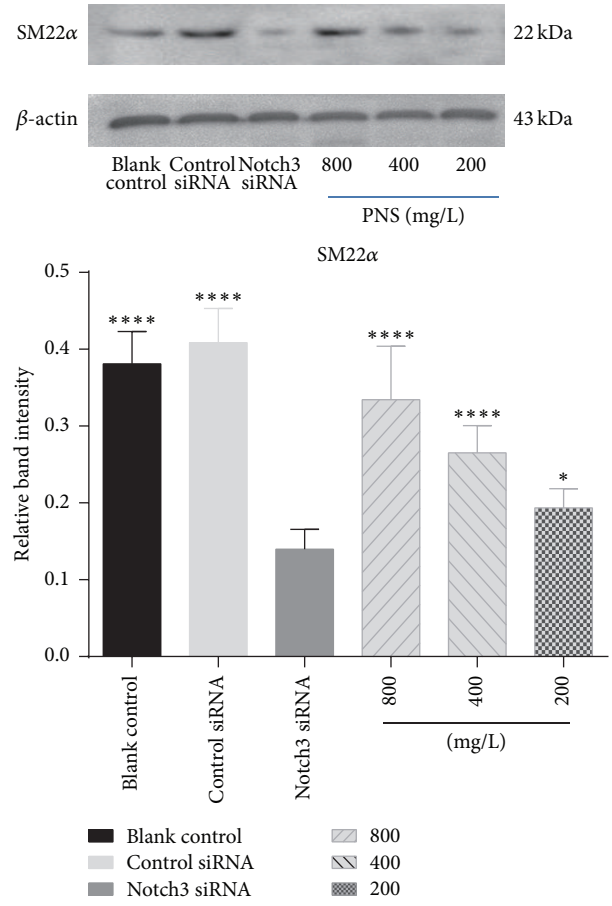

Figure 3: Effects of PNS on SM22α in VSMCs transfected with a Notch3 siRNA. SM22α was examined by Western blot. The data represent mean ± S.D. $^{****}P < 0.0001$ or $^{*}P < 0.05$ versus Notch3 siRNA VSMCs.

pass transmembrane receptor, is exclusively expressed almost in VSMCs and pericytes, the specialized VSMCs, but is not detectable in endothelial cell which is important for survival of VSMCs and plays a critical role of Notch3 for VSMCs in blood vessel integrity and blood-brain barrier function in the mammalian vasculature [2]. Notch3 is the first cell-autonomous regulator of arterial differentiation and maturation of VSMCs. In vivo studies have shown that Notch3−/− vessels lost their arterial phenotype, from contractile to synthetic, indicating that Notch3 is crucial for the phenotypic integrity of VSMCs [19]. There is growing evidence for a pivotal role of VSMC plasticity and phenotypic switching in vascular diseases, such as atherosclerosis, vein graft stenosis, and restenosis following angioplasty and stenting [20]. In our study, using the RNA interference approach, we studied the role of Notch3 in the phenotype switch of VSMCs. In order to tackle this problem, we do some work from two aspects: morphological pattern observed by laser scanning confocal microscope and the marker proteins of VSMCs detecting by Western Blot.

In physiological state, VSMCs are large and elongated and have abundant cytoskeleton and prominent nucleus. In culture, these cells orient themselves into parallel bundles and become spindle-shaped. Notch3 siRNA VSMCs, lacking actin cytoskeleton, change their shape from elongated to more rounded and irregular [21]. These cells have more pseudopods. This is identical to our observation (Figure 1). However, the morphology of Notch3 siRNA VSMCs with PNS was better than control cells. Their shapes were regular without much pseudopods. Then we further investigated the cytoskeleton and ECM related to VSMCs phenotypic switching. α-SM-actin and SM22α are considered VSMC-specific contractile proteins as well as important cytoskeletal proteins. OPN is one of the synthetic VSMCs markers and a multifunctional protein in ECM. It is hardly expressed by contractile VSMCs. VSMCs in the blank control treated with the control siRNA only maintain the contractile phenotype and hardly expressed OPN. This is consistent with our result in Western blot (Figure 4).

VSMCs phenotype switching from contractile to synthetic is a key step in which VSMCs revert to an immature, proliferative phenotype, leading to pathological luminal narrowing. This process involves a reduction in the expression of the VSMCs contractile proteins such as α-SM-actin and

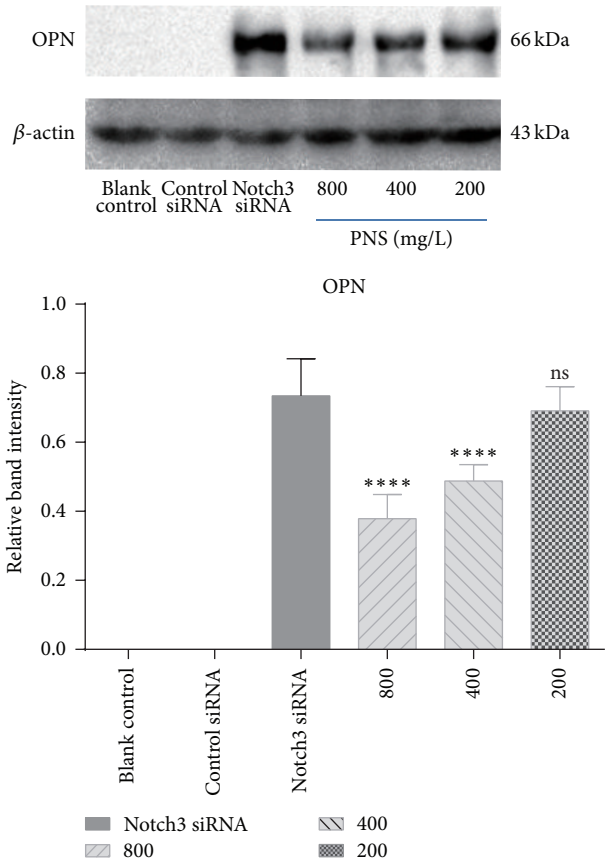

Figure 4: Effects of PNS on OPN in VSMCs transfected with a Notch3 siRNA. OPN was examined with Western blot. The data represent mean ± S.D. $^{****}P < 0.0001$ versus Notch3 siRNA VSMCs.

SM22α that are the hallmarks of quiescent, mature VSMCs [22]. Meanwhile, the expression level of OPN increases gradually. It has been reported that secretory calcitonin gene-related peptide (CGRP) and CGRP receptor modified mesenchymal stem cells on proliferation and phenotypic transformation of VSMCs. They found that the expression of contractile phenotype protein α-SM-actin declined while intermediate phenotype OPN increased significantly [23]. However, only two markers proteins seemed to be insufficient to support phenotypic changes. Another study showed that α-SM-actin and calponin protein levels significantly decreased by OPN overexpression. Downregulation of α-SM-actin and calponin was also observed on extracellular treatment of mouse VSMCs with recombinant OPN [24]. It is worth noting that our study found that there is a negative relation between α-SM-actin, SM22α, and OPN, which has never been reported before. And we observed that PNS could increase the expression of contractile markers α-SM-actin and SM22α and decrease the expression of synthetic marker OPN in a dose-dependent manner. PNS at concentration of 200 mg/L only increased the expression of SM22α in control cells and had little influence on the expression of α-SM-actin and OPN. This suggested PNS at high concentration of 400 and 800 mg/L had a better protective effect than that at low concentration of 200 mg/L.

5. Conclusions

Notch3 plays an important role in the phenotype switch of VSMCs and may represent a target for treatment of atherosclerotic diseases. We showed improved morphology by PNS in VSMCs treated with a Notch3 siRNA: the polymorphous cells became regular with PNS treatment. Notch3 siRNA transfection decreased α-SM-actin and SM22α and increased OPN. PNS attenuated these changes, particularly at high concentration range. These results suggested that PNS could maintain VSMCs contractile phenotype and encourage exploring of the therapeutic potentials of PNS in vascular diseases.

A few limitations of this study need to be mentioned. First, the migration ability of VSMCs was only assessed morphologically. Secondly, this study focused on the phenotype switch of VSMCs by detecting marker proteins. Future studies are needed to address signal pathways through that phenotype switch of VSMCs.

Conflict of Interests

The authors declare that there is no conflict of interests regarding the publication of this paper.

Authors' Contribution

Nan Liu and Dazhi Shan contributed equally to this study.

Acknowledgment

This study was supported by the National Natural Science Foundation of China (Project no. 30800357).

References

[1] A. Tedgui and Z. Mallat, "Cytokines in atherosclerosis: pathogenic and regulatory pathways," *Physiological Reviews*, vol. 86, no. 2, pp. 515–581, 2006.

[2] T. L. Henshall, A. Keller, L. He et al., "Notch3 is necessary for blood vessel integrity in the central nervous system," *Arteriosclerosis, Thrombosis, and Vascular Biology*, vol. 35, no. 2, pp. 409–420, 2015.

[3] W. Zhang, G. Chen, and C.-Q. Deng, "Effects and mechanisms of total Panax notoginseng saponins on proliferation of vascular smooth muscle cells with plasma pharmacology method," *Journal of Pharmacy and Pharmacology*, vol. 64, no. 1, pp. 139–145, 2012.

[4] P. Chan, G. N. Thomas, and B. Tomlinson, "Protective effects of trilinolein extracted from *Panax notoginseng* against cardiovascular disease," *Acta Pharmacologica Sinica*, vol. 23, no. 12, pp. 1157–1162, 2002.

[5] K.-W. Leung, H.-M. Ng, M. K. S. Tang, C. C. K. Wong, R. N. S. Wong, and A. S. T. Wong, "Ginsenoside-Rg1 mediates a hypoxia-independent upregulation of hypoxia-inducible factor-1α to promote angiogenesis," *Angiogenesis*, vol. 14, no. 4, pp. 515–522, 2011.

[6] Y.-G. Zhang, H.-G. Zhang, G.-Y. Zhang et al., "Panax notoginseng saponins attenuate atherosclerosis in rats by regulating the blood lipid profile and an anti-inflammatory action," *Clinical*

and Experimental Pharmacology and Physiology, vol. 35, no. 10, pp. 1238–1244, 2008.

[7] L. Wu, W. Zhang, Y.-H. Tang et al., "Effect of total saponins of 'panax notoginseng root' on aortic intimal hyperplasia and the expressions of cell cycle protein and extracellular matrix in rats," *Phytomedicine*, vol. 17, no. 3-4, pp. 233–240, 2010.

[8] J. Wang, L. Wu, W. Zhang, and C. Deng, "Effect of Panax notoginseng saponins on vascular intima hyperplasia and PCNA expression in rat aorta after balloon angioplasty," *Zhongguo Zhong Yao Za Zhi*, vol. 34, no. 6, pp. 735–739, 2009.

[9] Z. Yuan, Y. Liao, G. Tian et al., "Panax notoginseng saponins inhibit Zymosan A induced atherosclerosis by suppressing integrin expression, FAK activation and NF-kappaB translocation," *Journal of Ethnopharmacology*, vol. 138, no. 1, pp. 150–155, 2011.

[10] L. Xu, J.-T. Liu, N. Liu, P.-P. Lu, and X.-M. Pang, "Effects of Panax notoginseng saponins on proliferation and apoptosis of vascular smooth muscle cells," *Journal of Ethnopharmacology*, vol. 137, no. 1, pp. 226–230, 2011.

[11] T. Wang, M. Baron, and D. Trump, "An overview of Notch3 function in vascular smooth muscle cells," *Progress in Biophysics and Molecular Biology*, vol. 96, no. 1–3, pp. 499–509, 2008.

[12] V. Domenga, P. Fardoux, P. Lacombe et al., "Notch3 is required for arterial identity and maturation of vascular smooth muscle cells," *Genes and Development*, vol. 18, no. 22, pp. 2730–2735, 2004.

[13] G. Zhu, H. Chen, and W. Zhang, "Phenotype switch of vascular smooth muscle cells after siRNA silencing of filamin," *Cell Biochemistry and Biophysics*, vol. 61, no. 1, pp. 47–52, 2011.

[14] F. T. L. van der Loop, G. Schaart, E. D. J. Timmer, F. C. S. Ramaekers, and G. J. J. M. van Eys, "Smoothelin, a novel cytoskeletal protein specific for smooth muscle cells," *Journal of Cell Biology*, vol. 134, no. 2, pp. 401–411, 1996.

[15] C. M. Shanahan, P. L. Weissberg, and J. C. Metcalfe, "Isolation of gene markers of differentiated and proliferating vascular smooth muscle cells," *Circulation Research*, vol. 73, no. 1, pp. 193–204, 1993.

[16] V. Lesauskaite, M. C. Epistolato, M. Castagnini, S. Urbonavicius, and P. Tanganelli, "Expression of matrix metalloproteinases, their tissue inhibitors, and osteopontin in the wall of thoracic and abdominal aortas with dilatative pathology," *Human Pathology*, vol. 37, no. 8, pp. 1076–1084, 2006.

[17] G. K. Owens, M. S. Kumar, and B. R. Wamhoff, "Molecular regulation of vascular smooth muscle cell differentiation in development and disease," *Physiological Reviews*, vol. 84, no. 3, pp. 767–801, 2004.

[18] G.-M. Zhu, H.-E. Guo, and W.-W. Zhang, "Knockdown of Notch3 expression in VSMC by RNA interference," *Chinese Journal of Geriatric Heart Brain and Vessel Diseases*, vol. 12, pp. 1127–1129, 2011.

[19] A. Ishiko, A. Shimizu, E. Nagata, K. Takahashi, T. Tabira, and N. Suzuki, "Notch3 ectodomain is a major component of granular osmiophilic material (GOM) in CADASIL," *Acta Neuropathologica*, vol. 112, no. 3, pp. 333–339, 2006.

[20] A. C. Doran, N. Meller, and C. A. McNamara, "Role of smooth muscle cells in the initiation and early progression of atherosclerosis," *Arteriosclerosis, Thrombosis, and Vascular Biology*, vol. 28, no. 5, pp. 812–819, 2008.

[21] S. Tikka, Y. Peng Ng, G. Di Maio et al., "CADASIL mutations and shRNA silencing of *NOTCH3* affect actin organization in cultured vascular smooth muscle cells," *Journal of Cerebral Blood Flow and Metabolism*, vol. 32, no. 12, pp. 2171–2180, 2012.

[22] C. P. Regan, P. J. Adam, C. S. Madsen, and G. K. Owens, "Molecular mechanisms of decreased smooth muscle differentiation marker expression after vascular injury," *Journal of Clinical Investigation*, vol. 106, no. 9, pp. 1139–1147, 2000.

[23] B. Shi, C. Cui, X. P. Long et al., "Effects of CGRP and CGRP receptor modified mesenchymal stem cells on proliferation and phenotypic transformation of vascular smooth muscle cells," *National Medical Journal of China*, vol. 93, no. 30, pp. 2372–2376, 2013.

[24] H. Gao, M. C. Steffen, and K. S. Ramos, "Osteopontin regulates α-smooth muscle actin and calponin in vascular smooth muscle cells," *Cell Biology International*, vol. 36, no. 2, pp. 155–161, 2012.

Hindawi Publishing Corporation
Evidence-Based Complementary and Alternative Medicine
Volume 2015, Article ID 358028, 8 pages
http://dx.doi.org/10.1155/2015/358028

Review Article

An Overview of Meta-Analyses of Danhong Injection for Unstable Angina

Xiaoxia Zhang,[1,2] Hui Wang,[3] Yanxu Chang,[2] Yuefei Wang,[2] Xiang Lei,[3] Shufei Fu,[3] and Junhua Zhang[3]

[1]*College of Management and Economics, Tianjin University, Tianjin 300072, China*
[2]*Tianjin State Key Laboratory of Modern Chinese Medicine, Tianjin University of Traditional Chinese Medicine, Tianjin 300193, China*
[3]*Institute of Traditional Chinese Medicine, Evidence-Based Medicine Center, Tianjin University of Traditional Chinese Medicine, Tianjin 300193, China*

Correspondence should be addressed to Xiaoxia Zhang; zhangxiaoxia@tjutcm.edu.cn and Junhua Zhang; zjhtcm@foxmail.com

Received 6 May 2015; Revised 29 July 2015; Accepted 4 August 2015

Academic Editor: Dan Hu

Objective. To systematically collect evidence and evaluate the effects of Danhong injection (DHI) for unstable angina (UA). *Methods*. A comprehensive search was conducted in seven electronic databases up to January 2015. The methodological and reporting quality of included studies was assessed by using AMSTAR and PRISMA. *Result*. Five articles were included. The conclusions suggest that DHI plus conventional medicine treatment was effective for UA pectoris treatment, could alleviate symptoms of angina and ameliorate electrocardiograms. Flaws of the original studies and systematic reviews weaken the strength of evidence. Limitations of the methodology quality include performing an incomprehensive literature search, lacking detailed characteristics, ignoring clinical heterogeneity, and not assessing publication bias and other forms of bias. The flaws of reporting systematic reviews included the following: not providing a structured summary, no standardized search strategy. For the pooled findings, researchers took statistical heterogeneity into consideration, but clinical and methodology heterogeneity were ignored. *Conclusion*. DHI plus conventional medicine treatment generally appears to be effective for UA treatment. However, the evidence is not hard enough due to methodological flaws in original clinical trials and systematic reviews. Furthermore, rigorous designed randomized controlled trials are also needed. The methodology and reporting quality of systematic reviews should be improved.

1. Introduction

A report from World Health Organization indicates that ischemic heart disease is a leading cause of death in the world [1, 2]. In 2010, 2150 deaths occurred every day in the United States due to cardiovascular disease (CVD). The direct and indirect cost of CVD was USD 3154 billion in 2010 in the United States [3]. Antiplatelet drugs [4], anticoagulant [5], nitrates [6, 7], calcium channel blockers [8], and beta blockers [9] are commonly used treatments for high-risk patients with CVD. However, many patients are still not satisfied with these routine treatments. Traditional Chinese medicinal drugs have been used for cardiovascular diseases for a long time. From the perspective of traditional Chinese medicine (TCM), the pathogenesis of UA is mainly blood stagnation [10]. Danhong injection (DHI), which is typically used to resolve blood stasis [11], has been widely used in clinical practice for the treatment of UA in China. DHI is made of the extraction from Danshen (the root and rhizome of *Salvia miltiorrhiza* Bge.) and Honghua (the flower of *Carthamus tinctorius* L.). The ingredients of DHI are mainly *Salvia* phenolic acids, flavonoids safflower, benzene diene glycosides, and nucleosides. Jiang et al. [12] identified 30 compounds in DHI, including mono- and oligo-saccharide, amino acids, and low-molecular-weight organic acids (Figure 1). The quantitative nuclear magnetic resonance (qNMR) technique is utilized to quantitatively measure amino acids, mono- and oligo-saccharide, and small molecular organic acids in DHI. This enhancement in technology enables the detection of ingredients previously undetectable using the HPLC-DAD method [13, 14]. Experimental studies have shown that DHI can increase coronary blood flow [15], improve cardiac

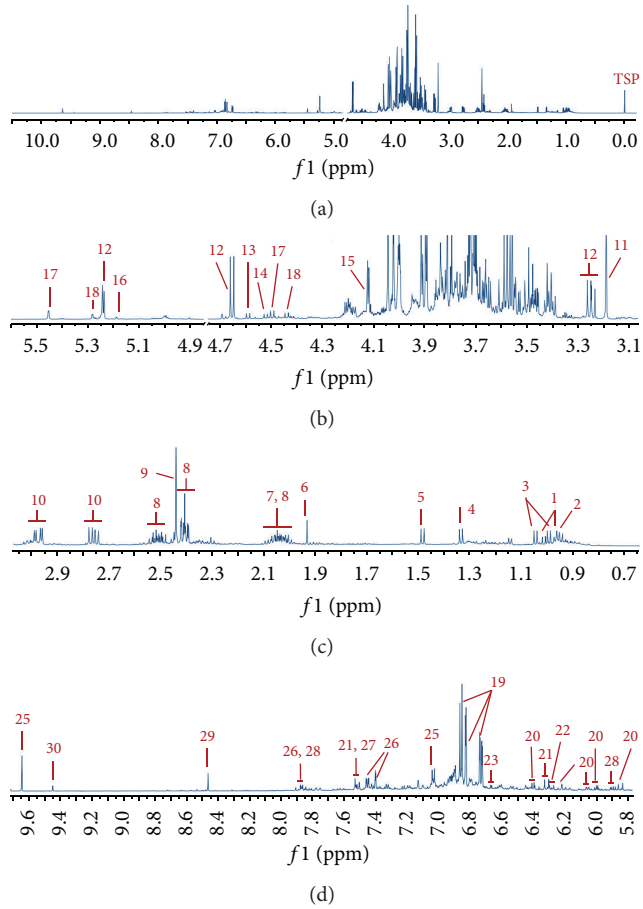

Figure 1: Representative ^{1}H NMR spectra of DHI. Peaks: 1, isoleucine; 2, leucine 3, valine; 4, threonine; 5, alanine; 6, acetate; 7, proline; 8, pyroglutamate; 9, succinate; 10, asparagine; 11, malonate; 12, glucose; 13, galactose; 14, arabinose; 15, fructose 16, rhamnose 17, rutinose 18, rutinulose; 19, salvianic acid; 20, salvianolic acid B; 21, rosmarinic acid; 22, lithospermic acid 23, salvianolic acid A; 24, procatechuic acid; 25, procatechuic aldehyde; 26, 4-hydroxybenzoic acid; 27, 4-hydroxycinnamic acid; 28, uridine; 29, formate; 30, 5-(hydroxymethyl)-2-furaldehyde.

microcirculation [16], scavenge for free radicals [17], prevent platelet aggregation [13], and accommodate blood lipids [18]. Meanwhile, some studies indicated that conventional intervention plus DHI can enhance the therapeutic effect and lessen side effects of chemical drugs [19, 20]. Many clinical trials of DHI for UA have been conducted and are mainly published in Chinese journals. Furthermore, there were also some published systematic reviews/meta-analyses about DHI for UA [19, 20]. However, the quality of methodology and the conclusions of the systematic reviews/meta-analyses have not been critically assessed. This paper aimed to evaluate the quality of published systematic reviews and summarize the clinical evidence of DHI for UA.

2. Method

2.1. Inclusion Criteria. Systematic reviews of DHI for UA were included irrespective of whether meta-analysis was used. Patients should be diagnosed as UA. There were no limitations to the publishing date, language, and outcome measures.

2.2. Literature Searching Strategy. Seven electronic literature databases were searched to recruit candidate studies up to January 2015. Three of the databases were English databases (PubMed, Web of Science, and the Cochrane Library), and the others were Chinese-literature databases (China National Knowledge Infrastructure, Wanfang Data, sinomed, and VIP Database for Chinese technical journals). The words used for English databases were "Danhong" OR "Dan hong" OR "Danhong Injection" AND "Systematic review" OR "meta-analysis" OR "systematic reviews" OR "meta analyse."

2.3. Quality Assessment

2.3.1. Assessment of the Methodological Quality. AMSTAR (a measurement tool to assess the methodological quality of systematic reviews) which is a reliable and valid measurement tool for the "assessment of multiple systematic reviews" was used in this study [24, 25]. AMSTAR consists of 11 items. For each item, there are four answer options: "cannot answer," "yes," "no," and "not applicable."

2.3.2. Assessment of the Reporting Quality. PRISMA (preferred reporting items for systematic reviews and meta-analyses) was used to assess the reporting quality of included

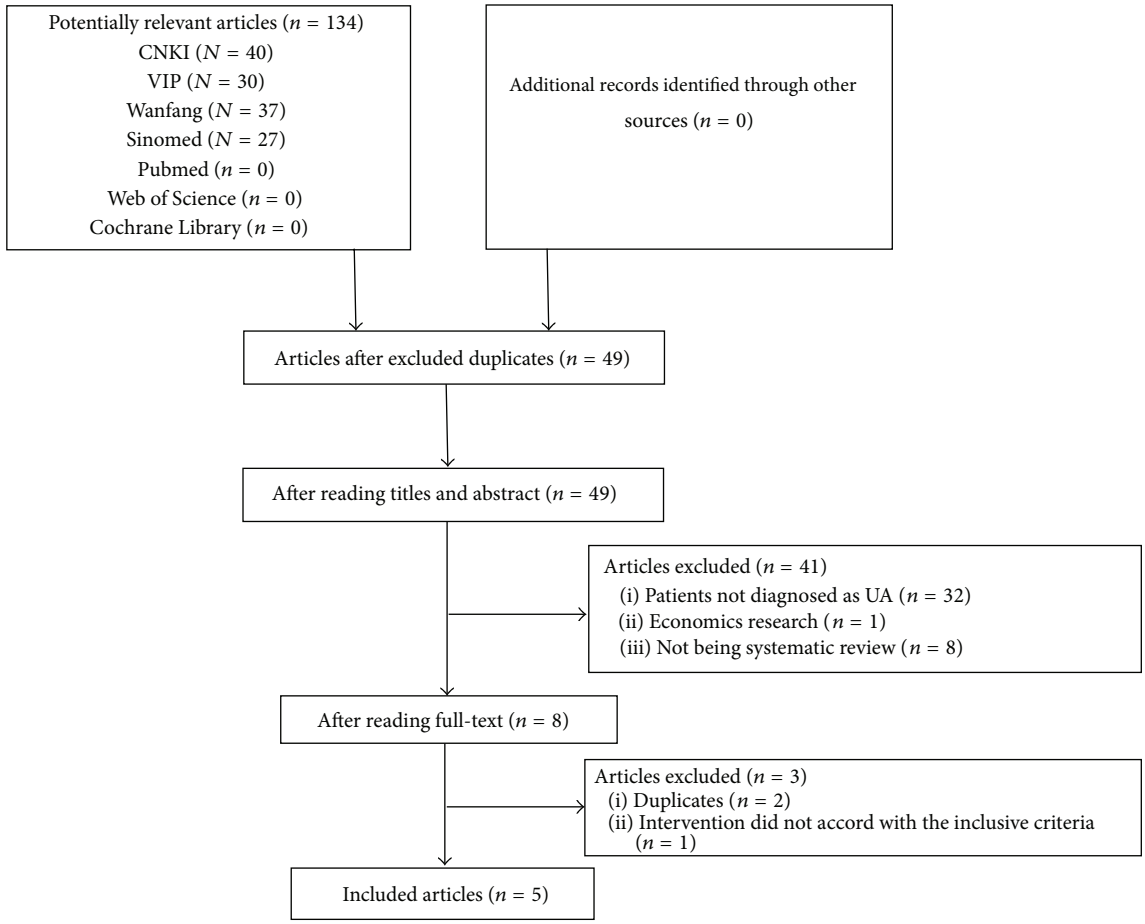

Figure 2: PRISMA 2009 flow diagram.

systematic reviews [26, 27]. Each included review was assessed by two independent reviewers (Xiaoxia Zhang and Hui Wang). Any disagreements were resolved by discussion with other authors. The PRISMA statement consists of 27 items and aims to improve the reporting quality of meta-analyses and systematic reviews. For each item, there are three answers: "adequate," "inadequate," and " inconformity."

3. Results

Initially, 134 articles were identified for further investigation according to the search strategy. After duplicates were removed, 49 records remained. After further screening, 41 studies were excluded according to the inclusion criteria. Three more studies were excluded after reading the full content. Finally, 5 studies were included for analyses (Figure 2).

3.1. Characteristics of Selected Studies. Five systematic reviews were published in Chinese from 2010 to 2012. There were 76 original studies with 7906 participants. As shown in Table 1, all included original studies are randomized clinical trials (RCT). The Jadad scores were used in 4 systematic reviews (the other one did not mention tool for quality evaluation), and most of the primary studies were of poor quality. A mean of 15 studies was included in each systematic review. The treatment courses of original studies ranged from 7 to 28 days. The main outcomes were alleviation of angina symptom and amelioration of electrocardiograms (ECG). The conclusions of the five studies were consistent, which suggest that DHI plus conventional medicine treatment was effective for UA pectoris treatment.

Wang and Hu [19] evaluated the effectiveness of DHI treatments for UA by a meta-analysis including 13 randomized controlled trials (RCTs) with 1183 participants: 623 patients in DHI treatment group and 560 patients in comparison group. The age of patients ranged from 31 to 84 years. There were 11 RCTs of DHI plus conventional treatment compared with the same conventional treatment. The remaining two RCTs were DHI compared with a 20 mL of Danshen injection and 5 mL of nitroglycerin based on conventional treatments. The meta-analysis showed that the DHI group performed significantly better than the control group in two parameters: angina symptoms (RAS) (OR = 4.98, 95% CI: 3.49~7.11) and ECG (OR = 2.48, 95% CI: 1.85~3.32). Two patients from the DHI group reported headaches, dizziness, and nausea, and 1 patient reported low blood pressure. After the drip speed of the intravenous drip was turned down, the patients recovered. There were 14 patients from the control group who reported headache. Among

Table 1: Characteristics of included trials.

Author Year	Electronic databases	Assessment tool of primary studies	Study type	Study time	Number of trails (participants)	Experiment group (participants)	Control group (participants)	Course (d)	Main outcome	Adverse events	Authors' conclusion
Wangand Hu, 2010 [19]※	VIP, CNKI, and Wanfang	Jadad	RCT	2000–2009	13 (1183)	CMT plus DHI (623)	CMT (560)	7–15	Effectiveness for RAS and ECG	Yes	Effectiveness of RAS and ECG Incidence of heart event
Xu et al., 2010 [20]	Cochrane Library, Medline, Embase, CBM disc, and CNKI	Jadad	RCT	1991–2010	9 (771)	CMT plus DHI (401)	CMT (370)	10–15	Effectiveness for RAS and ECG	No	Effectiveness and safety for UA
Xu et al., 2011 [21]	Cochrane Library, Medline, Embase, CBM disc, and CNKI	Jadad	RCT	1991–2009	19 (1940)	CMT plus DHI (991)	CMT (949)	10–21	Effectiveness for RAS and ECG	Yes	Effectiveness for UA
Yang et al., 2011 [22]	CNKI, Wanfang, VIP, and CBM disc	NM	RCT	2000–2010	12 (1337)	CMT plus DHI (NM)	CMT (NM)	NM	Effectiveness for ECG and RAS	NM	Effectiveness and safety for UA
Cui et al., 2012 [23]	Pubmed, Medline, CNKI, Wanfang, and Cochrane Library	Jadad	RCT	Up to 2010	23 (2675)	CMT plus DHI (1382)	CMT (1293)	10–28	Effectiveness for ECG and RAS Regulation of HDL-C, LDL-C, and HS-CRP	NM Or no	Effectiveness for ECG Regulation of HDL-C, LDL-C, and HS-CRP

DHI: Danhong injection; NM: not mentioned; CMT: conventional medicine treatment, including the combination of platelet aggregation inhibitor (aspirin), nitrates, beta-blockers, calcium channel blockers, and ACE inhibitors; RAS: resolution of angina symptoms; ECG: electrocardiogram; HDL-C: high density lipoprotein-cholesterol; LDL-C: low density lipoprotein-cholesterol; HS-CRP: high sensitive C-reactive protein; ※ indicates the intervention of 2 trials that were conventional medicine treatment plus DHI versus conventional medicine treatment plus Danshen injection; CNKI: China National Knowledge Infrastructure; CBM disc: Chinese Biology Medicine disc.

those 13 reports, no detailed information reported early termination or loss to follow-up. All the 13 articles were marked as low quality using the Jadad scale. Additionally, there was publication bias in the included articles.

Xu et al. [20] assessed the efficacy and safety of DHI treatments for UA in 9 RCTs, with a total of 771 participants aged 60 years or older. The meta-analysis showed that DHI plus conventional medicine was better than the conventional medicine alone in two outcome measures: RAS (OR = 3.83, 95% CI: 2.52~5.82) and ECG (OR = 2.51, 95% CI: 1.79~3.53). There was no report on adverse effects. All the included articles had low-quality grades according to the Jadad scale (score = 2). Publication bias was reported in the included articles.

Xu et al. [21] showed that DHI can effectively improve ECG (OR = 2.87, 95% CI: 2.30~3.59) and RAS (OR = 3.96, 95% CI: 3.00~5.24) in patients with UA. There were no severe adverse effects during treatment duration. There was 1 patient who appeared fatigued in DHI group. There were 2 patients who reported headaches, dizziness, and nausea in control group. Included studies were of low quality; only one reached 3 on Jadad score. There was publication bias based on the funnel plot. Few trials mentioned a randomization method or allocation concealment. Only one trial mentioned a method of blinding.

Yang et al. [22] examined 12 RCTs with 1337 participants ranging from 43 to 78 years of age. The meta-analysis showed that there was significant improvement of clinical symptoms in the DHI group compared with conventional medicine, RAS (OR = 4.01, 95% CI: 2.80~5.76). The difference between the two groups in ECG improvement was statistically significant (OR = 2.60, 95% CI: 1.98~3.41). Adverse events were not mentioned. Publication bias existed. Except for 2 trials (one that described single blinding and one that mentioned double-blinding); most of the trials did not mention blinding.

Cui et al. [23] assessed the effects of DHI on UA in 23 RCTs with a total of 2675 participants ranging from 39 to 82 years of age, and the duration of disease ranged from 21 days to 15 years. The results of the meta-analysis showed that the DHI group was superior to the control group in 5 parameters: ECG (RR = 2.84, 95% CI: 2.28~3.55), RAS (RR = 4.13, 95% CI: 3.12~5.47), increasing the serum level of HDLC (WMD = 0.29, 95% CI: 0.05~0.52), decreasing low density LDLC (WMD = −0.98, 95% CI: −1.33~0.63), and HS-CRP (WMD = −1.42, 95% CI: −2.18~−0.65). Adverse events were not mentioned, and no side effects were reported. More double-blinding RCTs with large-scale and high-quality are needed.

3.2. Quality of Methodology. Methodological quality of the included systematic reviews is summarized in Table 2. For the included 5 systematic reviews, none of them reported "a priori" designs. Literature searches were performed with keywords; however, the search strategy was not provided in the included reviews. Language bias existed in all 5 articles, and 2 reviews only searched Chinese databases.

All the reviews provided a list of included studies, while a list of excluded studies was not provided. The scientific quality of the included studies in formulating conclusions and methods used to combine the findings of studies were not appropriately used. A fixed-effects model was applied in 5 systematic reviews. None of the authors stated whether they included grey literature. Three (60%) of the studies showed that there was duplicate study selection and data extraction. Data were independently extracted by two researchers, and disagreements were resolved by discussion. The detailed characteristics of the included articles were provided in 3 (60%) articles. Funnel plots were applied in 3 (60%) reviews. The scientific quality of the studies were assessed and documented by 4 authors.

Table 2: Methodological quality assessment of systems review/meta-analysis [24, 25].

AMSTAR	Yes		No		Cannot answer		Not applicable	
Items	*n*	%	*n*	%	*n*	%	*n*	%
1	0	0	5	100	0	0	0	0
2	3	60	0	0	2	40	0	0
3	0	0	0	0	5	100	0	0
4	0	0	5	100	0	0	0	0
5	0	0	5	100	0	0	0	0
6	3	60	2	40	0	0	0	0
7	4	80	1	20	0	0	0	0
8	0	0	5	100	0	0	0	0
9	0	0	5	100	0	0	0	0
10	3	60	2	40	0	0	0	0
11	1	20	4	80	0	0	0	0

(1) Was an "a priori" design provided? (2) Were there duplicate study selection and data extraction? (3) Was a comprehensive literature search performed? (4) Was the status of publication (i.e., grey literature) used as an inclusion criterion? (5) Was a list of studies (included and excluded) provided? (6) Were the characteristics of the included studies provided? (7) Was the scientific quality of the included studies assessed and documented? (8) Was the scientific quality of the included studies used appropriately in formulating conclusions? (9) Were the methods used to combine the findings of studies appropriate? (10) Was the likelihood of publication bias assessed? (11) Was the conflict of interest stated?

3.3. Quality of Reporting. Quality of reporting was shown in Table 3. Reporting quality of included systematic reviews was generally poor. The sections of *title, abstract,* and *introduction* were inadequately reported in all the 5 reviews.

"Systematic review" or "meta-analysis" was stated in the titles of all the reports. However, whether the studies were systematic reviews, meta-analyses, or both was not identifiable from the titles.

In the *abstract* sections, structured summary was not clearly reported in all the systematic reviews.

In Section 1, rationale of doing a systematic review was not clearly reported in all the 5 reviews.

In Section 2, three items were well reported including eligibility criteria, data collection process, and summary measures. In the items of protocol and registration, search, synthesis of results, and additional analyses were inadequately reported in 5 reviews. Eligibility criteria were stated in the 5 reviews. Five studies stated their method of data extraction and the principal summary measures. Only two reviews stated a comprehensive electronic search database,

Table 3: Report quality evaluation of system review/meta-analysis.

PRISMA		Adequate		Inadequate		Inconformity	
Section/topic		*n*	%	*n*	%	*n*	%
Title	Title	0	0	5	100	0	0
Abstract	Structured summary	0	0	5	100	0	0
Introduction	Rationale	0	0	5	100	0	0
	Objectives	0	0	5	100	0	0
Methods	Protocol and registration	0	0	0	0	5	100
	Eligibility criteria	5	100	0	0	0	0
	Information sources	2	40	3	60	0	0
	Search	0	0	5	100	0	0
	Study selection	3	60	2	40	0	0
	Data collection process	5	100	0	0	0	0
	Data items	1	20	4	80	0	0
	Risk of bias in individual studies	3	60	2	40	0	0
	Summary measures	5	100	0	0	0	0
	Synthesis of results	0	0	5	100	0	0
	Risk of bias across studies	4	80	1	20	0	0
	Additional analyses	0	0	5	100	0	0
Results	Study selection	0	0	5	100	0	0
	Study characteristics	3	60	2	40	0	0
	Risk of bias within studies	3	60	2	40	0	0
	Results of individual studies	5	100	0	0	0	0
	Synthesis of results	0	0	5	100	0	0
	Risk of bias across studies	4	80	1	20	0	0
	Additional analysis	0	0	5	100	0	0
Discussion	Summary of evidence	1	20	4	80	0	0
	Limitations	0	0	5	100	0	0
	Conclusions	1	20	4	80	0	0
Funding		1	20	0	0	4	80

while others were lacking additional search information. All five studies did not provided search formula. There was no review describing the registration information. As for the synthesis of results and additional analysis, none of authors gave adequate descriptions. There were 3 reviews that presented the process for selecting studies and risk of bias of individual studies.

In Section 3, the reporting quality of *results of individual studies* was good. As for the three items including *study selection, synthesis of results,* and *additional analysis*, inadequate reporting was detected in 5 reviews. No review reported flow diagrams and present well-synthesized results. Clinical heterogeneity was ignored in the 5 reviews. Characteristics and risk of bias across studies were described in 3 reviews. Sensitivity analyses and subgroup analyses were not provided in all of the included studies.

In Section 4, only 1 review summarized the evidence. All researchers did not completely discuss the limitations.

Only one review presented sources of funding for the systematic review.

4. Discussion

4.1. Primary Outcomes. Five systematic reviews published from 2010 to 2012 drew the same conclusion that DHI plus conventional medicine treatment for UA is effective and safe in alleviating angina symptoms and ameliorating ECG. Four systematic reviews reported side effects, and one did not mention side effects. The rate of adverse effects is low from the included systematic reviews.

4.2. The Quality of Methodology and Reporting. Generally speaking, the quality of the included systematic reviews is low. The limitations of the methodology quality of those studies included the following: no a priori design was provided; incomprehensive literature searches was performed; and the search strategy was not provided in most of the included reviews. Language bias existed in all reviews. There were 3 reviews that only searched Chinese databases. None of the authors stated whether they included grey literature. Selection bias should be controlled in the processes of

study selection and data extraction. In each study, at least two independent data extractors participated, and disagreements should be checked. For meta-analysis, researchers only checked the statistical heterogeneity, but clinical and methodology heterogeneity were ignored. So, the results of meta-analyses might be incorrect or meaningless.

The flaws in reporting included the following: systematic reviews and meta-analyses were not clear in the title of reviews and the main content of the article did not show up in the summary. All the five systematic reviews were published from 2010 to 2012. In accordance with the requirements of systematic reviews, the rationale of the research should be demonstrated. In addition, the necessity and significance of doing a systematic reviews should be described in the introduction. However, the follow-up studies did not mention previously published systematic reviews; that is, the follow-up studies did not fully demonstrate rationale. In conclusion, systematic reviews of some TCM were done without clinical or scientific significance, which might be due to no registration mechanism for systematic reviews in TCM. No studies specified search strategies; thus, selection bias cannot be ignored. Although flow diagrams were an ideal tool to illustrate study selection, they were not used in the five reviews.

Because not all the characteristics of studies were presented (e.g., course, follow-up period, and interventions), clinical and methodology heterogeneity were hard to evaluate. In the synthesis of results, researchers considered statistical heterogeneity, but clinical and methodology heterogeneity were ignored. Clinical and methodology heterogeneity were significant among the original clinical trials. So, dogmatic data combing with different controls, follow-up periods, and interventions would affect the result of meta-analyses. Limitations were not adequately discussed and did not deeply analyze the risk of bias such as whether the outcome and course were reasonable. The requirement of the reporting of system reviews was not strictly enforced in Chinese journals, leading to poor quality of reporting; thus, training concerning relevant knowledge is needed for journal editors.

4.3. Limitations of Current Evidence. The flaws in methodology and reporting weaken the results of systematic reviews. Improper use of meta-analysis will exaggerate the bias and draw the wrong conclusions. In addition to publication bias and incomprehensive search, all the included reviews were published in Chinese and reached positive conclusions, which affected the quality of the systematic reviews.

There were some limitations for this study. Inaccurate assessment of each item in AMSTAR and PRISMA may exist due to subjective judgment. Inadequate reporting of systematic reviews affected the evaluation process although inconsistencies were solved by discussion.

5. Conclusions

This study summarized the evidence of DHI for UA and obtained a positive result. However, poor quality of systematic reviews/meta-analyses affected reliability of current evidence. In the future, rigorous clinical trials with larger samples are needed to confirm this conclusion. The methodological and reporting quality of systematic reviews and meta-analysis should be improved.

Conflict of Interests

The authors declare that there is no conflict of interests.

Authors' Contribution

Xiaoxia Zhang and Hui Wang contributed equally to this paper. Xiaoxia Zhang and Hui Wang performed literature search, data extraction, data analysis, and paper preparation. Yanxu Chang and Yuefei Wang performed chemical ingredients analyses and paper preparation. Xiang Lei and Shufei Fu performed literature search and selection. Junhua Zhang performed protocol design, quality evaluation, and data analysis.

Acknowledgments

This work was supported by the Tianjin Research Program of Application Foundation and Advanced Technology (12JCQNJC08800 and 13ZLZLZF03400) and the National Key Basic Research Program (973 Project, nos. 2014CB542902 and 2012CB518401).

References

[1] World Health Orgnizaton, *World Health Statistics Annual*, World Health Orgnizaton, Geneva, Switzerland, 2012, http://www.who.int/mediacentre/factsheets/fs310/en/.

[2] C. J. L. Murray and A. D. Lopez, "Mortality by cause for eight regions of the world: Global Burden of Disease Study," *The Lancet*, vol. 349, no. 9061, pp. 1269–1276, 1997.

[3] E. A. Amsterdam, N. K. Wenger, R. G. Brindis et al., "2014 AHA/ACC Guideline for the management of patients with non-st-elevation acute coronary syndromes: executive summary: a report of the American college of cardiology/American heart association task force on practice guidelines," *Circulation*, vol. 130, no. 25, pp. 2354–2394, 2014.

[4] A. B. McCann and M. R. Jaff, "Treatment strategies for peripheral artery disease," *Expert Opinion on Pharmacotherapy*, vol. 10, no. 10, pp. 1571–1586, 2009.

[5] D. T. Mangano, "Aspirin and mortality from coronary bypass surgery," *The New England Journal of Medicine*, vol. 347, no. 17, pp. 1309–1317, 2002.

[6] N. Hirai, H. Kawano, H. Yasue et al., "Attenuation of nitrate tolerance and oxidative stress by an angiotensin II receptor blocker in patients with coronary spastic angina," *Circulation*, vol. 108, no. 12, pp. 1446–1450, 2003.

[7] U. Thadani, "Nitrate tolerance, rebound, and their clinical relevance in stable angina pectoris, unstable angina, and heart failure," *Cardiovascular Drugs and Therapy*, vol. 10, no. 6, pp. 735–742, 1997.

[8] P. Chandrasekar and A. Wilbert, "Treatment of stable angina pectoris," *American Journal of Therapeutics*, vol. 18, no. 5, pp. 138–152, 2011.

[9] R. L. Frye, P. August, M. M. Brooks et al., "A randomized trial of therapies for type 2 diabetes and coronary artery disease," *The New England Journal of Medicine*, vol. 360, no. 24, pp. 2503–2515, 2009.

[10] K.-W. Yao, Q.-Y. He, F. Teng, and J. Wang, "Logistic regression analysis of syndrome essential factors in patients with unstable angina pectoris," *Journal of Traditional Chinese Medicine*, vol. 31, no. 4, pp. 273–276, 2011.

[11] J. P. Yang, X. J. Wang, and F. Zhao, "Advances in clinical application of Danhong injection in the treatment of cardiovascular and cerebrovascular diseases," *Contemporary Medicine*, vol. 20, no. 13, pp. 144–145, 2014.

[12] M. Jiang, Y. Jiao, Y. Wang et al., "Quantitative profiling of polar metabolites in herbal medicine injections for multivariate statistical evaluation based on independence principal component analysis," *PLoS ONE*, vol. 9, no. 8, Article ID e105412, 2014.

[13] H.-T. Liu, Y.-F. Wang, O. Olaleye et al., "Characterization of in vivo antioxidant constituents and dual-standard quality assessment of Danhong injection," *Biomedical Chromatography*, vol. 27, no. 5, pp. 655–663, 2013.

[14] X. Liu, Z. Z. Wu, K. Yang, H. Y. Ding, and Y. J. Wu, "Quantitative analysis combined with chromatographic fingerprint for comprehensive evaluation of Danhong injection using HPLC-DAD," *Journal of Pharmaceutical and Biomedical Analysis*, vol. 76, pp. 70–74, 2013.

[15] Y. Liu, H.-J. Yin, D.-Z. Shi, and K.-J. Chen, "Chinese herb and formulas for promoting blood circulation and removing blood stasis and antiplatelet therapies," *Evidence-Based Complementary and Alternative Medicine*, vol. 2012, Article ID 184503, 8 pages, 2012.

[16] H. Fan, Y. Z. Shen, and X. H. Wang, "Effect of Danhong injection on the microcirculation of patients with acute pancreatitis," *Beijing Medical Journal*, vol. 2, no. 2, pp. 43–45, 2009.

[17] L.-M. Wan, L. Tan, Z.-R. Wang et al., "Preventive and therapeutic effects of Danhong injection on lipopolysaccharide induced acute lung injury in mice," *Journal of Ethnopharmacology*, vol. 149, no. 1, pp. 352–359, 2013.

[18] J. Luo and H. Xu, "Outcome measures of Chinese herbal medicine for coronary heart disease: an overview of systematic reviews," *Evidence-Based Complementary and Alternative Medicine*, vol. 2012, Article ID 927392, 9 pages, 2012.

[19] Z. X. Wang and Y. Hu, "Meta-analysis of Danhong injection in treating unstable angina pectoris," *Chinese Journal of Hospital Pharmacy*, vol. 30, no. 19, pp. 1671–1674, 2010.

[20] G. L. Xu, H. Xu, H. Y. Cao, and L. Qin, "A systemic review of Danhong injection in treating elderly patients with unstable angina," *Liaoning Journal of Traditional Chinese Medicine*, vol. 37, no. 10, pp. 1960–1962, 2010.

[21] G. L. Xu, S. M. Lin, H. Xu, and L. Qin, "Meta analysis of Danhong injection in the treatment of unstable angina," *Lishizhen Medicine and Materia Medica Research*, vol. 22, no. 3, pp. 765–767, 2011.

[22] T. F. Yang, W. Zhang, Z. X. Ding, and X. X. Wang, "Meta-analysis of Danhong injection in the treatment of unstable angina," *China Pharmacy*, vol. 22, no. 15, pp. 1423–1425, 2011.

[23] R. Cui, K. Xia, P. Shi, and X. M. Nie, "Danhong injection combined conventional western medicine treatmentof unstable angina efficacy and safety evaluation system," *Journal of Anhui Traditional Chinese Medical College*, vol. 31, no. 1, pp. 14–19, 2012.

[24] B. J. Shea, J. M. Grimshaw, G. A. Wells et al., "Development of AMSTAR: a measurement tool to assess the methodological quality of systematic reviews," *BMC Medical Research Methodology*, vol. 7, article 10, pp. 133–139, 2007.

[25] J. Xiong and R.-X. Chen, "An introduction to a measurement tool to assess the methodological quality of systematic reviews/meta-analysis: AMSTAR," *Chinese Journal of Evidence-Based Medicine*, vol. 11, no. 9, pp. 1084–1089, 2011.

[26] K. Knobloch, U. Yoon, and P. M. Vogt, "Preferred reporting items for systematic reviews and meta-analyses (PRISMA) statement and publication bias," *Journal of Cranio-Maxillofacial Surgery*, vol. 39, no. 2, pp. 91–92, 2011.

[27] D. Moher, A. Liberati, J. Tetzlaff, and D. G. Altman, "Preferred reporting items for systematic reviews and meta-analyses: the PRISMA statement," *Journal of Clinical Epidemiology*, vol. 62, pp. 1006–1012, 2009.

Hindawi Publishing Corporation
Evidence-Based Complementary and Alternative Medicine
Volume 2015, Article ID 270498, 7 pages
http://dx.doi.org/10.1155/2015/270498

Research Article

The Clinical Relevance of Serum NDKA, NMDA, PARK7, and UFDP Levels with Phlegm-Heat Syndrome and Treatment Efficacy Evaluation of Traditional Chinese Medicine in Acute Ischemic Stroke

Xiuxiu Han,[1] Yonghong Gao,[2] Bin Ma,[1] Ying Gao,[1] Yikun Sun,[2] Ru Jiang,[1] and Yayun Wang[1]

[1]*Department of Neurology, Dongzhimen Hospital Affiliated to Beijing University of Chinese Medicine, Beijing 100700, China*
[2]*Key Laboratory of Chinese Internal Medicine of Ministry of Education, Dongzhimen Hospital Affiliated to Beijing University of Chinese Medicine, Beijing 100700, China*

Correspondence should be addressed to Bin Ma; mabin0352@126.com

Received 8 May 2015; Revised 16 August 2015; Accepted 23 August 2015

Academic Editor: Dan Hu

According to the methods of Patient-Reported Outcome (PRO) based on the patient reports internationally and referring to U.S. Food and Drug Administration (FDA) guide, some scholars developed this PRO of stroke which is consistent with China's national conditions, and using it the feel of stroke patients was introduced into the clinical efficacy evaluation system of stoke. "Ischemic Stroke TCM Syndrome Factor Diagnostic Scale (ISTSFDS)" and "Ischemic Stroke TCM Syndrome Factor Evaluation Scale (ISTSFES)" were by "Major State Basic Research Development Program of China (973 Program) (number 2003CB517102)." ISTSFDS can help to classify and diagnose the CM syndrome reasonably and objectively with application of syndrome factors. Six syndrome factors, internal-wind syndrome, internal-fire syndrome, phlegm-dampness syndrome, blood-stasis syndrome, qi-deficiency syndrome, and yin-deficiency syndrome, were included in ISTSFDS and ISTSFES. TCM syndrome factor was considered to be present if the score was greater than or equal to 10 according to ISTSFDS. In our study, patients with phlegm-heat syndrome were recruited, who met the diagnosis of both "phlegm-dampness" and "internal-fire" according to ISTSFDS. ISTSFES was used to assess the syndrome severity; in our study it was used to assess the severity of phlegm-heat syndrome (phlegm-heat syndrome scores = phlegm-dampness syndrome scores + internal-fire syndrome scores).

1. Introduction

With the aging of the global population, stroke and related diseases have become a serious threat to human health [1]. Recent studies have shown that stroke has become the leading cause of death in China [2], in which ischemic stroke patients account for about 80% of all stroke patients [3] with a high morbidity. Traditional Chinese medicine (TCM) plays an important role in the prevention and treatment of strokes in China. The application of laboratory technology has been widely used for explaining the nature of the syndrome in stroke diseases. Moreover, biological markers have played an important role in the clinical diagnosis and treatment evaluation in many diseases. In general, biological markers closely associated with the pathogenesis of cerebral ischemia and reperfusion, blood-brain barrier damage, and cerebral infarction could be used for the diagnosis and clinical evaluation of acute ischemic stroke as a microindicator and are becoming a hot research topic.

Recent studies have demonstrated an association between stroke syndromes and changes in biological markers [4, 5]. For example, interleukin-6 (IL-6) and tumor necrosis factor-α (TNF-α) have been demonstrated to be positively associated with the fire-heat syndrome scores in acute ischemic stroke patients and it was suggested that elevated IL-6 and TNF-α levels can be used as indicators to distinguish between

the fire-heat and non-fire-heat syndrome [6]. For a biomarker to be of optimal use, it should be rapid, cost-effective, specific, sensitive, as is the case for B-type natriuretic peptide (BNP) in the assessment of congestive heart failure [7]. However, there is still a lack of specific biomarkers for diagnosis of TCM syndromes of acute stroke [8].

Currently, the "integrating disease and syndrome" evaluation model is a widely acceptable model for clinical efficacy evaluation of TCM stroke by the TCM scholars [9]. This model combines the evaluation methods of Chinese and western medicine. For instance, at the disease level, the model adopted the US National Institutes of Health Stroke Scale (NIHSS) [10], Barthel Index (BI) [10], and Patient-Reported Outcome (PRO) [11], which are mature efficacy evaluation scales in western medicine. The evaluation of the level of the syndrome used the "Ischemic Stroke TCM Syndrome Factor Diagnostic Scale (ISTSFDS)" and "Ischemic Stroke TCM Syndrome Factor Evaluation Scale (ISTSFES)" [12]. Although the objectivity of clinical efficacy evaluation has been improved by the combination of these scales, the model lacks accurate and objective laboratory parameters to evaluate the clinical efficacy of acute stroke [13].

Analyzing current literatures linked with ischemic stroke, we found some novel biological indicators as follows: NDKA (nucleoside diphosphate kinase A) is an ubiquitous enzyme that catalyzes the exchange of terminal phosphate between different nucleoside diphosphates and is thought to be involved in the ischemic cascade after stroke [14, 15]. Previous studies found that NDKA was an early biomarker since its level was already elevated in blood of patients within 3 h after the stroke onset [15, 16]. The excitatory NMDA (N-methyl-D-aspartate) receptor is one of the key regulators of nerve cell membrane functions in the process embolic or thrombotic vascular occlusion stimulating the cascade of neurotoxicity, causing biochemical changes in brain tissue, the blood-brain barrier, and brain vessels. Recently, researches had investigated antibodies to the glutamate NDMA-R that had a 97% sensitivity and 98% specificity to distinguish ischemic stroke from control at 3 h [17]. PARK7 (Polyploidy-Associated Protein Kinase) is a highly conserved protein with unclear function. Allard et al. found that serum PARK7 levels were significantly increased in stroke patients 30 min to 3 hrs after onset with a sensitivity of 54%–91% and specificity of 80%–90% in diagnosis of stroke [15]. The studies found that UFDP (ubiquitin fusion degradation protein 1) was increased in human postmortem CSF, a model of global brain insult, and also was released in the blood of patients affected by a brain injury [18]. These biomarkers maybe used in clinical practice in further as indexes for diagnosis in acute ischemic stroke.

In this study, we examined the association between serum NDKA, NMDA, PARK7, and UFDP levels and the phlegm-heat syndromes of acute ischemic stroke and explored their value in evaluating the clinical efficacy of stroke.

2. Materials and Methods

2.1. Participants. Biological samples and medical records of fifty-one stroke patients with phlegm-heat syndrome that met the inclusion and exclusion criteria were obtained to form a biomarkers and clinical information database, which was established since January 2009 by the Clinical Research Centers of Dongzhimen Hospital, Beijing University of Chinese Medicine. The inclusive criteria were (1) meeting the diagnosis of cerebral infarction according to the "2010 China acute ischemic stroke diagnosis and treatment guidelines"; (2) both the diagnosis of "phlegm-dampness" and "internal-fire" existing (phlegm-dampness syndrome scores ≥10 points, internal-fire syndrome scores ≥10 points) according to the "Ischemic Stroke TCM Syndrome Factor Diagnostic Scale (ISTSFDS)"; (3) NIHSS scores being ≥5 points, but ≤22 points; (4) onset being within 72 hours; and (5) age being ≤75 years and ≥35 years. The exclusion criteria were (1) patients who were diagnosed with transient ischemic attack or cerebral hemorrhage or subarachnoid hemorrhage and (2) patients who had drag-over disease with liver, kidney, hematopoietic system, and endocrine system diseases, bone and joint diseases, mental illness, dementia, stroke sequelae, and stroke caused by brain tumor, traumatic brain injury, blood disease, and rheumatic heart disease. Ninety-five age and gender matched healthy people were recruited as controls. Signed informed consents were obtained from all subjects.

2.2. Clinical Evaluation. Basic information such as age and sex and fasting blood samples were collected from healthy controls. The clinical data for each patient was collected by the neurologist.

2.2.1. General Information. The demographic data, medical history, lifestyle, blood test information (blood count, blood chemistry, blood clotting, etc.), and imaging data (CT or head MRI) of the 51 patients were collected at the day of recruiting.

2.2.2. Biological Samples. Five mL of venous blood was collected from patients within 3 days of onset and 7 and 14 days after onset. The serum NDKA, NMDA, PARK7, and UFDP levels were measured using the enzyme-linked immunosorbent assay kits by following the manufacturer's instruction.

2.2.3. The Observations of Therapeutic Efficacy. The evaluation of clinical therapeutic efficacy in stroke patients included disease evaluation and syndrome evaluation. Disease evaluation used the NIHSS (National Institutes of Health Stroke Scale) to assess the neurological impairment. Syndrome evaluation used the "Ischemic Stroke TCM Syndrome Factor Evaluation Scale (ISTSFES)" to assess the syndrome severity (phlegm-heat syndrome scores = phlegm-dampness syndrome scores + internal-fire syndrome scores). Evaluation point is within 3 days of onset and at day 7 and day 14 after onset (Figure 1).

2.3. Statistical Analysis. Statistical analyses were performed using SPSS 21 software (IBM, NC, USA). Data with normal distribution were expressed as mean ± standard errors. If the data showed homogeneity of variance, differences between

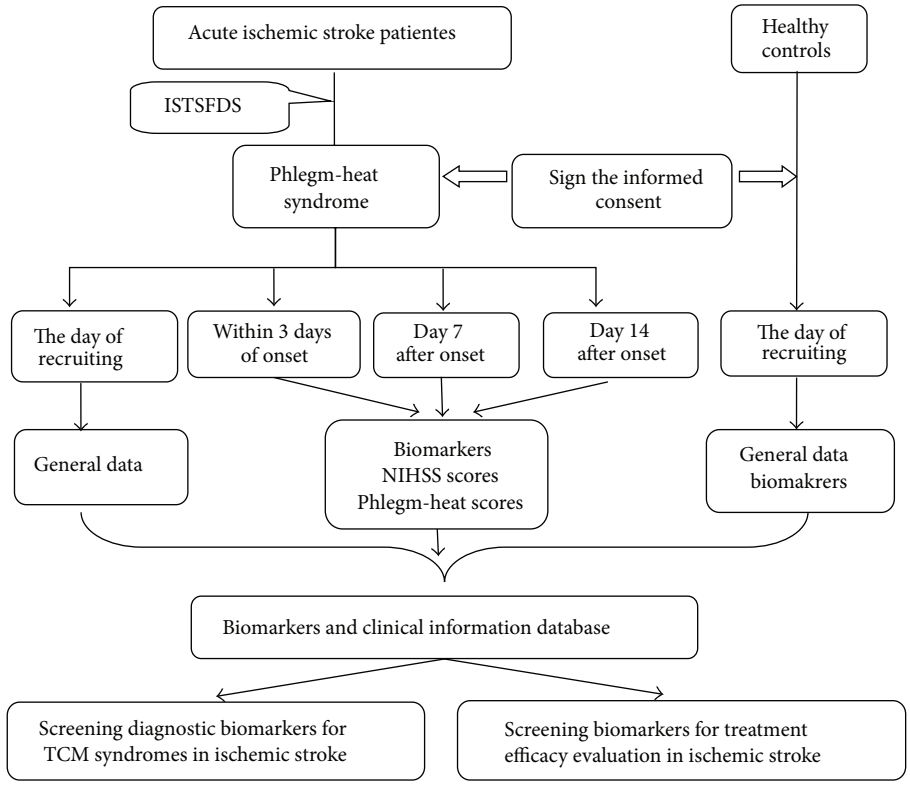

Figure 1: Flow chart of the study.

groups were analyzed using independent samples t-test. If not, differences between groups was analyzed using nonparametric tests (Kruskal-Wallis H test). The receiver operating characteristic curve (ROC) analysis was used to elucidate the diagnostic value of biological markers for phlegm-heat syndrome. Single factor repeated measures analysis was used for assessment of the variance in biological indicators, NIHSS scores, and phlegm-heat syndrome scores in stroke patients within 3 days of onset and at 7 and 14 days after onset. Linear regression analysis was used for the correlation between changes of biological parameters and NIHSS scores or phlegm-heat syndrome scores. $P < 0.05$ was considered statistically significant.

Table 1: General data.

Items	Patients	Healthy controls
N	51	95
Age (Yr., $\overline{x} \pm s$)	62.27 ± 9.27	31.23 ± 9.74
Females (case (%))	43.1	46.3
Hypertension (case (%))	28 (54.9)	NA
Coronary heart disease (case (%))	9 (17.6)	NA
Diabetes mellitus (case (%))	9 (17.6)	NA
Hyperlipidemia (case (%))	16 (31.4)	NA
Previous stroke (case (%))	22 (43.1)	NA
Smoking (case (%))	18 (35.3)	NA
Alcohol (case (%))	10 (19.6)	NA

Note. NA indicates not applicable.

3. Results

3.1. General Data. This study included 95 healthy controls and 51 patients. The general characteristics, including gender and age of healthy controls, were collected, and, beyond that, diseases of hypertension, diabetes mellitus and so forth of patients were collect (Table 1).

3.2. Serum NDKA, NMDA, PARK7, and UFDP Levels and Diagnosis Value. Differences in these four biomarkers between ischemic stroke patients within 3 days of onset and healthy controls was analyzed using independent samples t-test or nonparametric tests (Kruskal-Wallis H test). The result showed a significant difference in serum PARK7 ($P = 0.003$) and UFDP ($P = 0.045$) between groups; in contrast, there was no significant difference in serum NDKA ($P = 0.384$) and NMDA ($P = 0.774$) between groups. Comparing the mean of these two groups, we found that the serum NMDA and PARK7 levels were higher than that in the healthy controls, whereas the serum NDKA and UFDP levels were lower than that in the healthy controls (Figure 2(a)).

Receiver operator characteristic curves (ROC) were used to evaluate the diagnostic value of the biological markers in the early stage of stroke with phlegm-heat syndrome. Results showed that NMDA, PARK7, and UFDP exhibited certain diagnostic accuracy with an AUC of 0.639, 0.669, and

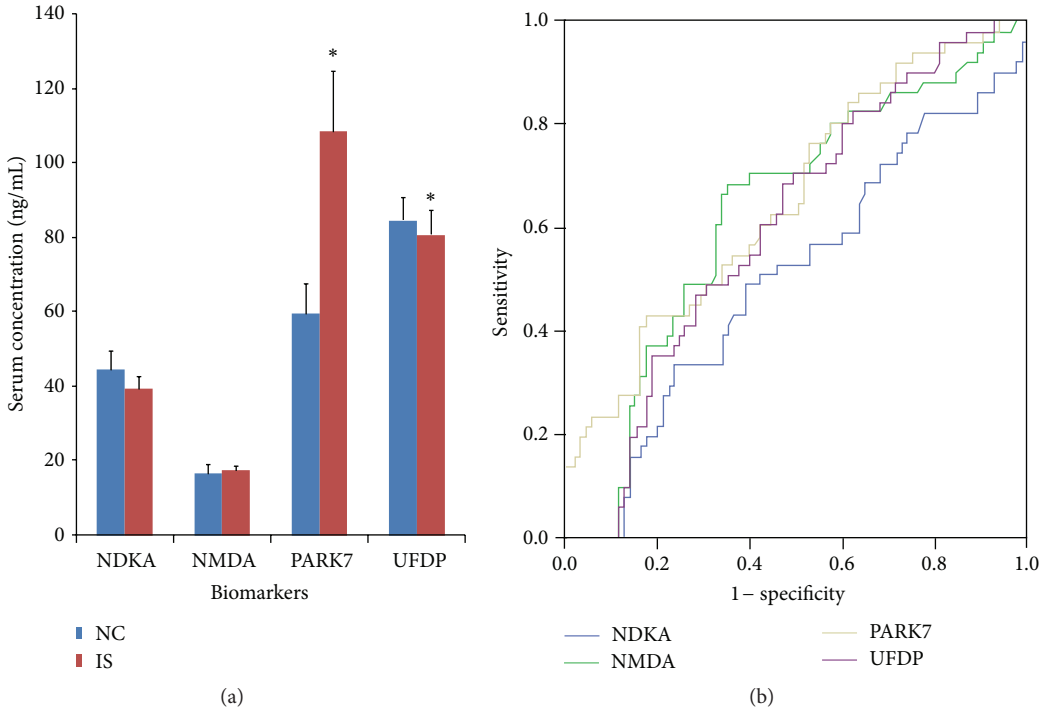

Figure 2: Serum NDKA, NMDA, PARK7, and UFDP levels and diagnostic value of phlegm-heat syndrome in acute ischemic stroke. (a) Comparison of serum NDKA, NMDA, PARK7, and UFDP levels between stroke patients within 3 days of onset and healthy controls. $^{*}P < 0.05$ versus controls. (b) Receiver operator characteristic (ROC) curves of serum NDKA, NMDA, PARK7, and UFDP levels. The area under ROC was 0.501, 0.639, 0.669, and 0.634, respectively.

0.634, respectively, and specificity of 54.1%–83.5%. The cut-off values of serum NMDA, PARK7, and UFDP levels for the diagnosis of phlegm-heat syndrome were 11.465 ng/mL, 74.152 ng/mL, and 46.950 ng/mL, respectively (Figure 2(b)). Serum NDKA level showed no diagnostic accuracy for the phlegm-heat syndrome (AUC 0.501) (Figure 2(b)).

3.3. Dynamic Changes in NDKA, NMDA, PARK7, and UFDP Levels. Single factor repeated measures analysis was used to measure the dynamic changes in serum NDKA, NMDA, PARK7, and UFDP levels within 3 days of onset and 7 and 14 days after the onset. Mauchly sphericity test showed that there was significant association between repeated measures data of NDKA ($W = 0.841$, $P = 0.014$) and PARK7 ($W = 0.664$, $P = 0.000$) and the need for freedom correction. In contrast, no significant associations between repeated measures data of NMDA ($W = 0.936$, $P = 0.198$) and UFDP ($W = 0.954$, $P = 0.318$) were observed and there was no need for freedom correction. ANOVA analysis showed a significant difference in serum NMDA ($F = 5.301$, $P = 0.006$), PARK7 ($F = 17.472$, $P = 0.000$), and UFDP ($F = 10.518$, $P = 0.000$) levels between 3 time points. In contrast, no significant difference in serum NDKA ($F = 0.784$, $P = 0.446$) level was observed between 3 time points. The pairwise comparison showed that the serum level of NMDA within 3 days was not significantly different from the level at 7 days ($P = 0.564$), whereas significant differences in serum NMDA levels were observed between the levels within 3 days and 14 days ($P = 0.009$) and between 7 days and 14 days ($P = 0.009$). Similarly, serum PARK7 and UFDP levels within 3 days were not significantly different from the levels on day 7 ($P = 0.977$ and $P = 0.868$, resp.), but significant differences were observed between the levels within 3 days and at day 14 ($P = 0.000$) and between day 7 and day 14 ($P = 0.000$ and $P = 0.009$, resp.) (Figure 3(a)). These observations suggested that serum NMDA, PARK7, and UFDP levels showed an increasing trend within 14 days of onset.

3.4. Correlations between Serum NDKA, NMDA, PARK7, and UFDP Levels and Treatment Efficacy Evaluation in Stroke Patients

3.4.1. Correlations between These Biomarkers Levels and the Therapeutic Efficacy of Disease. The NIHSS Scale (NIH Stroke Scale) was used to evaluate the severity of defects in neural function in acute stroke patients as to the severity of stroke disease within 3 days of onset and at day 7 and day 14 after the onset of stroke. Single factor repeated measures analysis was used to measure its dynamic changes. Mauchly sphericity test revealed a significant association between repeated measures NIHSS scores ($W = 0.621$, $P = 0.000$) and the need for freedom correction. ANOVA analysis showed a significant difference in the NIHSS scores ($F = 57.641$, $P = 0.000$) between 3 time points. The pairwise comparison of two time points showed significant difference in NIHSS scores between the scores within 3 days and at day 7 or

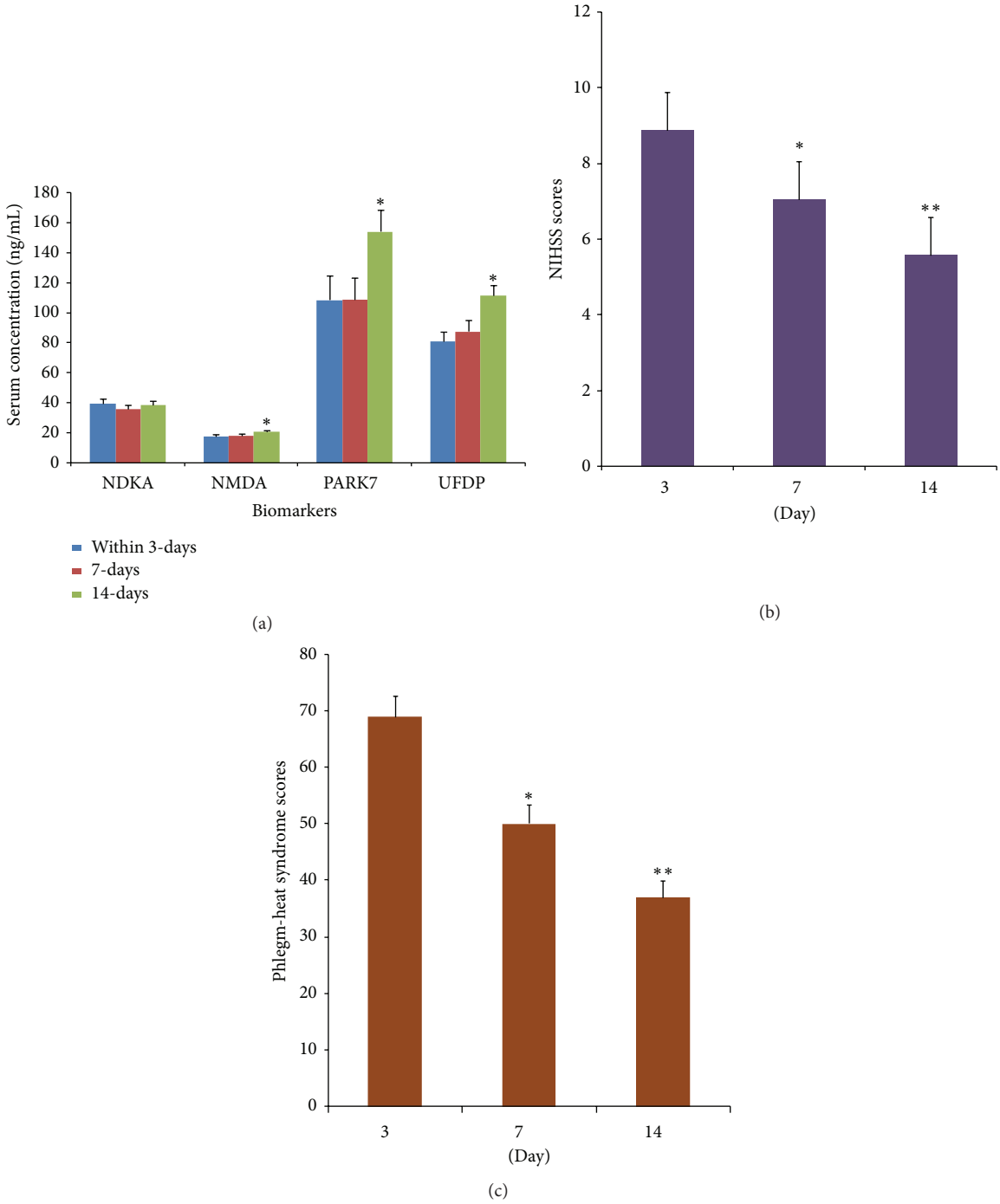

FIGURE 3: Dynamic changes of serum biological markers and scale scores of therapeutic efficacy in patients within 3 days of onset and 7 and 14 days after onset of stroke. (a) Serum NDKA, NMDA, PARK7, and UFDP levels in patients within 3 days of onset and 7 and 14 days after onset of stroke. $^{*}P < 0.05$ (14 days versus 7 days and 3 days). (b) NIHSS scores within the onset of 3 days and 7 and 14 days after onset. $^{*}P < 0.05$ (3 days versus 7 days), $^{**}P < 0.05$ (7 days versus 14 days). (c) Phlegm-heat syndrome scores within the onset of 3 days and 7 and 14 days after onset. $^{*}P < 0.05$ (3 days versus 7 days), $^{**}P < 0.05$ (7 days versus 14 days).

day 14 after onset ($P = 0.000$) and between day 7 and day 14 after onset ($P = 0.000$). These observations suggested that NIHSS scores were decreased gradually, indicating the gradual improvement in neurological functions and disease condition (Figure 3(b)).

Correlation analysis between changes of day 7 and day 14 serum NDKA, NMDA, PARK7, and UFDP levels (dependent variable) and NIHSS scores (independent variable) showed that serum NDKA, NMDA, PARK7, and UFDP levels were not significantly associated with NIHSS scores ($P > 0.05$)

Table 2: Correlation between NIHSS scores and serum NDKA, NMDA, PARK7, and UFDP levels.

Dependent variables	Independent variable	r	P
NDKA	NIHSS scores	−0.056	0.696
NMDA		0.050	0.727
PARK7		0.086	0.546
UFDP		0.149	0.295

Table 3: Correlation between phlegm-heat syndrome scores and serum NDKA, NMDA, PARK7, and UFDP levels.

Dependent variables	Independent variable	r	P
NDKA	Phlegm-heat syndrome scores	0.074	0.608
NMDA		−0.206	0.146
PARK7		−0.111	0.437
UFDP		−0.218	0.125

(Table 2). These results suggested that serum NDKA, NMDA, PARK7, and UFDP levels are not biomarkers to evaluate the therapeutic efficacy of disease in stroke patients.

3.4.2. Correlations between These Biomarkers Levels and the Therapeutic Efficacy of Phlegm-Heat Syndrome. The ischemic stroke syndrome rating scale was used to evaluate the severity of syndrome within 3 days and at day 7 and day 14 of the onset of stroke. Single factor repeated measures analysis was used to measure its dynamic changes. Mauchly sphericity test revealed a significant association between repeated measured phlegm-heat syndrome scores ($W = 0.655$, $P = 0.000$) and the need for freedom correction. ANOVA analysis showed a significant difference in the phlegm-heat syndrome scores between the 3 time points ($F = 62.462$, $P = 0.000$). The pairwise comparison of two time points showed significant difference in phlegm-heat syndrome scores between the scores within 3 days and at day 7 or day 14 after onset ($P = 0.000$) and between day 7 and day 14 ($P = 0.000$). These observations suggested that phlegm-heat syndrome scores were decreased gradually, indicating the gradual improvement in phlegm-heat syndrome (Figure 3(c)).

Correlation analysis between changes of day 7 and day 14 serum NDKA, NMDA, PARK7, and UFDP levels (dependent variable) and phlegm-heat syndrome scores (independent variable) showed that serum NDKA, NMDA, PARK7, and UFDP levels were not significantly associated with the phlegm-heat syndrome scores ($P > 0.05$) (Table 3). These results suggested that serum NDKA, NMDA, PARK7, and UFDP levels are not biomarkers to evaluate the therapeutic efficacy of phlegm-heat syndrome in stroke patients.

4. Discussion

This study included 95 healthy subjects and 51 acute ischemic stroke patients with phlegm-heat syndrome. The serum NDKA, NMDA, PARK7, and UFDP levels; NIHSS scores; and phlegm-heat syndrome scores were measured within 3 days of onset and at 7 days and 14 days after the onset of stroke in 51 acute ischemic stroke patients. The associations between the serum levels of the tested biomarkers and phlegm-heat syndrome in acute ischemic stroke were analyzed within 3 days of the onset. The diagnostic value of each biological marker on the phlegm-heat syndrome in acute stroke patients was analyzed by ROC curve. The association between these biomarkers and treatment efficacy evaluation was analyzed by exploring the correlation of dynamic changes between the test biomarkers levels and the NIHSS scores as well as the phlegm-heat syndrome scores within 3 days of onset and at 7 days and 14 days after the onset. Our results demonstrated that the serum PARK7 and UFDP concentration have diagnostic value for the phlegm-heat syndrome of acute ischemic stroke. However, serum NDKA, NMDA, PARK7, and UFDP levels are not biomarkers for predicting the therapeutic efficacy of the disease and the phlegm-heat syndrome.

Previous studies have revealed that NDKA, NMDA, PARK7, and UFDP levels were significantly elevated in stroke patients within 3 h of onset and had certain sensitivity and specificity in the diagnosis of ischemic stroke [14–18]. This study found that serum PARK7 and UFDP levels in stroke patients with phlegm-heat syndrome within 3 days of onset were statistically different from the healthy subjects. The serum PARK7 level was elevated whereas UFDP level was lowered. The ROC curve analysis showed that serum PARK7 and UFDP levels had some diagnostic value on the phlegm-heat syndrome in ischemic stroke patients. However, currently, there were no reports on the associations between serum PARK7 and UFDP levels and other diseases such as coronary heart diseases and hypertension as well as stroke patients without phlegm-heat syndrome. Therefore, serum PARK7 and UFDP levels could not be used as a marker for the diagnosis of stroke with phlegm-heat syndrome currently. In addition, this study looked at the changing trends of serum NDKA, NMDA, PARK7, and UFDP levels and found that serum NDKA levels were not significantly changed within 3 days of onset to day 14 after onset. While no significant differences in the serum NMDA, PARK7, and UFDP levels were observed between the levels within 3 days of onset and at day 7 after onset, significant differences in serum levels of these 3 markers were observed between day 7 and day 14 after onset, and their levels had a tendency of increase. Our findings provided a complement to previous findings.

This study analyzed the associations between biological parameters and the clinical efficacy of acute stroke patients at the disease level and syndrome level. At the disease level, these biological markers showed no significant association with NIHSS scores at 3 time points. This indicated that these biomarkers lack value for evaluating the severity of defects in neural function in acute stroke patients. At the syndrome level, these biological markers exhibited no significant associations with the phlegm-heat syndrome scores and less efficacy in evaluating the severity of phlegm-heat syndrome. Therefore, these biomarkers cannot be used as indicators of clinical efficacy of therapy in acute stroke patients with phlegm-heat syndrome. However, this study found that the serum NMDA, PARK7, and UFDP levels had a tendency of increase at day 14 compared to day 7 after onset. Similarly,

the NIHSS scores and phlegm-heat syndrome scores showed a tendency of decrease at day 14 compared to day 7 after onset. These observations may suggest a relationship between the biological markers and the clinical efficacy of therapy. No significant differences were observed, which may be a bias caused by the small sample size. Despite the failure to obtain statistical difference, using biological markers to evaluate the therapeutic efficacy of Chinese medical syndromes is a new idea.

We acknowledge the limitations in the present study. (1) This study lacks control of syndromes and cannot determine the relevance between these biological markers and other disease syndromes of stroke. (2) The sample size was relatively small and may cause biases in outcomes.

5. Conclusion

Serum PARK7 and UFDP levels within 3 days of onset of acute stroke with phlegm-heat syndrome have some diagnostic value in phlegm-heat syndrome. The serum NDKA, NDMA, PARK7, and UFDP levels did not show a significant tendency in day 7 compared to day 3 within onset, while the serum NDMA, PARK7, and UFDP, but not NDKA, levels exhibited a tendency of increase in day 14 compared to day 7. Although the tendency of increase of NDMA, PARK7, and UFDP levels shown parallels the decreases in NIHSS scores and phlegm-heat syndrome scores at day 14 compared to day 7 after onset, no statistical significance between the serum levels of these biomarkers and treatment efficacy evaluation was obtained. A study with larger sample size and a control of syndromes is necessary to establish the statistical association between these biological markers and the therapeutic efficacy of acute stroke.

Conflict of Interests

The authors declared that there is no conflict of interests.

Authors' Contribution

Xiuxiu Han and Yonghong Gao contributed equally to this work.

Acknowledgments

This study was supported by the National Natural Science Foundation of China (no. 81173230) and a major national project "Significant Drug Discovery" (no. 2009ZX09502-028).

References

[1] G. A. Donnan, M. Fisher, M. Macleod, and S. M. Davis, "Stroke," *The Lancet*, vol. 371, no. 9624, pp. 1612–1623, 2008.

[2] C. F. Tsai, B. Thomas, and C. L. Sudlow, "Epidemiology of stroke and its subtypes in Chinese vs white populations: a systematic review," *Neurology*, vol. 81, no. 3, pp. 264–272, 2013.

[3] L. B. Goldstein, R. Adams, K. Becker et al., "Primary prevention of ischemic stroke: a statement for healthcare professionals from the stroke council of the American Heart Association," *Stroke*, vol. 32, no. 1, pp. 280–299, 2001.

[4] Z. Chang and Y. Jiang, "The relationship between acute cerebral infarction TCM Syndrome and cytokines," *Sichuan Traditional Chinese Medicine*, vol. 24, pp. 19–21, 2006.

[5] J. Chen, "The relationship between diabetic ischemic stroke syndromes and serum inflammatory cell factors," *Chinese Journal of Integrated Traditional and Western Medicine*, vol. 7, p. 147, 2000.

[6] S. Guan, J. Chen, and Y. Ma, "Relation between the initial state fiery syndrome of acute cerebral infarction and immune cell factors," *Journal of Radioimmunoassay*, vol. 13, pp. 331–332, 2000.

[7] R. W. Troughton, C. M. Frampton, T. G. Yandle, E. A. Espiner, M. G. Nicholls, and A. M. Richards, "Treatment of heart failure guided by plasma aminoterminal brain natriuretic peptide (N-BNP) concentrations," *The Lancet*, vol. 355, no. 9210, pp. 1126–1130, 2000.

[8] S. Wang, W. Zhang, and R. Tian, "Correlation of stroke syndromes and biological indicator and progress (review)," *Traditional Chinese Medicine of Beijing University*, vol. 30, pp. 279–281, 2007.

[9] B. Ma and Y. Gao, "Stroke outcome evaluation and establishment of clinical evaluation model of disease and syndrome," *Chinese Journal of Clinical Rehabilitation*, vol. 10, pp. 155–158, 2006.

[10] B. Zhang and Y. Wang, "Research and evaluation of comprehensive treatment program for acute stroke—with 522 cases of clinical studies," *Chinese Medicine*, vol. 17, pp. 259–263, 2005.

[11] X. Wang, Q. Liu, H. Zhong et al., "Second round of clinical validation of the outcome rating scale based on reports of stroke patients," *Chinese Medicine*, vol. 27, pp. 1245–1248, 2012.

[12] Y. Gao, B. Ma, and Q. Liu, "Development and methodology study of the diagnosis scale of ischemic stroke syndrome factors," *Traditional Chinese Medicine*, vol. 52, pp. 2097–2101, 2011.

[13] B. Ma, Z. Wang, X. Han et al., "Study of biological evaluation indicators in the system of stroke TCM clinical efficacy evaluation," *Journal of Integrative Medicine Heart Disease*, vol. 12, pp. 1012–1013, 2014.

[14] P. Lescuyer, L. Allard, C. G. Zimmermann-Ivol et al., "Identification of post-mortem cerebrospinal fluid proteins as potential biomarkers of ischemia and neurodegeneration," *Proteomics*, vol. 4, no. 8, pp. 2234–2241, 2004.

[15] L. Allard, P. R. Burkhard, P. Lescuyer et al., "PARK7 and nucleoside diphosphate kinase A as plasma markers for the early diagnosis of stroke," *Clinical Chemistry*, vol. 51, no. 11, pp. 2043–2051, 2005.

[16] S. Dabernat, M. Larou, K. Massé et al., "Cloning of a second nm23-M1 cDNA: expression in the central nervous system of adult mouse and comparison with nm23-M2 mRNA distribution," *Molecular Brain Research*, vol. 63, no. 2, pp. 351–365, 1999.

[17] S. A. Dambinova, G. A. Khounteev, G. A. Izykenova, I. G. Zavolokov, A. Y. Ilyukhina, and A. A. Skoromets, "Blood test detecting autoantibodies to *N*-methyl-D-aspartate neuroreceptors for evaluation of patients with transient ischemic attack and stroke," *Clinical Chemistry*, vol. 49, no. 10, pp. 1752–1762, 2003.

[18] L. Allard, N. Turck, P. R. Burkhard et al., "Ubiquitin fusion degradation protein 1 as a blood marker for the early diagnosis of ischemic stroke," *Biomarker Insights*, vol. 2, article 155, 2007.

Hindawi Publishing Corporation
Evidence-Based Complementary and Alternative Medicine
Volume 2015, Article ID 827472, 12 pages
http://dx.doi.org/10.1155/2015/827472

Research Article

The Protective Effects of Curcumin on Obesity-Related Glomerulopathy Are Associated with Inhibition of Wnt/β-Catenin Signaling Activation in Podocytes

Bao-li Liu,[1,2] Yi-pu Chen,[1] Hong Cheng,[1] Yan-yan Wang,[1] Hong-liang Rui,[1] Min Yang,[1] Hong-rui Dong,[1] Dan-nuo Han,[1] and Jing Dong[1]

[1]*Division of Nephrology, Beijing Anzhen Hospital, Capital Medical University, Beijing 100029, China*
[2]*Division of Nephrology, Beijing Traditional Chinese Medicine Hospital, Capital Medical University, Beijing 100010, China*

Correspondence should be addressed to Yi-pu Chen; chen_yipu@medmail.com.cn

Received 3 February 2015; Accepted 14 March 2015

Academic Editor: Dan Hu

The present study investigated the effects of curcumin, one of the most important active ingredients of turmeric, on podocyte injury *in vitro* and obesity-related glomerulopathy (ORG) *in vivo*. Cellular experiments *in vitro* showed that curcumin significantly antagonized leptin-induced downregulation of the mRNA and protein expression of podocyte-associated molecules including nephrin, podocin, podoplanin, and podocalyxin. Animal experiments *in vivo* showed that curcumin significantly reduced the body weight, Lee's index, abdominal fat index, urinary protein excretion, and average glomerular diameter and significantly upregulated the mRNA and protein expressions of the above podocyte-associated molecules in ORG mice. Furthermore, the experiments *in vitro* and *in vivo* both displayed that curcumin could downregulate the mRNA and protein expressions of Wnt1, Wnt2b, Wnt6, and β-catenin and upregulate the phosphorylation level of β-catenin protein in podocytes and renal tissue. In conclusion, curcumin is able to alleviate the harmful reaction of leptin on podocytes and reduce the severity of ORG. The above protective effects are associated with the inhibition of Wnt/β-catenin signaling activation in podocytes.

1. Introduction

In the past two decades, the obese patients were obviously increased with the improvement of life conditions in China. Obesity is a risk factor not only for diabetes mellitus and cardiovascular diseases, but also for kidney disease, which can induce obesity-related glomerulopathy (ORG) [1, 2]. As early as 1974, Weisinger and colleagues [3] firstly found that the severely obese individuals might be associated with massive proteinuria. With a rise in the number of obese patients, the incidence of ORG was rapidly increased. Kambham and colleagues [4] reported that among 6818 patients who underwent renal biopsy, the percentage of ORG patients increased from 0.2% in 1986–1990 to 2% in 1996–2000. Cheng and Chen [5] reported that ORG patients accounted for 3.8% in 1186 cases of renal biopsy during 2006–2008. Progression of ORG is relatively slow, but finally it still can enter into end stage renal disease (ESRD). Therefore, prevention and treatment of ORG have attracted more and more attention [1, 2].

Unfortunately except restricting dietary caloric intake, appropriately increasing physical activity and taking insulin sensitizing agent, so far there are scarcely other measures that can effectively interfere with ORG. So it is very important to look for available medicines. Curcumin, one of the most important active ingredients of turmeric, is a possible candidate. The modern laboratory and clinical research work in China and other countries has showed that curcumin is able to promote body weight loss and reduce incidence of some obesity-related diseases, such as diabetes mellitus, ischemic heart disease, stroke, and cancer [6–9]. In the present study, we are going to investigate the effects of curcumin on prevention and treatment of ORG and to explore its possible signal transduction pathway by the use of cellular experiments *in vitro* and animal experiments *in vivo*.

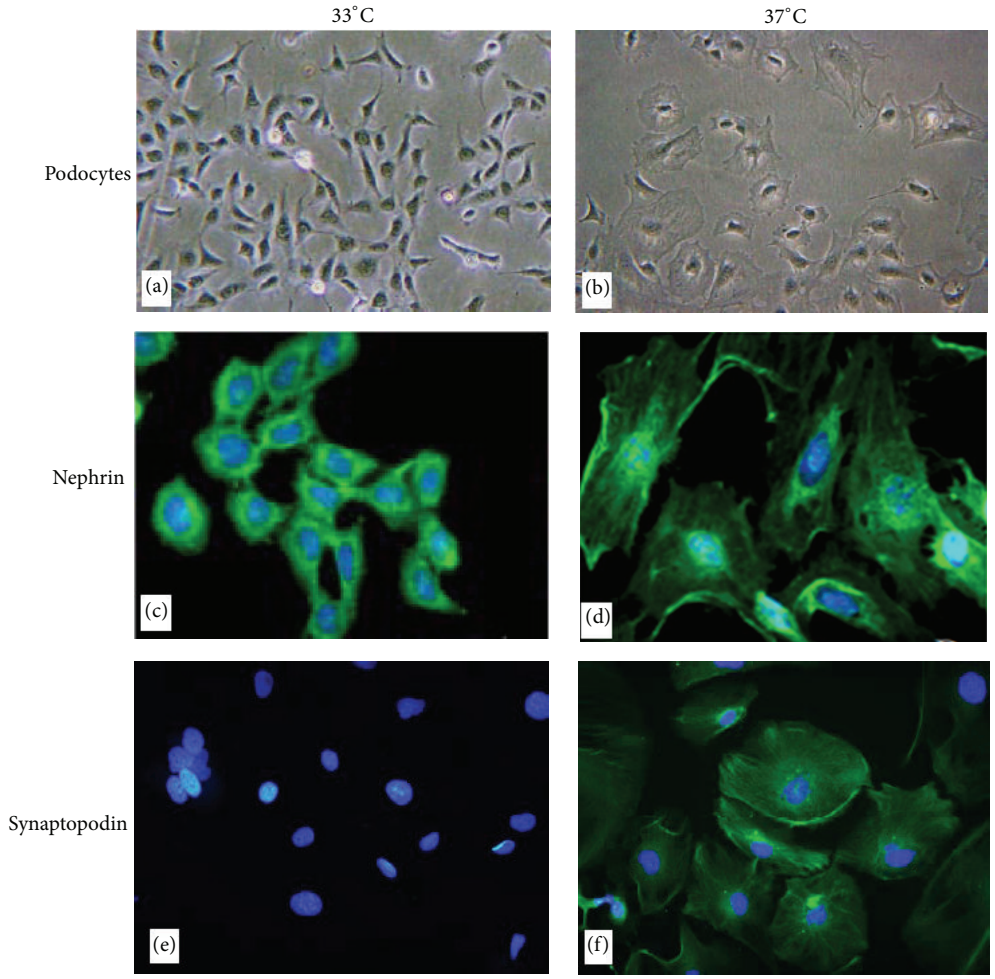

Figure 1: Cultured conditionally immortalized mouse podocytes in undifferentiated and differentiated statuses. (a) and (b) Morphology of cultured podocytes in undifferentiated status (left) and differentiated status (enlarged cell bodies with short and long projections, right) (phase microscopy ×200). (c) and (d) Diffuse cytoplasmic expression of nephrin in undifferentiated status (left); cell surface and cytoplasmic expression of nephrin in differentiated status (right) (immunofluorescence microscopy ×1000). (e) and (f) No expression of synaptopodin in undifferentiated status (left); filamentous and cell surface expression of synaptopodin in differentiated status (right) (immunofluorescence microscopy ×1000).

2. Materials and Methods

2.1. Cellular Experiments

2.1.1. Cell Culture. The conditionally immortalized mouse podocyte cell line was kindly provided by Proffessor Maria Pia Rastaldi (S. Carlo Hospital, University of Milan). Cells were incubated in RPMI-1640 medium (Gibco) containing 10% inactivated fetal bovine serum (FBS) and 10 u/mL interferon-γ (IFN-γ) (Cell Signaling Technology) at 33°C in humidified air with 5% CO_2. When cells reached 70% to 80% confluence, the cells were transferred in RPMI-1640 medium containing 10% inactivated FBS without IFN-γ and incubated at 37°C with 5% CO_2 to induce differentiation. The cells would completely differentiate in 10 to 14 days.

2.1.2. Immunofluorescent Staining of Nephrin and Synaptopodin on Podocytes. Before cellular experiments, differentiated status of podocytes was inspected by the indirect immunofluorescent staining of nephrin and synaptopodin, the marker proteins of podocytes [10]. Podocytes on the cover slip were fixed in 4% paraformaldehyde and permeabilized with 0.1% Triton X-100. Fixed podocytes were incubated overnight at 4°C with either rabbit anti-nephrin antibodies (1 : 100, Abcam) or mouse anti-synaptopodin antibodies (1 : 100, Acris GmbH). After washing with PBS for 3 times, podocytes were incubated with FITC-labeled goat anti-rabbit IgG antibodies (Dako) or FITC-labeled goat anti-mouse IgG antibodies (Dako) for 1 h at room temperature, mounted with a Hochst33342 containing mounting solution, and then observed with a fluorescent microscope (Nikon, Japan). The images of undifferentiated and differentiated podocytes were shown in Figure 1.

2.1.3. Effects of Leptin and Curcumin on the Podocytes. The podocytes were incubated in RPMI-1640 medium, medium containing 15 ng/mL leptin (Abcam), medium containing

Table 1: Sequence of oligo used in the study.

Name	Oligo sequence	Length of PCR products (bp)
Nephrin	Forward 5′-GTCTGGGGACCCCTCTATGA Reverse 5′-CAGGTCTTCTCCAAGGCTGT	209
Podocin	Forward 5′-CTGCAGAAGGGGAAAAGGCT Reverse 5′-TGATGCTCCCTTGTGCTCTG	205
Podoplanin	Forward 5′-AGGGAGGGACTATAGGCGTG Reverse 5′-GCTGAGGTGGACAGTTCCTC	202
Podocalyxin	Forward 5′-AGCCTGTGGATTCTTCACCG Reverse 5′-GTGTGGAGACGGGCAATGTA	210
Wnt1	Forward 5′-CGAACGACCGTGTTCTCTGA Reverse 5′-GCTCCAGGCGCAGCAG	191
Wnt2b	Forward 5′-GATGGGGCCAATTTCACAGC Reverse 5′-AGTTGTGTCATACCCTCGGC	202
Wnt6	Forward 5′-CAACTGGCTCTCCAGATGCT Reverse 5′-TGGCACTTACACTCGGTGC	203
β-catenin	Forward 5′-ACTGGAGCTCTCCACATCCT Reverse 5′-GTGGCTCCCTCAGCTTCAAT	191
GADPH	Forward 5′-TGTGAACGGATTTGGCCGTA Reverse 5′-GATGGGCTTCCCGTTGATGA-3′	206

5 μmol/L curcumin (Sigma-Aldrich), or medium containing both 15 ng/mL leptin and 5 μmol/L curcumin, respectively. Curcumin 3.684 mg was dissolved in dimethyl sulphoxide (DMSO) 1 mL and then diluted into concentration of 5 μmol/L with RPMI-1640 medium for experiment. After 9 h and 24 h of incubation, the mRNA and protein expression of nephrin, podocin, podoplanin, and podocalyxin of podocytes were determined by real-time PCR and Western blot, respectively. After 8 hours of incubation, the protein expression of phosphorylated β-catenin and total β-catenin of podocytes was measured by Western blot.

2.1.4. Effects of Wnt Signaling Inhibitor DKK1 on the Podocytes. The podocytes were incubated in RPMI-1640 medium, medium containing 15 ng/mL leptin (Abcam), medium containing 200 ng/mL DKK1, that is, Dickkopf-1 (R&D), or medium containing both 15 ng/mL leptin and 200 ng/mL DKK1, respectively. Incubation time and observation items were the same as in Section 2.1.3.

2.2. Animal Experiments

2.2.1. Animal Model and Grouping. Twenty-one male 5-week-old C57BL/6J mice were randomly divided into the following three groups: control group, ORG model group, and curcumin intervention group. The mice in control group were fed with common food which contains fat accounting for 10% kcal. The mice in model group and curcumin group were fed with high fat diet which contains fat accounting for 60% kcal according to the method described by us previously [11]. From 8th week to 12th week, the mice in curcumin group were subcutaneously injected 150 mg/kg/d curcumin that was dissolved in 75% polyethylene glycol 400 to a final concentration of 30 mg/mL. The same dosage of polyethylene glycol 400 was given to the mice in control and model groups in the same time. All the mice were sacrificed at the end of 12th week. A part of kidney tissue was fixed in 4% neutral formaldehyde solution for light microscopy, and another part of kidney tissue was rapidly preserved in liquid nitrogen for real-time PCR and Western blot assays.

2.2.2. Physicochemical Parameters. Body weight was measured every week and body length was measured at the 12th week. The samples of nocturnal 12 h urine were collected at 0 week and 12th week, respectively, for the detection of urinary protein excretion. Blood and urine samples were collected at the 12th week to test serum cholesterol, blood glucose, and blood and urine creatinine levels (Olympus AU5400). The weight of visceral fat mass was measured after the mouse was sacrificed.

The calculation formulas were as follows: Lee's index = $[\text{body weight (g)} \times 1000]^{1/3} \div$ body length (cm); visceral fat index = visceral fat mass (g) ÷ body weight (g) × 100%; creatinine clearance rate (CCr) = urine creatinine × urine volume ÷ serum creatinine (mL/min).

2.2.3. Glomerular Diameter Measurement. The tissue of kidney cortex was conventionally dehydrated, embedded, cut into sections, and stained with periodic acid-Schiff reagent. Twenty images of glomerular maximal profiles with vascular pole and/or urinary pole were taken under high-power microscope and were then analyzed by Nikon NIS-Elements BR image analysis software. The two longest perpendicular diameters of every glomerular capillary tuft without Bowman's space were measured and their mean value was calculated [11].

2.3. RNA Extraction and Real-Time PCR. Total RNA of each sample was extracted using TRIzol reagent (Invitrogen) according to the manufacturer's description. 2 μg mRNA from each sample was reverse-transcribed to cDNA with

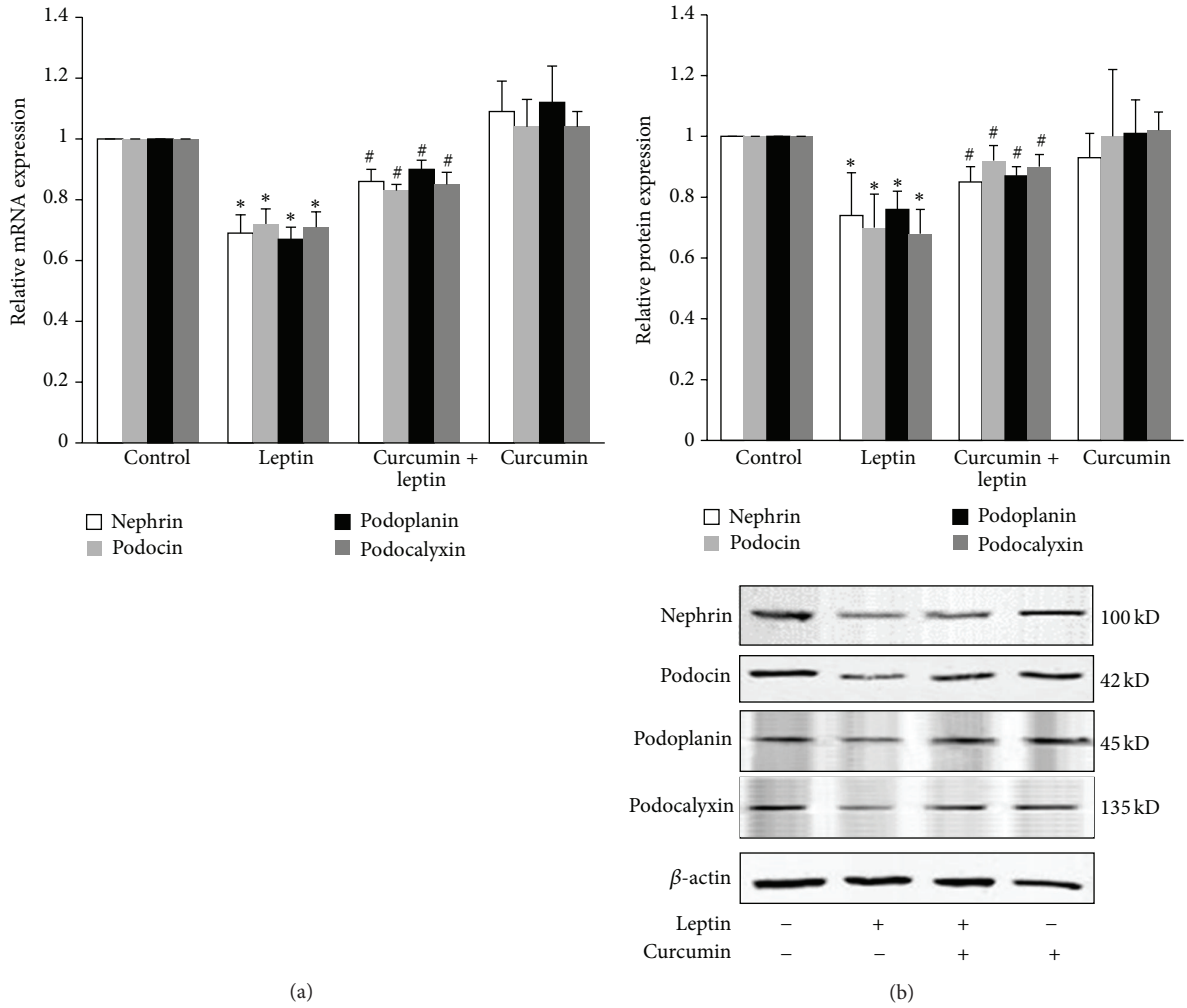

Figure 2: Effects of curcumin on leptin-mediated podocyte injury. Well-differentiated conditionally immortalized mouse podocytes were incubated in normal medium, medium containing 15 ng/mL leptin, medium containing 5 μmol/L curcumin, or medium containing both 15 ng/mL leptin and 5 μmol/L curcumin, respectively. (a) After 9 h, cells were collected and the relative mRNA expression levels of nephrin, podocin, podoplanin, and podocalyxin were measured by relative quantitative real-time RT-PCR. (b) After 24 h, cells were lysed and total lysates were analyzed by Western blot assay with antibodies of nephrin, podocin, podoplanin, podocalyxin, and β-actin, respectively. The relative protein level was expressed as the protein/β-actin ratio. Values are represented as mean ± SD ($n = 3$). $^{*}P < 0.05$ versus control group and $^{\#}P < 0.05$ versus leptin alone group.

Moloney murine leukemia virus reverse transcriptase (Transgene). Gene-specific primers were designed and synthesized by SBS Genetech Co., Ltd (Table 1). Relatively quantitative real-time PCR was performed in a total volume of 50 μL containing 2 μL of cDNA, 0.2 μM each primer, and 25 μL SYBR Green I Real-time PCR Master Mix (Transgene) using Rotor-Gene 6000. A thermal cycling profile consisted of a preincubation step at 94°C for 5 min, followed by 50 cycles of denaturation (94°C, 15 s), annealing (58°C, 15 s), and extension (72°C, 45 s). The specificity of the primers was verified by melting curves, and amplified products were sequenced to ensure the validity. Reactions were performed in triplicate, and threshold cycle numbers were averaged. A no template control was used as a negative control. The GAPDH fragment was amplified as a reference gene. The relative quantity of mRNA expression was calculated according to the formula $2^{-(\text{target gene Ct}-\text{GAPDH Ct})} \times 10^3$, where Ct is the threshold cycle number [12].

2.4. Western Blot Assay. Total protein was extracted from the cultured podocytes or mouse renal cortex using cell lysis buffer. Protein samples were boiled for 5 minutes, separated by 10% sodium dodecyl sulphate-polyacrylamide gel electrophoresis (SDS-PAGE), and then transferred to nitrocellulose membranes (Amersham Pharmacia Biotech). After blocking with 5% skim milk in phosphate-buffered saline with 0.1% Tween 20 for 1 hour, the membranes were incubated with primary antibody at 4°C overnight and then incubated with secondary antibody in room temperature for 1 hour. Details regarding primary and secondary antibodies are listed in Table 2. The blotted proteins were quantified using Odyssey infrared imaging system. β-actin as internal control

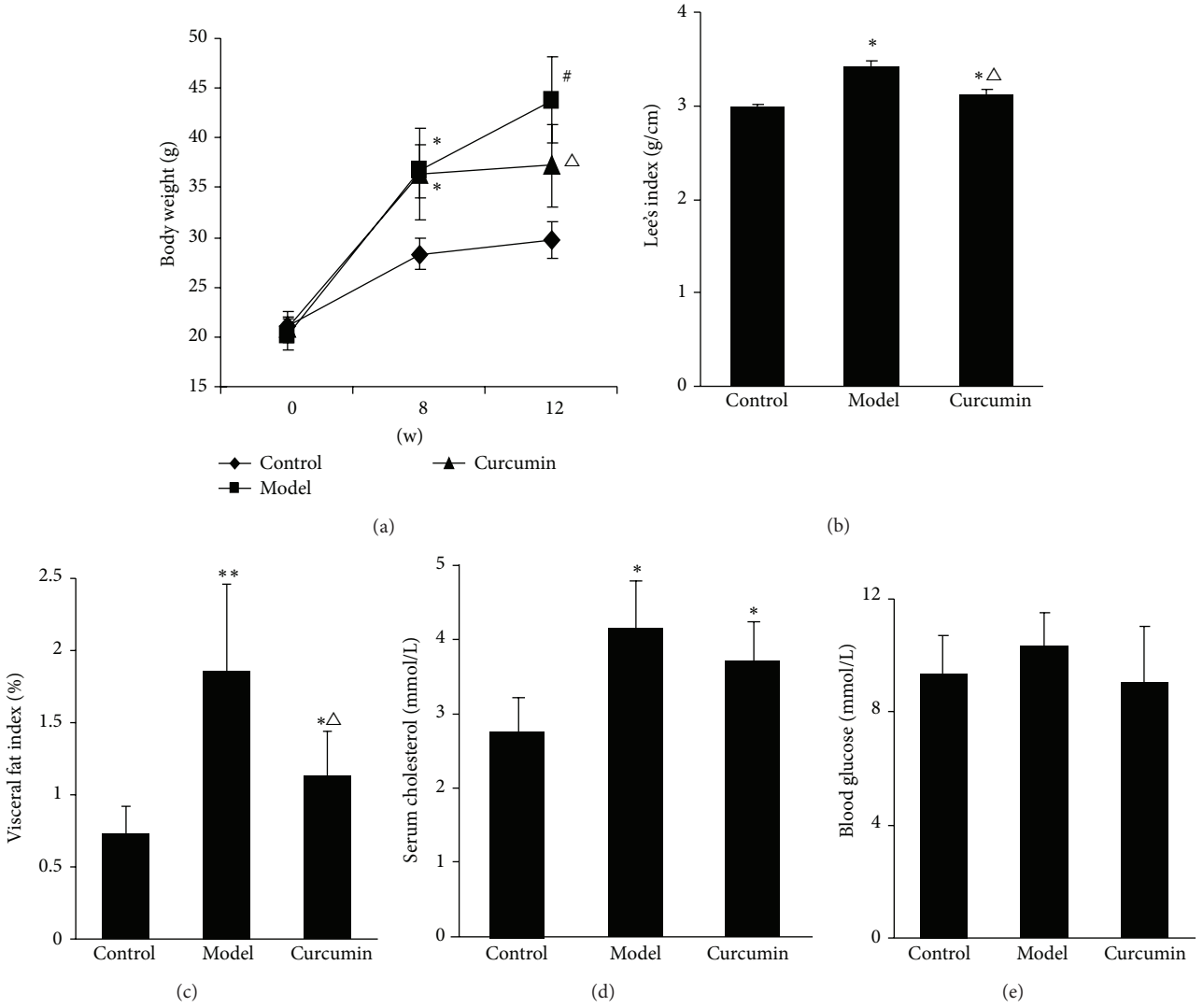

Figure 3: Effects of curcumin on body weight, Lee's index, visceral fat index, serum cholesterol, and blood glucose of ORG mice. (a) Average body weight of mice in model group and curcumin group was significantly higher than that in control group at the 8th week; it was significantly lighter in curcumin group than that in model group at the 12th week. $^{*}P < 0.05$ versus control group at 8th week, $^{\#}P < 0.05$ versus model group itself at 8th week, and $^{\triangle}P < 0.05$ versus model group at 12th week. (b), (c), and (d) Average Lee's index, visceral adiposity index, and serum cholesterol levels were significantly increased in mice of model group and curcumin group compared with control group, and the former two parameters were significantly reduced in curcumin group compared with model group at the 12th week. $^{*}P < 0.05$ versus control group, $^{**}P < 0.01$ versus control group, and $^{\triangle}P < 0.05$ versus model group. (e) Average levels of blood glucose in three groups had no significant difference at the 12th week. Values are represented as mean ± SD ($n = 7$).

was used to assess equal loading and the relative protein level was expressed as the protein/β-actin ratio [13]. All assays were performed at least in triplicate.

2.5. Statistical Analysis. All of the data of continuous variables were represented as mean ± SD and analyzed by using SPSS 19.0 statistical software. One-way ANOVA was used to test the differences among groups. Paired t-test was used for matched-pairs samples.

3. Results

3.1. Curcumin Can Reduce Podocyte Injury Induced by Leptin. In vitro cellular experiments showed that, compared with control group, leptin significantly downregulated the mRNA and protein expression of podocyte-associated molecules including nephrin, podocin, podoplanin, and podocalyxin ($P < 0.05$), while curcumin had no effect on their expression ($P > 0.05$). Compared with leptin group, curcumin significantly upregulated the mRNA and protein expression of above podocyte-associated molecules ($P < 0.05$) (Figure 2).

3.2. Curcumin Can Relieve Renal Damage in ORG Mice

3.2.1. Effects of Curcumin on the Physicochemical Parameters of Mice. In vivo animal experiments showed that, compared with control group, the body weight of mice in model group

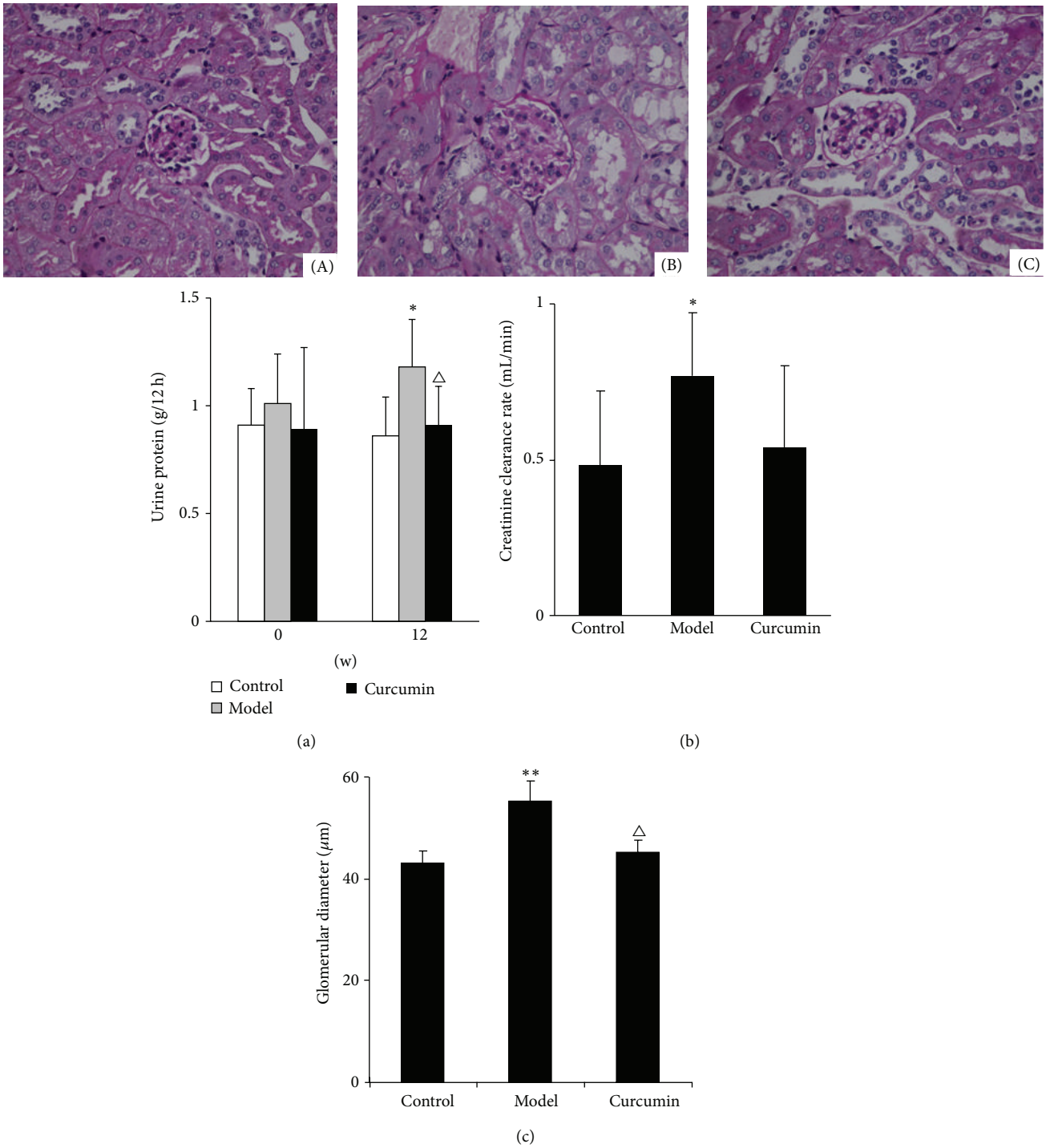

Figure 4: Effects of curcumin on renal damage of ORG mice. (a) Average level of nocturnal 12 h urine protein was significantly increased in mice of model group compared with control group and was significantly reduced in curcumin group compared with model group at the 12th week. (b) Average level of creatinine clearance rate was significantly increased in mice of model group compared with control group and was reduced in curcumin group compared with model, but the difference had not reached statistical significance at the 12th week. (c) Histology of kidney tissue from mice of control (A), model (B), and curcumin (C) groups (PAS staining ×400). The average glomerular diameter was significantly longer in the mice of model group than that in control group, while it was significantly shorter in curcumin group than that in model group at the 12th week. Values are represented as mean ± SD ($n = 7$). $^{*}P < 0.05$ versus control group, $^{**}P < 0.01$ versus control group, and $^{\triangle}P < 0.05$ versus model group.

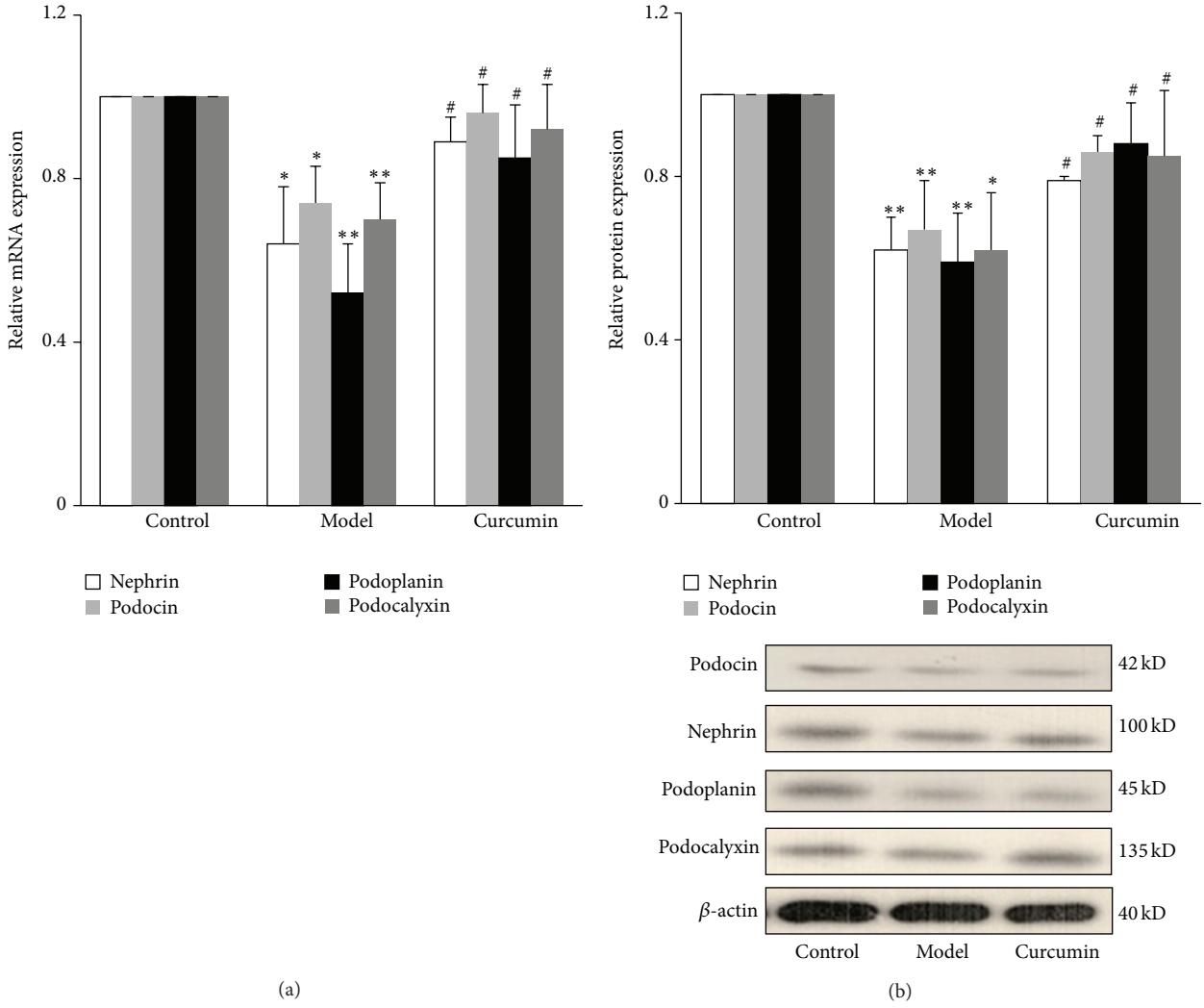

Figure 5: Effects of curcumin on podocyte-associated molecules of mice. (a) Mice sacrificed at the end of 12th week. Total RNA was extracted from kidney cortex, and then the relative mRNA expression levels of nephrin, podocin, podoplanin, and podocalyxin were measured by relative quantitative real-time RT-PCR. (b) Kidney cortex tissue was lysed and total lysates were analyzed by Western blot assay with antibodies of nephrin, podocin, podoplanin, podocalyxin, and β-actin antibody, respectively. The relative protein level was expressed as the protein/β-actin ratio. Values are represented as mean ± SD ($n = 7$). $^{*}P < 0.05$ versus control group, $^{**}P < 0.01$ versus control group, and $^{\#}P < 0.05$ versus model group.

and curcumin group was significantly increased at the 8th week ($P < 0.05$). Compared with their own body weight at the 8th week, it was significantly increased again in model group ($P < 0.05$) but had no significant change in curcumin group at the 12th week ($P > 0.05$). In addition, the body weight of mice in curcumin group was significantly lighter than that in model group at the 12th week ($P < 0.05$) (Figure 3).

The average Lee's index and abdominal fat index of mice were significantly increased in model and curcumin groups compared with control group ($P < 0.05$ or $P < 0.01$), while these two parameters in curcumin group were significantly lower than those in model group at the 12th week ($P < 0.05$) (Figure 3).

At the 12th week, the average serum cholesterol levels of mice in model and curcumin groups were significantly increased compared with control group ($P < 0.05$). The absolute value of this parameter in curcumin group was lower than that in model group, but the difference had not reached statistical significance ($P > 0.05$). There was no significant difference of average blood glucose levels among the three groups ($P > 0.05$) (Figure 3).

3.2.2. Effects of Curcumin on the Proteinuria and CCr of Mice. There was no difference of the nocturnal 12 h urinary protein excretion among the three groups at the beginning of the experiment ($P > 0.05$). Compared with the beginning of the experiment, the nocturnal 12 h urinary protein excretion was significantly increased in model group ($P < 0.05$), but it had no significant change in curcumin or control groups at the 12th week ($P > 0.05$). In addition, the nocturnal 12 h

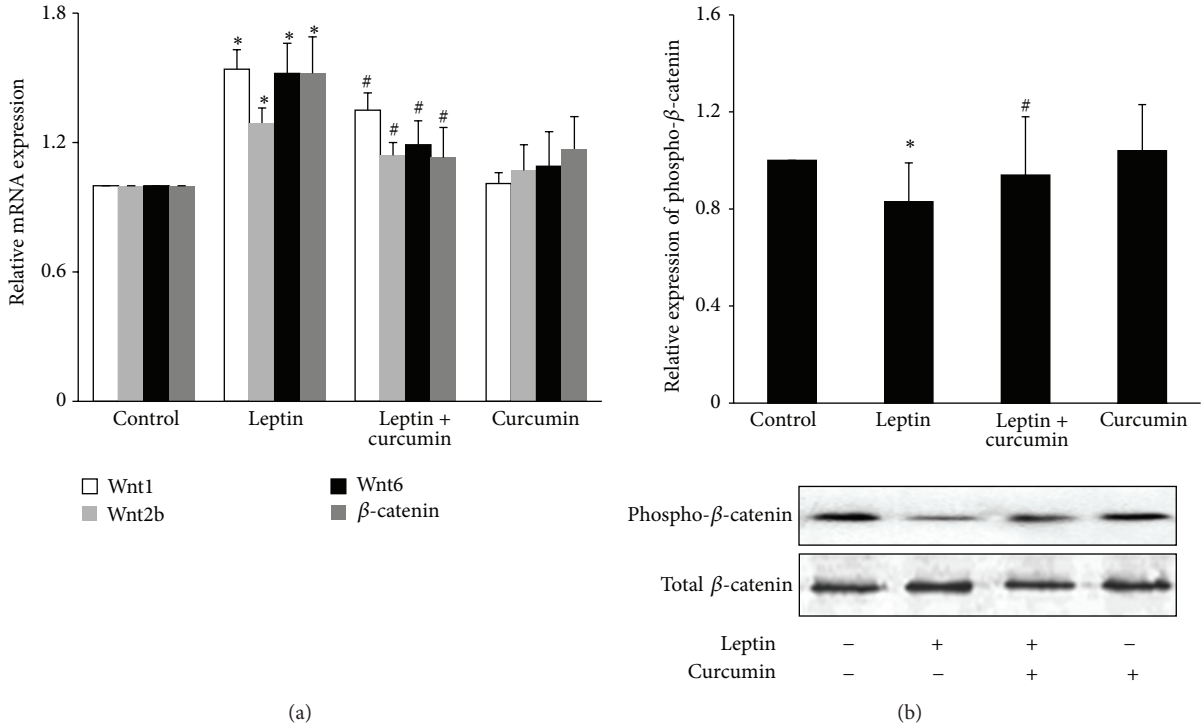

Figure 6: Effects of curcumin on leptin-activated Wnt/β-catenin signaling in cultured podocytes. Well-differentiated conditionally immortalized mouse podocytes were incubated in normal medium, medium containing 15 ng/mL leptin, medium containing 5 μmol/L curcumin, or medium containing both 15 ng/mL leptin and 5 μmol/L curcumin, respectively. (a) After 9 h, cells were collected and the mRNA expression levels of Wnt1, Wnt2b, Wnt6, and β-catenin were measured by relative quantitative real-time RT-PCR. (b) After 24 h, cells were lysed and total lysates were analyzed by Western blot assay with anti-phosphorylated β-catenin antibody and total β-catenin antibody, respectively. The relative phosphorylated β-catenin level was expressed as the phosphorylated β-catenin/total β-catenin ratio. Values are represented as mean ± SD ($n = 3$). $^{*}P < 0.05$ versus control group and $^{\#}P < 0.05$ versus leptin alone group.

urinary protein excretion in model group was significantly higher than that in control group ($P < 0.05$), while in the curcumin group it was significantly lower than that in model group at the 12th week ($P < 0.05$) (Figure 4).

At the 12th week, the average CCr of mice in model group was significantly increased compared with control group ($P < 0.05$). The absolute value of CCr in curcumin group was lower than that in model group, but the difference had not reached statistical significance ($P > 0.05$) (Figure 4).

3.2.3. Effect of Curcumin on Glomerular Size of Mice. The average glomerular size, which was expressed as average glomerular diameter in the present study, was significantly larger in the model group than that in control group ($P < 0.01$), while it was significantly smaller in curcumin group than that in model group at the 12th week ($P < 0.05$) (Figure 4).

3.2.4. Effects of Curcumin on Podocyte-Associated Molecules of Mice. Compared with control group, the mRNA and protein expression of podocyte-associated molecules, including nephrin, podocin, podoplanin, and podocalyxin, were significantly decreased in the renal cortical tissue of mice in model group at the 12th week ($P < 0.05$ or $P < 0.01$). Compared with model group, the mRNA and protein expression of the above podocyte-associated molecule were significantly upregulated in curcumin group at the 12th week ($P < 0.05$) (Figure 5).

Table 2: Primary and secondary antibodies used in the study.

Primary antibody	Secondary antibody
Rabbit anti-mouse nephrin pAb (Abcam)	IRDye 800 conjugated goat anti-rabbit IgG Ab (Rockland)
Rabbit anti-mouse podocin pAb (Sigma-Aldrich)	Ditto
Rabbit anti-mouse podoplanin pAb (Biotechnology)	Ditto
Rabbit anti-mouse podocalyxin pAb (Biotechnology)	Ditto
Rabbit anti-mouse β-catenin pAb (Cell Signaling Technology)	Ditto
Rabbit anti-mouse phosphorylated β-catenin pAb (Cell Signaling Technology)	Ditto
Mouse anti-mouse β-actin mAb (Sigma-Aldrich)	IRDye 800 conjugated goat anti-mouse IgG Ab (Rockland)

pAb: polyclonal antibody; mAb: monoclonal antibody.

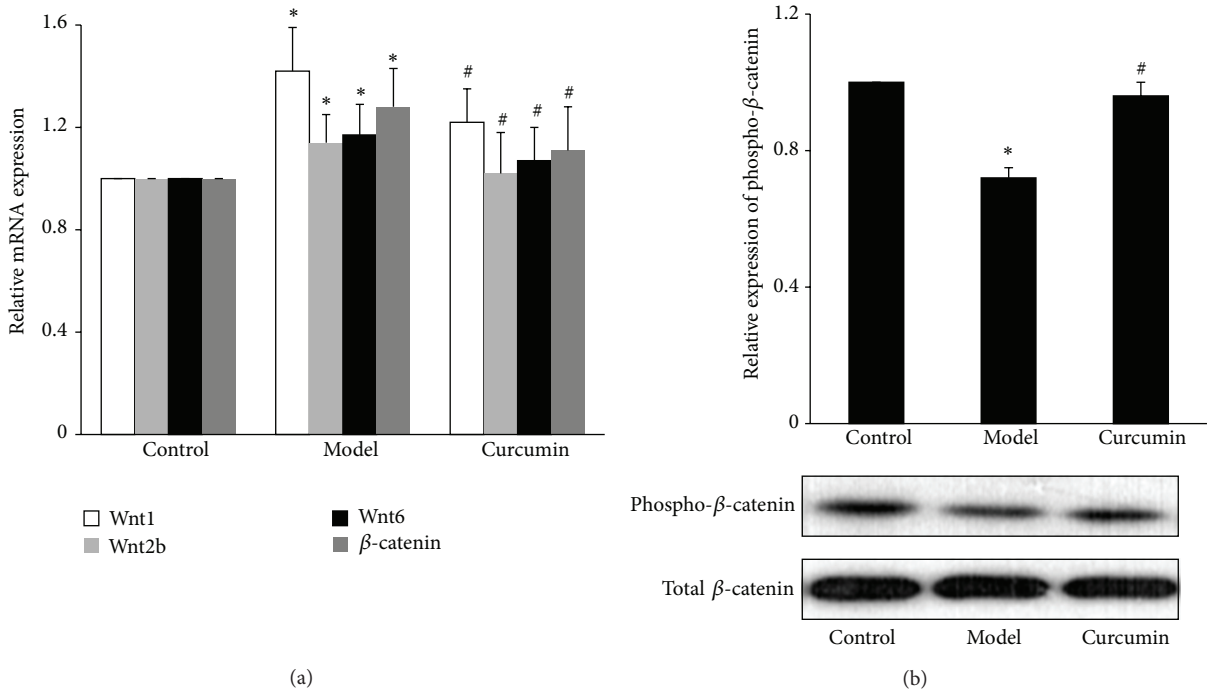

FIGURE 7: Effects of curcumin on Wnt/β-catenin signaling in the kidney tissue of ORG mice. (a) Mice sacrificed at the end of 12th week. Total RNA was extracted from kidney cortex, and then the relative mRNA expression levels of Wnt1, Wnt2b, Wnt6, and β-catenin were measured by relative quantitative real-time RT-PCR. (b) Kidney cortex was lysed and total lysates were analyzed by Western blot assay with anti-phosphorylated β-catenin antibody and total β-catenin antibody, respectively. The relative phosphorylated β-catenin level was expressed as the phosphorylated β-catenin/total β-catenin ratio. Values are represented as mean ± SD ($n = 7$). $^{*}P < 0.05$ versus control group and $^{\#}P < 0.05$ versus model group.

3.3. Curcumin Can Inhibit the Wnt/β-Catenin Signaling Activation in Podocytes

3.3.1. Inhibitory Effects of Curcumin on Podocyte Wnt/β-Catenin Signaling. In vitro cell experiments showed that, compared with control group, the mRNA expression of Wnt1, Wnt2b, Wnt6, and β-catenin was significantly upregulated ($P < 0.05$), and the level of phosphorylated β-catenin protein was significantly decreased in leptin group ($P < 0.05$). Curcumin alone had no effect on podocyte Wnt/β-catenin signaling pathway ($P > 0.05$) (Figure 6).

Compared with leptin group, the mRNA expression of the Wnt1, Wnt2b, Wnt6, and β-catenin was significantly downregulated ($P < 0.05$), and the level of phosphorylated β-catenin protein was significantly increased in curcumin group ($P < 0.05$) (Figure 6).

3.3.2. Inhibitory Effects of Curcumin on Wnt/β-Catenin Signaling in the Kidney Cortex Tissue of ORG Mice. The mRNA expression of Wnt1, Wnt2b, Wnt6, and β-catenin was significantly upregulated in model group compared with control group ($P < 0.05$) and was significantly downregulated in curcumin group compared with model group at the 12th week ($P < 0.05$) (Figure 7).

At the 12th week, the level of phosphorylated β-catenin protein was significantly decreased in model group compared with control group ($P < 0.05$) and significantly increased in curcumin group compared with model group ($P < 0.05$) (Figure 7).

3.3.3. Inhibition of Wnt/β-Catenin Signaling Activation Can Reduce Podocyte Injury. To test whether Wnt/β-catenin signaling activation was involved in the podocyte injury induced by leptin, the inhibitor of Wnt/β-catenin signaling DKK1 was used for cellular experiments. Result showed that the mRNA and protein expression of nephrin, podocin, podoplanin, and podocalyxin in leptin group were significantly downregulated compared with control group ($P < 0.05$ or $P < 0.01$), while DKK1 group was significantly upregulated compared with leptin group ($P < 0.05$) (Figure 8).

4. Discussion

Turmeric belongs to plants of ginger family. Its rhizome is used as a traditional Chinese herb. Turmeric contains a wide variety of phytochemicals in which curcumin is the most important pharmacodynamic ingredient and makes up about 2–5% of turmeric [14]. Curcumin is a natural polyphenolic compound with a molecular formula of $C_{21}H_{20}O_6$ [8, 14]. For investigating the action of curcumin on ORG and podocyte injury, it was used in cellular and animal experiments in the present study.

Podocyte injury and dysfunction are hallmark of ORG. Pathological examination in the kidney tissue of patients with

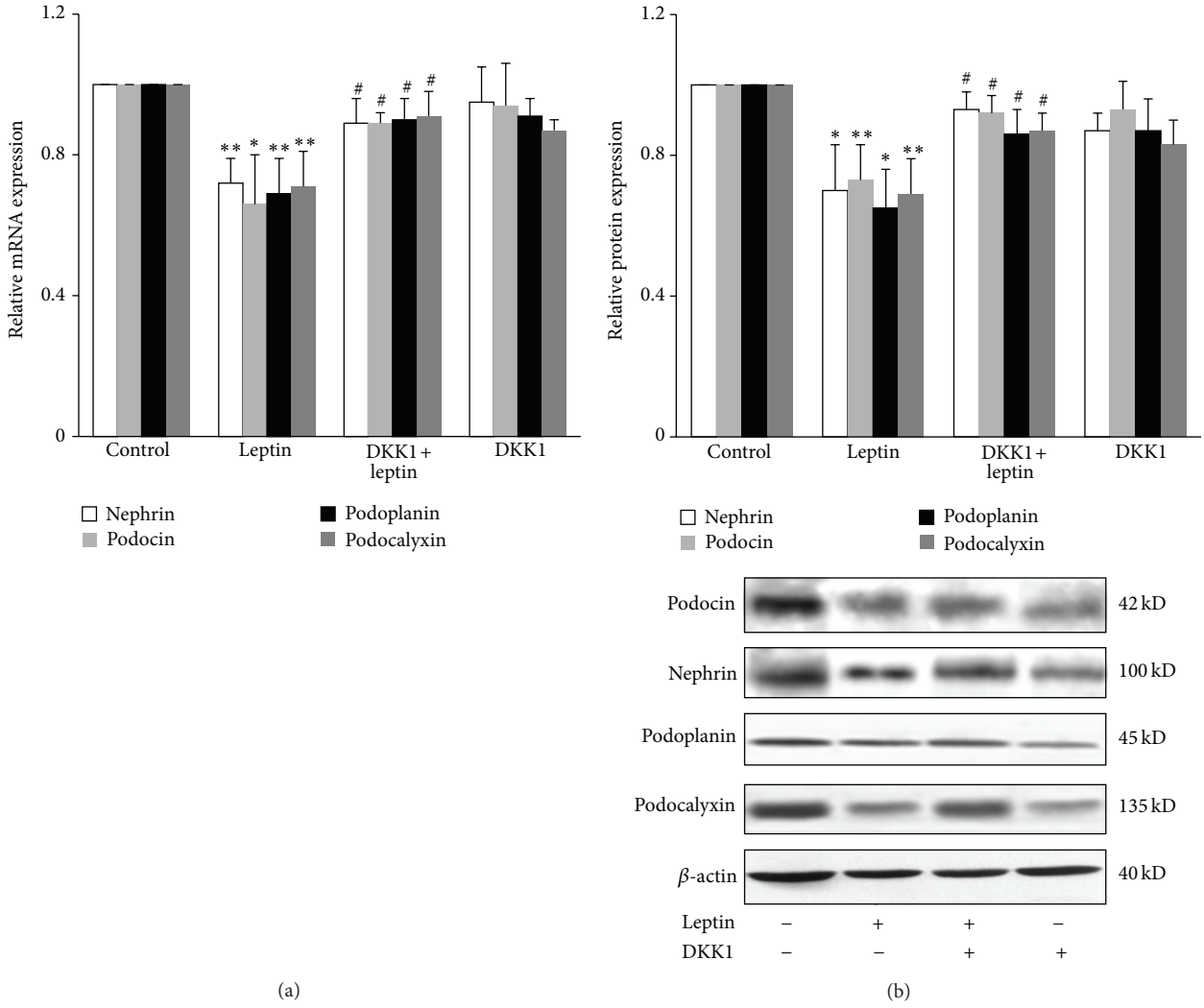

Figure 8: Effects of DKK1 on leptin-mediated podocyte injury. Well-differentiated conditionally immortalized mouse podocytes were incubated in normal media, media containing 15 ng/mL leptin and medium containing both 15 ng/mL leptin and 200 ng/mL DKK1, a well-known inhibitor of Wnt/β-catenin signaling, respectively. (a) After 9 h, cells were collected and the mRNA expression levels of nephrin, podocin, podoplanin, and podocalyxin were measured by relative quantitative real-time RT-PCR. (b) After 24 h, cells were lysed and total lysates were analyzed by Western blot assay with antibodies of nephrin, podocin, podoplanin, podocalyxin, and β-actin, respectively. The relative protein level was expressed as the protein/β-actin ratio. Values are represented as mean ± SD ($n = 3$). $^{*}P < 0.05$ versus control group, $^{**}P < 0.01$ versus control group, and $^{\#}P < 0.05$ versus leptin alone group.

ORG showed podocyte swelling, hypertrophy and vacuolar degeneration, increase of foot process width, fusion of foot process, decrease of podocyte density and number, the stripping of podocyte from the basement membrane, and so forth. Furthermore, these podocyte injuries were closely associated with proteinuria and renal function damage [15, 16]. In addition, it has been known that obese patients often have hyperleptinemia and leptin may play a role in the genesis of ORG [17, 18]. Therefore, in the *in vitro* cellular experiments of this study mouse podocytes were incubated with leptin, accompanied with curcumin or not, to observe the changes of podocytes. Results showed that leptin downregulated the mRNA and protein expression of podocyte-associated molecules including nephrin, podocin, podoplanin, and podocalyxin. The above podocyte-associated molecules are located at the slit diaphragm, basolateral region, basal aspect, and apical part of foot process, respectively, and have very important role in maintaining normal podocyte architecture and glomerular filtration function. The downregulation of their mRNA and protein expressions indicates podocyte injury [19]. However, our study results showed that curcumin could antagonize the harmful action of leptin and relieve the podocyte injury that resulted from leptin.

On the basis of cellular experiments, we carried out *in vivo* animal experiments using the mouse ORG model which was successfully established by our research team [11]. Study results showed that, compared with model group, the body weight, Lee's index, and abdominal fat index of mice in curcumin intervention group were significantly decreased, which suggests that curcumin has an effect against obesity

including abdominal obesity. Study results also showed that the mice in curcumin intervention group had less urinary protein excretion, less severe glomerulomegaly, and enhanced mRNA and protein expressions of podocyte-associated molecules compared with model group, which suggests that curcumin also has a good effect on prevention and treatment of ORG.

It is reported that Wnt/β-catenin signaling in podocytes plays a critical role in integrating cell adhesion, motility, differentiation and survival [20], and Wnt/β-catenin signaling activation-mediated podocyte injury and proteinuria caused by puromycin, adriamycin, or TGF-β [21–23]. So, the present study investigated the effects of curcumin on Wnt/β-catenin signaling pathway in podocytes. The results of *in vitro* cellular experiments and *in vivo* animal experiments both showed that curcumin was able to downregulate the high expression of Wnt1, Wnt2b, Wnt6, and β-catenin and to raise the low phosphorylation level of β-catenin protein, which suggests that curcumin has an inhibition action on Wnt/β-catenin signaling activation in podocytes. In order to better understand the effect of inhibiting Wnt/β-catenin signaling on podocytes, the inhibitor of Wnt signaling DKK1 was used in the cellular experiment. Experimental result showed that inhibition of Wnt/β-catenin signaling did alleviate podocyte injury. So, we consider that the inhibition action of curcumin on Wnt/β-catenin signaling probably is one of its important mechanisms for prevention and treatment of ORG.

However, when Ahn and colleagues [24] studied the action of curcumin on 3T3-L1 preadipocytes, they found that curcumin was able to activate Wnt/β-catenin signaling, and therefore the differentiation and maturation of preadipocytes were suppressed. So, we speculate that curcumin may have different effects on the Wnt signaling pathway in different cells, which is quite worth a further study in the future. In addition, it has been known that curcumin can regulate multiple signaling pathways besides Wnt/β-catenin signaling [25], so is there another signaling pathway which also participates in the actions of curcumin on prevention and treatment of ORG? This is also worth our further research in the future.

5. Conclusion

Curcumin is able to alleviate the harmful reaction of leptin on podocytes and reduce the severity of ORG. The above protective effects are associated with the inhibition of Wnt/β-catenin signaling activation in podocytes. This study will provide a preliminary experimental basis to better use curcumin in prevention and treatment of ORG. To our knowledge, no similar study has been reported in the literature.

Conflict of Interests

The authors declare that there is no conflict of interests regarding the publication of this paper.

Acknowledgments

This research was supported by the following 3 Grants: Chinese Postdoctoral Science Foundation (2013M530667), National Natural Science Fund Project (81241115), and Beijing Development Foundation of Traditional Chinese Medicine (JJ2012-20).

References

[1] Y. P. Chen, *Nephrology*, People's Medical Publishing House, Beijing, China, 1st edition, 2008.

[2] H.-M. Chen, S.-J. Li, H.-P. Chen, Q.-W. Wang, L.-S. Li, and Z.-H. Liu, "Obesity-related glomerulopathy in China: a case series of 90 patients," *American Journal of Kidney Diseases*, vol. 52, no. 1, pp. 58–65, 2008.

[3] J. R. Weisinger, R. L. Kempson, F. L. Eldridge, and R. S. Swenson, "The nephrotic syndrome: a complication of massive obesity," *Annals of Internal Medicine*, vol. 81, no. 4, pp. 440–447, 1974.

[4] N. Kambham, G. S. Markowitz, A. M. Valeri, J. Lin, and V. D. D'Agati, "Obesity-related glomerulopathy: an emerging epidemic," *Kidney International*, vol. 59, no. 4, pp. 1498–1509, 2001.

[5] H. Cheng and Y. P. Chen, "The compare study of clinical manifestations and pathological features between two kinds of obesity-related glomerulopathy," *Chinese Journal of Nephrology*, vol. 25, no. 4, pp. 261–264, 2009.

[6] Y. Yan, Y. Hong, H. Senke et al., "The study of weight control and the mechanism on the model of simplicity obesity rats by curcumin," *Journal of Xi'an Jiaotong University (Medical Sciences)*, vol. 27, no. 4, pp. 387–390, 2006.

[7] Y. Yu, S.-K. Hu, and H. Yan, "The study of insulin resistance and leptin resistance on the model of simplicity obesity rats by curcumin," *Chinese Journal of Preventive Medicine*, vol. 42, no. 11, pp. 818–822, 2008.

[8] L. Alappat and A. B. Awad, "Curcumin and obesity: evidence and mechanisms," *Nutrition Reviews*, vol. 68, no. 12, pp. 729–738, 2010.

[9] P. G. Bradford, "Curcumin and obesity," *BioFactors*, vol. 39, no. 1, pp. 78–87, 2013.

[10] S. Chittiprol, P. Chen, D. Petrovic-Djergovic, T. Eichler, and R. F. Ransom, "Marker expression, behaviors, and responses vary in different lines of conditionally immortalized cultured podocytes," *The American Journal of Physiology—Renal Physiology*, vol. 301, no. 3, pp. F660–F371, 2011.

[11] Y. Pei, M. Yang, H. Rui et al., "The establishment of obesity-related glomerulopathy mouse model," *Chinese Journal of Integrated Traditional and Western Nephrology*, vol. 15, no. 2, pp. 110–113, 2014.

[12] H. Cheng, Y.-P. Chen, H.-R. Dong, Y.-Y. Wang, and H.-L. Rui, "Study of glomerular podocyte injury induced by aristolochic acid," *Chinese Journal of Nephrology*, vol. 28, no. 3, pp. 222–225, 2012.

[13] P.-L. Bao, G.-Q. Wang, H.-R. Dong et al., "Wnt-7a inhibites epithelial to mesenchymal transition in mice of unilateral ureteral obstruction model," *Chinese Journal of Nephrology*, vol. 28, no. 9, pp. 720–724, 2012.

[14] S. Shishodia, G. Sethi, and B. B. Aggarwal, "Curcumin: getting back to the roots," *Annals of the New York Academy of Sciences*, vol. 1056, pp. 206–217, 2005.

[15] H. M. Chen, Z. H. Liu, C. H. Zeng, S. J. Li, Q. W. Wang, and L. S. Li, "Podocyte lesions in patients with obesity-related glomerulopathy," *The American Journal of Kidney Diseases*, vol. 48, no. 5, pp. 772–779, 2006.

[16] M. Camici, F. Galetta, N. Abraham, and A. Carpi, "Obesity-related glomerulopathy and podocyte injury: a mini review," *Frontiers in Bioscience—Elite*, vol. 4, no. 3, pp. 1058–1070, 2012.

[17] D.-K. Papafragkaki and G. Tolis, "Obesity and renal disease: a possible role of leptin," *Hormones (Athens)*, vol. 4, no. 2, pp. 90–95, 2005.

[18] J. F. Briffa, A. J. McAinch, P. Poronnik, and D. H. Hryciw, "Adipokines as a link between obesity and chronic kidney disease," *The American Journal of Physiology—Renal Physiology*, vol. 305, no. 12, pp. F1629–F1636, 2013.

[19] A. Greka and P. Mundel, "Cell biology and pathology of podocytes," *Annual Review of Physiology*, vol. 74, pp. 299–323, 2012.

[20] H. Kato, A. Gruenwald, J. H. Suh et al., "Wnt/β-catenin pathway in podocytes integrates cell adhesion, differentiation, and survival," *The Journal of Biological Chemistry*, vol. 286, no. 29, pp. 26003–26015, 2011.

[21] I. Matsui, T. Ito, H. Kurihara, E. Imai, T. Ogihara, and M. Hori, "Snail, a transcriptional regulator, represses nephrin expression in glomerular epithelial cells of nephrotic rats," *Laboratory Investigation*, vol. 87, no. 3, pp. 273–283, 2007.

[22] C. Dai, D. B. Stolz, L. P. Kiss, S. P. Monga, L. B. Holzman, and Y. Liu, "Wnt/β-catenin signaling promotes podocyte dysfunction and albuminuria," *Journal of the American Society of Nephrology*, vol. 20, no. 9, pp. 1997–2008, 2009.

[23] D. Wang, C. Dai, Y. Li, and Y. Liu, "Canonical Wnt/β-catenin signaling mediates transforming growth factor-B1-driven podocyte injury and proteinuria," *Kidney International*, vol. 80, no. 11, pp. 1159–1169, 2011.

[24] J. Ahn, H. Lee, S. Kim, and T. Ha, "Curcumin-induced suppression of adipogenic differentiation is accompanied by activation of Wnt/beta-catenin signaling," *The American Journal of Physiology—Cell Physiology*, vol. 298, no. 6, pp. C1510–C1516, 2010.

[25] Y. P. Chen, "Attention should be paid to the prospects of curcumin in prevention and treatment of kidney diseases," *Chinese Journal of Integrated Traditional and Western Nephrology*, vol. 15, no. 1, pp. 5–6, 2014.